ACTA SILVATICA
&
LIGNARIA
HUNGARICA

Acta Silvatica & Lignaria Hungarica

An International Journal in Forest, Wood and Environmental Sciences

Volume 9
2013

UNIVERSITY OF WEST HUNGARY PRESS

ACTA SILVATICA ET LIGNARIA HUNGARICA
AN INTERNATIONAL JOURNAL IN FOREST, WOOD AND ENVIRONMENTAL SCIENCES
issued by the Forestry Commission of the Hungarian Academy of Sciences

The journal is financially supported by the
Hungarian Academy of Sciences (HAS),
Faculty of Forestry, University of West Hungary (FF-UWH),
Faculty of Wood Sciences, University of West Hungary (FWS-UWH),
Hungarian Forest Research Institute (HFRI),
Instiute of Wildlife Management, University of West Hungary (IWM-UWH),
Sopron Scientists' Society of the Hungarian Academy of Sciences (SSS).

HU ISSN 1786-691X (Print)
HU ISSN 1787-064X (Online)

Manuscripts and editorial correspondence should be addressed to
MAGDOLNA STARK, ASLH EDITORIAL OFFICE
UNIVERSITY OF WEST HUNGARY,
PF. 132, H-9401 SOPRON, HUNGARY

Phone: +36 99 518 122
Fax: +36 99 329 911
E-mail: aslh@nyme.hu
Information and electronic edition: http://aslh.nyme.hu

The journal is indexed in the CAB ABSTRACTS database of CAB International; by SCOPUS, Elsevier's Bibliographic Database, by EBSCOhost database and by De Gruyter Open Sp. z. o. o., Warsaw

Published by UNIVERSITY OF WEST HUNGARY PRESS,
BAJCSY-ZS. U. 4., H-9400 SOPRON, HUNGARY
Cover design by ANDREA KLAUSZ
Printed by LŐVÉR-PRINT KFT., SOPRON

Contents

Tartalomjegyzék

DE GRUYTER OPEN DOI: 10.2478/aslh-2013-0001 Acta Silv. Lign. Hung., Vol. 9 (2013) 9–24

Comparison of Several Methods for Calculation of Reference Evapotranspiration

Csaba RÁCZ* – János NAGY – Attila Csaba DOBOS

Institute for Land Utilisation, Regional Development and Technology,
Centre for Agricultural and Applied Economic Sciences, University of Debrecen, Debrecen, Hungary

Abstract – The knowledge of the evapotranspiration of natural ecosystems and plant populations is of fundamental importance in several branches of science, research and practical uses. Nevertheless, the harmonisation of the large number of methods and user needs often causes problems. The objective of the analyses was to explore the output range and sensitivity of models of different physical approaches under local conditions. We performed descriptive statistical and sensitivity analysis of 10 commonly used estimation models – one of them with two variants. Correlation between modelled and measured evapotranspiration data series was assessed. The magnitude of the model outputs, their variability and responses to the changes of selected atmospheric parameters were evaluated. Priestley–Taylor, Penman–Monteith–FAO-56, Shuttleworth–Wallace (parameterized with alternative radiation balance), Szász and Makkink proved to be the most sensitive methods. As regards the systematic error, Makkink and Shuttleworth–Wallace showed the best agreement with pan evaporation, while Shuttleworth–Wallace, Blaney–Criddle and Makkink models were found to be the closest to the Penman–Monteith–FAO-56 method as a reference value.

evapotranspiration /estimation models / sensitivity analysis

Kivonat – **A referencia párolgás néhány becslő módszerének összehasonlító vizsgálata.** Számos tudományterület és kutatási téma, valamint gyakorlati alkalmazás számára bír alapvető fontossággal a növényállományok, természetes ökoszisztémák evapotranspirációjának ismerete. A nagyszámú módszer és a változó felhasználói igények összeegyeztetése azonban gyakran problémát okoz. A vizsgálatok célja az volt, hogy helyi viszonyok között is megismerhessük az eltérő fizikai megközelítést tükröző modellek kimeneti értéktartományát, érzékenységét. Leíró statisztikai-, valamint érzékenységvizsgálatot végeztünk 10 gyakran alkalmazott becslő modell eredményeire, ezek egyikének esetében két modellváltozatra is. Vizsgáltuk a kiválasztott módszerek korrelációját egymáshoz, illetve mért adatsorhoz képest. Értékeltük a modellkimenetek nagyságrendjét, azok változékonyságát, valamint az egyes légköri paraméterek változására adott reakcióját. A vizsgált módszerek közül a Priestley–Taylor, Penman–Monteith–FAO-56, Shuttleworth–Wallace (egyedi sugárzási egyenleggel parametrizálva), Szász és Makkink modell bizonyult a legérzékenyebbnek. Szisztematikus hiba tekintetében a Makkink és a Shuttleworth–Wallace mutatta a legjobb egyezést a mért értékekkel, míg a Penman–Monteith–FAO-56 módszert referenciaként választva ahhoz a Shuttleworth–Wallace, a Blaney–Criddle és a Makkink modell állt a legközelebb.

evapotranspiráció / becslő modellek / érzékenységvizsgálat

*Corresponding author: raczcs@agr.unideb.hu; H–4032 DEBRECEN, Böszörményi út 138.

1 INTRODUCTION

Research of evapotranspiration plays an important role in the field of agro- and hydrometeorology. Due to the complexity of evapotranspiration as a biophysical phenomenon, several approaches and variants were developed.

In physical sense, evapotranspiration (ET) is the sum of the evaporation (E) from the water and soil surfaces and the amount of water transpired by plants (transpiration, T). It is often limited by the currently available evaporable water, as well as by characteristics of the plant cover and the soil. Based on these factors, two values can be distinguished, namely potential (PET or ET_p) and actual evapotranspiration (AET or ET_a). Reference evapotranspiration (ET_0) represents theoretical evapotranspiration from an extensive surface of green grass of uniform height, actively growing, completely shading the ground, and not short of water (Allen et al. 1998). This concept is suitable for deriving ET values for any crop, although significant differences between values of diverse model equations may be confusing for practical users.

For each of the wide range of applications, such as hydrological and ecosystem models, aridity assessments, or irrigation planning etc. (FAO 1996, Lieth 1975), it is crucial to find the most appropriate method to estimate ET_0. Differences among methods often reach hundreds of millimetres per growing season (Federer et al. 1996), and accuracy of a given method depends heavily on the climatic conditions of the study site. For humid climate the Penman-Monteith-FAO-56 method is generally recommended (Jensen et al. 1990, Sumner – Jacobs 2005, Yoder et al. 2005, McMahon et al. 2012), and its extensions e.g. the Shuttleworth–Wallace equation also proved to be effective (Zhou 2011) because of its robust physical basis. Several studies preferring Priestley-Taylor's approach (Lu et al. 2005, Adeboye et al. 2009), point out that under such climatic conditions it performs better than any other radiation and temperature based methods. Most of the authors confirmed that temperature and radiation based methods tend to give the highest, while pan-coefficient based ones result in the lowest ET_0 values (Yates – Strzepek 1994, Tabari et al. 2011). Under arid and semi-arid climates radiation based models may perform poorly (Er-Raki et al. 2010), however, use of locally calibrated equations can make them more accurate than temperature based and even combination type ones (Bois et al. 2005, Schneider et al. 2007). In general, Penman-Monteith-FAO-56 and radiation based methods estimate ET_0 higher than pan-coefficient methods do (Rao – Rajput 1992) in arid environment.

The necessity of comparison, sensitivity testing and calibration of methods in a local context is emphasized by a large number of studies. Additionally, in continental climate of Eastern Hungary, there is a considerable variability of humid and arid characteristics, thus, to find the most suitable models, a local test appeared to be indispensable.

For our assessment we selected two methods of each the four basic ET_0 approaches. Since it is also highly recommended by literature (Federer et al. 1996, McMahon et al. 2012) to consider locally measured data, we decided to involve pan evaporation data series as a reference value.

The main objectives of our study were the following:

- statistical evaluation of the outputs of several approaches to evapotranspiration assessment,
- evaluation of the sensitivity of addressed approaches to change in input climate variables.

2 DATA AND METHODS

2.1 Climate data

The weather data used in our study were daily mean values derived from hourly values of the basic parameters (global radiation (kJ m^{-2} $hour^{-1}$), temperature at 2 m (°C), relative humidity (%), sunshine duration (hour day^{-1}) and wind speed at 10 m height (m s^{-1}), all measured at Debrecen Airport station of the Hungarian Meteorological Service. Therefore, we obtained a useful basis for comparison with the pan evaporation values measured at the same location.

Pan evaporation measurements represent a conventional measurement method and long data series are available at several Hungarian meteorological stations. The method refers to the daily amount of water evaporated from the open surface of a water filled pan. Although such measurements may be subject to error due to e.g. oasis effect, drinking animals, etc. (Tanner 1968, Lim et al. 2011), it is still a widely used method. Our data series contains the daily *ET* ('Pan', E_{pan} in mm day^{-1}) data measured by class-A evaporation pan at Debrecen Airport station (lat.: N47.490°; lon.: E21.611°) of the Hungarian Meteorological Service (OMSZ) during the growing seasons (April – October) of test years (2005–2010). In *Table 1.* we provide the descriptive statistics for the pan evaporation data series.

Table 1. Descriptive statistics of the pan evaporation data for the growing season (Apr.–Oct.)

	2005	2006	2007	2008	2009	2010
Sum	613.6	751.1	1015	802.8	1091	750.7
Mean	87.66	107.3	145	114.7	155.8	107.2
St.D.	1.59	1.88	2.60	2.01	2.29	2.04
CV	1.81	1.75	1.79	1.75	1.47	1.90

Unit: mm day^{-1}
St.D.: standard deviation, **CV**: coefficient of variation (%)

2.2 Methods for modelling potential evapotranspiration

Equations for the applied models can be seen below, sorted by type.

Pan coefficient-based methods ***(time step: day)***

Pereira model: (Pereira et al. 1995): *('Per', hereinafter)*

$$ET_0 = E_{pan} \cdot K_1 \quad (1)$$

$$K_1 = \frac{0.85(\Delta + \gamma)}{[\Delta + \gamma(1 + 0.33u_2)]} \quad (2)$$

FAO-56 (Allen et al. 1998): ('FAO56')

$$ET_0 = E_{pan} \cdot K_2 \quad (3)$$

$$K_2 = 0.51206 - (0.000321u_2 + 0.0422\ln(F) + 0.1434\ln(RH) - 0.000631[\ln(F)]^2 \ln(RH) \quad (4)$$

Temperature-based methods ***(time step: month or longer)***

Blaney–Criddle-model: (Blaney–Criddle 1950, Doorenbos–Pruitt 1977a, Burman–Pochop 1994): *('B&C')*

$$ET_0 = a_1 + b_1[p(0.46T + 8.13)] \quad (5)$$

$$a_1 = 0.0043RH_{\min} - (n/N) - 1.41 \quad (6)$$

$$b_1 = 0.82 - 0.0041RH_{\min} + 1.07(n/N) + 0.066u_{2d} - 0.006RH_{\min}(n/N) - 0.0006RH_{\min}u_{2d} \quad (7)$$

Szász method (Szász 1973): *('Szász')*

$$ET_0 = 0.00536 \cdot (T+21)^2 \cdot (1-RH)^{\frac{2}{3}} \cdot f(u) \quad (8)$$

$$f(u) = 0.0519 \cdot u_2 + 0.905 \quad (9)$$

Radiation-based methods ***(time step: day/month)***

Makkink–FAO-24 (Makkink 1957, Doorenbos–Pruitt 1977b): *('Mak')*

$$ET_0 = a_2 + b_2\left(\frac{\Delta}{\Delta+\gamma}\right)\frac{R_g}{\lambda} \quad (10)$$

$a_2 = -0{,}3$ (11)

$$b_2 = c_0 + c_1RH + c_2u_{2d} + c_3RHu_{2d} + c_4RH^2 + c_5u_{2d} \quad (12)$$

Priestley–Taylor-model (Priestley–Taylor 1972, McNaughton – Jarvis, 1983): *('P&T')*

$$ET_0 = \frac{\alpha\frac{\Delta}{\Delta+\gamma}(R_n - G)}{\lambda} \quad (13)$$

$$\alpha = 1 + \frac{\gamma}{\Delta+\gamma} \cdot \frac{r_c}{r_a} \quad (14)$$

Methods based on mass-transfer ***(time step: day)***

WMO-1966 (WMO 1966): *('WMO66')*

$$ET_0 = (0.1298 + 0.0934u_2) \cdot (e_s - e_a) \quad (15)$$

Mahringer-model (Mahringer 1970): *('Mah')*

$$ET_0 = 0.1572 \cdot \sqrt{3.6u_2} \cdot (e_s - e_a) \quad (16)$$

Combination-type methods ***(time step: day)***

Penman–Monteith–FAO-56-model (Allen et al. 1998): *('PMF56')*

$$ET_0 = \frac{0.408\Delta(R_n - G) + \gamma\frac{900}{T+273}u_2(e_s - e_a)}{\Delta + \gamma(1 + 0.34u_2)} \quad (17)$$

Shuttleworth–Wallace-model (Shuttleworth–Wallace 1985): *('S&W' and 'S&W#2')*

$$ET_0 = \frac{C_c \cdot ET_c + C_s \cdot ET_s}{\lambda} \quad (18)$$

Terms of the above equations are given in details in *Table 2*.

Table 2. Abbreviation of variables, coefficients and units used in equations 1–17

Notation	Name of variable	Unit	Equation no.
u_2	daily mean wind speed at 2 m height	km day^{-1}	2, 4, 9, 15, 16, 17
u_{2d}	mean wind speed of daylight hours at 2 m height	m s^{-1}	7, 12
γ	psychrometric constant	kPa °C^{-1}	2, 10, 13, 14, 17
Δ	slope of the vapor pressure curve	kPa °C^{-1}	2, 4, 10, 13, 14, 17
F	the fetch distance above the reference surface	m	4
RH	daily mean relative humidity	%	4, 8, 12
RH_{min}	daily minimum of relative humidity	%	6, 7
a_1, b_1	parameters for equation 5	–	5
a_2, b_2	parameters for equation 10	–	10
(n/N)	relative sunshine duration	–	6, 7
T	daily mean temperature at 2 m height	°C	5, 7, 8, 17
c_0, c_1, c_2, c_3, c_4, c_5	coefficients for equation 12	–	12
R_g	global radiation	cal m^{-2} day^{-1}	10
R_n	net radiation	MJ m^{-2} day^{-1}	13
	water equivalent of net radiation	mm day^{-1}	17
G	soil heat flux	MJ m^{-2} day^{-1}	13
	water equivalent of soil heat flux	mm day^{-1}	17
λ	latent heat of vaporization	cal m^{-2} day^{-1}	10
		MJ kg^{-1}	13, 18
α	Priestley-Taylor coefficient	–	13
r_a	aerodynamic resistance	s m^{-1}	14
r_c	canopy resistance	s m^{-1}	14
e_s	saturation vapor pressure	hPa	15, 16
		kPa	17
e_a	actual vapor pressure	hPa	15, 16
		kPa	17
C_c	weighting coefficient for canopy	–	18
C_s	weighting coefficient for soil	–	18
ET_c	transpiration	mm day^{-1}	18
ET_s	evaporation	mm day^{-1}	18

During the selection of the models, attributes taken into consideration were input data requirements, sensitivity for different climatic variables and suitability to different humidity conditions according to literature.

Pan-evaporation derived methods are relatively simple, computation is based on measured E_{pan} values and an empirically determined pan-coefficient as a correction factor. An advantage of these methods, such as Per and FAO56, is their very little input data.

Temperature- and radiation based methods are also simple with low number of input variables, however, calculation of empirical coefficients used can be difficult. These methods are recommended to be used for monthly or longer periods of time.

Methods based on mass-transfer mainly use temperature and humidity parameters. This approach considers the energy and water vapour transfer between the surface and the air. Equations are typically simple, with daily time step.

Combination-type methods unify aerodynamic and energy-balance theories. PMF56 and S&W methods are particularly widely used and considered to be accurate and robust models with the disadvantage of high input data requirements. S&W equation, which is a modification of PMF56, allows for local calibration and parameterization, though it requires abundant data describing air, soil and vegetation conditions either.

The analysis was performed for the period of 2005–2010. Winter periods during the analysis, were deliberately neglected. However, daily values of ET_0 could be considerable in several cases, it has very little significance for agro- and hydrometeorological use.

For our alternative Shuttleworth-Wallace 'S&W#2' test-variant, estimated net radiation values were used. Net radiation data was calculated from global radiation of D.-Airport, with linear regression method on the basis of four components net radiation measurements. Net radiation was measured at Debrecen-Kismacs Agrometeorological Observatory (lat.: N47.577°; lon.: E21.582°), approximately 10 km north to the Airport station.

2.3 Methods for data analysis

The comparative analysis consisted of two parts. First, a descriptive analysis was performed; the values of the final results obtained from each estimation algorithm, i.e., evapotranspiration sums during the growing season and monthly amounts were examined in six test years. Furthermore, the average differences of values from the pan evaporation data were also evaluated in the respective periods. By means of basic descriptive statistical indices, such as absolute maximum, absolute minimum, mean value, total range of values, standard deviation, coefficient of variation and variance, models were subjected to a statistical. Also, cross analysis of the models' root mean square error (RMSE) between model outputs was performed. RMSE is an informative which denotes the error between a model and a certain basis for comparison. In this study we paired every single model to all the others to assess the magnitude of discrepancy between each pair. In a similar way we carried out a Pearson's correlation test. In addition to cross-analyses we examined residues calculated on the basis of Pan and PMF-56 methods. Outputs of each model were compared to Pan and PMF-56 thus, and for ΔET_0 values basic statistics (e.g. absolute maximum and minimum, mean bias error (MBE), standard deviation, variance and total range) were calculated.

All the indices were calculated on the basis of daily data in the entire examination period except for the analysis of monthly or seasonal sums.

Next, a sensitivity analysis was carried out to evaluate the response of calculated ET to selected atmospheric parameters. Changes of model outputs and their variability induced by change in atmospheric variables were evaluated. Reason for the selection of these variables, such as temperature measured at 2 m height (T), relative humidity (RH), global radiation (R_g) and wind speed measured at 10 m (u), was that these variables are thought of as the most decisive in the control of ET values in most of equations used.

Mean values of these parameters and also from the ET_0 values of each model were calculated. Then we calculated the deviation (Δ) from these means for the daily data of the atmospheric parameters and the ET_0 values, respectively. In order to reach the best comparability between the effects of changes in all atmospheric variables, Δ values of each parameter and ET_0 were converted to changes in percentage. Finally, the mean of output changes (mean ΔET_0) and the total range (R) of the changes for the period were shown in diagrams indicating the magnitude of changes in the input on the x-axis.

3 COMPARATIVE ANALYSIS AND SENSITIVITY ANALYSIS

3.1 Descriptive statistics

Data in *Table 3* indicate that yearly sums of modelled ET_0 values differ remarkably among years and models. This high level of divergence occurs mostly between different types (e.g. temperature-based, radiation based, etc.) of methods and only to a lesser extent between methods of the same type.

Table 3. Sums of ET_0 during the growing seasons of the examined years

Year	Pan	Per	FAO56	B&C	Szász	Mak	P&T	WMO66	Mah	S&W	PMF56	S&W#2
2005	649	425	517	914	692	861	663	481	582	864	925	828
2006	751	493	597	951	708	893	674	520	628	895	948	853
2007	1015	644	771	1126	797	1046	746	755	885	1113	1148	1065
2008	803	512	628	971	708	923	710	557	657	922	979	883
2009	1091	690	830	1153	789	1041	737	799	937	1164	1183	1117
2010	751	477	595	877	648	844	683	446	527	799	868	763

ET_0: reference evapotranspiration (mm)

Table 4 implies that there are differences between the selected models in terms of their range and standard deviation. In addition, the group of models which estimate the highest maximum – and the widest range – of ET_0 (mass-transfer based and combination type methods) and those which show the highest standard deviation (B&C, Mak and combination type methods) is not necessarily the same. Notwithstanding, we could distinguish large fluctuation models by their high range and standard deviation values (Pan, B&C, mass-transfer based and combination-type methods) and also 'conservative' ones with less fluctuation can be specified (pan coefficient-based, Szász and P&T methods).

Table 4. Descriptive statistics calculated for the whole examined period (2005–2010)

	Pan	Per	FAO56	B&C	Szász	Mak	P&T	WMO66	Mah	S&W	PMF56	S&W#2
Max.	12.10	7.67	8.18	11.79	6.49	9.70	7.17	16.05	17.30	14.76	12.85	14.92
Min.	0.00	0.00	0.00	0.33	0.21	–0.05	0.24	0.04	0.05	0.15	0.23	0.08
Avg.	3.94	2.52	3.07	4.67	3.38	4.37	3.28	2.77	3.28	4.48	4.71	4.29
R.	12.10	7.67	8.18	11.46	6.28	9.75	6.93	16.00	17.25	14.61	12.62	14.84
St.D.	2.18	1.41	1.61	2.32	1.51	2.31	1.55	1.82	2.04	2.22	2.22	2.22
CV	0.55	0.56	0.53	0.50	0.45	0.53	0.47	0.66	0.62	0.50	0.47	0.52
Var.	4.75	2.00	2.60	5.40	2.27	5.35	2.41	3.32	4.18	4.92	4.91	4.94

Max.: absolute maximum (mm day^{-1}), **Min.**: absolute minimum (mm day^{-1}), **Avg.**: mean value (mm day^{-1}), **R.**: total range (mm day^{-1}), **St.D.**: standard deviation, **CV**: coefficient of variation, **Var.**: variance
For explanation of method abbreviations see chapter 2.2

Annual time series of residuals *(Figure 1.)* indicate that differences between modelled and measured values were relatively stable, but not constant. There are major changes in residuals either between model outputs or between Pan data and modelled ET_0 values.

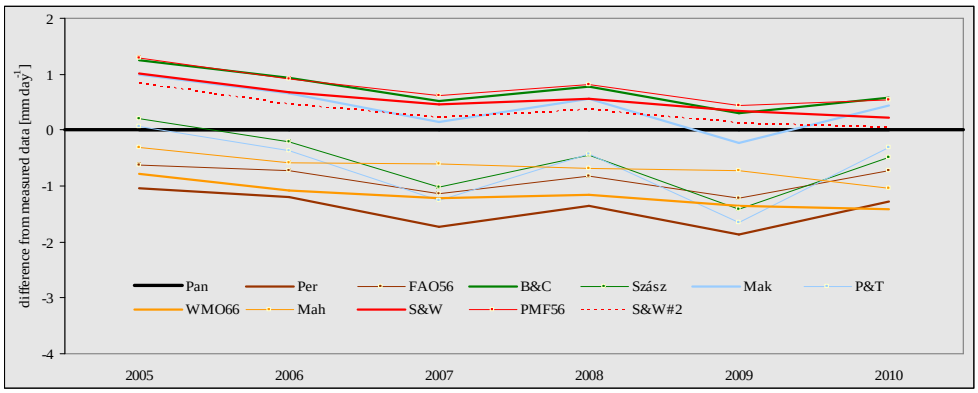

(Meanings of abbreviations are given in chapter 2.2)

Figure 1. Average daily difference of the model outputs and measured values in the period 2005–2010

The temporal course of the differences compared to Pan data and the precipitation sums of the examined growing seasons correlates well in case of certain models. The following precipitation sums were recorded in the interval between April and October: 473 mm (2005), 438 mm (2006), 369 mm (2007), 396 mm (2008), 256 mm (2009) and 571 mm (2010). The value of the coefficients of determination (R^2) are 0.79 (Per), 0.82 (FAO56), 0.72 (Szász), 0.69 (Mak) and 0.82 (P&T**)**.

It shows the fact that model response to the amount of evaporable water is stronger than that of the evaporation pan. Although it should be noted that in case of other models correlation was much weaker.

The quantification of the correlation of the models and the residuals compared to each other is closely linked to our statistical examinations. Correlation was calculated for each pair of models instead of averaging within model types. *Table 5* summarises the values of Pearson's correlation coefficient.

Table 5. Cross analysis of Pearson's correlation between modelled daily ET_0 data (2005–2010)

	Pan	Per	FAO56	B&C	Szász	Mak	P&T	WMO66	Mah	S&W	PMF56	S&W#2
Pan	–	0.97	0.99	0.83	0.78	0.81	0.80	0.81	0.82	0.87	0.86	0.85
Per	0.97	–	0.99	0.87	0.83	0.84	0.81	0.75	0.79	0.85	0.84	0.84
FAO56	0.99	0.99	–	0.84	0.80	0.82	0.81	0.76	0.79	0.84	0.84	0.83
B&C	0.83	0.87	0.84	–	0.95	0.96	0.92	0.81	0.85	0.93	0.94	0.90
Szász	0.78	0.83	0.80	0.95	–	0.97	0.95	0.72	0.77	0.89	0.91	0.86
Mak	0.81	0.84	0.82	0.96	0.97	–	0.97	0.75	0.80	0.92	0.95	0.89
P&T	0.80	0.81	0.81	0.92	0.95	0.97	–	0.70	0.73	0.88	0.92	0.85
WMO66	0.81	0.75	0.76	0.81	0.72	0.75	0.70	–	0.99	0.93	0.90	0.92
Mah	0.82	0.79	0.79	0.85	0.77	0.80	0.73	0.99	–	0.95	0.91	0.94
S&W	0.87	0.85	0.84	0.93	0.89	0.92	0.88	0.93	0.95	–	0.99	0.98
PMF56	0.86	0.84	0.84	0.94	0.91	0.95	0.92	0.90	0.91	0.99	–	0.97
S&W#2	0.85	0.84	0.83	0.90	0.86	0.89	0.85	0.92	0.94	0.98	0.97	–

n (number of cases) = 1284. Method abbreviations are explained in chapter 2.2

The closest correlation was observed between Pan and pan-based models due to the fact that these algorithms are closely related to the measured data by the use of a correction factor. Models that showed the weakest correlation with any other were mass-transfer-based ones. The weakest correlation of all has been found between mass-transfer and radiation-based methods. Also, from a different perspective, the difference between the two model types can be explained by use of different atmospheric parameters.

The same analysis was performed with RMSE (*Table 6*) to determine 'alignment' of the models compared to one another. With this analysis our purpose was to find possible reference values and evaluate error between models in this comparison.

Using *pan evaporation* measurement (Pan) as a standard Per and FAO56 models can be highlighted by their lowest RMSE values. Choosing *PMF56* to be the basis of comparison, the two variants of S&W show the best accordance, also because of belonging to the same type. As an alternative, we searched for the models that are closest to the *majority of methods* by selecting the lowest average RMSE. It is found that Per (0.7), Szász (0.73) and even P&T (0.78) showed considerably lower values than the rest of the models.

Table 6 Cross analysis of the Root-Mean-Square Error (RMSE) of modelled daily ET_0 data (2005–2010)

	Pan	Per	FAO56	B&C	Szász	Mak	P&T	WMO66	Mah	S&W	PMF56	S&W#2
Pan	–	0.34	0.20	1.31	0.94	1.36	0.94	1.06	1.16	1.11	1.14	1.17
Per	0.53	–	0.24	1.14	0.84	1.27	0.90	1.20	1.24	1.18	1.19	1.21
FAO56	0.28	0.21	–	1.27	0.91	1.33	0.91	1.18	1.26	1.19	1.20	1.24
B&C	1.23	0.69	0.88	–	0.45	0.65	0.61	1.08	1.06	0.80	0.77	0.95
Szász	1.36	0.79	0.97	0.69	–	0.57	0.50	1.26	1.30	1.01	0.90	1.13
Mak	1.28	0.77	0.93	0.66	0.37	–	0.37	1.20	1.24	0.86	0.70	1.02
P&T	1.31	0.82	0.95	0.92	0.49	0.55	–	1.30	1.40	1.05	0.88	1.18
WMO66	1.27	0.93	1.05	1.38	1.04	1.52	1.11	–	0.28	0.79	0.98	0.87
Mah	1.23	0.86	1.00	1.21	0.96	1.40	1.06	0.25	–	0.68	0.90	0.76
S&W	1.09	0.75	0.87	0.84	0.68	0.89	0.74	0.65	0.62	–	0.32	0.49
PMF56	1.12	0.76	0.88	0.81	0.61	0.73	0.62	0.81	0.83	0.32	–	0.51
S&W#2	1.15	0.77	0.90	1.00	0.76	1.07	0.82	0.72	0.70	0.49	0.50	–

n (number of cases) = 1284

Table 7. Descriptive statistics calculated for residues based on Pan and PMF56 (2005–2010)

ΔET_{0pan}

	Per	FAO56	B&C	Szász	Mak	P&T	WMO66	Mah	S&W	PMF56	S&W#2
Max.	0.00	0.00	5.21	3.44	4.91	3.20	4.68	5.20	6.44	6.21	7.15
Min.	–5.76	–4.00	–6.01	–7.76	–6.60	–7.39	–6.37	–6.16	–4.56	–4.33	–4.87
Avg. (MBE)	–1.42	–0.87	0.73	–0.56	0.43	–0.66	–1.17	–0.66	0.54	0.77	0.35
St.D.	0.88	0.61	1.34	1.38	1.40	1.33	1.27	1.26	1.14	1.17	1.21
Var.	0.77	0.38	1.79	1.89	1.95	1.76	1.62	1.58	1.30	1.37	1.46
R.	5.8	4.0	11.2	11.2	11.5	10.6	11.0	11.4	11.0	10.5	12.0

ΔET_{0PMF56}

	Pan	Per	FAO56	B&C	Szász	Mak	P&T	WMO66	Mah	S&W	S&W#2
Max.	4.33	2.07	2.88	3.20	0.24	1.24	0.35	3.19	4.45	1.91	3.68
Min.	–6.21	–8.96	–8.30	–3.90	–7.52	–4.35	–7.16	–4.42	–3.77	–2.27	–1.66
Avg. (MBE)	–0.77	–2.19	–1.65	–0.05	–1.33	–0.35	–1.43	–1.94	–1.43	–0.23	–0.42
St.D.	1.17	1.28	1.23	0.81	1.04	0.73	1.00	1.00	0.90	0.32	0.51
Var.	1.37	1.63	1.51	0.66	1.08	0.54	1.01	1.00	0.80	0.10	0.26
R.	10.5	11.0	11.2	7.1	7.8	5.6	7.5	7.6	8.2	4.2	5.3

Δ**ET_0**: residues compared to Pan and PMF56 daily output data, respectively; **Max.**: absolute maximum, **Min.**: absolute minimum, **Avg. (MBE)**: mean value, (i.e., systematic error, MBE – Mean Bias Error), all in mm day^{-1}; **St.D.**: standard deviation, **Var.**: variance, **R.**: total range

General descriptive statistics was performed for the residues (ΔET_0) specifically calculated based on the comparison outlined above, but only in relation to Pan and PMF56 *(Table 7)*. The smallest MBE, i.e. systematic error compared to the measured pan data was shown by Mak and the S&W#2 with modified radiation balance calculation. It is however the consequence of the fact that the differences having high standard deviation and variance compensate each other because of their inverse signs. Therefore, despite the less correlation, these models provided a relatively small MBE, which also implies a larger proportion of non-systematic error.

In comparison with the PMF56 model, the B&C and Mak models show the same features as the above, while S&W method provides a very similar result to the standard both in terms of its MBE and RMSE values. The real reason for this phenomenon is the similarity of the

principal bases of these two methods. The error of the mentioned methods thus presumed mostly non-systematic.

3.2 Sensitivity analysis

In *Figure 2a*, the impact of temperature on the models and the measured 'Pan' data set is shown. The curve of average change (ΔET_0) of all models runs together in the –60 – +40% range, divergence can be seen above or below this range only. At the same time, the correlation between the input and output data changes is nearly linear. Total range (R) of the changes follows a typical span in most models *(Figure 2b)*. Small differences can be seen in case of input change is in the negative range, mostly peaking near the mean, then starting to decrease again with higher differences between the models. Nevertheless, the different behaviour of mass-transfer-based algorithms can be seen in this case, too, the total range of the output change continuously extends in these models. The lowest deviation of the two temperature-based (B&C, Szász) and the radiation-based (Mak, P&T) models is worth mentioning, as the model response to the change of T is the most stable in these methods.

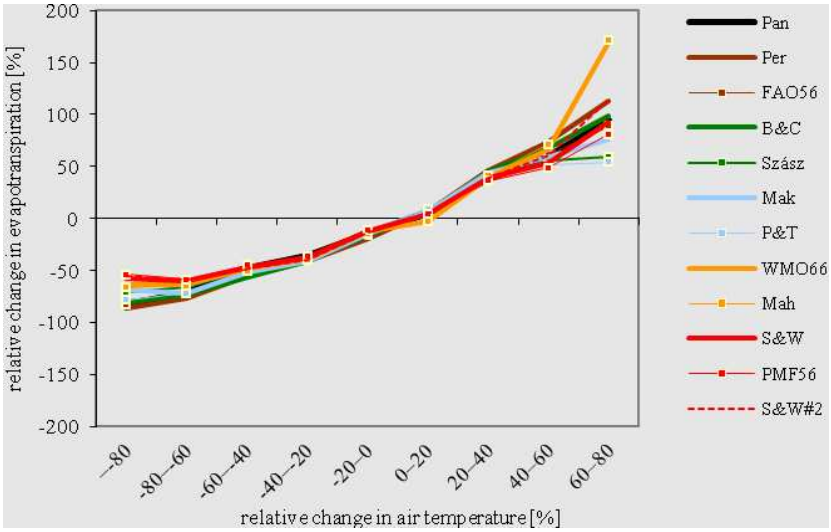

a)

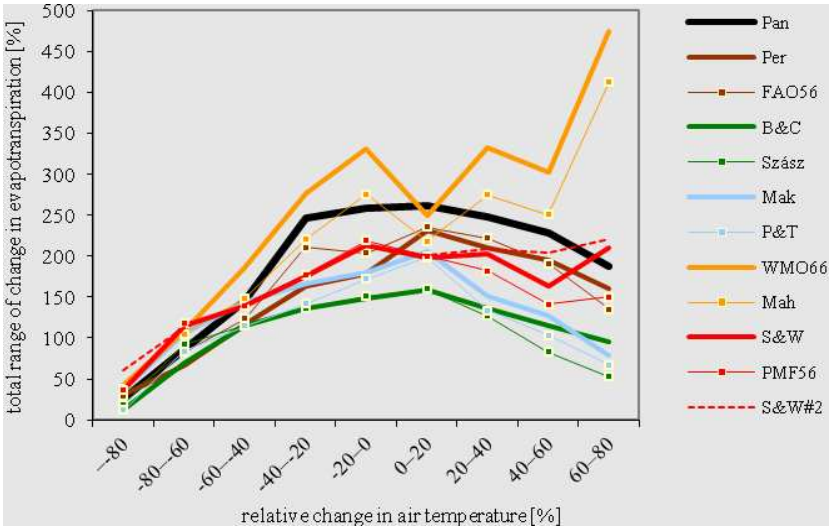

b)

In parameter changes 0% equals to 17.1 (lowest value: 1.3, highest value: 30.4) °C mean daily temperature.
Meanings of abbreviations are given in chapter 2.2

Figure 2a–b. Impact of the change of temperature on model outputs

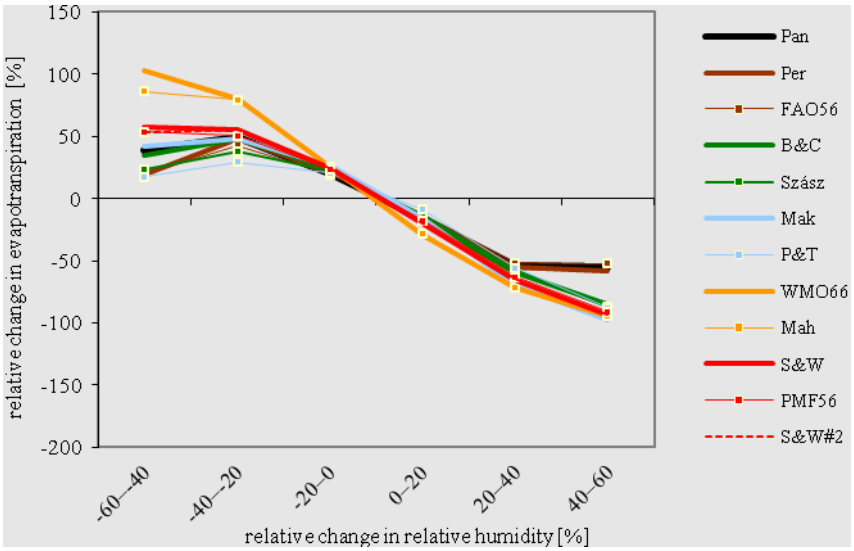

a)

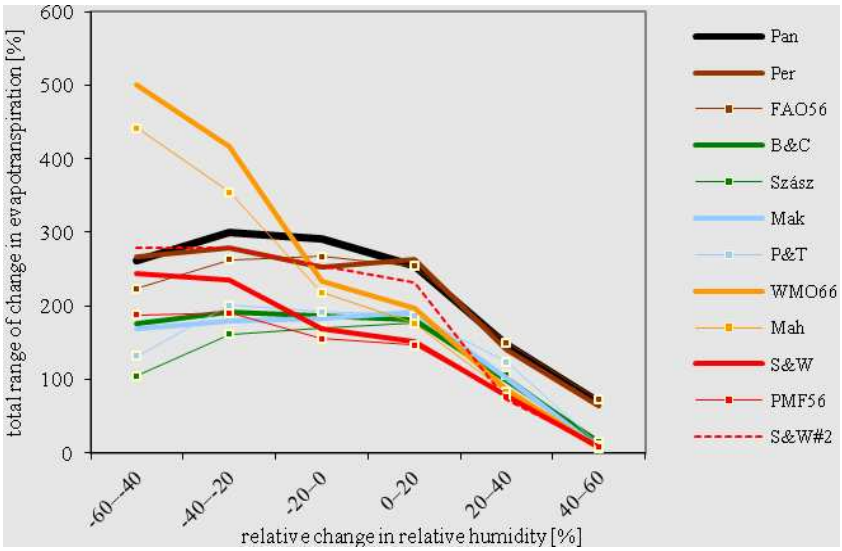

b)

In parameter changes 0% equals to 67.9 (lowest value: 30.7, highest value: 99.0) % mean daily rel. humidity. Meanings of abbreviations are given in chapter 2.2

Figure 3a–b. Impact of the change of relative humidity on model outputs

Figure 3a shows the results of the sensitivity analyses performed in relation to relative humidity. Due to the set of RH values, the curve shapes are inverted, results of the analysis were still similar to temperature. The reason for the similarities is that relative humidity depends on temperature; therefore, the two parameters are related. Nevertheless, the correlation between the change in air humidity and the output changes can be best described with a logistic trend. It is a further difference that the models start to diverge after a 20% reduction of the parameter value. Also, as regards to the total range (*Figure 3b)*, Szász, S&W, Mak and PMF56 models resulted in the lowest values. Mass-transfer-based models proved to be of different behaviour again: their total range of change in output was above at 200% at -20% RH differences and below.

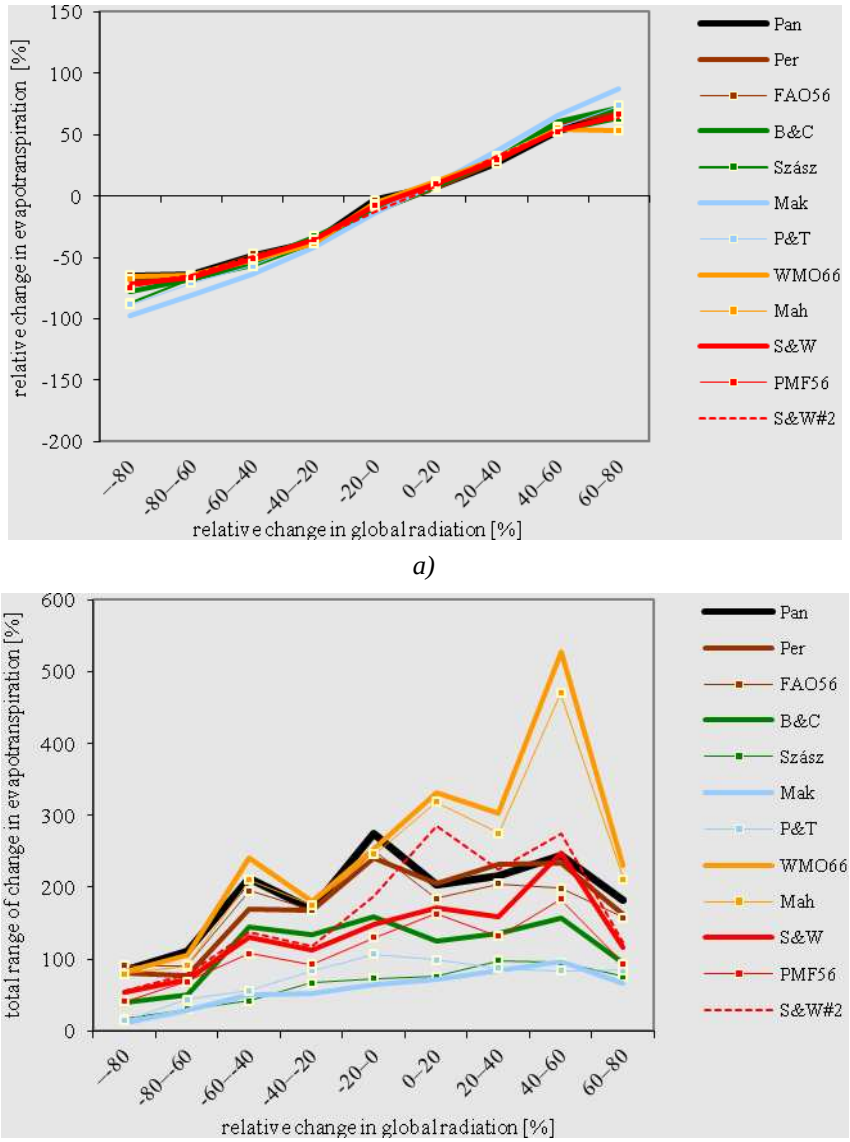

In parameter changes 0% equals to 17.1 (lowest value: 1.0, highest value: 30.3) MJ m^{-2} day^{-1} daily sum of global radiation. Meanings of abbreviations are given in chapter 2.2

Figure 4a–b. Impact of global radiation changes on the model outputs

The value of ET_0 estimated by the models linearly increases with the increase of global radiation (*Figure 4a*). Of the four meteorological parameters, it is the one where the correlation can be determined most clearly in relation to the models. The usual divergence can only be observed from around the ±80% levels. As regards the range of the output changes, mass-transfer-based models can be distinguished again, while the higher stability was observed in case of the Mak, Szász and P&T models. The benefits of using the latter model concerning the availability of the measured radiation data are also confirmed by other sources (Lu et al. 2005). The extent of total range is the lowest around the negative extreme value, above the mean value (17.1 MJ m^{-2} day^{-1}) it stagnates or slightly decreases at high uncertainty in the case of the majority of models (*Figure 4b*).

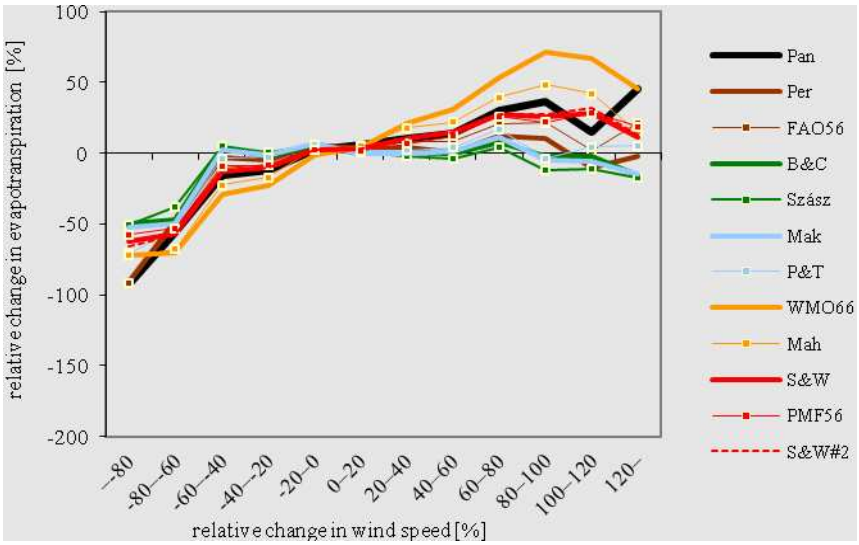

a)

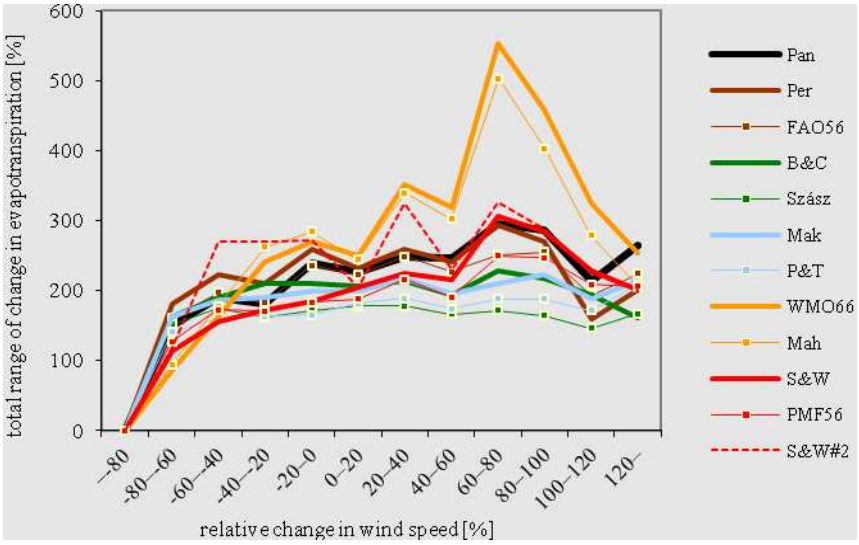

b)

In parameter changes 0% equals to 2.8 (lowest value: 0, highest value: 9.3) m s^{-1} mean daily wind speed. Meanings of abbreviations are given in chapter 2.2

Figure 5a–b. Impact of wind speed change on the model outputs

Figure 5a shows ET response to change in wind speed. As opposed to the other parameters, there is not even a temporary linear correlation between the change dynamics of the parameter and the output in relation to wind. In this case, the correlation type is presumably logarithmic. On days with wind speed below the average (0.5–2.8 m s^{-1}) the models provide results with rather close correlation. Approximately above the level of –50% wind speed change (1.4 m s^{-1} and above), the extent of estimated evaporation abruptly increases in each model. After reaching the average value, the extent of evaporation keeps its level. It peaks mostly between 80–100% increases of wind speed (5.1–5.7 m s^{-1}), although 5 models do not show any increase notable. These models (Szász, P&T, B&C, Mak, Per) appear to be insensitive to any further stiffening of wind, as opposed to mass-transfer-based models. As regards the total range of the deviation (*Figure 5b)*, the same models are the steadiest (except for the Pereira model); thereby further strengthening their 'conservative' classification.

4 CONCLUSIONS

Based on monthly and yearly amounts of estimated ET_0, it was concluded that evaluation on the basis of seasonal sums is very sensitive to systematic differences between daily model results. Differences of the order of even several hundred millimetres can evolve during a growing season. Nevertheless, the highest sums were provided by the Blaney–Criddle, Penman–Monteith–FAO-56, Shuttleworth–Wallace and Makkink methods, while the lowest amounts were provided by the Pereira, FAO-56, WMO-1966 and Mahringer models.

On the basis of seasonal dynamics of the model outputs, the distinct behaviour of mass-transfer-based models (WMO-1966, Mahringer) and the sensitivity of pan-coefficient models (Pereira, FAO-56), temperature-based (Szász), and radiation-based models (Makkink and Priestley–Taylor) to the precipitation amounts could be detected.

Large fluctuation models with high R and St.D. values (Pan, B&C, mass-transfer based and combination-type methods) and 'steady' ones (pan coefficient-based, Szász and P&T methods) with less variability of outputs were identified. Furthermore, mass-transfer-based methods showed wide standard deviation and total range of the output data even in the case of relatively low ET_0 levels.

Based on the correlations between the model results, Pereira and FAO-56 models agreed the most to the pan evaporation measurements, while Shuttleworth-Wallace model showed the most similarity to the Penman–Monteith–FAO-56 method. As regards the systematic error, Makkink and Shuttleworth–Wallace model were the closest to pan evaporation, while Shuttleworth–Wallace, Blaney–Criddle and Makkink models were the closest to the Penman–Monteith method.

With the sensitivity analyses, two main groups were defined: the Szász, Makkink, Priestley–Taylor and Penman–Monteith–FAO-56 models can be considered steady, i.e. these methods responded with lower fluctuations to the changes of atmospheric variables. At the same time, WMO-1966, Mahringer, Shuttleworth–Wallace methods, the pan evaporation measurements and Pereira model are rather sensitive. These showed large magnitude and high range of changes in ET_0 as a response to the increase or decrease of the four main atmospheric inputs (temperature, air humidity, global radiation and wind).

In the light of these conclusions, Priestley–Taylor, Penman–Monteith–FAO-56, Shuttleworth–Wallace parameterized with alternative radiation balance, Szász and Makkink methods were found to be the best performing models for ET calculation. In order to perform properly accurate estimations, however, it is necessary to carry out further parameterization of each model in accordance with local circumstances.

Acknowledgements: Authors gratefully acknowledge the Hungarian Meteorological Service for making the meteorological datasets from Debrecen-Airport station available. Furthermore, research has been supported by TECH-08 „Improving quality production and yield safety with modern water management and irrigation", FP-7-2010-1 REGPOT „Improving research potential of the Institution for Land Utilization, Technology and Regional Development on the field of GIS, precision agriculture, land use and regional development" and the funds from TÁMOP-4.2.2/B-10/1-2010-0024 projects.

REFERENCES

ADEBOYE, O. B. – OSUNBITAN J. A. – ADEKALU K. O. – OKUNADE D. A. (2009): Evaluation of FAO-56 Penman-Monteith and Temperature Based Models in Estimating Reference Evapotranspiration Using Complete and Limited Data, Application to Nigeria. Agricultural Engineering International: CIGR Journal. 11:1–25.

ALLEN, R.G. – PEREIRA, L.S. – RAES, D. – SMITH, M. (1998): Crop evapotranspiration. Guidelines for computing crop water requirements. FAO Irrigation and Drainage. Paper No. 56. FAO, Rome

BLANEY, H.F. – CRIDDLE, W.D. (1950): Determining water requirements in irrigated areas from climatological and irrigation data. Soil conservation service technical paper 96. Soil conservation service. US. Department of Agriculture, Washington

BOIS, B. – PIERI, P. – VAN LEEUWEN, C. – GAUDILLÉRE, J.P. (2005): XIV International GESCO Viticulture Congress, Geisenheim, Germany, 23–27 August, 2005 2005. 187–193

BURMAN, R. – POCHOP, L.O. (1994): Evaporation, evapotranspiration and climatic data. Developments in Atmospheric Science, 22. Elsevier, Amsterdam

DOORENBOS, J. – PRUITT, W.O. (1977a): Crop water requirements. FAO Irrigation and Drainage. Paper No.24. (rev.) FAO, Rome

DOORENBOS, J. – PRUITT, W.O. (1977b): Guidelines for predicting crop water requirements. FAO, UN, Irrigation and Drainage. Paper No.24. (2nd Ed.) FAO, Rome

ER-RAKI, S. – CHEHBOUNI, A. – KHABBA, S. – SIMONNEAUX, V. – JARLAN, L. – OULDBBA, A. – RODRIGUEZ, J.C. – ALLEN, R. (2010): Assessment of reference evapotranspiration methods in semi-arid regions: Can weather forecast data be used as alternate of ground meteorological parameters? Journal of Arid Environments, Vol. 74. 1587–1596.

FAO (Food and Agriculture Organization) (1996): Guidelines: Agro-ecological zoning. FAO Soils Bulletin 73. Rome, FAO

FEDERER, C.A., C. VÖRÖSMARTY, AND B. FEKETE, (1996): Intercomparison of Methods for Calculating Potential Evaporation in Regional and Global Water Balance Models. Water Resources Research. 32 (7): 2315–2321.

JENSEN, M.E. – BURMAN, R.D. – ALLEN, R.G. (1990): Evapotranspiration and Irrigation Water Requirements. ASCE Manuals and Reports on Engineering Practice. No. 70.

LIETH, H. (1975): Modeling the primary productivity of the world. In: LIETH, H. – WHITTAKER, R. H. (eds.): Primary productivity of the biosphere. Ecological studies; Vol. 14. Springer – Verlag New York. 237–263.

LIM, W.H. – RODERICK, M.L. – HOBBINS, M.T. – WONG, S.C. – GROENEVELD, P.J. – SUN, F. FARQUHAR, G.D. (2011): The aerodynamics of pan evaporation. Agricultural and Forest Meteorology. Vol. 152. (2012) 31–43.

LU, J. – SUN, G. – MC NULTY, S.G. – AMATYA, D.M. (2005) A comparison of six potential evapotranspiration methods for regional use in the south-eastern United States. Journal of the American Water Resources Association. Vol. 41 (3). 621–633.

MAHRINGER, W. (1970): Verdunstungsstudien am Neusiedler See. Theoretical and Applied Climatology. 18. (1): 1–20.

MAKKINK, G.F. (1957): Testing the Penman formula by means of lysimeters. Journal of the Institution of Water Engineers and Scientists. Vol. 11. 277–288.

MCMAHON, T. A. – PEEL, M. C. – LOWE, L. – SRIKANTHAN, R. – MCVICAR, T. R. (2012): Estimating actual, potential, reference crop and pan evaporation using standard meteorological data: a pragmatic synthesis Hydrology and Earth System Sciences Discuss., 9, 11829–11910.

MCNAUGHTON, K. G. – JARVIS, P. G. (1983): Predicting effects of vegetation changes on transpiration and evaporation. In: Kozlowski, T. T. (Ed.) Water Deficits and Plant Growth, vol. VII. Academic Press, pp. 1–47.

PEREIRA, A.R. – VILLANOVA, N. – PEREIRA, A.S. – BAEBIERI, V.A. (1995): A model for the class-A pan coefficient. Agricultural Water Management. 76 : 75–82.

PRIESTLEY, C.H.B. – TAYLOR, R.J. (1972): On the assessment of surface heat flux and evaporation using large scale parameters. Monthly Weather Reviews. 100: 81–92.

RAO, G. G. S. N – RAJPUT, R. K. (1992): Evapotranspiration estimates for crop water requirements under different agro-climatic conditions in India In: Proceedings of the International Commission on Irrigation and Drainage 16th European Regional Conference Vol 2. Ecological, Technical and Social-Economical Impacts on Agricultural Water Management Budapest, Hungary, June 21–27. 1992. 277–288.

SCHNEIDER, K. – KETZER, B. – BREUER, L. – VACHÉ, K. B. – BERNHOFER, C. – FREDE, H.-G. (2007): Evaluation of evapotranspiration methods for model validation in a semi-arid watershed in northern China Advances in Geosciences 11, 37–42.

SHUTTLEWORTH, W.J. – WALLACE, J.S. (1985): Evaporation from sparse canopy: an energy combination theory. Quarterly Journal of Met. Soc. 111: 839–855.

SUMNER, D.M. – JACOBS, J.M. (2005): Utility of Penman–Monteith, Priestley–Taylor, reference evapotranspiration, and pan evaporation methods to estimate pasture evapotranspiration. Journal of Hydrology. Vol. 308. (2005): 81–104.

SZÁSZ, G. (1973): A potenciális párolgás meghatározásának új módszere. [New method for calculating potential evapotranspiration] Hidrológiai Közlöny. 435–442. (in Hungarian)

TABARI, – H. GRISMER, M.E. – TRAJKOVIC, S. (2005): Comparative analysis of 31 reference evapotranspiration methods under humid conditions. Irrigation Science Vol. 23 (4). 1–11.

TANNER, B.C. (1968): Evaporation of water from plants and soil. In: KOZLOWSKI, T.T. (ed.): Water deficits and plant growth. Academic Press, Vol.1. Development, Control and Measurement, New York. 73–106.

WMO (1966): Measurement and estimation of evaporation and evapotranspiration. Technical Paper (CIMO-Rep.) No. 83. Genf

YATES, D. – STRZEPEK, K. (1994): Potential evapotranspiration methods and their impact on the assessment of river basin runoff under climate change. International Institute of Applied Systems Analysis Working Papers 94–46. 28.

YODER, R. E. – ODHIAMBO, L. O. – WRIGHT, W. C. (2005): Evaluation of methods for estimating daily reference crop evapotranspiration at a site in humid Southeast United States Applied Engineering in Agriculture 21(2): 197−202.

ZHOU, M. (2011). Estimates of Evapotranspiration and Their Implication in the Mekong and Yellow River Basins, Evapotranspiration, Leszek Labedzki (Ed.), ISBN: 978-953-307-251-7, InTech, DOI: 10.5772/14791.

DE GRUYTER OPEN DOI: 10.2478/aslh-2013-0002 Acta Silv. Lign. Hung., Vol. 9 (2013) 25–33

Dehydrogenase Activity in a Litter Manipulation Experiment in Temperate Forest Soil

Zsuzsa VERES* – Zsolt KOTROCZÓ – Kornél MAGYAROS – János Attila TÓTH – Béla TÓTHMÉRÉSZ

Department of Ecology, University of Debrecen, Debrecen, Hungary

Abstract – Soil enzyme activities are "sensors" of soil organic matter (SOM) decomposition since they integrate information about microbial status and physico-chemical condition of soils. We measured dehydrogenase enzyme activity in a deciduous temperate oak forest in Hungary under litter manipulation treatments. The Síkfőkút Detritus Input and Removal Treatments (DIRT) Project includes treatments with doubling of leaf litter and woody debris inputs as well as removal of leaf litter and trenching to prevent root inputs. We hypothesized that increased detrital inputs increase labile carbon substrates to soils and would increase enzyme activities particularly that of dehydrogenase, which has been used as an indicator of soil microbial activity. We also hypothesized that enzyme activities would decrease with detritus removal plots and decrease labile carbon inputs to soil. After ten years of treatments, litter removal had a stronger effect on soil dehydrogenase activity than did litter additions. These results showed that in this forest ecosystem the changed litter production affected soil microbial activity: reduced litter production decreased the soil dehydrogenase activity; increased litter production had no significant effect on the enzyme activity.

oak forest / dehydrogenase activity / Síkfőkút Project / litter input / litter removal / soil enzymes

Kivonat – Az avar mennyiségének hatása egy cseres-tölgyes erdő talajában a dehidrogenáz enzim aktivitására. A talajenzimek a talajban lévő szerves anyag (SOM) bomlásának "szenzorai", mivel információt adnak a talaj mikrobiológiai és fizikai-kémiai állapotáról. Egy magyarországi mérsékelt övi tölgyerdőben mértük a dehidrogenáz enzim aktivitását az avar mennyiségének csökkentésével és növelésével. A Síkfőkút DIRT Projectben (Detritus Input and Removal Treatments) az alábbi kezeléseket alkalmaztuk: dupla mennyiségű levél avar, dupla mennyiségű ágavar, valamint levél és gyökér megvonásos kezelések, ahol a gyökereknek a parcellákra történő benövését akadályozzuk meg. Azt feltételeztük, hogy a megnövelt avar input hatására megnövekszik a talajban a labilis, azaz a könnyen bontható szén szubsztrátok mennyisége és az enzimek aktivitása. Különösen a dehidrogenáz enzim aktivitásának változását vártuk, ami az egyik legáltalánosabban használt mutató a talaj mikrobiális aktivitásának mérésére. Továbbá azt feltételeztük, hogy a talaj enzim aktivitása csökkenni fog az avarmegvonásos kezelésekben, a labilis szén szubsztrátok mennyiségének csökkenésével. Eredményeink azt mutatják, hogy tíz év elteltével az avar produkció csökkenése ebben az erdei ökoszisztémában a talaj dehidrogenáz enzim aktivitásának csökkenését okozta, ugyanakkor az avarprodukció növekedése nem okozott szignifikáns változást az enzim aktivitásában

tölgyerdő / dehidrogenáz aktivitás / Síkfőkút Project / avarmennyiség megduplázása / avarmegvonás / talajenzimek

* Corresponding author: veres.zsu@gmail.com; H-4032 DEBRECEN, Egyetem tér 1.

1 INTRODUCTION

Soil enzyme activities are “sensors” of soil organic matter (SOM) decomposition since they integrate information about microbial status and physico-chemical condition of soils (Aon – Colaneri 2001, Baum et al. 2003). All soils contain a group of enzymes that determine soil metabolic processes (McLaren 1975) which, in turn, depend on its physical, chemical, microbiological and biochemical properties (Makoi and Ndakidemi 2008). Enzymatic processes are closely related to soil quality, they participate in the processing of unavailable forms of nutrients readily assimilated by plants (Sinsabaugh et al. 1994).

Soil dehydrogenase enzymes (DHA) (EC 1.1.1.1) are one of the main components of soil enzymatic activities participating in and assuring the correct sequence of all the biochemical routes in soil biogeochemical cycles (Ladd 1985). Determination of DHA in soil gives large amount of information about biological characteristic of the soil (Wolińska – Stępniewska 2012). Dehydrogenase enzyme is often used as a measure of any disruption caused by pesticides, trace elements or management practices to the soil, as well as a direct measure of soil microbial activity (Chendrayan et al. 1979; Trevors et al. 1982; McCarthy et al. 1994). Soil DHA is considered to exist in soils as integral parts of intact cells (Taylor et al. 2002). Dehydrogenase enzyme is known to oxidize soil organic matter by transferring protons and electrons from substrates to acceptors (Makoi – Ndakidemi 2008). These processes are part of respiration pathways of soil micro-organisms and are closely related to the type of soil and soil air-water conditions (Kandeler et al. 1996). Several environmental factors, including soil moisture, oxygen availability, oxidation reduction potential, pH, organic matter content, depth of the soil profile, temperature, season of the year, heavy metal contamination and soil fertilization or pesticide use can affect significantly DHA in the soil environment (Dkhar – Mishra 1983; Baruah – Mishra 1984; Sinsabaugh et al. 2008; Xiang et al. 2008; Wolińska – Stępniewska 2012; Kumar et al. 2013).

We measured DHA in a deciduous temperate oak forest in Hungary under litter manipulation treatments. Our research in the Síkfőkút DIRT Project (SIK) constitutes an important part of an international long term project which involves five experimental sites in the USA (H.J. Andrews Experimental Forest, Bousson Experimental Forest, Harvard Forest, University of Michigan Biological Station, Santa Rita) (Nadelhoffer et al. 2004) and one in Germany (Universität Bayreuth BITÖK). We hypothesized that increased detrital inputs would provide increased labile carbon substrates to soils and increase dehydrogenase activities, which is used as indicator of soil microbial activity (Thalmann 1968a; Chendrayan et al. 1979; Nannipieri et al. 2002). We also hypothesized that dehydrogenase activities would decrease in detritus removal plots with decreases in labile carbon inputs to soil.

2 METHODS

2.1 Area and project descriptions

The Síkfőkút Project was established in 1972 for the long-term study of forest ecosystems. It is located in the south part of the Bükk Mountains in North-Eastern Hungary N 47°55’ E 20°46’ at 325 m altitude. This forest has been protected since 1976, and it is part of the Bükk National Park. Mean annual temperature (MAT) is 10°C and Mean Annual Precipitation (MAP) is 550 mm (Antal et al. 1997). Soil pH ranged between 4.85 and 5.50 depending on the plots (Tóth et al. 2007). Both soil pH and humus content was lower in detritus removal treatments. Humus content ranged between 2.66% and 3.14% (Varga et al. 2008). In the control plots the carbon content was 5.19% (0–5 cm), and 3.25% (5–15 cm) (Tóth et al. 2011). According to the FAO Soil Classification, the soil is a Cambisols. This

forest is a semi-natural stand (Quercetum petraeae-cerris community) without forest management activity (Jakucs 1985; Kotroczó et al. 2012). The Síkfőkút Project is a member site of the Hungarian LTER Network (Long Term Ecological Research) and the ILTER Network (International Long Term Ecological Research) from 1995 (Kovács-Láng et al. 2000).

Six treatments were established at the Síkfőkút DIRT experimental site in the autumn of 2000 each in three replicates on 7 × 7 m (49 m2) plots. Detritus was not manipulated in the Control plots (CO). There were normal litter inputs in the CO plots. The average leaf-litter production was 3547 kg $ha^{-1}year^{-1}$ between 2003 and 2010 (Kotroczó et al. 2012). There were two types of detritus additions: double the normal amount of leaf litter was applied to the Double Litter (DL) plots by adding leaf litter removed from NL plots; while in the Double Wood plots (DW) the amount of wood detritus (branches, twigs and bark) was doubled. Annual wood litter amount was measured by boxes placed to the site and its double amount was applied in the case of every DW plots (average 17 kg $year^{-1}$). In three treatments of detritus removal were also applied: aboveground detritus removed by rake in the No Litter plots (NL), living roots severed by trenching in the No Roots plots (NR), and both NL and NR treatments in No Inputs plots (NI). The NR and NI plots were trenched around 40 cm wide and 100 cm deep. The soil dug out was placed outside the plot. Root-proof Delta MS 500 PE foil was put in the trenches, which was 0.6 mm thick and 1 m wide. Then the trenches were filled with soil. Plants were cleared to eliminate root production (bushes were cut out at the establishment). Weeds were also controlled by Medalon (agent: 480 g l^{-1} glifosate-ammonium) and dry plant residues were raked. The detailed description of the treatments is in Nadelhoffer et al. (2004), Sulzman et al. (2005), Kotroczó et al. (2008). These processes were replayed every year.

2.2 Soil sampling and measuring of dehydrogenase enzyme activity

Soil samples were collected 11 times from February 2010 to November 2012. Five cores were taken from each plot 15 cm depth with a 2 cm diameter Oakfield soil corer (Oakfield Apparatus Company, USA). Three analytical replicates per sample per assay were used. The samples were homogenized and stored for one week at 4°C.

DHA was determined using the reduction of 2.3.5-triphenyltetrazolium chloride (TTC) method (Thalmann 1968b). Samples of 2 g field-moist soils were mixed with 2 ml 1.5% TTC thoroughly into test tubes. The samples were mixed on a vortex and incubated at 30°C. The control contains only 2 ml Tris buffer (without TTC). After 24 h, the triphenyl formazan, a product from the reduction of TTC, was extracted by adding 10 ml ethanol to each tube and shaken for 1 min. Samples were further incubated at room temperature for 2 h in the dark (shaking the tubes at intervals). The soil suspensions (12 ml) were then filtered and the optical density of the clear supernatant was measured against the blank (ethanol) at 546 nm (red color) at Genesys 10 spectrophotometer. A standard curve was plotted using a range of triphenyl formazan (TPF) (Reanal, Budapest, Hungary) concentrations between 0 and 40 µg TPF ml^{-1}. DHA was expressed as µg TPF g^{-1} dry soil 24 h^{-1}.

Soil moisture content was measured by TDR 300 (Time Domain Reflectometer) instrument in the field in volumetric water content per cent (vwc%). There were two measurements at each plot at the time of soil sampling to determine DHA. Soil temperature was measured by an ONSET, StowAway TidbiT-type data-logger (Onset Computer Corporation, USA), in the middle of each plot at 10 cm depth. Data-loggers were programmed to measure soil temperature every hour; daily mean of the soil temperature values was used in the paper.

2.3 Statistical analyzes

We used one-way ANOVA to determine significant treatment effects; significant mean differences were evaluated at the level of p=0.05 using Tukey's test.

3 RESULTS AND DISCUSSION

We started to measure soil DHA in 2010, ten years after the establishment of treatments. In general, activities were lower in removal treatments (NL, NR, NI) than the control (CO) or addition treatments (DL, DW). Our data show that the dehydrogenase activity is fairly stable in the control plots compared to the treated plots (*Figure 1*). There is a temporal trend in dehydrogenase activity; the effect of detritus removal is increased.

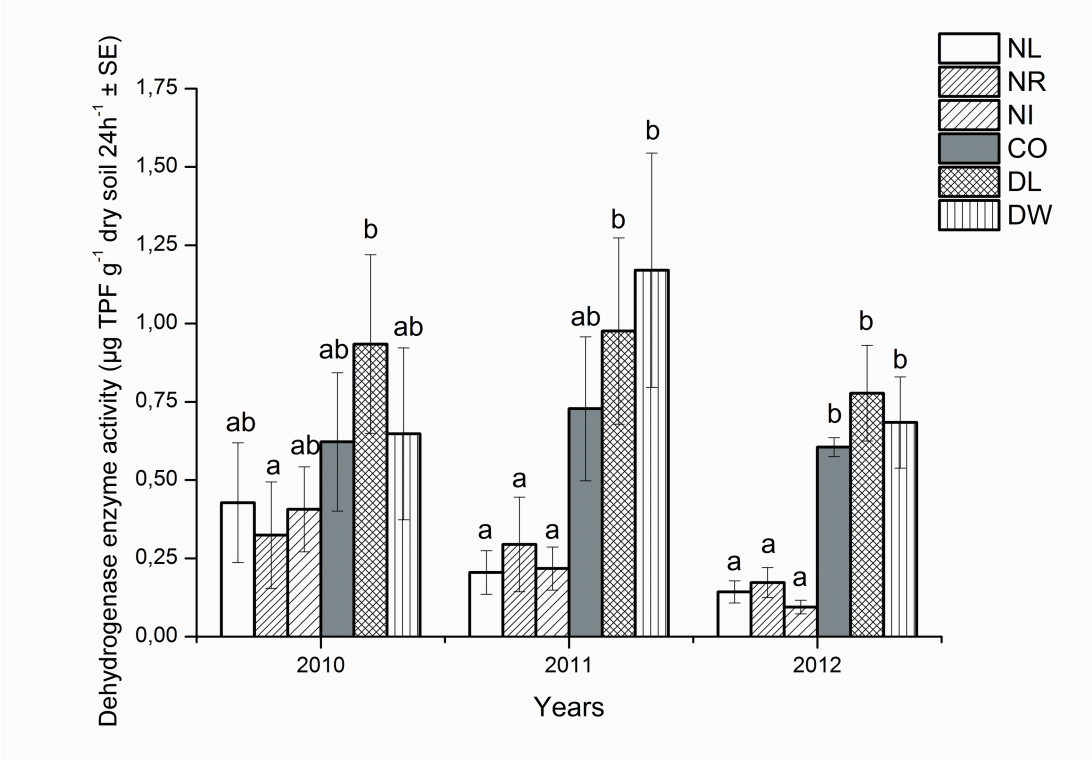

Figure 1. Soil dehydrogenase enzyme activity among treatments between 2010 and 2012 (µg TPF g^{-1} dry soil $24h^{-1}$ ± SE). Different letters denote significant treatment differences within each year (p<0.05, ANOVA and Tukey's test).

DHA were significant lower in NR than in DL treatments in 2010 (p=0.029). In 2011 there were higher significant differences in dehydrogenase activity among treatments, enzyme activity was higher in DL and DW treatments than in all removal plots (p<0.001). In 2012 litter removal treatments differed significantly not only to DL and DW treatments but also controls (p<0.001) (*Figure 1*). The enzyme activities were higher in DL and DW treatments than controls, but not significantly. In contrast to our initial hypothesis, dehydrogenase activities did not increase significantly with either leaf litter or wood additions. This is generally in agreement with our earlier results for litter decomposition (Fekete et al. 2007), soil respiration (Kotroczó et al. 2008), arylsulphatase and saccharase activities (Fekete et al. 2011). At the other DIRT site in H.J. Andrews Experimental Forest (HJA) in Oregon, Brant et al. (2006a) showed that, soil from the doubled wood treatment had a higher fungal:bacterial ratio, and soil from the no inputs treatment had a lower fungal:bacterial ratio, than the control soil. These changes were the result of alteration in the size and composition of the microbial

community. Brant et al. (2006b) reported microbial biomass values at three DIRT sites: HJA, SIK and BOU (Bousson Experimental Forest in Pennsylvania). They found significant differences in biomass between treatments at SIK. At that site DW plots had a larger biomass than the NR plots and suggestive evidence that the DW plots had a larger biomass than the NI plots. Błońska et al. (2013) report that, DHA is increasing with the diversity of plant communities; this suggest that there is a relationship between the composition of soil organic matter and microbial enzymatic activity. Mamatha et al. (2001) studying soil from red sandy loam areas show that, the DHA is higher in soil covered by plants and in the rhizosphere than non-rhizosphere.

Table 1. Mean values and standard errors of dehydrogenase activity, soil moisture content and soil temperature in terms of the treatments. (Soil moisture and temperature values are the mean values of the days of the measurements). Significant differences in dehydrogenase activity between treatments showed in Figure 1 ($p<0.05$, ANOVA and Tukey's test).

Treatments	Dehydrogenase activity (μg TPF g^{-1} dry soil $24h^{-1}\pm$ SE)	Soil moisture (vwc% ± SE)	Soil temperature (°C)
2010			
NL	0.43±0.12	34.07±1.95	8.29±4.09
NR	0.32±0.12	41.00±2.01	9.63±4.20
NI	0.41±0.10	38.36±2.02	9.46±4.26
CO	0.62±0.12	34.84±2.63	8.92±3.86
DL	0.93±0.17	34.38±2.56	9.28±3.64
DW	0.65±0.17	35.07±2.99	9.60±4.14
	p=0.029	p>0.05	p>0.05
2011			
NL	0.20±0.08	18.82±3.39	17.69±3.21
NR	0.29±0.11	25.89±4.84	17.93±3.22
NI	0.22±0.08	21.68±4.44	18.02±3.30
CO	0.73±0.13	20.88±4.44	17.86±3.20
DL	0.98±0.20	21.87±4.41	17.13±2.96
DW	1.17±0.23	21.30±4.62	18.07±3.27
	p<0.001	p>0.05	p>0.05
2012			
NL	0.14±0.03	19.93±3.22	12.50±5.68
NR	0.17±0.03	20.66±3.59	12.46±5.75
NI	0.09±0.03	21.32±3.87	12.52±5.76
CO	0.60±0.06	16.18±2.51	12.47±5.76
DL	0.78±0.10	17.36±2.67	12.87±5.34
DW	0.68±0.10	18.26±3.12	12.58±5.75
	p<0.001	p>0.05	p>0.05

We measured the soil moisture and soil temperature at the days when soil sampling was made to determine DHA. We did not find significant treatment differences within each year in soil moisture and in soil temperature (*Table 1*). The soil moisture values were the highest in 2010 (*Figure 2*); this year was extremely rainy. Contrarily, years 2011 and 2012 were dry and warm; instead of that the DHA showed same values in the CO plots than in 2010. In the

removal plots DHA decreased in 2011 and 2012. Probably the higher soil moisture caused the higher DHA in 2010. However, we did not find correlation between soil moisture and DHA in years 2010, 2011 and 2012. Kumar et al. (2013) showed significant correlation between DHA and soil moisture. Other authors also attributed the increase in microbial activity in forest soil to higher soil moisture (Görres et al. 1998). Fekete et al. (2011) also found correlation between soil moisture and enzyme activities (arylsulphatase and saccharase) in Síkfőkút between 2004 and 2006. Our results suggest that, changes in soil organic matter content had higher effect on DHA than soil moisture. In other studies also found that more organic matter maintained larger and more active microbial biomass and higher DHA (Chodak et al. 2010; Bonanomi et al. 2011).

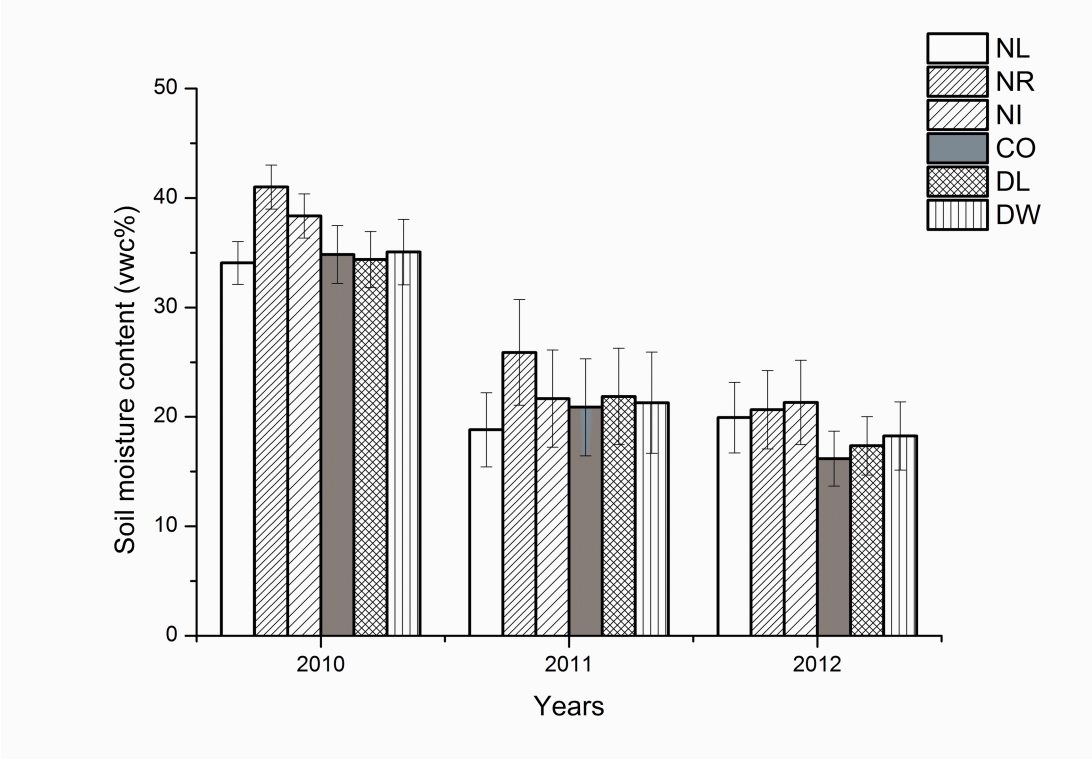

Figure 2. Soil moisture content (vwc%) among treatments between 2010 and 2012.

After ten years of treatments, litter removal had a stronger effect through time on soil dehydrogenase activities than did increase litter inputs. Ectomycorrhizal fungi associated with roots of trees in deciduous forests produce enzymes and thus can increase the surrounding soil enzyme activities (Colpaert – van Laere 2006; Smith – Read 2008). These fungi are responsible for the mobilization of essential plant nutrients by decomposing litter and soil organic materials (Courty et al. 2006). Decomposition of severed roots (NR and NI) would result in the disappearance of mycorrhizal fungi and rhizosphere microbes, causing a considerable reduction in microbial and enzyme activities (Fekete et al. 2011).

4 CONCLUSION

Our findings showed that the changes of litter production significantly affected soil microbial activity, and by extension general nutrient cycling and SOM dynamics in this forest ecosystem. When the litter production decreased, soil dehydrogenase activity also decreased. Increased litter production caused no significant increase in enzyme activity. After ten years of treatments, loss of inputs had a greater impact than increased inputs.

Acknowledgments: We thank Csabáné Koncz for long hours of field and laboratory work. Special thanks are due to Dr. Kate Lajtha and Bruce Caldwell (Oregon State University, Corvallis, USA) and Dr. Kristin Vanderbilt (University of New Mexico, Albuquerque, USA) for their substantial contribution in establishing the experiment. This research was supported by the European Union and the State of Hungary, co-financed by the European Social Fund in the framework of TÁMOP 4.2.4. A/2-11-1-2012-0001 'National Excellence Program'. The work was supported by TÁMOP 4.2.1./B-09/1/KONV-2010-0007, TÁMOP-4.2.2_B-10_1-2010-0024 and TÁMOP-4.2.2.C-11/1/KONV-2012-0010 projects. The TÁMOP projects are implemented through the New Hungary Development Plan, co-financed by the European Social Fund and the European Regional Development Fund.

REFERENCES

ANTAL, E. – BERKI, I. – JUSTYÁK, J. – KISS, GY. – TARR, K. – VIG, P. (1997): A síkfőkúti erdőtársulás hő- és vízháztartási viszonyainak vizsgálata az erdőpusztulás és az éghajlatváltozás tükrében, Debrecen. pp 83. (in Hungarian).

AON, M. A. – COLANER, A. C. (2001): Temporal and spatial evolution of enzymatic activities and physico-chemical properties in an agricultural soil. Applied Soil Ecology 18: 255–270.

BARUAH, M. – MISHRA, R. R. (1984): Dehydrogenase and urease activities in rice field soils. Soil Biology and Biochemistry 16: 423–424.

BAUM, C. – LEINWEBER, P. – SCHLICHTING, A. (2003): Effects of chemical conditions in re-wetted peats temporal variation in microbial biomass and acid phosphatase activity within the growing season. Applied Soil Ecology 22: 167–174.

BŁOŃSKA, E. – LASOTA, J. – JANUSZEK, K. (2013): Variability of enzymatic activity in forest Cambisols and Brunic Arenosols of Polish lowland areas. Soil Science Annual 64: 54–59.

BONANOMIA, G. – D'ASCOLIC, R. – ANTIGNANIA, V. – CAPODILUPOA, M. – COZZOLINOA, L. – MARZAIOLIC, R. – PUOPOLOA, G. – RUTIGLIANOC, F. A. – SCELZAB, R. – SCOTTI, R. – RAOB, M. A. – ZOINAA, A. (2011): Assessing soil quality under intensive cultivation and tree orchards in Southern Italy. Applied Soil Ecology 47: 184–194.

BRANT, J. B. – MYROLD, D. D. – SULZMAN, E. W. (2006b): Root controls on soil microbial community structure in forest soils. Oecologia 148: 650–659.

BRANT, J. B. – SULZMAN, E. W. – MYROLD, D. D. (2006a): Microbial community utilization of added carbon substrates in response to long-term carbon input manipulation. Soil Biology and Biochemistry 38: 2219–2232.

CHENDRAYAN, K. – AHLYA, T. K. – SETHUNATHAN, N. (1979): Dehydrogenase and invertase activities of flooded soils. Soil Biology and Biochemistry 12: 217–273.

CHODAK, M. – NIKLINSKA, M. (2010): Effect of texture and tree species on microbial properties of mine soils. Applied Soil Ecology 46: 268–275.

COLPAERT, J. V. – VAN LAERE, A. (2006): A comparison of the extracellular enzyme activities of two ectomycorrhizal and a leaf-saprotrophic basidiomycete colonizing beech leaf litter. New Phytologist 134: 133–141.

COURTY, P. E. – POUYSEGUR, R. – BUÉE, M. – GARBAYE, J. (2006): Laccase and phosphatase activities of the dominant ectomycorrhizal types in a lowland oak forest. Soil Biology and Biochemistry 38: 1219–1222.

DKHAR, M. S. – MISHRA, R. R. (1983): Dehydrogenase and urease activities of maize (Zea mays L.) filed crops. Plant and Soil 70: 327–333.

FEKETE, I. – VARGA, CS. – KOTROCZÓ, ZS. – KRAKOMPERGER, ZS. – TÓTH, J. A. (2007): The effect of temperature and moisture on enzyme activity in Síkfőkút Site. Cereal Research Communication 35: 381–385.

FEKETE, I. – VARGA, CS. – KOTROCZÓ, ZS. – TÓTH, J. A. – VÁRBIRÓ, G. (2011): The relation between various detritus inputs and soil enzyme activities in a Central European deciduous forest. Geoderma 167–168: 15–21.

GÖRRES, J. H. – DICHIARO, M. J. – LYONS, J. B. – AMADOR, J. A. (1998): Spatial and temporal patterns of soil biological activity in a forest and an old field. Soil Biology and Biochemistry 30: 219–230.

JAKUCS, P (ed.) (1985): Ecology of an Oak Forest in Hungary I. Akadémiai Kiadó, Budapest.

KANDELER, E. (1996): Nitrate. In: Schinner, F. – Öhlinger, R. – Kandeler, E. – Margesin, R. (ed). Methods in soil biology. Springer. Berlin, Heidelberg, New York. pp. 408–410.

KOTROCZÓ, ZS. – FEKETE, I. – TÓTH, J. A. – TÓTHMÉRÉSZ, B. (2008): Effect of leaf- and root-litter manipulation for carbon-dioxide efflux in forest soil. Cereal Research Communication 36: 663–666.

KOTROCZÓ, ZS. – VERES, ZS. – FEKETE, I. – PAPP, M. – TÓTH, J. A. (2012): Effects of Climate Change on Litter Production in a Quercetum petraeae-cerris Forest in Hungary. Acta Silvatica et Ligniaria Hungarica 8: 31–38.

KOVÁCS-LÁNG, E. – HERODEK, S. – TÓTH, J. A. (2000): Long Term Ecological Research in Hungary. In: The International Long Term Ecological Research Network. Perspectives from Participating Networks. Compiled by the US LTER Network Office Albuquerque New Mexico. 38–40.

KUMAR, S. – CHAUDHURI, S. – MAITI, S. K. (2013): Soil Dehydrogenase Enzyme Activity in Natural and Mine Soil - A Review. Middle-East Journal of Scientific Research 13: 898–906.

LADD, J. N. (1985): Soil enzymes. In: Soil Organic Matter and Biological Activity. Nijhoff, Dordecht

MAKOI, J. H. J. R. – NDAKIDEMI, P. A. (2008): Selected soil enzymes: Examples of their potential roles in the ecosystem. African Journal of Biotechnology 3: 181–191.

MAMATHA, G. – JAYANTHI, S. – BAGYARAJ, D. J – SURESH, C. K. (2001): Microbial and enzymatic analysis from sandal root zone soil growing in red sandy loam. Indian Journal of Microbiology 41: 219–221.

MCCARTHY, G. W. – SIDDARAMAPPA, R. – REIGHT, R. J. – CODDLING, E. E. – GAO, G. (1994): Evaluation of coal combustion by products as soil liming materials: their influence on soil pH and enzyme activities. Biology and Fertility of Soils 17: 167–172.

MCLAREN, A. D. (1975): Soil as a system of humus and clay immobilised enzymes. Chemica Scripta 8: 97–99.

NADELHOFFER, K. – BOONE, R. – BOWDEN, R. – CANARY, J. – KAYE, J. – MICKS, P. – RICCA, A. – MCDOWELL, W. – AITKENHEAD, J. (2004): The DIRT experiment. In: Foster, D. R. – Aber, D. J. (ed) Forests in Time. Yale Univ. Press, Michigan.

NANNIPIERI, P. – KANDELER, E. – RUGGIERO, P. (2002): Enzyme activities and microbiological and biochemical processes in soil. In: Burns, R. G. and Dick, R. P. (ed.) Enzymes in the Environment: Activity, Ecology, and Applications. Marcel Dekker, New York. pp. 1–33.

SINSABAUGH, R. L. – MOORHEAD, D. L. (1994): Resource allocation to extracellular enzyme production: a model for nitrogen and phosphorus control of litter decomposition. Soil Biology and Biochemistry 26: 1305–1311.

SINSABAUGH, R. L. – LAUBER, C. L. – WEINTRAUB, M. N. – AHMED, B. – ALLISON, S. D. – CHELSEA, C. – CONTOSTA, A. R. – CUSACK, D. – FREY, S. – GALLO, M. E. – GARTNER, T. B. – HOBBIE, S. E. – HOLLAND, K. – KEELER, B. L. – POWERS, J. S. – STURSOVA, M. – TAKACS-VESBACH, C. – WALDROP, M. P – WALLENSTEIN, M. D. – ZAK, D. R. – ZEGLIN, L. H. (2008): Stoichiometry of soil enzyme activity at global scale. Ecology Letters 11: 1252–1264.

SMITH, S. E. – READ, D. (2008): Mycorrhizal Symbiosis, 3rd edn. Academic Press is an imprint of Elsevier, New York, London, pp. 365.

SULZMAN, E. W. – BRANT, J. B. – BOWDEN, R. D. – LAJTHA, K. (2005): Contribution of aboveground litter, belowground litter, and rhizosphere respiration to total soil CO2 efflux in an old growth coniferous forest. Biogeochemistry 73: 231–256.

TAYLOR, J. P. – WILSON, B. – MILLS, M. S. – BURNS, R. G. (2002): Comparison of microbial numbers and enzymatic activities in surface soils and subsoils using various techniques. Soil Biology and Biochemistry 34: 387–401.

THALMANN, A. (1968a): Zur Methodik der Bestimmung der Dehydrogenaseaktivit□t im Boden mittels Triphenyltetrazoliumchlorid (TTC). Landwirtschaftliche Forschung 21: 249–258.

THALMANN, A. (1968b): Dehydrogenase activity. In: Alef K. and Nannipieri P. (ed) (1995): Methods in Applied Soil Microbiology and Biochemistry. Academic Press Ltd. pp. 228–230.

TÓTH, J. A. – LAJTHA, K. – KOTROCZÓ, ZS. – KRAKOMPERGER, ZS. – CALDWEL, B. – BOWDEN, R. D. – PAPP, M. (2007): The effect of climate change on soil organic matter decomposition. Acta Silvatica et Ligniaria Hungarica 3: 75–85.

TÓTH, J. A. – NAGY, P. T. – KRAKOMPERGER, ZS. – VERES, ZS. – KOTROCZÓ, ZS. – KINCSES, S. – FEKETE, I. – PAPP, M. – LAJTHA, K. (2011): Effect of Litter Fall on Soil Nutrient Content and pH, and its Consequences in View of Climate Change (Síkfőkút DIRT Project). Acta Silvatica et Ligniaria Hungarica 7: 75–86.

TREVORS, J. T – MAYFIELD, C. I. – INNISS, W. E. (1982): Measurement of electron transport system (ETS) activity in soil. Microbial Ecology 8: 163–168.

VARGA, CS. – FEKETE, I. – KOTROCZÓ, ZS. – KRAKOMPERGER, ZS. – VINCZE, GY. (2008): Effect of litter amount on soil organic matter (SOM) turnover in Síkfőkút site. Cereal Research Communications 36: 547–550.

WOLIŃSKA, A. – STE□PNIEWSKA, Z. (2012): Dehydrogenase Activity in the Soil Environment, Dehydrogenases. Prof. Rosa Angela Canuto (ed). ISBN: 978-953-307-019-3. InTech. DOI: 10.5772/48294.

XIANG, S. – R. – DOYLE, A. – HOLDEN, P. A. – SCHIMEL, J. P. (2008): Drying and rewetting effects on C and N mineralization and microbial activity in surface and subsurface California grassland soils. Soil Biology and Biochemistry 40: 2281–2289.

DE GRUYTER OPEN DOI: 10.2478/aslh-2013-0003 Acta Silv. Lign. Hung., Vol. 9 (2013) 35–42

Juvenile Growth and Morphological Traits of Micropropagated Black Locust (*Robinia Pseudoacacia* L.) Clones under Arid Site Conditions

Károly RÉDEI[a*] – Zsolt KESERŰ[a] – Imre CSIHA[a] – János RÁSÓ[a] – Ágnes KAMANDINÉ VÉGH[a] – Borbála ANTAL[b]

[a] Department of Plantation Forestry, Hungarian Forest Research Institute, Sárvár, Hungary
[b] Faculty of Agriculture, University of Debrecen, Hungary

Abstract – In Hungary black locust (*Robinia pseudoacacia* L.) is considered as an important exotic stand-forming tree species growing mostly under unfavourable ecological conditions for forest management. Due to climate change effects its importance is increasing in many other countries, too. As a result of a selection programme new black locust clones were tested in clone trials. Juvenile growth and the morphological as well as phenological traits of four micropropagated black locust clones were evaluated in central Hungary under dry site conditions. Significant differences (P<5%) were found for DBH and field survival rate values. At age of 7 the clone R.p. 'Bácska' ('KH 56A 2/5') appears to be especially promising for mass propagation. Tissue culture can be considered as a suitable tool for propagating superior individuals and offers new prospects for the rapid cloning of selected genotypes used for plantation forestry.

Black locust *(Robinia pseudoacacia* L.) / clone trial / juvenile growth / micropropagation

Kivonat – Mikroszaporított fehér akác (*Robinia pseudoacacia* L.) klónok fiatalkori növekedése és morfológiai jellemzői száraz termőhelyeken. Magyarországon a fehér akác (*Robinia pseudoacacia* L.) fontos állományalkotó egzóta fafaj, főként az erdőgazdálkodás számára kedvezőtlen termőhelyeken. A klímaváltozás hatásai miatt a fafaj jelentősége folyamatosan növekszik több más országban is. Egy szelekciós program eredményeként új akác klónokat állítottunk elő klónkísérletek létesítése céljából. Jelen tanulmányban négy mikroszaporítással előállított akác klónt értékeltünk fiatalkori növekedésük, továbbá morfológiai és fenológiai jellemzőik alapján Közép-Magyarországon száraz termőhelyi viszonyok között. Szignifikáns különbséget (P<5%) találtunk a mellmagassági átmérő és a megmaradási értékek tekintetében. 7 éves korban az R.p. 'Bácska' ('KH 56A 2/5') klón különösen ígéretesnek tűnik a tömegszaporításra. A szövettenyésztéses szaporítási eljárás megfelelő eszköznek tekinthető az ültetvényes fatermesztés területén kiváló minőségű egyedek klónos elszaporítására, új távlatokat nyújtva ezzel a kiválasztott genotípusok gyors klónozására.

Fehér akác *(Robinia pseudoacacia* L.) / klónkísérlet / fiatalkori növekedés / mikroszaporítás

* Corresponding author: redei.karoly@t-online.hu; H-4150 PÜSPÖKLADÁNY, Farkassziget 3.

1 INTRODUCTION

Black locust (*Robinia pseudoacacia* L.) was introduced to Europe from its natural range in south-eastern United States more than 300 years ago. It has been well adapted for growth in a wide variety of ecological conditions and planted throughout the world from temperate to subtropical areas. It is fast growing, excellent coppicing, drought tolerant, has high survival rates and yield as well as very hard durable wood. Due to its symbiosis with the nitrogen fixing bacteria, *Rhizobium* sp. black locust is capable of colonising very low nutrient substrates. Black locust is also a promising tree species for short rotation forestry (SRF) including energy plantations. The development of an integrated landscape includes forests, agricultural fields and shelterbelts. In these cases afforestation with black locust is focused on improving the natural environment and the living conditions of the population as well (Führer – Rédei 2003, Rédei et al. 2011).

Several countries have started research programmes on improving black locust wood quality and/or increasing production of biomass for energy purpose. Black locust has also been considered as a promising tree species for animal feeding and for recultivation of drying out devastated lands as well as nectar production. At present, black locust breeding and improvement is undertaken in the United States (Bongarten et al. 1991, 1992) Greece (Dini-Papanastasi – Panetsos 2000), Germany (Liesebach et al. 2004, Böhm et al. 2011), Slovakia (Chalupa 1992), Poland (Kraszkiewicz 2013), Turkey (Dengiz et al. 2010), India (Sharma 2000, Swamy et al. 2002), China (Dunlun et al. 1995), South Korea (Lee et al. 2007). Increasingly, countries are interested in black locust improvement and management paying special attention to its response to climate change effects.

The primary requirement for reproducing black locust clones (varieties) to establish clone trials, seed orchards and seed production stands was to reliable vegetative methods. Propagation from root cuttings and tissue culture propagation are suitable for reproduction of superior traits of the selected trees. Brown (1980) was the first to report a successful in vitro method for mass production of black locust. Enescu and Jucan (1985) started experiments in Romania with similar results. Balla and Vértesy in 1985 had the first success in the sterile production of four Hungarian state-approved black locust cultivars. Balla et al. (1998) published the improvement of the acclimatization results of micropropagated black locust using symbiotic microorganisms.

Because of the fact that black locust is easy to clone and also exhibits wide adaptation to ecological (site) conditions, there is also an opportunity to develop basic information on genotype by environment interaction for traits of interest (Hanover 1992). In Hungary, black locust has played a role of great importance in the forest management for more than 280 years, covering approximately 23% of the forested area (445.000 ha) and providing about 20% of the annual timber output of the country. Being aware of the importance of black locust, forest research in Hungary has been engaged in resolving various problems of black locust management for a long time, and numerous research results have already been implemented in the practice (Keresztesi 1988, Rédei et al. 2007). In the country in the lowlands characterized with forest steppe climatic type, the annual precipitation is not more than 500 mm, most of which is outside the growing season. Thus, drought is a frequent phenomenon in the summer period coupled with very high atmospheric temperatures. Due to these facts about 40% of the black locust stands in Hungary grow under marginal site conditions (Rédei 2003, Rédei et al. 2008). Considering the above-mentioned circumstances a *new black locust selection work* started 12 years ago to find and improve black locust clones and cultivars which perform good stem form, provide good-quality wood material for industrial purposes, and which are able to tolerate the dry ecological conditions as well. As a result of the selection programme some new black locust clones have been improved. In this

paper one of the trials established *with micropropagated black locust clones* is evaluated with special regard to their juvenile growth rate and morphological traits. By applying micropropagation, superior traits of the selected trees can be preserved in the clones and it can also be considered as an effective tool for producing improved initial propagation material.

2 MATERIALS AND METHODS

2.1 Study site

Data used in this study came from a black locust clone trial established in the forest subcompartment Kecskemét 16CS/1 (N46^{0}54'44", E19^{0}41'51") in Central-Hungary between the Danube and Tisza rivers (*Figure 1*). The forest subcompartment has slightly humous sandy soil without ground-water influence. The annual precipitation amounts to only 500 mm in some years, of which less than 300 mm comes in the dry summer period; water supply is a limiting factor. The trial at Kecskemét is not among the best sites available in Hungary but can be considered as an average yield class site for black locust (Rédei – Gál 1985).

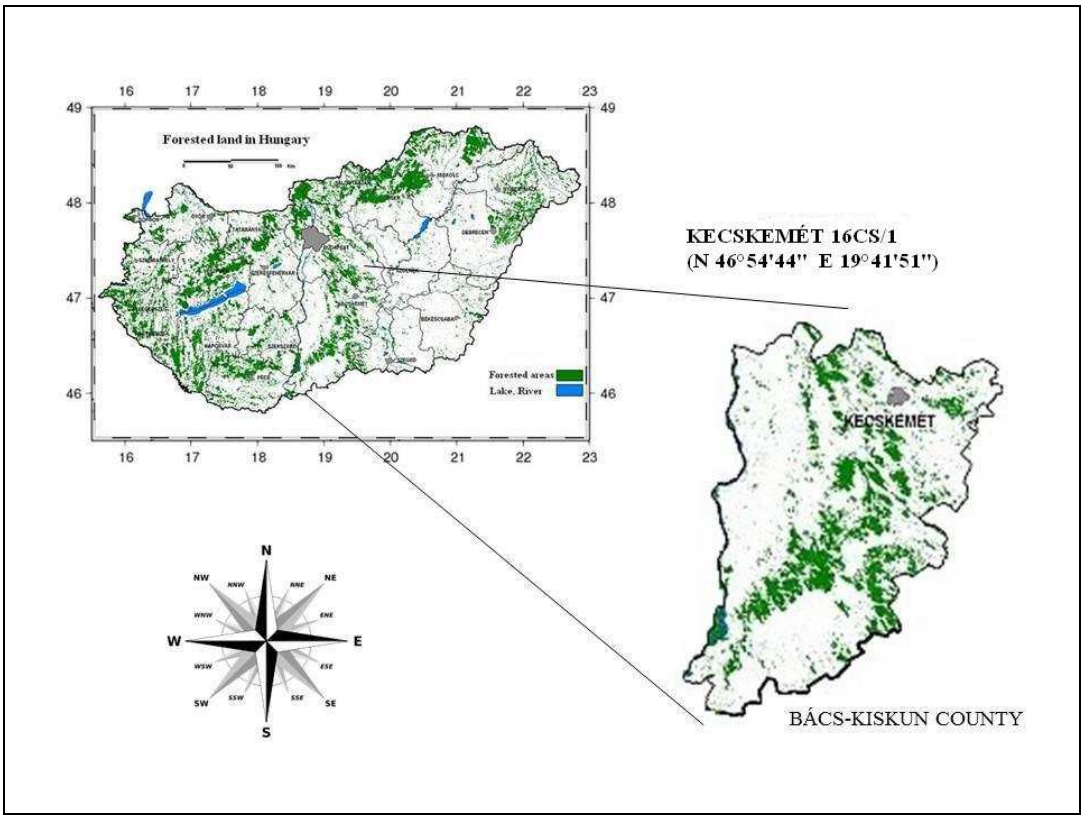

Figure 1. Location of the study site

The main ecological conditions of the study area are as follows: relative air humidity below 50%, hydrology: free draining, genetic soil type: humus sand soil, annual precipitation is less than 550 mm (between 1st April and 26th September in 2011 the precipitation was only 288 mm).

2.2 Materials

The trial, with three replications was established at a spacing of 2.0 m × 1.0 m. Common black locust and four black locust clones, i.e. R.p. 'Bácska' ('KH 56A 2/5'), 'KH 56A 2/6', 'MB 17D 4/1'and 'CST 61A 3/1' were selected. Each treatment corresponds to a plot of 15 by 20 m. For the clones one-year-old micropropagated plants were used and one-year-old seedlings for common black locust. Plant tissue culture method provided us with an effective means to accelerate vegetative propagation of the newly selected clones and to establish new clone trials (Rédei et al. 2002).

2.3 Methods

The following parameters were measured and calculated at age of 7: number of stems, tree height (also at 1, 3 and 5 years), dbh (diameter at breast height) over bark, stem volume and mean tree volume. We used arithmetic mean in case of tree height and dbh because it is more appropriate for certain types of experimental studies, for example, clone trials where it is primarily important to measure the responses of the trees to the experimental treatments during the first years after plantation establishment. The stem volume was calculated using the volume function based on the volume table for black locust (Kolozs – Sopp 2000):

$$v = 10^{-8} d^{2} h^{1} \left(h/\left[h-1.3\right]\right)^{2} \left(-0.6326dh + 20.23d + 3034\right),$$

where

v is stem volume (m^3),
d is diameter at breast height (cm),
h is tree height (m).

The mean tree volume (v_m, m^3/tree) was calculated using the means of stem volume (h, dbh) for each of the experimental plots.

The following classifications were used for the evaluation of the morphological and phenological traits:

- Stem form = 1: straight, 2: more or less straight, 3: declining, 4: strongly declining.
- Bud break intensity = 1: very poorly budding, 2: poorly budding, 3: mediocre, 4: vigorously budding.
- Foliage density = 1: loose foliage, 2: mediocre foliage, 3: dense foliage.
- Forking = 1: not forking, 2: forking in the crown, 3: the crown starts with forking, 4: the stem is forking.
- Branching = 1: thick branches, 2: medium thick branches, 3: thick branches in the crown only.
- Blooming intensity = 1: complete, 2: abundant, 3: mediocre, 4: scarce, 5: sporadic, 6: no flowers.

The collected data were analyzed by STATISTICA 8.0 (data analysis software system – StatSoft, Inc., 2008) programme. Analysis of variance (one-way ANOVA) was done for height, dbh and mean tree volume to consider the trial with having completely randomized design.

3 RESULTS

Table 1 illustrates the most important stand structure parameters and the survival rate. According to the significance test at P = 5% level significant differences were found in DBH and in the survival rate.

Comparison of mean height illustrated that clones ‘KH 56 A2/5’ and ‘KH 56 A 2/6’ achieved the higher value (9.4 and 9.5 m) and the height growth patterns of the clones and the control at different ages were similar (*Figure 2*).

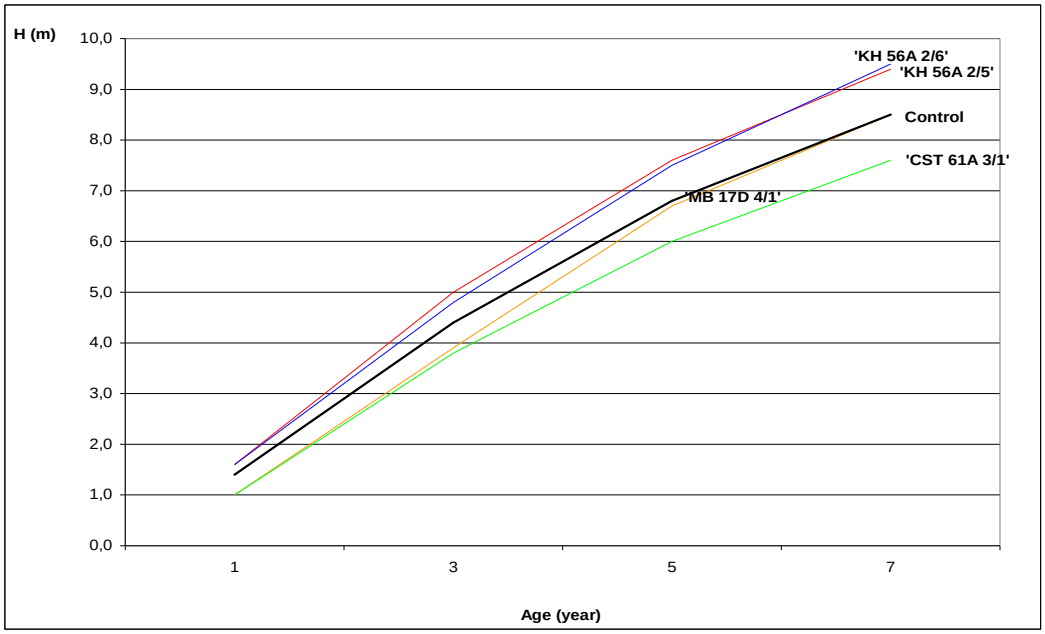

Figure 2. Height growth patterns of micropropagated black locust (Robinia pseudoacacia L.) clones at the age of 1, 3, 5 and 7 years

Comparison of mean DBH indicated that the clone ‘KH 56 A 2/5‘ had maximum growth. The same result was obtained in the case of mean tree volume for ‘KH 56A 2/5’ and ’KH 56 A 2/6’.

Table 1. Stand characteristics of micropropagated black locust clones at age of 7 years

Clone name	Plot number	Height (m)	DBH (cm)	Survival %	Height (m)	DBH (cm)	Mean tree volume (m^3)	Survival %
					plot average values			
Kéleshalom 56A 2/5 ('KH 56A 2/5')	1	8.5	6.9	81	9.4	7.1**	0.0497	83**
	9	9.0	6.3	94				
	18	10.7	8.2	75				
Kéleshalom 56A 2/6 ('KH 56A 2/6')	2	9.0	5.8	62	9.5	6.1	0.0496	69*
	12	11.6	7.3	75				
	15	7.9	5.2	69				
Mikebuda 17D 4/1 (’MB 17D 4/1')	3	8.3	5.4	69	8.5	5.4	0.0373	73
	13	9.3	5.5	75				
	16	7.8	5.2	75				
Császártöltés 61A 3/1 (’CST 61A3/1’)	5	6.7	4.3	94	7.6	5.1*	0.0310	87**
	8	8.4	5.6	87				
	14	7.8	5.5	81				
Common black locust	6	8.0	5.6	56	8.5	6.1	0.0389	69*
	10	7.1	4.8	75				
	17	10.5	7.9	75				

*, **: P<5%

Table 2. Analysis of variance for height, diameter at breast height, mean tree volume and survival rate of the four tested black locust clones

Source of variation	Degrees of freedom (df)	Sum squares (SS)	Mean squares (MS)	F	Significance
		Height (m)			
Total	14	26.47			
Replication	2	2.12			
Treatment	4	8.09	2.0225		
Error	8	16.26	2.0325	0.99508	
		Diameter at breast height (cm)			
Total	14	17.85			***
Replication	2	1.63			
Treatment	4	7.35	1.8375		
Error	8	8.87	1.10875	1.657272	
		Mean tree volume (m^3)			
Total	14	0.0022			
Replication	2	0.0002			
Treatment	4	0.0006	0.00015		
Error	8	0.0014	0.000175	0.857143	
		Survival rate (%)			
Total	14	1518.4			***
Replication	2	204.4			
Treatment	4	895.73	223.9325		
Error	8	418.27	52.28375	4.283023	

***: P<5%

Table 3 contains some morphological and phenological characteristics of the selected black locust clones at age of 7. As the general evaluation of the morphological characteristics is concerned, the succession from best to worst is: ‘KH 56A 2/5’, ‘KH 56A 2/6’, ‘MB 17D 4/1’ and ’CST 61A 3/1’. The phenological evaluation for blooming intensity indicated the highest quality in ’KH 56A 2/5’. The micropropagated trees began to flower in the fifth growing season after field planting and produced seeds with germination comparable to that of common black locust trees.

Table 3. Morphological and phenological data of 7-year-old clones as a mean of plots

Morphological and phenological traits	Stem form	Bud break intensity	Foliage density	Forking	Branching	Blooming intensity
Clone name	(1–4)	(1–4)	(1–3)	(1–4)	(1–3)	(1–6)
'KH 56A 2/5'	1.5	3.1	2.0	1.2	2.1	2.6
'KH 56A 2/6'	1.7	2.8	1.9	1.3	1.9	3.1
'MB 17D 4/1'	2.1	2.8	2.3	1.2	2.1	3.5
'CST 61A 3/1'	1.6	2.8	2.5	1.2	1.8	4.5
Common black locust	2.0	2.9	2.2	1.3	2.0	3.5

4 DISCUSSION AND CONCLUSIONS

For some decades black locust has received increased attention in more and more countries for the following reasons:

1) the energy crisis has stimulated research on relatively rapid growing, nitrogen-fixing trees such as black locust;
2) the species has a great many characteristics from both the practical and biological research standpoints; and
3) application of genetic improvement and biotechnology techniques may remove several hindrances to the widespread use of black locust in some, potentially promising countries from black locust growing point of view.

Black locust's fast growth and site condition tolerance are important characteristics for short rotation cycle silviculture (SRF), as well. Because of its many desirable attributes, the species is admirably suited to utilization in many areas of the world. Plant tissue culture methods provide us with relatively new means to speed up vegetative propagation of recently selected clones and give us opportunity to establish healthy stock plantations. According to our experiences and investigations (Rédei et al. 2007) black locust trees show considerable variability in stem and branching form, wood quality and stress tolerance. Well designed clone trials (clonal tests) are needed to improve varieties best adapted to certain environments.

This study leads to the following conclusions: (1) the trial demonstrated that micropropagated trees can be successfully transplanted into soil, hardened and grown in the field. Micropropagated trees exhibited normal growth and appearance; (2) the results at the end of the 7th growing season demonstrated that the DBH and seedling survival differed significantly among the tested clones; (3) the investigations showed that clone R.p. 'Bácska'('KH 56 A 2/5') achieved the highest growth rate in mean tree volume with having the best morphological and phenological characteristics; (4) micropropagation has proved as a suitable mean in the field of black locust clonal selection.

To consider the effects of the global climate change and the regional growing experiences, in the future would be two regions, where the fast spread of black locust could be expected. In Europe some Mediterranean countries (Turkey, Italy), while in Asia China and Korea may be the most prominent black locust growers.

Acknowledgements: The authors would like to express their appreciation to the Korea Forest Research Institute for its financial support to bring the join black locust improvement project to fruition. The authors also gratefully acknowledge the valuable comments on the manuscript made by P.J. Smallidge, PhD, Director, Arnot Teaching and Research Forest, Cornell University, Ithaca, NY, US.

REFERENCES

BALLA, I. – VÉRTESY, J. (1985): Experiences and problems related to the micropropagation of black locust. In: Symposium on In Vitro Problems Related to Mass Propagation of Horticultural Plants, Book of Abstracts II. International Society of Horticultural Science, Gembloux, Belgium.

BALLA, I. – VÉRTESY, J. – KÖVES-PÉCSI, K. – VÖRÖS, I. – OSVÁTH-BUJTÁS, Z. – BÍRÓ, B. (1998): Acclimation results of micropropagated black locust (*Robinia pseudoacacia* L.) improved by symbiotic microorganism. Plant Cell Tissue Organ Culture Vol. (52): 113–115.

BÖHM, CH. – QUINKENSTEIN, A. – FREESE D. (2011): Yield prediction of young black locust (*Robinia pseudoacacia* L.) plantation for woody biomass production using allometric relations. Ann. For. Res. 54(2): 215–227.

BONGARTEN, B.C. – MERKLE, S.A. – HANOVER, J.W. (1991): Genetically improved black locust for biomass production in short-rotation plantations. In: Energy from Biomass and Wastes XV (KLASS, D.L. ed.), Institute of Gas Technology, Chicago, IL. 391–409.

BONGARTEN, B.C. – HUBER, D.A. – APSLEY, D.K. (1992): Environmental and genetic influences on short-rotation biomass production of black locust (*Robinia pseudoacacia* L.) in the Georgia Piedmont. For. Ecol. Manage. Vol. (55): 315–331.

BROWN, C. L. (1980): Application of tissue culture technology to production of woody biomass. In: Tissue Culture in Forestry. J. M. Bonga, and D. J. Durzan (eds.) Martinus Nijhoff, The Hague, 137–145.

CHALUPA, V. (1992): Tissue culture propagation of black locust. In: Black locust: Biology, Culture and Utilization (Hanover, J.W., Miller, K. & Plesko, S. eds.). Michigan State University, East Lansing, 115–125.

DENGIZ, O. – GOL, C. – SARIOGLU, F. E. – EDIS, S. (2010): Parametric approach to land evaluation for forest plantation: A methodological study using GIS model. African Journal of Agricultural Research. 5 (12): 1482–1496.

DINI-PAPANASTASI, O. – PANETSOS, C.P. (2000): Relation between growth and morphological traits and genetic parameters of *Robinia pseudoacacia* var. monophylla DC in northern Greece. Silvae Genet. Vol. (49): 37–44.

DUNLUN, Z. – ZHENFEN, Z. – FANGQUAN, W. (1995): Progress in clonal selection and breeding of black locust (*Robinia pseudoacacia* L.) In: Forest Tree Improvement in the Asia-Pacific Region (Xihuan Shen): China Forestry Publishing House, Beijing, 152–156.

ENESCU, V. – JUCAN, A. (1985): Problems of the in vitro micropropagation of black locust (*Robinia pseudoacacia* L.). In: New Ways in Forest Genetics: Proceeding of the 20th Canadian Tree Improvement Association Meeting, Quebec. F. Caron, A. G. Corriveau and T.J.B. Boyle (eds.) 179–184.

FÜHRER, E. – RÉDEI, K. (2003): The role of black locust (*Robinia pseudoacacia* L.) in the Great Hungarian Plain. Proceedings of Scientific Paper, 2. Sofia. 67–73.

HANOVER, J. (1992): Black locust: An Historical Perspective. In: Black Locust: Biology, Culture and Utilization (Hanover, J. W. – Miller, K. – Plesko, S. eds.). Michigan State University, East Lansing, 7–20.

KERESZTESI, B. (ed.) (1988): The Black Locust. Academic Publishing House. Budapest.

KOLOZS, L. – SOPP, L. (2000): Volume tables. Forest Service, Budapest. 58–66.

KRASZKIEWICZ, A. (2013): Evaluation of the possibility of energy use black locust (*Robinia pseudoacacia* L.) dendromass acquired in forest stands growing on clay soils. Journal of Central European Agriculture. 14(1): 388–399.

LEE, K. J. – SOHN, J. H. – RÉDEI, K. – YUN, H. Y. (2007): Selection of Early and Late Flowering *Robinia pseudoacacia* from Domesticated and Introduced Cultivars in Korea and Prediction of Flowering Period by Accumulated Temperature. Journal of Korean Forest Society 96 (2): 170–177.

LIESEBACH, H. – YANG M.S. – SCHNECK, V. (2004): Genetic diversity and differentiation in a black locust (*Robinia pseudoacacia* L.) progeny test. Forest Genetics 11 (2): 151–161.

RÉDEI, K. – GÁL, J. (1985): Akácosok fatermése. Erdészeti Kutatások, Vol. (76–77) : 195–203.

RÉDEI, K. – OSVÁTH-BUJTÁS, Z. – BALLA, I. (2002): Clonal approaches to growing black locust (*Robinia pseudoacacia*) in Hungary: a review. Forestry, 75(5): 547–552.

RÉDEI, K. (ed.) (2003): Black Locust (*Robinia pseudoacacia* L.) Growing in Hungary. Publications of the Hungarian Forest Research Institute, Budapest.

RÉDEI, K. – OSVÁTH-BUJTÁS, Z. – KESERŰ, ZS. – YOUNG-GOO PARK. (2007): Clonal Selection of Black Locust (*Robinia pseudoacacia* L.) in Hungary: a Review. Korean J. Apiculture, 22 (2):189–193.

RÉDEI, K. – OSVÁTH-BUJTÁS, Z. – VEPERDI, I. (2008): Black Locust (*Robinia pseudoacacia* L.) Improvement in Hungary: a Review. Acta Silvatica et Lignaria Hungarica. Vol.4:127–132.

RÉDEI, K. – CSIHA, I. – KESERŰ, ZS. – KAMANDINÉ VÉGH Á. – GYŐRI, J. (2011): The Silviculture of Black Locust (Robinia pseudoacacia L.) in Hungary: a Review. SEEFOR, 2 (2.) 101–107. Zagreb, Croatia.

SHARMA, K.R. (2000): Variation in wood characteristics of *Robinia pseudoacacia* L. managed under high density short rotation system. IUFRO World Congress held in Malaysia.

SWAMY, S.L. – PURI, S. – KANWAR, K. (2002): Propagation of *Robinia pseudoacacia* Linn. and *Grewia optiva* Drummond from rooted stem cuttings. Agrofor. Syst. Vol. 55: 231–237.

DE GRUYTER OPEN DOI: 10.2478/aslh-2013-0004 Acta Silv. Lign. Hung., Vol. 9 (2013) 43–56

The Effect of Herb Layer on Nocturnal Macrolepidoptera (Lepidoptera: Macroheterocera) Communities

Bálint HORVÁTH[a*] – Viktória TÓTH[a] – Gyula KOVÁCS[b]

[a] Institute of Silviculture and Forest Protection, University of West Hungary, Sopron, Hungary
[b] Institute of Wildlife Management and Vertebrate Zoology, University of West Hungary, Sopron, Hungary

Abstract – Vegetation beneath the canopy might be an important factor for macromoth community composition in forest ecosystems, strongly determined by forest management practices. Herein, we compared nocturnal macrolepidoptera communities and herb layers in young and old sessile oak (*Quercus petraea*) dominated forest stands in the Sopron Mountains (Western Hungary). The investigation of Lepidoptera species was performed 15 times from the end of March to the end of October in 2011. Portable light traps were used, and a total of 257 species and 5503 individuals were identified. The Geometridae family was the most abundant, followed by Noctuidae and Notodontidae. To investigate vascular plant species in the herb layer, circular plots with a 10-m radius around the moth traps were used. In each plot, we estimated the abundance of plant species in 20 sub-plots with a 1-m radius from May to July of 2011. The abundance of macromoth species was higher in the old forest stand, which might be influenced by the trees' higher foliar biomass. However, the mean abundance of herbs was lower in the old forest. Diversity of both the herb layer and the moth community were significantly higher in the young forest. However we found higher species richness of moths in the old forest. For additional analyses, moths feeding on plants in the herb layer were selected, but neither the difference in species number, neither mean abundance between the young and old forest were significant. Our results suggest that the herb layer is not a key factor for macrolepidoptera communities in Hungarian sessile oak forest stands.

Sopron Mountains / diversity / sessile oak (*Quercus petraea*) / Lepidoptera / vascular plants

Kivonat – Éjszakai nagylepke közösségek (Lepidoptera: Macroheterocera) és a gyepszint diverzitásának kapcsolata. Az erdei ökoszisztémák éjszakai lepkeközösségének összetételét a lombkoronaszint alatti növényzet erősen befolyásolja, amely közvetett úton az erdészeti kezelések következménye. A szerzők jelen dolgozatban egy idős és egy fiatal, kocsánytalan tölgy (*Quercus petraea*) által dominált erdőállomány gyepszintjének és éjszakai nagylepke közösségének kapcsolatát vizsgálták. Összesen 15 alkalommal történt éjszakai lepke mintavétel, 2011 márciusától novemberéig, hordozható fénycsapdák alkalmazásával. A vizsgálat során 257 nagylepke faj 5503 egyedét figyeltük meg. Fajokban leggazdagabb az araszoló lepkék családja (*Geometridae*) volt, ezt követték a bagolylepkék (*Noctuidae*) és a púposszövők (*Notodontidae*) családja. A gyepszint növényzetét 20 darab 1 méter sugarú mintavételi körben vizsgáltuk, a csapdák 10 méteres körzetében. A mintavételezést 2011 májusától júliusáig végeztük. Az éjszakai nagylepkék egyedszáma az idős erdőben volt magasabb, ami az idősebb fák nagyobb biomassza produktumával magyarázható.

* Corresponding author: hbalint@emk.nyme.hu; H–9400 SOPRON, Bajcsy-Zs. u. 4.

Ugyanakkor a gyepszint növényfajainak abundanciája alacsonyabb volt az idős erdőben. A gyepszint és az éjszakai nagylepkék diverzitási indexei szignifikánsan magasabb értéket mutattak a fiatal erdőben, az éjszakai nagylepkék fajszámát az idős erdőben találtuk magasabbnak. További elemzéseket végeztünk a gyepszintben (illetve a gyepszintben is) fejlődő lepkefajokon, mint modellcsoporton, de sem a fajszámban, sem a mintánkénti átlagos egyedszámban nem volt szignifikáns különbség a mintaterületek között. Eredményeink alapján arra következtethetünk, hogy a gyepszint önmagában nem meghatározó tényezője az éjszakai nagylepke közösségeknek, a vizsgáltakhoz hasonló hazai kocsánytalan tölgyes erdőkben.

Soproni-hegység / diverzitás / kocsánytalan tölgy (*Quercus petraea*) / Lepidoptera / lágyszárú edényes növények

1 INTRODUCTION

A question posed by many community ecologists is which factors influence biodiversity. The answer is multiple factors, but specialists have agreed that plants have an important role. One of the key components in maintaining the biodiversity of temperate forests is the vegetation (Thomas – Packham 2007, Schowalter 2011). The largest mass of herbivores is represented by insects, an abundant and diverse group. In addition, numerous insects have adapted to special environmental conditions, and thus are suitable as indicators of biodiversity (New 2009, Park et al. 2009). Numerous insect species respond rapidly to changes in their habitat (Wood – Storer 2003). For that reason, the structure of the forest vegetation is important for insect herbivores, which closely depend on plants for their development and survival (Summerville – Crist 2003). The density and species richness of forest insects are strongly determined by forest management – especially for specialist insects, which feed on a limited number of plant species (Thomas – Packham 2007). Forests in Hungary are often under pressure from intensive timber harvesting, which possibly have a significant influence on the vegetation and animals.

Lepidoptera species are among the most studied insects in the world, and they have been widely used in ecological studies (Kitching et al. 2000, Summerville – Crist 2003, Summerville et al. 2004, Park et al. 2009). Although butterflies are more often investigated (e.g. Jeanneret et al. 2003, Tudor et al. 2004, Benes et al. 2006, Cleary – Genner 2006), however moth species play a more significant role in forest ecosystems because the species richness of butterflies is much lower in forests (Scoble 1992, Schmitt 2003).

The effect of herb layer on Lepidoptera species in Hungarian forests is less studied. In this study, we investigated the relationship between the herb layer and macromoth community in two Hungarian forest stands. We supposed there was an influence of vascular plants on macromoths.

2 MATERIALS AND METHODS

2.1 Study area

The investigation was conducted in an area of approximately 5000 hectares in the Sopron Mountains in the Lower Austroalpides. Approximately 90% of the area is forested (Dövényi 2010). The intensive use of the forests near Sopron has started in the 12th or 13th century. After 1850, many indigenous forests were replaced by pine cultures, and the proportion of the deciduous forests continually decreased until the 1980's. This is the primary reason why the composition of several forests differs from the natural stands in the Sopron Mountains (Tamás 1955, Szmorad 2011).

One of the most common forest types in the Sopron Mountains are sessile oak-hornbeam woodlands. These forests are dominated by *Quercus petraea* agg. and *Carpinus betulus*. In the tree layer, *Tilia cordata*, *Castanea sativa*, *Fagus sylvatica* and *Cerasus avium* are the most common additional species, although coniferous tree species (e.g., *Larix decidua*, *Pinus sylvetris,* and *Picea abies*) also occur. The shrub layer is usually not dense, comprising of young tree species (*Carpinus betulus*, *Tilia cordata* and *Castanea sativa*) and some mesic shrub species (*Cornus sanguinea* and *Corylus avellana*). The herb layer is strongly varied according to ecological conditions, but both general and mesic forest species elements compose the undergrowth (Szmorad 2011, Bölöni et al. 2008).

Conifer forests were avoided in this study, as we focused only on two indigenous, sessile oak dominated forest stands: young (23 years old) and old (84 years old).

2.2 Moth sampling

Within each forest stand, nocturnal Lepidoptera species were sampled 15 times from the end of March to the end of October in 2011, every two weeks, using portable light traps (using a 3 piece UV LED, peak wavelength 400–410 nm, operated by a 4.5 V battery). Although light traps operated with various light sources have different levels of attraction for Lepidoptera families (Nowinszky – Ekk 1996, Puskás – Nowinszky 2011), UV light traps are widely used for sampling moth communities (Summerville – Crist 2003). This method is used for collecting phototactic species. Two traps were used in each forest stand, positioned on the ground and with 50 m apart. Samples in the two sites were taken simultaneously. Light trapping was regularly performed during the night (from sunset to sunrise) and ceased during heavy rain. Attracted moths were sacrificed using ethyl acetate as a killing agent inside the traps.

The collected Lepidoptera specimens were frozen until the identification. Most of the individuals were identified by macro-morphological features. The exceptions were *Eupithecia* sp., *Mesapamea* sp. and damaged specimens, which were identified by genitalia investigation. The abdomens of specimen were macerated in 10% cold KOH overnight, than hot for a few minutes before the identification.

2.3 Vascular plant sampling

Vascular plant species in the herb layer were screened from May to July in 2011, using Simon's (2000) nomenclature. Vegetation was semi-systematically sampled. Circular plots with a 10-m radius around the moth traps were used. In each plot, we selected 20 sub-plots with a 1-m radius each. We used 4 sub-plots among 4-m radius circle and 8–8 sub-plots among 6-m and 10-m radius circle. Presence and absence data were recorded within the sub-plots. To estimate the abundances of the vascular plants, we calculated the frequency, which is a generally used method to survey herb layer (Morrison et al. 1995).

2.4 Data analysis

The community and ecological parameters of the Lepidoptera and vascular plant communities were examined and compared in the sampling sites using the Past package (Paleontological Statistics Software 2.17) (Hammer et al. 2001).

The dominance of the most abundant Lepidoptera families was compared using the χ^2-test. The measure of diversity was determined by the Shannon index (Shannon – Weaver 1949), Simpson index (Simpson 1949) and Pielou's equitability formula (Pielou 1966). We used the bootstrap method to compare the diversities (Efron 1979).

The general trends of the Lepidoptera dominance structure and abundance for each sampling site were displayed using a rank-abundance plot. A log-series model (Fisher et al. 1943) (with two parameters α and x) was used. The fitting algorithm was from Krebs (1989),

Sn=αxn/n, for the number of species (Sn) with n individuals; the fitting test was calculated using the χ^2-test.

To compare the mean of the Lepidoptera and vascular plant abundances, the t-test was used.

3 RESULTS

During our study, a total of 257 Lepidoptera species and 5503 individuals were identified from 9 families, using Varga's (2010) nomenclature (1. appendix). The most abundant was the Geometridae family, followed by Noctuidae and Notodontidae. The proportion of these three families was significantly different (χ^2=6.68, p=0.04) between the old and young forests (*Figure 1*). However, there was no significant difference in the comparison of the mean number of Lepidoptera individuals in each family (*Figure 2*).

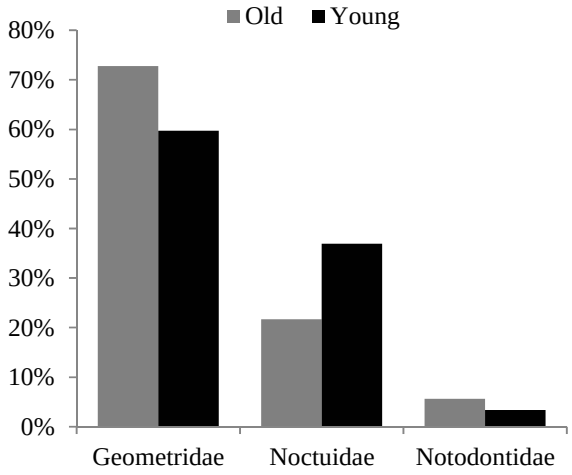

Figure 1. The proportion of the most abundant Lepidoptera families in the old and young forests

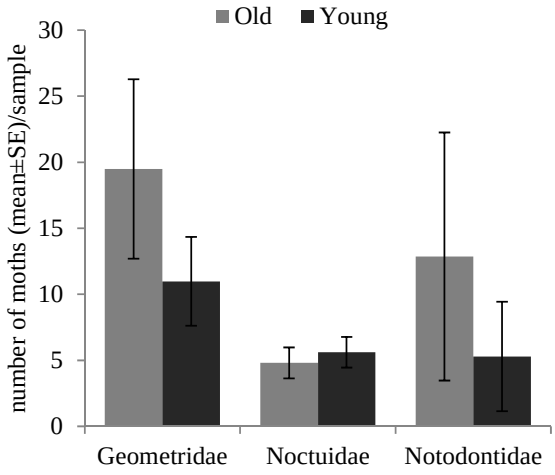

Figure 2. Average number of specimen per most abundant Lepidoptera families per study sites

Species richness of Lepidoptera was higher in the old forest, while species richness of the vascular plants was higher in the young forest. The abundance of Lepidoptera species was also higher in the old forest stand (old forest: 3270 specimens; young forest: 2233 specimens). The measure of the diversity indices (Shannon, Simpson and equitability) was higher in the young forest for both the Lepidoptera and vascular plant communities. The compared diversities showed significant differences between the sampling sites (*Table 1*).

Table 1. Diversity indices of nocturnal Lepidoptera and vascular plant communities in the old and young forests

	Moth			Plant		
	Old	Young	Bootstrap p	Old	Young	Bootstrap p
Species richness	203	192	–	28	32	–
Shannon index	3,668	3,994	0,001	0,908	0,942	0,002
Simpson index	0,929	0,957	0,001	2,748	3,056	0,015
Equitability	0,690	0,760	0,001	0,825	0,882	0,02

There were some differences also in proportions of dominant and rare Lepidoptera species between the sampling sites (old forest: α=47.9, x=0.986, χ^2=2123, p<0.05; young forest: α=50.32, x=0.978, χ^2=566.8, p<0.05). Most species were rare, as indicated by the step initial gradients in the rank abundance plot (*Figure 3*).

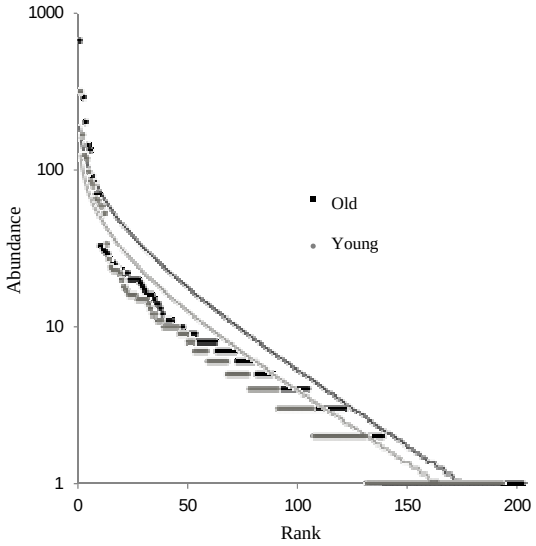

Figure 3. Rank-abundance plot of macromoth communities in old and young forests

We also found some differences in the mean vascular plant abundance of each sample (t-test t = 3.15, p = 0.003); however, this difference was not significant in the case of Lepidoptera abundance (t-test t = 0.97, p = 0.34). We choose the Lepidoptera species that develop on vascular plants as a model group for comparison but found no significant difference in the species number (old forest: 112; young forest: 112) or the mean abundance in each sample (t-test t = 0.28, p = 0.78) either (*Figure 4a-c*).

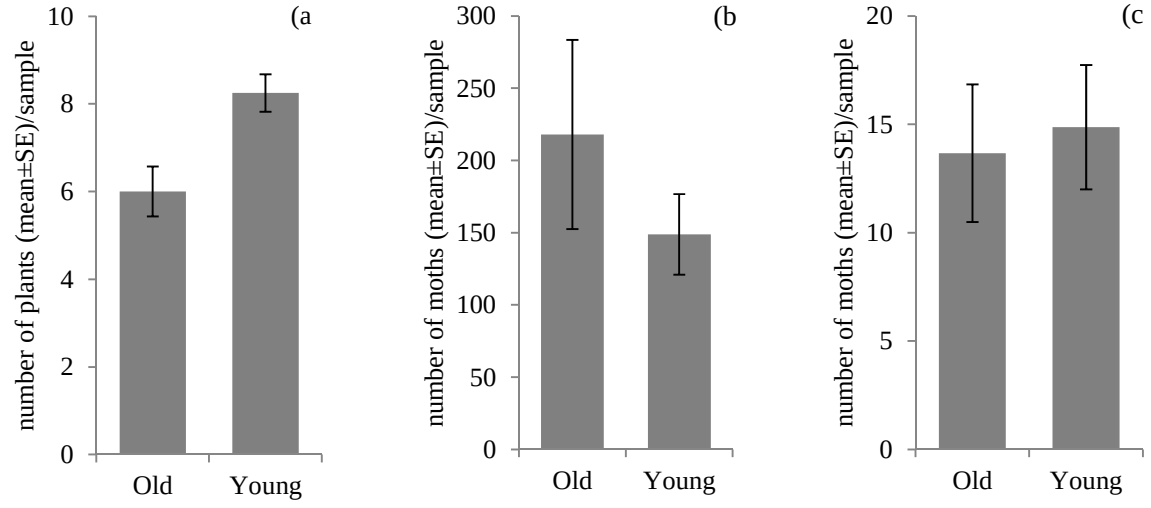

Figure 4a–c. Mean abundances per sample of a) vascular plants, b) nocturnal macrolepidoptera species and c) nocturnal macrolepidoptera species that develop on vascular plants

4 DISCUSSION

Macromoths in the Sopron area are faunistically well studied – approximately 800 species are known (Mészáros – Szabóky 1981, Leskó – Ambrus 1998, Sáfián et al. 2006, Sáfián – Szegedi 2008, Sáfián et al. 2009). Compared to that the number of comparative studies on nocturnal Lepidoptera species in the region is low (Ambrus 1979, Horváth 2013).

The Geometridae family was the most abundant in the investigated forests, although Noctuids are the most diverse group of macromoths in Hungary (Varga 2010). However, number of Geometridae species, which develop on oak species, is higher than in other Lepidoptera families (Csóka – Szabóky 2005). Nevertheless, species richness of Noctuidae was higher both in the old and young forests.

Species richness and abundance of Lepidoptera species were the highest in the old forest stand. This might be associated with the trees' higher foliar biomass product in the old forest (Powers 2001). However, the vascular plant species richness was higher in the young forest. Many species of the ground vegetation survived from the forest clearing. These species will definitely disappear in the growing young forest. Csontos (1996) found similar results in sessile oak - Turkey oak forests regeneration. Nevertheless, there was no difference in the richness of model species (macromoths which develop on vascular plants) between the study sites. Haddad et al. (2001) found a significant positive relationship between insect abundance and plant species richness, however their study was not confined only to the herb layer.

The calculated diversity indices (Shannon, Simpson and Pielou's equitability) were significantly higher in the young forest (both macromoths and vascular plants). The Shannon and Simpson indices show different sensitivities to dominant and rare species and to the equitability. The Shannon diversity formula is calculated using the degree of evenness of the species abundances, whereas the Simpson index is heavily weighted towards the most abundant species in the sample (Peet 1974). It can explain the higher diversity values of macromoths in young forest; however, species richness and abundance of Lepidoptera species were higher in the old forest. Comparison of nocturnal macrolepidoptera species that develop on vascular plants did not show difference between the study sites.

The effect of the vegetation composition on arthropod (especially Lepidoptera) assemblages was proven by many authors (e.g., Axmacher et al. 2009, Taki et al. 2010, Oxbrough et al. 2012). Forest management has an impact on the vegetation, e.g., species richness and species composition (Mark – Lawesson 2000). Nevertheless, forest management also plays an important role in the maintenance of a favourable forest structure for Lepidoptera communities. The forest structure is in under the high influence of the logging method used. Unlogged or selectively cut forest stands are more favourable for diversity and abundance of macromoths (Summerville – Crist 2002, Summerville et al. 2009). Some authors found that the vegetation beneath the forest canopy strongly determines the moth community structure in North-American forested ecosystems (Usher – Keiller 1998, Ober – Hayes 2010). Although the effect of understorey on Lepidoptera species in Hungarian forests is less studied. We supposed that there was an influence of herb layer on macromoths. In contrast, our result did not show an undisputed role of the vascular understory on nocturnal Lepidoptera communities. The explanation of our results may be in connection with the number of study sites and sampling occasion, furthermore with the tight scope of investigated vegetation layer. Henceforward, we suppose a substantial effect of the herb layer on nocturnal Lepidoptera communities, but the complex vegetation structure or other vegetation layers likely play a more significant role in sessile oak forests. The verification of the effect of the different vegetation level and structure on Lepidoptera communities requires further investigations.

Acknowledgements: We express our grateful thanks to Marianna Forgács and Tamás Márton Németh for their help with the field work. The financial backing for the language review was the TÁMOP-4.2.2.B-10/1-2010-0018 project. Further support was provided by the TÁMOP-4.2.2.A-11/1/KONV-2012-0004 project.

REFERENCES

AMBRUS, A. (1979): Újabb adatok a Soproni hegyvidék lepke-faunájához [New data to the Lepidoptera fauna of the Sopron Mountains] Manuscript, Erdészeti és Faipari Egyetem, kézirat, 25 pp + 8 oldal melléklet. (in Hungarian)

AXMACHER, J. C. – BREHM, G. – HEMP, A. – TÜNTE, H. – LYARUU, H. V. M. – MÜLLER-HOHENSTEIN, K. – FIEDLER, K. (2009): Determinants of diversity in afrotropical herbivorous insects (Lepidoptera: Geometridae): plant diversity, vegetation structure or abiotic factors. Journal of Biogeography 36: 337□349.

BENES, J. – CIZEK, O. – DOVALA, J. – KONVIČKA, M. (2006): Intensive game keeping, coppicing and butterflies: The story of Milovicky Wood, Czech Republic. Forest Ecology and Management 237: 353−365.

BÖLÖNI, J. – MOLNÁR, ZS. – BÍRÓ, M. – HORVÁTH, F. (2008): Distribution of the (semi-) natural habitats in Hungary II. Woodlands and scrublands. Acta Botanica 50 (6): 107−148.

CLEARY, D. F. R. – GENNER, M. J. (2006): Diversity patterns of Bornean butterfly assemblages. Biodiversity and Conservation 15: 503−524.

CSÓKA, GY. – SZABÓKY, CS. (2005): Cheklist of Herbivorous Insects of Native and Exotic Oaks in Hungary I (Lepidoptera). Acta Silvatica et Lignaria Hungarica, 1: 59-72.

CSONTOS, P. (1996): Az aljnövényzet változásai cseres-tölgyes erdők regenerációs szukcessziójában [Regeneration succession of sessile oak - Turkey oak forests: Processes in the herb layer] Synbiologica Hungarica 2 (2): 6–122. (in Hungarian)

DÖVÉNYI, Z. (ed.) (2010): Magyarország kistájainak katasztere – Második, átdolgozott és bővített kiadás. MTA Földrajztudományi Kutatóintézet, Budapest, 876 pp. (in Hungarian)

EFRON, B. (1979): Bootstrap Methods: Another Look at the Jackknife. Annals of Statistics 7(1): 1–26.

FISHER, R. A. – CORBET, A. S. – WILLIAMS, C. B. (1943): The relation between the number of species and the number of individuals in a random sample of an animal population. Journal of Animal Ecology 12: 42–58.

HADDAD, N. M. (1999): Corridor and distance effects on interpatch movements: A landscape experiment with butterflies. Ecological Applications 9 (2): 612−622.

HADDAD, N. M. – TILMAN, D. – HAARSTAD, J. – RITCHIE, M. – KNOPS, J. M. H. (2001): Contrasting Effects of Plant Richness and Composition on Insect Communities: A Field Experiment. The American Naturalist 158 (1): 17□35.

HAMMER, Ř. – HARPER, D. A. T. – RYAN, P. D. (2001): PAST – Paleontological Statistics Software Package for Education and Data Analysis. Palaeontologia Electronica 4(1): 9 pp.

HORVÁTH, B. (2013): Diversity comparison of nocturnal macrolepidoptera communities (Lepidoptera: Macroheterocera) in different forest stands. Natura Somogyiensis 23: 229□238.

JEANNERET, P. H. – SCHÜPBACH, B. – LUKA, H. (2003): Quantifying the impact of landscape and habitat features on biodiversity in cultivated landscapes. Agriculture, Ecosystems & Environment 98: 311–320.

KITCHING, L. R. – ORR, A. G. – THALIB, L. – MITCHELL, H. – HOPKINS, M. S. – GRAHAM, A. W. (2000): Moth assemblages as indicators of environmental quality in remnants of upland Australian rain forest. Journal of Applied Ecology 37: 284−297.

KREBS, C. J. (1989): Ecological Methodology. Harper and Row Publisher, New York, 654 pp.

LESKÓ, K. – AMBRUS, A. (1998): Sopron környékének nagylepkefaunája fénycsapdás gyűjtések alapján. [Macrolepidoptera fauna based on light trappings in the surrounding of Sopron] Erdészeti Kutatások 88: 273–304. (in Hungarian)

MARK, S. – LAWESSON, J. E. (2000): Plants as indicators of the conservation value of Danish beech forests. Paper read at Proceedings IAVS Symposium, at Uppsala, Sweden, 26 July–1 August 1998, p. 158–161.

MÉSZÁROS, Z. – SZABÓKY, CS. (1981): A Fertő-tó nádrontó lepkéi. [Lepidoptera damaging reed in the region of Fertő lake]. Növényvédelem 17 (9):372−375. (in Hungarian)

MIRONOV, V. (2003): The Geometrid Moth of Europe, Volume 4. Larentiinae II. (Perizomini and Eupithechini). Apollo Books, Stenstrup, Denmark, 464 pp.

MORRISON, D. A. – LE BROCQUE, A. F. – CLARKE, P. J. (1995): An assessment of some improved techniques for estimating the abundance (frequency) of sedentary organisms. Vegetation 120:131□145.

NEW, T. R. (2009): Insect Species Conservation. Cambridge University Press, New York, 256 pp.

NOVINSZKY, L. – EKK, I. (1996): Normál és UV fénycsapdák Macrolepidoptera anyagának összehasonlítása. [Comparative study of Macrolepidoptera caught in light traps operating with normal and ultra-violet light waves]. Növényvédelem 32 (11): 557−567. (in Hungarian)

OBER, H. K. – HAYES, J. P. (2010): Determinants of nocturnal Lepidopteran diversity and community structure in a conifer-dominated forest. Biodiversity and Conservation 19 (3): 761−774.

OXBROUGH, A. – FRENCH, V. – IRWIN, S. – KELLY, T. C. – SMIDDY, P. – O'HALLORAN, J. (2012): Can mixed species stand enhance arthropod diversity in plantation forest? Forest Ecology and Management 270: 11□18.

PARK, M. – AN, J-S. – LEE, J. – LIM, J-T. – CHOI, S-W. (2009): Diversity of Moths (Insecta: Lepidoptera) on Bogildo Island, Wando-gun, Jeonnam, Korea. Journal of Ecology and Field Biology 32 (2): 129−135.

PIELOU, E. C. (1966): The measurement of diversity in different types of biological collection. Journal of Theoretical Biology 13: 131–144.

POWERS, R. F. (2001): Assessing Potential Sustainable Wood Yield. In: Evans, J. (ed.): The Forests Handbook. Volume 2. Applying Forest Science For Sustainable Management. Blackwell Science Ltd., London, UK, p. 105–128.

PUSKÁS, J. – NOWINSZKY, L. (2011): Light-trap catch of Macrolepidoptera species compared the 100 W normal and 125 W BL lamps. e-Acta Naturalia Pannonica 2 (2): 179−192.

SÁFIÁN, SZ. – AMBRUS, A. – HORVÁTH, B. (2009): Új fajok Sopron környékének éjjeli nagylepkefaunájában (Lepidoptera: Macroheterocera). [New nocturnal Macrolepidoptera species in the fauna of Sopron and its vicinity (Lepidoptera: Macroheterocera)]. Praenorica Folia Historico-Naturalia 11: 189−201. (in Hungarian)

SÁFIÁN, SZ. – HADARICS, T. – SZEGEDI, B. – HORVÁTH Á. (2006): Ritka lepkefajok (*Lepidoptera*) előfordulási adatai egy Fertőrákos melletti mészkőbányából. [Occurrence of rare butterfly and moth species (*Lepidoptera*) from a limestone quarry at Fertőrákos]. Szélkiáltó 12: 28–32. (in Hungarian)

SÁFIÁN, SZ. – SZEGEDI, B. (2008): A behurcolt tölgy-selyemlepke (*Antheraea yamamai* Guérin-Méneville, 1861) (*Saturniidae*: *Lepidoptera*) megjelenése a Soproni-hegyvidéken. [The appearence of Japanese Oak Silkmoth (*Antheraea yamamai Lepidoptera*: *Saturniidae*), an introduced species in the Sopron Mountains (North-West Hungary)]. Szélkiáltó 13: 29. (in Hungarian)

SCHMITT, T. (2003): Influence of forest and grassland management on the diversity and conservation of butterflies and burnet moths (Lepidoptera, Papilionoidea, Hesperiidae, Zygaenidae). Animal Biodiversity and Conservation 26 (2): 51−67.

SCHOWALTER, T. D. (2011): Insect Ecology. An Ecosystem Approach. Third Edition. Academic Press, London, 656 pp.

SCOBLE, M. J. (1992): The Lepidoptera: Form, Function, and Diversity. Oxford University Press, New York, 404 pp.

SHANNON, C. E. – WEAVER, W. (1949): The mathematical theory of communication. Urbana, Illionis, Univ. Illionis Press, 125 pp.

SIMON, T. (ed). (2000): A magyarországi edényes flóra határozója. [Manual of the Vascular Flora of Hungary] Harasztok-virágos növények. Nemzeti Tankönyvkiadó, Budapest, 976 pp.

SIMPSON, E. H. (1949): Measurement of diversity. Nature 163: 688.

SUMMERVILLE, K. S. – CRIST, T. O. (2002): Effects of timber harvest on forest Lepidoptera: Community, guild, and species responses. Ecological Applications 12 (3): 820−835.

SUMMERVILLE, K. S. – CRIST, T. O. (2003): Determinants of lepidopteran community composition and species diversity in eastern deciduous forests: roles of season, eco-region and patch size. Oikos 100: 134−148.

SUMMERVILLE, K. S. – COURARD-HAURI, D. – DUPONT, M. M. (2009): The legacy of timber harvest: Do patterns of species dominance suggest recovery of lepidopteran communities in managed hardwood stands? Forest Ecology and Management 259: 8□13.

SUMMERVILLE, K. S. – RITTER, L. M. – CRIST, T. O. (2004): Forest moth taxa as indicators of lepidopteran richness and habitat disturbance: a preliminary assessment. Biological Conservation 116: 9−18.

SZMORAD, F. (2011): A Soproni-hegység erdeinek történeti, növényföldrajzi és cönológiai vizsgálata. [Historical, phytogeographical and coenological investigations in the forests of the Sopron Hills.]. Tilia XVI., 205 pp. + 61 pp. melléklet. (in Hungarian)

TAKI, H. – INOUE, T. – TANAKA, H. – MAKIHARA, H. – SUEYOSHI, M. – ISONO, M. – OKABE, K. (2010): Response of community structure, diversity, and abundance of understory plants and insect assemblages to thinning in plantation. Forest Ecology and Management 259: 607□613.

TAMÁS, J. (1955): A soproni hegyvidéki erdők történelmi fejlődése, tájleírásai a fafaj, elegyarány és korosztály viszonylatában napjainkig. [Historical development, silvicultural state and description of the forests of the Sopron Mountains] Manuscript, Nyugat-magyarországi Egyetem, Növénytani és Természetvédelmi Intézet, Sopron, 149 pp. (in Hungarian)

THOMAS, P. A. – PACKHAM, J. R. (2007): Ecology of Woodlands and Forests. Description, Dynamics and Diversity. Cambridge University Press, Cambridge, United Kingdoom, 528 pp.

TUDOR, O. – DENNIS, R. L. H. – GREATOREX-DAEVIS, J. N. – SPARKS, T. H. (2004): Flower preferences of woodland butterflies in the UK: nectaring specialists are species of conservation concern. Biological Conservation 119 (3): 397–403.

USHER, M. B. – KEILLER, S. W. J. (1998): The macrolepidoptera of farm woodlands: determinants of diversity and community structure. Biodiversity and Conservation 7: 725−748.

VARGA, Z. (ed.) (2010): Magyarország nagylepkéi. [Macrolepidoptera of Hungary]. Heterocera Press, Budapest, 253 pp.

WOOD, D. L. – STORER, A. J. (2003): Forest Habitats. In: Resh, V. H. – Cardé, R. T. (eds.): Encyclopedia of Insects, Academic Press, London, p. 442−454.

1. Appendix: Taxonomic list of collected Lepidoptera species in the sampling sites

Species	Old	Young	Sum
Lasiocampidae			
Poecliocampa populi (Linnaeus, 1758)	1	0	1
Euthrix potatoria (Linnaeus, 1758)	0	1	1
Lasiocampa quercus (Linnaeus, 1758)	1	0	1
Dendrolimus pini (Linnaeus, 1758)	3	0	3
Endromidae			
Endromis versicolora (Linnaeus, 1758)	1	0	1
Shingidae			
Sphinx ligustri (Linneaus, 1758)	13	0	13
Hyloicus pinastri (Linnaeus, 1758)	9	0	9
Laothoe populi (Linneaus, 1758)	1	0	1
Saturniidae			
Aglia tau (Linnaeus, 1758)	3	1	4
Drepanidae			
Watsonalla binaria (Hufnagel, 1767)	1	9	10
Watsonalla cultraria (Fabricius, 1775)	0	1	1
Thyatiridae			
Thyatira batis (Linnaeus, 1758)	5	5	10
Habrosyne pyritoides (Hufnagel, 1766)	10	11	21
Cymatophorima diluta ([Denis et Schiffermüller], 1775)	6	0	6
Achyla flavicornis (Linnaeus, 1758)	1	0	1
Geometridae			
Geometra papilionaria (Linnaeus, 1758)	4	1	5
Comibaena bajularia ([Denis et Schiffermüller], 1775)	9	1	10
Jodis lactearia (Linnaeus, 1758)	3	0	3
Thalera fimbrialis (Scopoli, 1763)	2	8	10
Hemithea aestivaria (Hübner, 1789)	3	0	3
Idaea dimidiata (Hufnagel, 1767)	0	1	1
Idaea trigeminata (Haworth, 1809)	4	1	5
Idaea biselata (Hufnagel, 1767)	8	8	16
Idaea aversata (Linnaeus, 1758)	22	7	29
Idaea degeneraria (Hübner, 1799)	3	4	7
Idaea deversaria (Herrich-Schäffer, 1847)	10	1	11
Scopula nigropunctata (Hufnagel, 1767)	6	2	8
Scopula floslactata (Haworth, 1809)	7	20	27
Rhodostrophia vibicaria (Clerck, 1759)	1	0	1
Timandra comae Schmidt, 1931	1	3	4
Cyclophora annularia (Fabricius, 1775)	9	5	14
Cyclophora quercimontaria (Bastelberger, 1897)	0	1	1
Cyclophora ruficiliaria (Herrich-Schäffer, 1855)	4	7	11
Cyclophora porata (Linnaeus, 1767)	1	6	7
Cyclophora punctaria (Linnaeus, 1758)	20	18	38
Cyclophora linearia (Hübner, 1799)	6	4	10
Xanthorhoe spadicearia ([Denis et Schiffermüller], 1775)	6	3	9
Xanthorhoe ferrugata (Clerck, 1759)	11	3	14
Xanthorhoe quadrifasciata (Clerck, 1759)	1	0	1
Xanthorhoe fluctuata (Linnaeus, 1758)	5	1	6
Catarhoe rubidata ([Denis et Schiffermüller], 1775)	2	0	2
Epirrhoe alternata (Müller, 1764)	1	4	5
Euphyia biangulata (Haworth, 1809)	7	16	23
Euphyia unangulata (Haworth, 1809)	1	0	1
Camptogramma bilineata (Linnaeus, 1758)	0	6	6
Anticlea badiata ([Denis et Schiffermüller], 1775)	1	1	2
Mesoleuca albicillata (Linnaeus, 1758)	9	3	12
Lampropteryx suffumata ([Denis et Schiffermüller], 1775)	23	4	27

Species	Old	Young	Sum
Cosmorhoe ocellata (Linnaeus, 1758)	1	1	2
Nebula salicata ([Denis et Schiffermüller], 1775)	4	1	5
Eulithis populata (Linnaeus, 1758)	2	0	2
Ecliptopera silaceata ([Denis et Schiffermüller], 1775)	1	0	1
Chloroclysta siterata (Hufnagel, 1767)	1	1	2
Chloroclysta miata (Linnaeus, 1758)	1	0	1
Dysstroma truncata (Hufnagel, 1767)	2	1	3
Thera variata ([Denis et Schiffermüller], 1775)	11	0	11
Thera britannica (Turner, 1925)	4	2	6
Electrophaes corylata (Thunberg, 1792)	1	1	2
Colostygia olivata ([Denis et Schiffermüller], 1775)	23	4	27
Colostygia pectinataria (Knoch, 1781)	30	6	36
Horisme tersata ([Denis et Schiffermüller], 1775)	0	1	1
Melanthia procellata ([Denis et Schiffermüller], 1775)	7	2	9
Anticollix sparsata (Treitschke, 1828)	5	1	6
Triphosa dubitata (Linnaeus, 1758)	1	0	1
Philereme transversata (Hufnagel, 1767)	0	1	1
Epirrita dilutata ([Denis et Schiffermüller], 1775)	318	124	442
Perizoma alchemillata (Linnaeus, 1758)	8	10	18
Perizoma albulata ([Denis et Schiffermüller], 1775)	3	0	3
Eupithecia plumbeolata (Haworth, 1809)	2	0	2
Eupithecia abbreviata Stephens, 1831	20	5	25
Eupithecia tantillaria Boisduval, 1840	4	2	6
Eupithecia lariciata (Freyer, 1842)	1	0	1
Eupithecia subfuscata (Haworth, 1809)	1	2	3
Aplocera plagiata (Linnaeus, 1758)	1	0	1
Asthena albulata (Hufnagel, 1767)	33	17	50
Trichopteryx carpinata (Borkhausen, 1794)	0	1	1
Acasis viretata (Hübner, 1799)	0	1	1
Abraxas grossulariata (Linnaeus, 1758)	1	1	2
Lomaspilis marginata (Linnaeus, 1758)	1	1	2
Ligdia adustata ([Denis et Schiffermüller], 1775)	16	34	50
Macaria notata (Linnaeus, 1758)	7	6	13
Macaria alternata ([Denis et Schiffermüller], 1775)	1	6	7
Macaria liturata (Clerck, 1759)	11	0	11
Plagodis pulveraria (Linnaeus, 1758)	19	23	42
Plagodis dolabraria (Linnaeus, 1767)	25	7	32
Hypoxystis pluviaria (Fabricius, 1787)	0	1	1
Apeira syringaria (Linnaeus, 1758)	0	4	4
Ennomos autumnaria (Werneburg, 1859)	0	1	1
Ennomos quercinaria (Hufnagel, 1767)	83	66	149
Selenia dentaria (Fabricius, 1775)	6	5	11
Selenia lunularia (Hübner, 1788)	4	4	8
Selenia tetralunaria (Hufnagel, 1767)	20	15	35
Crocallis elinguaria (Linnaeus, 1758)	4	10	14
Odontopera bidentata (Clerck, 1759)	2	0	2
Colotois pennaria (Linnaeus, 1761)	671	167	838
Angerona prunaria (Linnaeus, 1758)	7	12	19
Lycia hirtaria (Clerck, 1759)	0	1	1
Biston betularia (Linnaeus, 1758)	3	0	3
Agriopis leucophaearia ([Denis et Schiffermüller], 1775)	0	2	2
Agriopis aurantiaria (Hübner, 1799)	14	9	23
Agriopis marginaria (Fabricius, 1776)	0	16	16
Erannis defoliaria (Clerck, 1759)	14	3	17
Peribatodes rhomboidaria ([Denis et Schiffermüller], 1775)	31	118	149
Alcis repandata (Linnaeus, 1758)	8	2	10
Alcis bastelbergeri (Hirschke, 1908)	4	0	4
Hypomecis roboraria ([Denis et Schiffermüller], 1775)	70	4	74

Species	Old	Young	Sum
Hypomecis punctinalis (Scopoli, 1763)	291	53	344
Fagivorina arenaria (Hufnagel, 1767)	20	0	20
Ectropis crepuscularia ([Denis et Schiffermüller], 1775)	91	64	155
Paradarisa consonaria (Hübner, 1799)	7	2	9
Parectropis similaria (Hufnagel, 1767)	4	15	19
Aethalura punctulata ([Denis et Schiffermüller], 1775)	1	2	3
Cabera pusaria (Linnaeus, 1758)	18	7	25
Cabera exanthemata (Scopoli, 1763)	3	10	13
Lomographa bimaculata (Fabricius, 1775)	4	3	7
Lomographa temerata ([Denis et Schiffermüller], 1775)	1	0	1
Campaea margaritata (Linnaeus, 1767)	202	320	522
Notodontidae			
Stauropus fagi (Linnaeus, 1758)	11	1	12
Drymonia dodonea ([Denis et Schiffermüller], 1775)	134	59	193
Drymonia ruficornis (Hufnagel, 1766)	2	6	8
Peridea anceps Goeze, 1781	3	3	6
Pterostoma palpina (Linnaeus, 1758)	0	2	2
Spatalia argentina ([Denis et Schiffermüller], 1775)	6	0	6
Ptilodon capucina (Linnaeus, 1758)	15	1	16
Ptilodon cucullina ([Denis et Schiffermüller], 1775)	3	0	3
Ptilophora plumigera ([Denis et Schiffermüller], 1775)	1	0	1
Phalera bucephala (Linnaeus, 1758)	4	2	6
Clostera pigra (Hufnagel, 1766)	1	0	1
Noctuidae			
Rivula sericealis (Scopoli, 1763)	10	4	14
Trisateles emortualis ([Denis et Schiffermüller], 1775)	4	7	11
Idia calvaria ([Denis et Schiffermüller], 1775)	0	1	1
Paracolax tristalis (Fabricius, 1794)	69	23	92
Herminia tarsipennalis Treitschke, 1835	0	4	4
Herminia tarsicrinalis (Knoch, 1782)	8	13	21
Herminia grisealis ([Denis et Schiffermüller], 1775)	24	23	47
Polypogon tentacularia (Linnaeus, 1758)	3	1	4
Zanclognatha lunalis (Scopoli, 1763)	16	8	24
Hypena proboscidalis (Linnaeus, 1758)	26	80	106
Colobochyla salicalis ([Denis et Schiffermüller], 1775)	1	1	2
Lymantria dispar Linnaeus, 1758	7	1	8
Lymantria monacha Linnaeus, 1758	22	0	22
Calliteara pudibunda (Linnaeus, 1758)	27	2	29
Spilarctia lutea (Hufnagel, 1766)	1	0	1
Diaphora mendica (Clerck, 1759)	0	1	1
Euplagia quadripunctaria (Poda, 1761)	2	3	5
Miltochrista miniata (J. R. Forster, 1771)	4	1	5
Lithosia quadra (Linnaeus, 1758)	0	1	1
Eilema depressa (Esper, [1787])	8	5	13
Eilema lurideola ([Zincken], 1817)	16	10	26
Dysauxes ancilla (Linnaeus, 1767)	1	1	2
Catephia alchymista ([Denis et Schiffermüller], 1775)	0	1	1
Minucia lunaris ([Denis et Schiffermüller], 1775)	1	1	2
Catocala nupta (Linnaeus, 1767)	6	0	6
Catocala promissa ([Denis et Schiffermüller], 1775)	3	3	6
Meganola strigula ([Denis et Schiffermüller], 1775)	7	0	7
Meganola albula ([Denis et Schiffermüller], 1775)	1	0	1
Pseudoips prasinana (Linnaeus, 1758)	0	2	2
Abrostola asclepiadis ([Denis et Schiffermüller], 1775)	1	0	1
Abrostola triplasia (Linnaeus, 1758)	1	1	2
Autographa gamma (Linnaeus, 1758)	1	0	1
Protodeltote pygarga (Hufnagel, 1766)	2	6	8
Deltote deceptoria (Scopoli, 1763)	1	0	1

Species	Old	Young	Sum
Colocasia coryli (Linnaeus, 1758)	144	85	229
Diloba caeruleocephala (Linnaeus, 1758)	1	0	1
Craniophora ligustri ([Denis et Schiffermüller], 1775)	0	2	2
Moma alpium (Osbeck, 1778)	1	3	4
Acronicta (*Jocheaera*) *alni* (Linnaeus, 1767)	0	1	1
Acronicta (*Triaena*) *tridens* ([Denis et Schiffermüller], 1775)	1	0	1
Acronicta (*Viminia*) *rumicis* (Linnaeus, 1758)	3	0	3
Amphipyra (*Amphipyra*) *pyramidea* (Linnaeus, 1758)	3	9	12
Amphipyra (*Amphipyra*) *berbera* Fletcher, 1971	1	0	1
Amphipyra (*Amphipyra*) *livida* ([Denis et Schiffermüller], 1775)	0	1	1
Amphipyra (*Amphipyra*) *tragopoginis* (Clerck, 1759)	0	1	1
Asteroscopus sphinx (Hufnagel, 1766)	8	15	23
Brachionycha nubeculosa (Esper, 1785)	0	1	1
Allophyes oxyacanthae (Linnaeus, 1758)	0	2	2
Helicoverpa armigera (Hübner, 1808)	1	0	1
Caradrina (*Caradrina*) *morpheus* (Hufnagel, 1766)	2	0	2
Caradrina (*Platyperigea*) *kadenii* Freyer, 1836	1	0	1
Caradrina (*Platyperigea*) *aspersa* Rambur, 1834	2	1	3
Hoplodrina octogenaria (Goeze, 1781)	2	0	2
Hoplodrina blanda ([Denis et Schiffermüller], 1775)	1	1	2
Hoplodrina superstes (Ochsenheimer, 1816)	1	1	2
Hoplodrina respersa ([Denis et Schiffermüller], 1775)	1	0	1
Hoplodrina ambigua ([Denis et Schiffermüller], 1775)	5	27	32
Charanyca trigrammica (Hufnagel, 1766)	0	3	3
Rusina ferruginea (Esper, 1785)	12	10	22
Athetis (*Athetis*) *furvula* (Hübner, 1808)	1	0	1
Dypterygia scabriuscula (Linnaeus, 1758)	8	14	22
Trachea atriplicis (Linnaeus, 1758)	9	5	14
Euplexia lucipara (Linnaeus, 1758)	4	15	19
Apamea monoglypha (Hufnagel, 1766)	1	0	1
Apamea syriaca tallosi Kovács et Varga, 1969	0	1	1
Apamea anceps ([Denis et Schiffermüller], 1775)	1	0	1
Loscopia scolopacina (Esper, 1788)	0	1	1
Mesapamea secalis (Linnaeus, 1758)	1	12	13
Mesapamea secalella Remm, 1983	0	3	3
Oligia latruncula ([Denis et Schiffermüller], 1775)	0	1	1
Cosmia (*Calymnia*) *trapezina* (Linnaeus, 1758)	29	98	127
Tiliacea citrago (Linnaeus, 1758)	2	6	8
Tiliacea aurago ([Denis et Schiffermüller], 1775)	1	0	1
Lithophane socia (Hufnagel, 1766)	1	3	4
Lithophane ornitopus (Hufnagel, 1766)	10	10	20
Eupsilia transversa (Hufnagel, 1766)	8	7	15
Conistra (*Conistra*) *vaccinii* (Linnaeus, 1761)	20	15	35
Conistra (*Conistra*) *rubiginosa* (Scopoli, 1763)	0	1	1
Conistra (*Conistra*) *veronicae* (Hübner, 1813)	1	0	1
Conistra (*Dasycampa*) *rubiginea* ([Denis et Schiffermüller], 1775)	0	3	3
Agrochola (*Anchoscelis*) *nitida* ([Denis et Schiffermüller], 1775)	0	1	1
Agrochola (*Anchoscelis*) *litura* (Linnaeus, 1758)	0	1	1
Agrochola (*Anchoscelis*) *helvola* (Linnaeus, 1758)	0	1	1
Agrochola (*Leptologia*) *macilenta* (Hübner, 1809)	5	6	11
Agrochola (*Sunira*) *circellaris* (Hufnagel, 1766)	0	1	1
Agrochola (*Propenistra*) *laevis* (Hübner, 1803)	7	22	29
Xanthia togata (Esper, 1788)	0	4	4
Xanthia icteritia (Hufnagel, 1766)	0	1	1
Xanthia ocellaris (Borkhausen, 1792)	0	1	1
Dichonia aeruginea (Hübner, 1808)	0	1	1
Dichonia aprilina (Linnaeus, 1758)	0	5	5

Species	Old	Young	Sum
Blepharita satura ([Denis et Schiffermüller], 1775)	17	59	76
Mythimna (*Mythimna*) *turca* (Linnaeus, 1761)	2	0	2
Mythimna (*Mythimna*) *pallens* (Linnaeus, 1758)	1	1	2
Mythimna (*Hyphilare*) *albipuncta* ([Denis et Schiffermüller], 1775)	0	4	4
Mythimna (*Hyphilare*) *ferrago* (Fabricius, 1787)	5	16	21
Polia nebulosa (Hufnagel, 1766)	0	1	1
Mamestra brassicae (Linnaeus, 1758)	4	2	6
Lacanobia (*Dianobia*) *thalassina* (Hufnagel, 1766)	5	0	5
Lacanobia (*Diataraxia*) *oleracea* (Linnaeus, 1758)	3	0	3
Hada plebeja (Linnaeus, 1761)	1	1	2
Lasionycta (*Lasionhada*) *proxima* (Hübner, 1809)	1	0	1
Orthosia (*Orthosia*) *incerta* (Hufnagel, 1766)	1	2	3
Orthosia (*Monima*) *cerasi* (Fabricius, 1775)	6	3	9
Orthosia (*Microorthosia*) *cruda* ([Denis et Schiffermüller], 1775)	22	24	46
Orthosia (*Poporthosia*) *populeti* (Fabricius, 1781)	0	2	2
Orthosia (*Cororthosia*) *opima* (Hübner, 1809)	1	0	1
Orthosia (*Semiophora*) *gothica* (Linnaeus, 1758)	3	11	14
Anorthoa munda ([Denis et Schiffermüller], 1775)	2	5	7
Agrotis exclamationis (Linnaeus, 1758)	1	2	3
Agrotis segetum ([Denis et Schiffermüller], 1775)	1	9	10
Agrotis ipsilon (Hufnagel, 1766)	0	4	4
Ochropleura plecta (Linnaeus, 1761)	5	2	7
Diarsia brunnea ([Denis et Schiffermüller], 1775)	1	0	1
Diarsia mendica (Fabricius, 1775)	1	0	1
Noctua pronuba Linnaeus, 1758	8	10	18
Noctua fimbriata (Schreber, 1759)	0	2	2
Noctua interposita (Hübner, 1790)	10	5	15
Noctua comes Hübner, 1813	3	5	8
Noctua janthina ([Denis et Schiffermüller], 1775)	0	2	2
Noctua janthe (Borkhausen, 1792)	0	1	1
Eurois occulta (Linnaeus, 1758)	0	2	2
Xestia (*Xestia*) *baja* ([Denis et Schiffermüller], 1775)	2	3	5
Xestia (*Xestia*) *stigmatica* (Hübner, 1813)	0	1	1
Xestia (*Xestia*) *castanea* (Esper, 1798)	1	0	1
Xestia (*Xestia*) *xanthographa* ([Denis et Schiffermüller], 1775)	0	2	2
Xestia (*Megasema*) *c-nigrum* (Linnaeus, 1758)	6	16	22
Xestia (*Megasema*) *triangulum* (Hufnagel, 1766)	2	0	2
Metagnorisma depuncta (Linnaeus, 1761)	9	11	20

DE GRUYTER OPEN DOI: 10.2478/aslh-2013-0005 Acta Silv. Lign. Hung., Vol. 9 (2013) 57–69

Occurrence and Diversity of Soilborne Phytophthoras in a Declining Black Walnut Stand in Hungary

Judit KOVÁCS* – Ferenc LAKATOS – Ilona SZABÓ

Institute of Silviculture and Forest Protection, University of West-Hungary, Sopron, Hungary

Abstract – The paper reports on the occurrence and impact of *Phytophthora* species in a declining eastern black walnut (*Juglans nigra*) stand in West Hungary. The health condition of the trees was investigated and soil samples were taken from the rhizosphere of the trees two times per year in 2011 and 2012 in order to isolate *Phytophthora* species. Altogether 20 trees were selected for investigations. The species identity of the isolates was determined by morphological and molecular methods. *Phytophthora cactorum* and *Phytophthora plurivora* were found as supposedly responsible for the decline of the trees. The abundance of the two species was changing at the different sampling times, presumably due to the different weather conditions. The intraspecific diversity of both species was estimated based on the ITS1-5.8S-ITS2 sequences of the isolates.

eastern black walnut / *Phytophthora cactorum* / *Phytophthora plurivora* / tree decline

Kivonat – Phytophthora fajok gyakorisága és diverzitása egy pusztuló feketedió állományban Magyarországon. A tanulmány egy pusztuló nyugat-magyarországi fekete dió (*Juglans nigra*) állományban előforduló *Phytophthora* fajokról, és azok faállományra gyakorolt hatásáról tudósít. A szerzők vizsgálták a faállomány egészségi állapotát, illetve talajmintákat gyűjtöttek a fák gyökérzónájából a *Phytophthora* fajok kitenyésztése céljából. A vizsgálatokat 20 megjelölt fán végezték, 2011-ben és 2012-ben, évente 2–2 alkalommal. Az izolátumok azonosítása morfológiai és molekuláris genetikai módszerekkel történt. *Phytophthora cactorum*-ot és *Phytophthora plurivora*-t találtak, mint a pusztulás valószínűsíthető okát. A két faj gyakorisága eltérő volt a különböző mintavételi időpontokban, feltehetően az eltérő időjárási viszonyok miatt. A két faj diverzitását az izolátumok ITS1 – 5.8S – ITS2 szekvenciái alapján becsülték.

fekete dió / *Phytophthora cactorum* / *Phytophthora plurivora* / fapusztulás

1 INTRODUCTION

Some species of the genus *Phytophthora* (*Oomycota*) are harmful and destructive pathogens of forest trees (Hansen 2008).These species cause root rot, bleeding cankers or wilting symptoms on susceptible forest trees (Erwin – Ribeiro 1996). There are soilborne, waterborne and aerial species within this genus. Inside a forest, or between woodlands, soilborne and waterborne species can spread via irrigation water, ground water or splashes. The spores of the aerial species are delivered by the wind. Phytophthoras can easily spread between

* Corresponding author: kovacsj@emk.nyme.hu; H-9400 SOPRON, Bajcsy-Zs. u. 4

countries or continents with infected plants or soil. Twenty-one percent of the invasive plant pathogens in Europe belong to the genus *Phytophthora* (Santini et al. 2012). The impact of these invasive pathogens is unpredictable (Brasier – Webber 2010). Under favourable conditions, the ecological and economical loss might be huge.

Up to 2010, 98 formally described species and 2 species hybrids belong to the genus *Phytophthora* (Érsek – Ribeiro 2010). The number of the described species grew and expectedly will continue growing because of multiple reasons: the available molecular tools enable a quick and accurate identification, the number of *Phytophthora* research groups and the attention on forest Phytophthoras grows worldwide, and also because of the recent evolutionary processes within the genus (Érsek – Ribeiro 2010).

Since the beginning of the 20th century, Phytophthoras have been responsible for many diseases and declines in European forests. The ink disease of sweet chestnut spread as an epidemic in the 1920–1940s and beyond the chestnut blight caused by *Cryphonectria parasitica*, it is still one of the main diseases of *Castanea sativa* (Vannini – Vettraino 2001). Since the 1990s, an upswing is present in the number of epidemics caused by *Phytophthora* species. *Phytophthora cinnamomi* endangers a uniqe agroforestal ecosystem, the so called 'dehesa' in the Iberian Peninsula by killing the holm oak (*Quercus ilex*) and cork oak (*Quercus suber*) since 1991 (Brasier 1996; Moralejo et al. 2009). The infected trees show wilting symptoms and die within a few years. The disease is spreading continuously.

A decline was noticed in the deciduous oak forests of North- and Central-Europe in the mid of the 1990s. The climatic instability, the acid soils with moderate water conditions and *Phytophthora* species, like *P. cambivora, P. citricola, P. gonapodyides, P. cactorum, P. syringae, P. europaea* and mainly *P. quercina* played a role in this complex decline (Jung et al. 1999, Jung et al. 2000, Balci - Halmschlager 2003).

In 1993, a decline of riverside alders *(Alnus glutinosa)* was noticed in Great Britain. The trees showed wilting symptoms. On the stem, cankers and tarry exudations were observed (Brasier et al. 1995). An unknown *Phytophthora* was isolated from the infected bark samples. The pathogen caused an epidemic across Europe. In 1995, it was found in Germany, Belgium, in the Netherlands and France, in 1996 also in Austria and Hungary (Cech 1997, Szabó et al. 2000). The molecular analysis of the isolates showed that it is a natural, interspecific hybrid. It was formally described as *Phytophthora alni* in 2004 (Brasier et al. 2004).

Many *Phytophthora* species were isolated from bleeding cankers found on Europaean beech *(Fagus sylvatica)* trunks or soil samples from the rhizosphere of declining beech trees since 2000. These species are *P. cactorum, P. cambivora, P. citricola, P. plurivora* and in Great Britain, 2 invasive quarantine species, *P kernoviae* and *P. ramorum* (Brasier et al. 2005, Weiland et al. 2010, Jung 2009). The last two species can became an extreme threat to the European and North-American forests. Pedunculate oak (*Quercus robur*) can be infected by *P. kernoviae* too (Brasier et al. 2005), while many other tree species, like North-American coastal live oaks, Douglas-fir (*Pseudotsuga menziesii*), coast redwood (*Sequoia sempervirens*) and yew (*Taxus baccata*), and ornamental shrubs like *Viburnum spp*., *Rhododendron spp*., *Syringa vulgaris*, *Pieris spp*. and *Vaccinium spp*. are also susceptible for *P. ramorum* (Grünwald et al. 2008). However, till 2009 the *P. ramorum* infections in European forests were local, mainly near highly susceptible viburnums and rhododendrons. An epidemic similar to the North-American Sudden Oak Death was noticed in 2009 in Japanese larch (*Larix kaempferi*) plantations in South-West England. This host jump elucidates the potential threats of invasive pathogens (Brasier – Webber 2010).

According to a previous research of the Institute of Sylviculture and Forest Protection, (University of West Hungary, Hungary) *Phytophthora* species infect common alder (*Alnus glutinosa*), eastern black walnut (*Juglans nigra*), sessile oak (*Quercus petraea*) and Turkey oak (*Quercus cerris*) stands in Hungary (Szabó – Lakatos 2008, Szabó et al. 2013).

The genus *Juglans* consists of ~21 taxa, with an extensive distribution from East Asia to the Americas. The black walnuts (Section *Rhysocaryon*) are native to the Americas. They include six North-American, three Central American and four South American species. An other American species (*Juglans cinerea*), native to eastern North America belongs to the section Trachycaryon. The English walnut (*Juglans regia*, Section *Juglans*) is the only native species in Europe. Its distribution is ranging from Europe to China and the Himalayas. The other species belonging to the Section *Cardiocaryon* are native to East Asia (Aradhya et al. 2007). English walnut is the most widely cultivated species from the genus throughout the world for nuts and also for timber production (Belisario – Galli 2013). However, black walnuts and hybrid rootstocks (i. e. Paradox rootstock) are widely cultivated, economically important species, too.

J. regia and *J. nigra* are two economically important hardwood species in Hungary. They grow on marshlands and riparian sites. Although the stands of eastern black walnut as an exotic tree species cover only 0,5% of Hungary's forest area, the timber of this species is valuable for furniture industry (Molnár – Bariska 2006).

The two closely related species share some common diseases. One of these is the *Phytophthora* root and collar rot of walnuts, which is an increasing cause of walnut loss in Europe and also in North America (Belisario – Galli 2013).

Twelve *Phytophthora* species are known as pathogens of walnut species, affecting seedlings and also mature trees worldwide. These species are *P. cactorum*, *P. citricola*, *P. cinnamomi*, *P. citrophthora*, *P. cryptogea*, *P. megasperma*, *P.cambivora*, *P. drechsleri*, *P. hedraiandra*, *P. nicotianae*, *P. palmivora* and *P. plurivora* (Mircetich – Matheron 1983, Belisario – Galli 2013).

There are no specific symptoms of *Phytophthora* infection in *Juglans* species. Laboratory methods are required to identify the cause of the decline. *Phytophthora* species can cause various disease symptoms on different parts of the tree. In the crown, wilting, small, yellowish leaves or sudden death can be observed. On the stem, bleeding cankers, tary spots or also large, dark, flame-shaped areas may be present. A main symptom of the disease is the rot of the root system. Usually the young feeder roots die first which is later followed by the death of the older roots (Belisario – Galli 2013). The development of visible symptoms depends always on the amount of infected roots, which is in context with the inoculum density of the soil. It can be a sudden death during summertime or a slow decline with a progressive reduction of foliage and fruit production over several years (Belisario – Galli 2013). Sudden death is mainly characteristic to infections caused by *P. cinnamomi* (Belisario – Galli 2013). In the case of a slow wilting, the infection may be undetected in the first years. Some trees also can survive the infection without notable crown symptoms (Belisario – Galli 2013).

The distribution of the pathogen, the infections and the disease severity is in context with the soil moisture and the duration of soil saturation (Belisario – Galli 2013). However, trees can be infected also by occasionally occurring floodings (Vettraino et al. 2003).

In the early 2000s, decline of eastern black walnut (*Juglans nigra*) stands was observed in Hungary, in South-Danubian floodplain forests in Gemenc. The canopy of over 80 years old trees showed wilting symptoms despite of adequate soil humidity and lack of any other visible reason of the decline. *Phytophthora* species were isolated from the soil. *P. cactorum* and *P. plurivora* were the most frequently occurring species. The pathogenicity of these species was confirmed by inoculation of black walnut seedlings (Szabó – Lakatos 2008). Since that time similar symptoms were observed in old black walnut stands in some other regions of Hungary, also in the north-western part of the country.

Many investigations have been done in the last decades in order to better understand the *Phytophthora* disease of English walnut. Matheron and Mircetich pointed out that the

susceptibility of *J. regia* seedlings against *P. citricola* shows seasonality. Their susceptibility is higher in summer and in the beginning of autumn than from late autumn to spring (Matheron – Mircetich 1985a). Vettraino et al. showed that the five most frequently isolated Phytophthoras cause different symptoms under the same conditions. According to their study, *P. cinnamomi* is the most pathogenic species against English walnut, *P. cactorum* and *P. cambivora* are slow colonizers which damages also lateral fine roots, while *P. citricola* causes the rot of lateral fine roots, but does not damage the taproot (Vettraino et al. 2003).

Our aims were to study the changes of health condition of an affected stand, the diversity of soilborne *Phytophthora* community in the rhizosphere of the trees, to test the pathogenicity of the isolated species against *J. nigra* seedlings and to study whether there is a seasonality or not in the *Phytopthora* composition of the soil of the infected trees.

2 MATERIALS AND METHODS

2.1 Sampling

Twenty black walnut trees were selected for sampling in a 73 years old marshland forest near Kapuvár, Hungary. The site investigated is on alluvial meadow soil with periodic water effect.

The health condition of the trees was evaluated based on the crown symptoms using the following 4-pointed scale:

1. Healthy crown.
2. Less than 20% of the crown is dying. Some leaves are yellowish.
3. 20–50% of the crown is dying. Leaves with yellowish discolouration in larger groups.
4. More than 50% of the crown is dead. Yellow leaves in large groups, or the remaining foliage is yellow.

Soil samples were taken from the rhizosphere of each investigated tree with a final volume of 1 litre. The sampling was done at four different point within 1 metre around each tree, from a depth of 5–30 centimetres. The aliquots were mixed.

2.2 Isolation

A quantity of approximately 250 mg from each mixed soil sample was flooded with 500 ml distilled water in a flat plastic container of a volume of 2 litres. The isolation of Phytophthoras was performed by using healthy, freshly picked, young *Rhododendron* and *Prunus laurocerasus* leaves as baits (Themann – Werres 1998, Nagy et al. 2000). The leaves were surface-disinfected with 10% NaOCl solution and rinsed in water before use. The samples were incubated in 22 °C, on daylight. Necrotic spots appeared on the leaves within 2-4 days. A piece of a size of 5x5 mm was cut from the infected leaf sections and put on the surface of *Phytophthora* selective agar plates (*Figure 1*). The medium used contained 1,5% malt extract and 2% bacteriological agar. Ampicillin (250 mg/l), Benomyl (15 mg/l) and hymexazol (50 mg/l) were added to the medium before use.

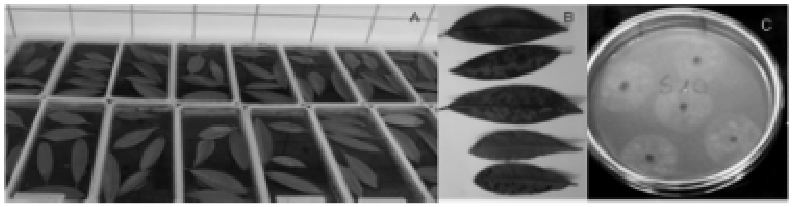

Figure 1. The method of isolation: A: leaf baits on the soil samples B: Characteristic lesions on the baits C: Phytophthora colonies on Phytophthora-selective agar media

2.3 Species identification

The species identification was done by using morphological features and ITS sequences.

The morphological features were studied on cultures grown on carrot agar (Brasier 1969), at 20°C, in the dark. The formation of sporangia was induced by non-sterile soil solution (Jeffers and Aldwinckle 1987). Daily growth rate, colony patterns and morphology of microscopic structures were investigated (Erwin – Ribeiro 1996).

The molecular identification of the isolates was made by amplifying and sequencing the ITS1-5.8S-ITS2 region of the rDNA of selected isolates. Pure mycelial cultures were used for DNA extraction or direct PCR. The DNA extraction and the PCR was made with the REDExtract N-Amp Plant Kit (Sigma – Aldrich), or with the PHIRE Plant Direct PCR Kit (Thermo Scientific) according to the user's guide of the manufacturers. ITS6 and ITS4 primer pair (Cooke – Duncan 1997) was used for PCR, in an Eppendorf Mastercycler Personal PCR machine. PCR conditions were as described by Cooke and Duncan (1997). The resulting PCR products were purified with EZ-10 Spin Column PCR Purification Kit (BioBasic Inc.), according to the user's guide of the manufacturer. The purified products were sequenced in both directions. Sequences were corrected and aligned with the ClustalX software. Homologs were searched in the GenBank (NCBI database) using BLASTN software (http://blast.ncbi.nlm.nih.gov/Blast.cgi).

2.4 Estimation of the genetic diversity

The genetic diversity of the isolated species was estimated based on the ITS1 – 5.8S – ITS2 sequences. The sequences were compared by using the Clustal X software. Only complete, error-free sequences were used for the comparison.

2.5 Pathogenicity tests

Two strains were used for pathogenicity tests. A *P. plurivora* strain (202a) isolated in September 2011 and a *P. cactorum* strain (174/2) isolated in June 2011 from the studied black walnut stand. The colonies used were 14 days old. They were grown on Potato-Dextrose Agar plates (39g/L, Microtrade Ltd., Budapest, Hungary).

3,5 months old black walnut seedlings were infected. The seedlings were grown from disinfected seeds in containers. The soil used for planting was investigated with the above mentioned leaf baiting method and proved to be free of Phytophthoras. Eight seedlings/isolate and eight seedlings as control (totally 24 seedlings) were used for the tests.

The infection was done on 8th September 2012. A wound of a diameter of 5 mm was made on the base of the stem and a piece of a 5mmx5mm size from the pathogen colony was put into the wound. After that, the wound was closed with plastic paraffin film (Parafilm® Pechiney Plastic Packaging Company). The wounds on the control seedlings were closed with Parafilm without any infection.

The seedlings were watered as it was necessary. They were overwintered in a frostfree, closed chamber. The mean temperature and the humidity of the chamber fluctuated according to the weather conditions outside. Their parameters (length and diameter of the shoots, length and width of the roots, health condition of the shoots and roots and especially the length and width of the bark necrosis caused by the pathogens on the stem) were measured after 10 months, in July 2013.

2.6 Data analysis

The health condition datasets were analysed with the IBM SPSS 20 Software (IBM Corp. 2011). We used Kruskall-Wallis and Mann-Whitney tests to see the change in the health condition of our sampling site.

Data resulted from the pathogenicity tests were also analysed with the IBM SPSS 20 Software. The Gaussian distribution of data sets was tested with the Shapiro-Wilks method. The homogenicity of variances of the variables was tested with Levene statistic, based on the median. To test differences between the two infected and the non-infected groups, One-Way ANOVA was used. Independent Samples T-test was used to test differences between the two infected groups in case of necrosis area data sets.

In order to understand the changes in species composition, daily temperature and precipitation data of the region were collected from the database of the Hungarian Meteorological Service (http://www.met.hu/idojaras/aktualis_idojaras/napijelentes/). Walter-Lieth diagrams were constructed from these data with a free, online software (http://www.zivatar.hu/script.php?id=walter-lieth).

3. RESULTS AND DISCUSSION

3.1 Changes in the health condition

The health condition of the trees (*Figure 2*.) got significantly (*P = 0,023*) worse during the experiment according to the Kruskal-Wallis test. Healthy tree could be found only at the very first investigation (1 tree). The number of trees belonging to the 2nd category decreased from 9 to 3 trees, while the number of trees in the 3rd and especially in the 4th category increased (from 7 to 8 in case of 3rd, and from 3 to 9 in case of 4th category). However, we couldn't find any dead trees till the end of the monitoring period.

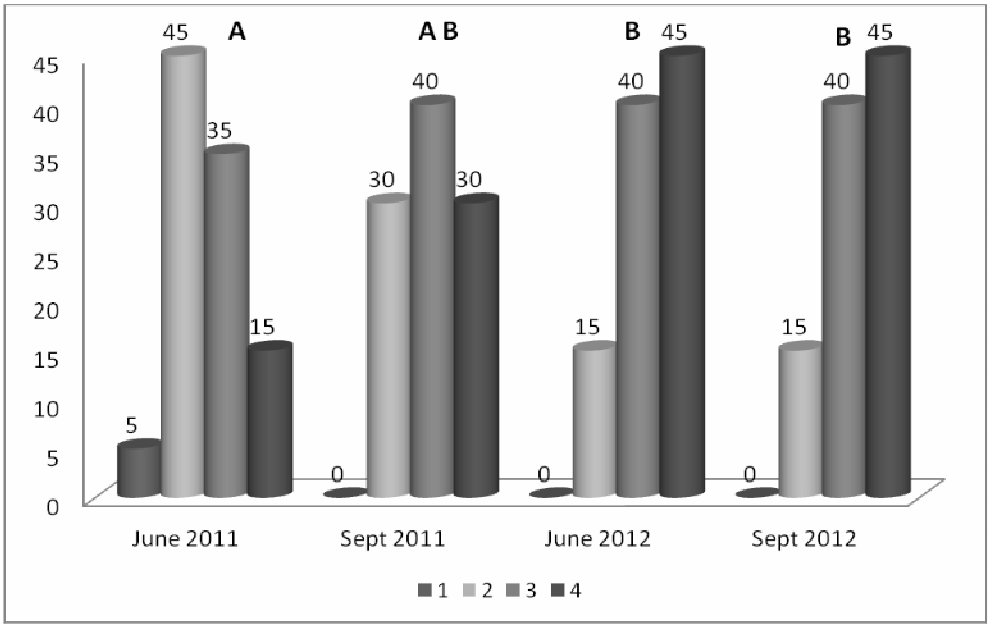

Figure 2: Changes in the health condition of the eastern black walnut trees. Categories: 1. Healthy crown; 2. Less than 20% of the crown is dying, some leaves are yellowish. 3. 20–50% of the crown is dying. Leaves with yellowish discolouration in larger groups. 4. More than 50% of the crown is dead. Yellow leaves in large groups or the remaining foliage is yellow. Values are in % of the investigated trees. The health condition of the trees in June 2011(A) is significantly different from their health condition in 2012 (B).

There was significant difference (*P = 0,009*) in the health condition of the sampling site between the investigations of June 2011 and June 2012 according to the Mann-Whitney test.

3.2 Isolation success and species composition

The isolation success was the highest in June 2011. Phytophthoras could be isolated from 75% of the collected soil samples then. After that, in September 2011 and June 2012 the isolation was succesfull only from 20% of the collected samples. The isolation success was a bit higher in September 2012. Phytophthoras could be isolated from 40% of the collected samples that time. There were two species constantly present in the soil samples: *P. plurivora* and *P. cactorum*. They were present in the rhizosphere of every selected tree, at least one time during the two – year period.

The distribution of the two species changed during the investigation (*Figure 3.*). Both species were present in June 2011 and September 2012, but only *P. plurivora* could be isolated at the other times.

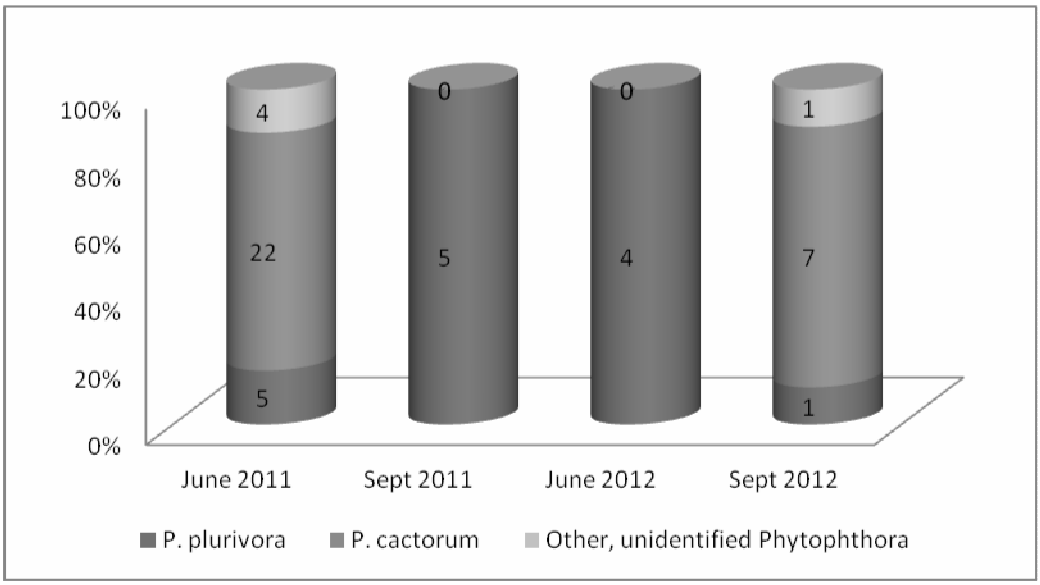

Figure 3. Species composition of Phytophthoras at different sampling times

This suggests that both species are constantly present in the soil of the forest stand. However, *P. cactorum* survives the unfavourable conditions with forming chlamydospores and oospores. When the environmental conditions become favourable, oospores and chlamydospores of *P. cactorum* can well germinate. The infection can be very serious in the case of heavy, flooded, poorly drained soils (Erwin – Ribeiro 1996).

Unlike *P. cactorum*, *P. plurivora* cannot form any chlamydospores. It can survive unfavourable environmental conditions only by forming oospores. This species is less competitive in wet, flooded soils, because supposedly semiarid – wet soils are optimal for it. However, it can infect walnut trees also under unflooded conditions (Matheron – Mircetich 1985b).

In the first year of our study, the spring and the first half of the summer was rainy. The Walter-Lieth diagram of the year 2011 (Figure 4.) shows this time as a humid period.

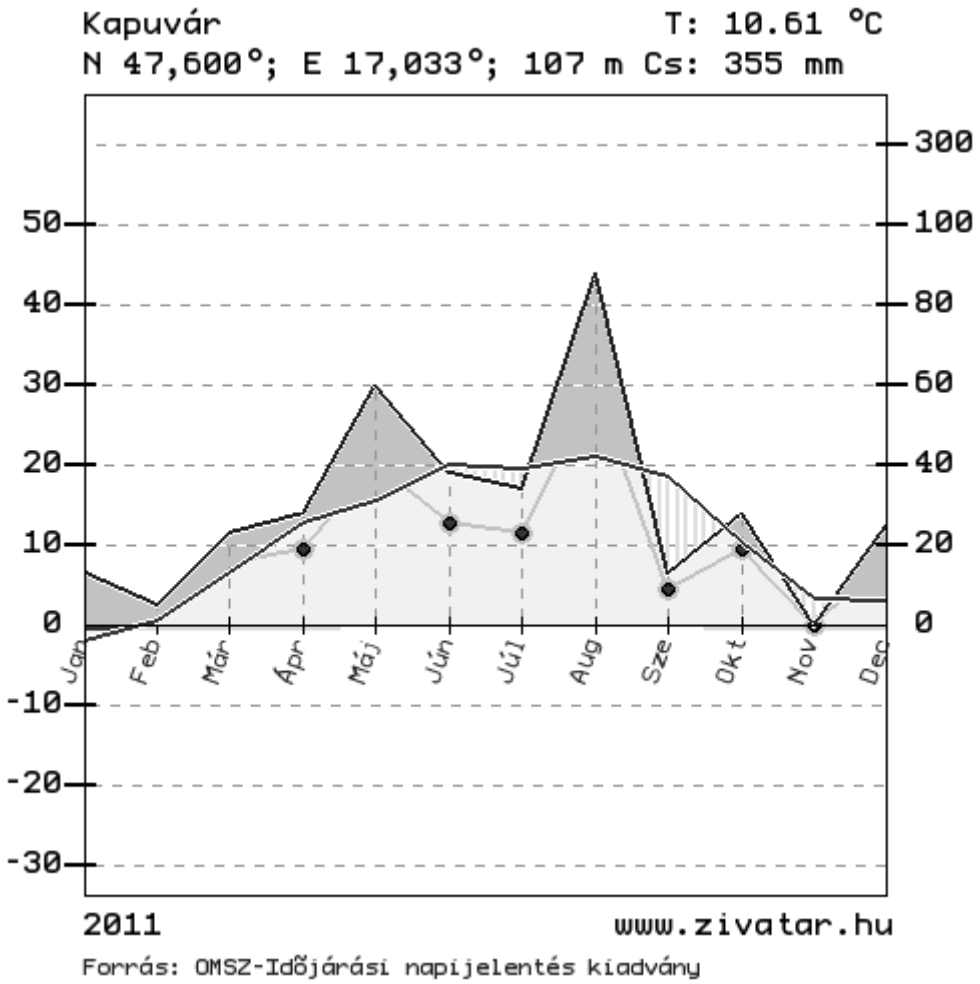

Figure 4. Walter-Lieth diagram of the sampling site in 2011 based on the data of the Hungarian Meteorological Service (http://www.met.hu/idojaras/aktualis_idojaras/napijelentes/). Dark grey: humid periods; striped: arid periods.

After 3 heavy rainfalls in the first week of August, the second half of the summer and the autumn was hot and dry, with unusual arid periods, especially in September. *P. cactorum* was dominant in June, when the forest soil was wet. Later, in mid of September, the soil was drier. This time the isolation success was lower, and we could only find *P. plurivora*.

Next year, after a dry autumn and winter in 2011, we had an extremely dry spring in 2012. According to the Walter-Lieth diagram of 2012 *(Figure 5*), the arid period began in May and lasted till September in the region.

The isolation success was low again in June, and only *P. plurivora* could be isolated. The summer was very hot, with a few big rainfall in the region mostly in the second half of July, and with some rainy days in August and September. The isolation success was a bit higher, and we could isolate mostly *P. cactorum* from the slightly wetter soil samples this time.

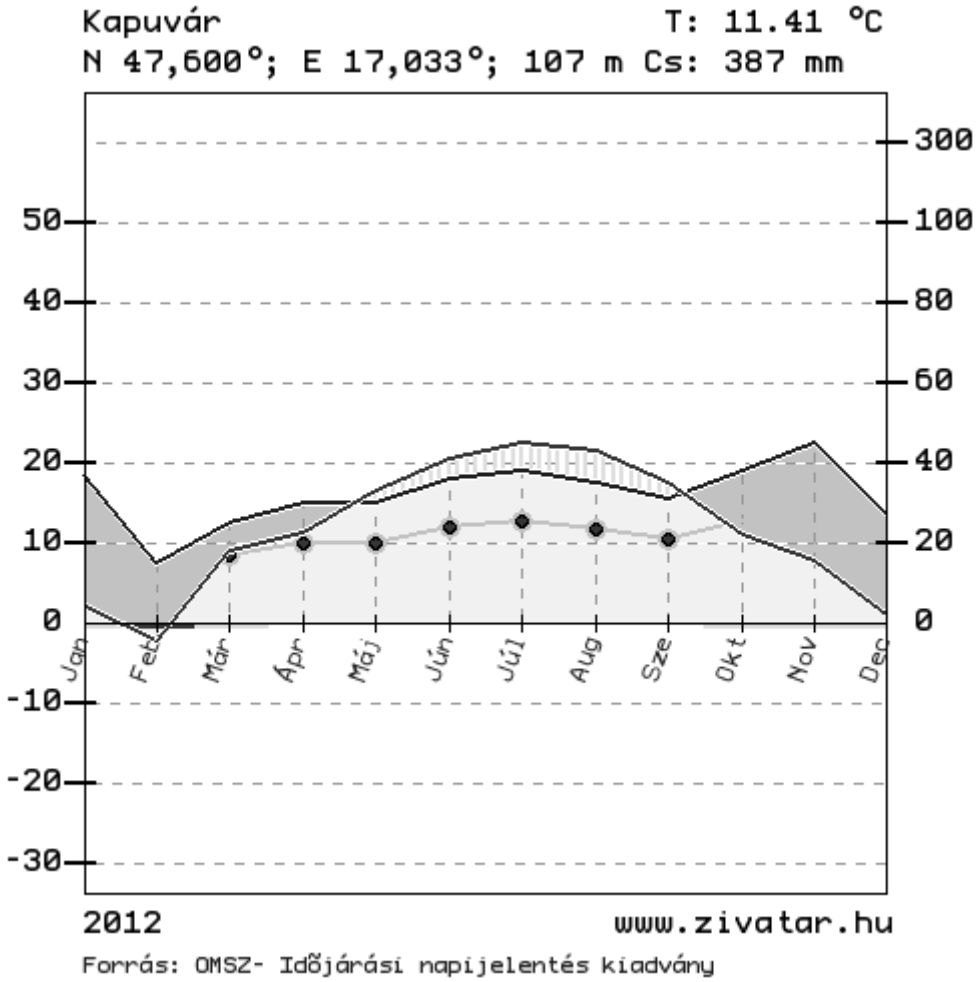

Figure 5. Walter-Lieth diagram of the sampling site in 2012 based on the data of the Hungarian Meteorological Service (http://www.met.hu/idojaras/aktualis_idojaras/napijelentes/). Dark grey: humid periods; striped: arid periods.

3.3 Intraspecific diversity

The genetic diversity of the two species was estimated based on ITS sequences. The examined fragment was 797bp long. 15 *P. cactorum* isolates and 8 *P. plurivora* isolates were analysed.

P. cactorum strains differed in 2 positions and 4 different haplotypes could be detected from which 3 haplotypes were frequent (*Table 1.*).

Table 1. Estimated haplotypes of P. cactorum *on the sampling site*

20	611	Haplotype	Number of isolates
–	A	CACTORUM 1	5
–	G	CACTORUM 2	4
A	A	CACTORUM 3	5
A	G	CACTORUM 4	1

P. plurivora strains were quite uniform, 2 haplotypes could be detected (*Table 2*). They differ only at one position. The first haplotype was much more frequent. The 2nd one is represented by only one isolate originating from the collection of the first sampling time.

Table 2. Estimated haplotypes of P. plurivora *on the sampling site*

402	Haplotype	Number of isolates
C	PLURIVORA 1	7
T	PLURIVORA 2	1

Both isolated species are cosmopolitan (Erwin – Ribeiro 1996). The poor genetic diversity especially in the case of *P. plurivora* can suggest that it might be a relatively new species in the studied region (Szabó et al. 2013).

3.4 Pathogenicity

All of the infected seedlings remained alive during the test period. Their health condition was similar as the health condition of the control plants. The stem diameter of the seedlings belonging to the control and the two infected groups was not significantly different (P = 0,107) at α=0,05 significance level according to the results of the One-Way ANOVA. However, according to the size of the necrosis on their stem, both pathogen strains turned to be moderately pathogenic to black walnut. The size of the necrosis in case of *P. plurivora* was 39,27–235,62 mm^2 (average size: 126,25 mm^2), while in case of *P. cactorum* it was 32,99-102,10 mm^2 (average: 62,93 mm^2). *P. plurivora* was slightly more aggressive than *P. cactorum*. This result agrees with the statement of Mircetich and Matheron (Mircetich – Matheron 1980). The area of the necrosis (Figure 6.) proved to be significantly larger in the two infected groups than in the case of the control seedlings at α=0,05 significance level, according to the One-Way ANOVA (P = 0,001). According to the T- test, *P. plurivora* caused significantly longer necrosis than *P. cactorum* did at α=0,05 significance level (P = 0,024).

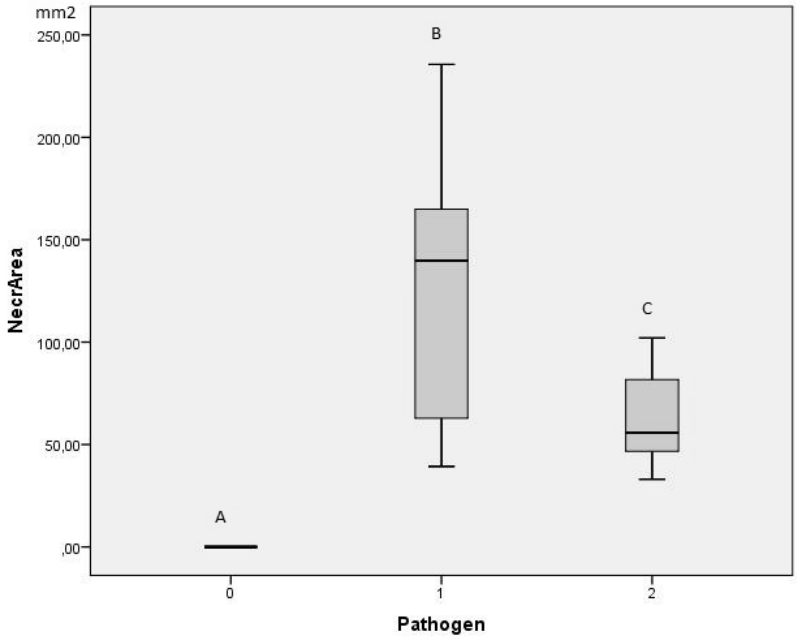

Figure 6. Necrosis area in case of the different groups. 0: seedlings without infection. 1: P. plurivora . 2: P. cactorum. The groups labelled with different letters are significantly different according to the One-Way ANOVAs and the t- test.

4. SUMMARY

Two *Phytophthora* species, *P. cactorum* and *P. pluri*vora were isolated from the rhizosphere soil of the declining old black walnut stand. These two species were also earlier frequently isolated by Szabó et al. (2013). However, we could not find *P. lacustris* as they did earlier. The health condition of the selected trees got worse during the two-years-period of the experiment. However, we couldn't find any dead trees yet. Changes could be observed in the isolation success. These changes don't show any seasonality. They could be related to the current environmental conditions, primarily with the humid or arid character of the weather conditions. The changes in the health condition of the studied eastern black walnut trees seem to confirm this. Their health condition continuously got worse in the first humid year of our investigation, while it was unaltered in the second, quite arid year. It would be necessary to continue the monitoring to find the correct correlation. Both *Phytophthora* species were isolated from the rhizosphere of every selected tree, at least at one sampling time.

The identified species composition had also changes during the two years. *P. plurivora* could be isolated always, while *P. cactorum* only in June 2011 and September 2012. When we could isolate both species, *P. cactorum* was more frequent than *P. plurivora*. We suppose that both species are present in the soil. However, *P. plurivora* is more competitive in semi-arid - wet soil, while *P. cactorum* prefers wet, flooded soil, where *P. plurivora* is less competitive. The poor genetic diversity of these species suggests that they were perhaps introduced into the region recently. Both isolated species proved to be moderately aggressive to eastern black walnut seedlings. The necroses caused by *P. plurivora* were longer than those caused by *P. cactorum*, suggesting that this species is slightly more aggressive to eastern black walnut seedlings than *P. cactorum*.

The above mentioned are preliminary results of a two-years long study. It would be necessary to do a proper analysis of weather condition data and to continue the monitoring in order to understand better the process of the decline.

Acknowledgements: We wish to thank to the staff of the KAEG State Forest Holding Company, who allowed us to do investigations in their black walnut stand, to Dr. Gy. Sipos , R. Dankóné, I. Kovács, E. Kovács and to B. Sárándi for their help. We also would like to thank to TÁMOP 4.2.1.B-09/1/KONV-2010-0006 and "TALENTUM" TÁMOP 4.2. 2/B – 10/1 – 2010 – 0018 for the financial support.

REFERENCES

ARADHYA, M. K. – POTTER, D. – GAO, F. – SIMON, C. J. (2007): Molecular phylogeny of *Juglans* (Juglandaceae): a biogeographic perspective. Tree Genetics & Genomes 3: 363–378.

BALCI, Y. – HALMSCHLAGER, E. (2003): Incidence of *Phytophthora* species in oak forests in Austria and their possible involvement in oak decline. Forest Pathology 33: 157–174.

BELISARIO, A. – GALLI, M. (2013): *Phytophthora* on *Juglans spp*. (walnuts). JKI Data Sheets: Plant Diseases and Diagnosis. 2012:7.

BRASIER, C. M. (1969): The effect of light and temperature on reproduction in vitro in two tropical species of *Phytophthora*. Transactions of the British Mycological Society 52: 105–113.

BRASIER, C. M. (1996): *Phytophthora cinnamomi* and oak decline in southern Europe. Environmental constraints including climate change. Annals of Forest Science 53: 347–358.

BRASIER, C. – WEBBER, J. (2010): Sudden larch death. Nature. 466: 824–825.

BRASIER, C. M. – ROSE, J. – GIBBS, J. N. (1995): An unusual *Phytophthora* associated with widespread alder mortality in Britain. Plant Pathology 44: 999–1007.

BRASIER, C. – KIRK, S. A. – DELCAN, J. – COOKE, D. E. L. – JUNG, T. – MAN IN'T VELD, W. A. (2004): *Phytophthora alni* sp. nov. and its variants: designation of emerging heteroploid hybrid pathogens spreading on *Alnus* trees. Mycological Research 108 (10): 1172–1184.

BRASIER, C. M. – BEALES, P. A – KIRK, S. A. – DENMAN, S., ROSE, J. (2005): *Phytophthora kernoviae* sp. nov., an invasive pathogen causing bleeding stem lesions on forest trees and foliar necrosis of ornamentals in the UK. Mycological Research 109 (8): 853–859.

CECH, T. (1997): *Phytophthora*- Krankheit der Erle in Österreich. Forstschutz Aktuell 19 (20): 14–16.

COOKE, D. E. L. – DUNCAN, J. M. (1997): Phylogenetic analysis of *Phytophthora* species based on the ITS1 and ITS2 sequences of ribosomal DNA. Mycological Research 101: 667–677.

ERWIN, D. C. – RIBEIRO, O. K. (1996): *Phytophthora* Diseases Worldwide. APS Press, St. Paul, Minnesota. 562p.

ÉRSEK, T. – RIBEIRO, O. K. (2010): Mini Review Article: An Annotated List of New *Phytophthora* Species Described Post 1996. Acta Phytopathologica et Entomologica Hungarica 45 (2): 251–266.

GRÜNWALD, N. J. – GOSS, E. M. – PRESS, C. M. (2008): *Phytophthora ramorum*: a pathogen with a remarkably wide host range causing sudden oak death on oaks and ramorum blight on woody ornamentals. Molecular Plant Pathology 9 (6): 729–740.

HANSEN, E. M. (2008): Alien forest pathogens: *Phytophthora* species are changing world forests. Boreal Environment Research 13: 33–41.

JEFFERS, S. N. – ALDWINCKLE, H. S. (1987): Enhancing detection of *Phytophthora cactorum* in naturally infested soil. Phytopathology 77: 1475–1482.

JUNG, T. (2009): Beech decline in Central Europe driven by the interaction between *Phytophthora* infections and climatic extremes. Forest pathology 39 (2009): 73–94.

JUNG, T. – COOKE, D. E. L. – BLASCHKE, H. – DUNCAN, J. M. – OßWALD, W. (1999): *Phytophthora quercina* sp. nov., causing root rot of European oaks. Mycological Research 103 (7): 785–798.

JUNG, T. – BLASCHKE, H. – OßWALD, W. (2000): Involvement of soilborne *Phytophthora* species in Central European oak decline and the effect of site factors on the disease. Plant Pathology 49: 706–718.

MATHERON, M. E. – MIRCETICH, S. M. (1985a): Seasonal Variation in Susceptibility of *Juglans hindsii* and Paradox Rootstocks of English Walnut Trees to *Phytophthora citricola*. Phytopathology 75: 970–972.

MATHERON, M. E. – MIRCETICH, S. M. (1985b): Influence of Flooding Duration on Development of *Phytophthora* Root and Crown Rot of *Juglans hindsii* and Paradox Walnut Rootstocks. Phytopathology 75: 973–976.

MIRCETICH, S. M. – MATHERON, M. E. (1980): *Phytophthora* root and crown rot of walnut trees. Walnut Research Reports (1980):21. http://walnutresearch.ucdavis.edu/year_results.asp 2012. 08. 16. 22:34.

MIRCETICH, S. M. – MATHERON, M. E. (1983): *Phytophthora* root and crown rot of walnut trees. Phytopathology 73: 1481–1488.

MOLNÁR, S. – BARISKA, M. (2006): Wood species of Hungary. Szaktudás Kiadó Ház, Budapest. 102 p.

MORALEJO, E. – PÉREZ–SIERRA, A. M. – ÁLVAREZ, L. A. – BELBAHRI, L. – LEFORT, F. – DESCALS, E. (2009): Multiple alien *Phytophthora* taxa discovered on diseased ornamental plants in Spain. Plant Pathology 58:100–110.

NAGY, Z. – SZABÓ, I. – BAKONYI, J. – VARGA, F. – ÉRSEK, T. (2000): A mézgás éger fitoftórás betegsége Magyarországon. [*Phytophthora* disease of common alder in Hungary.] Növényvédelem 36 (11): 573–579 (in Hungarian).

SANTINI, A. – GHELARDINI, L. – PACE, C.De. – DESPREZ-LOUSTAU, M. L. . – CAPRETTI, P. – CHANDELIER, A. – CECH, T. – CHIRA, D. – DIMANDIS, S. – GAITNIEKIS, T. – HANTULA, J. – HOLDENRIEDER,O. – JANKOVSKY, L. – JUNG, T. – JURC, D. – KIRISITS, T. – KUNCA, A. – LYGIS, V. – MALECKA, M. – MARCAIS, B. – SCHMITZ, S. – SCHUMACHER, J. – SOLHEIM, H. – SOLLA, A. – SZABÓ, I. – TSOPELAS, P – VANNINIA. – VETTRAINO, A. M. – WEBBER, J. – WOODWARD, S. – STENLID, J. (2012): Biogeographical patterns and determinants of invasion by forest pathogens in Europe. New Phytologist 197 (1): 238–250.

SZABÓ, I. – NAGY, Z. Á. – BAKONYI, J. – ÉRSEK, T. (2000): First report of *Phytophthora* root and collar rot of alder in Hungary. Plant Disease 84 (11): 1251.

SZABÓ, I. – LAKATOS, F. (2008): Pusztuló erdőállományokból izolált *Phytophthora* fajok Magyarországon. [*Phytophthora* species isolated from declining forests in Hungary.] Növényvédelem 44 (12): 607–613 (in Hungarian).

SZABÓ, I. – LAKATOS, F. – SIPOS, Gy.(2013): Occurrence of soilborne *Phytophthora* species in declining broadleaved forests in Hungary. European Journal of Plant Pathology 137 (1): 159–168.

THEMANN, K. – WERRES, S. (1998): Use of *Rhododendron* leaves to detect *Phytophthora* species in root and soil samples. Nachrichtenblatt des Deutschen Pflanzenschutzdienstes 50 (2): 37–45.

VANNINI, A. – VETTRAINO, A. M. (2001): Ink disease in chestnuts: impact on the European chestnut. Forest Snow and Landscape Research 76 (3): 345–350.

VETTRAINO, A. M. – BELISARIO, A. – MACCARONI, M. – VANNINI, A. (2003): Evaluation of root damage to English walnut caused by five *Phytophthora* species. Plant Pathology 52: 491–495.

WEILAND, J. E. – NELSON, A. H. – HUDLER, G. W. (2010): Aggressiveness of *Phytophthora cactorum, Phytophthora citricola* I. and *Phytophthora plurivora* from European Beech. Plant Disease 94 (8): 1009–1014.

Hungarian Meteorological Service (2013): Daily reports of the Hungarian Meteorological Service Online: http://www.met.hu/idojaras/aktualis_idojaras/napijelentes/ .

Online software for drawing Walter-Lieth diagram: http://www.zivatar.hu/script.php?id=walter-lieth

NCBI Database: http://blast.ncbi.nlm.nih.gov/Blast.cgr

DE GRUYTER OPEN DOI: 10.2478/aslh-2013-0005 Acta Silv. Lign. Hung., Vol. 9 (2013) 71–83

Distribution and Host Preference of Poroid Basidiomycetes in Hungary I. – *Ganoderma*

Viktor PAPP[a*] – Ilona SZABÓ[b]

[a] Department of Botany, Faculty of Horticulture Science, Corvinus University of Budapest, Hungary
[b] Institute of Silviculture and Forest Protection, University of West-Hungary, Sopron, Hungary

Abstract – From the economical point of view, the genus *Ganoderma* is one of the most important groups of Basidiomycetes due to their medicinal effects and also because they cause decay in a very wide range of tree species all over the world. In this study new data of the Hungarian *Ganoderma* species are published and the specimens in accessible Hungarian herbarium collections are processed and revised. The article includes the nomenclatural status, the morphological characters, the host preference, frequencies and the details of the fungarium samples of six *Ganoderma* species (*Ganoderma adspersum*, *G. applanatum*, *G. carnosum*, *G. cupreolaccatum*, *G. lucidum*, *G. resinaceum*) as well. In total 215 *Ganoderma* specimens are examined and 10 hosts of the six native *Ganoderma* species new for Hungary are presented. The Hungarian locality and time of the collection of the only *Ganoderma carnosum* (IZ3122) specimen and two new localities of this rare species is published here for the first time.

***Polyporaceae* / *G. carnosum* / *G. cupreolaccatum* / new host**

Kivonat – Taplógombák előfordulása és gazdanövényköre Magyarországon I. – *Ganoderma*. A taplók közül a *Ganoderma* P. Karst. 1881 gazdasági szempontból az egyik legfontosabb nemzetség, tekintettel növénykórtani jelentőségükre, valamint a gyógyászatban betöltött szerepükre. Jelen munkában feldolgoztuk és revideáltuk a Magyarországi gyűjteményekben elhelyezett hazai fungáriumi mintákat, továbbá újabb, korábban nem publikált adatokat is közlünk. A cikk tartalmazza a hazánkban előforduló hat *Ganoderma* faj (*Ganoderma adspersum*, *G. applanatum*, *G. carnosum*, *G. cupreolaccatum*, *G. lucidum*, *G. resinaceum*) nomenklatúrai helyzetét, az elkülönítő morfológiai bélyegeket, aljzataik gyakorisági megoszlását és a fungáriumi példányok részletes adatait megyék szerint csoportosítva. Összesen 215 *Ganoderma* taxon herbáriumi mintáját vizsgáltuk meg és 10 Magyarországon korábban nem ismert gazdanövényen való előfordulási adatot közlünk. Az eddig egyetlen hazánkból ismert *Ganoderma carnosum* mintának (IZ3122) lelőhelyét és gyűjtésének időpontját, valamint két további hazai minta adatát első alkalommal publikáljuk.

taplók / G. *carnosum* / *G. cupreolaccatum* / új gazdanövény

* Corresponding author: viktor.papp@uni-corvinus.hu; H-1118 BUDAPEST, Ménesi út 44.

1 INTRODUCTION

Ganoderma P. Karst. 1881 is a cosmopolitan, poroid basidiomycete genus, which contains mainly wood decaying fungi of different deciduous trees and conifers (Ryvarden – Gilbertson 1993). From the economical point of view, the genus *Ganoderma* is one of the most important groups of Basidiomycetes due to their medicinal effects (e.g. Papp et al 2012a, Paterson 2006, Trigos – Medellín 2011) and also because they cause decay in a very wide range of tree species all over the world (Flood et al. 2000; Schwarze – Ferner 2003). It is, however, taxonomically „the most difficult genus among polypores" (Ryvarden 1985) and in a state of taxonomical chaos (Ryvarden 1991). Nevertheless the situation is rather confusing even today. Up to now, all over the world, taxonomists have described 326 legitimate *Ganoderma* species and many forms, varieties and subspecies (Robert et al. 2013). Among these only 7 *Ganoderma* species (*G. adspersum*, *G. applanatum*, *G. carnosum*, *G. cupreolaccatum*, *G. lucidum*, *G. resinaceum*, *G. valesiacum*) are accepted in the European polypore monographs (e.g. Bernicchia 2005; Ryvarden – Gilbertson 1993). Moreover there are some species (e.g. *Ganoderma kosteri* Steyaert 1972, *G. puglisii* Steyaert 1972, *G. soniense* Steyaert 1961) which are described from Europe (Steyaert 1961, 1972) and have a modern description and type material, but the taxonomical state of these species is uncertain (Moncalvo – Ryvarden 1997).

The location and host plants of the Hungarian *Ganoderma* species was synthesized firstly by Igmándy (1968, 1970), however not all of his data have been published. The summarized data of the fungarium collection of Zoltán Igmándy was published by Szabó (2012), which mentioned *Ganoderma carnosum* from Hungary for the first time. The Hungarian distribution of *G. cupreolaccatum* (syn. *G. pfeifferi*) was processed by Papp and Siller (2012) and new occurrence data of this rare species have also been reported.

In this study the accessible Hungarian fungarium materials of *Ganoderma* were examined. The localities of the species are presented and the host preference is discussed.

2 MATERIALS AND METHODS

The identification of the Hungarian *Ganoderma* materials was done based on the taxons included in the European polypore monographs (Bernicchia 2005, Ryvarden – Gilberston 1993). In nomenclature, the MycoBank database (Robert et al. 2013) was followed, except for *G. applanatum* (syn. *G. lipsiense*), in which case the sanctioning proposal of Redhead et al. (2006) accepted by the Nomenclature Committee for Fungi (Norvell 2010, 2011) was taken into account. The herbarium of the Hungarian Natural History Museum (BP) and the polypore collection of Zoltán Igmándy (IZ) (which is kept at the Institute of Silviculture and Forest Protection of the University of West-Hungary Sopron) were examined. The new fungarium materials were placed into the first author's collection (PV) and can be accessed at the Botanical Department of the Corvinus University of Budapest (Faculty of Horticultural Science). For the microscopic studies a Zeiss Axio Imager. A2 type light microscope was used.

3 RESULTS

Ganoderma adspersum (Schulzer) Donk, Proceedings van de Koninklijke Nederlandse Akademie van Wetenschappen Section C, 72: 273, 1969

≡ *Polyporus adspersus* Schulzer 1878

= *Polyporus linhartii* Kalchbr. 1884 – *Ganoderma linhartii* (Kalchbr.) Z. Igmándy 1968

= *Ganoderma europaeum* Steyaert 1961

In European monographs, *Ganoderma adspersum* (e.g. Bernicchia 2005, Krieglsteiner 2000, Ryvarden – Gilbertson 1993) was found under the name *G. australe* (Fr.) Pat. 1889 (Bas.: *Polyporus australis* Fr. 1828), which originated from the Pacific Islands. The identity of the two taxa is ambiguous due to the lack of holotype and geographical distribution (Welti – Courtecuisse 2010). Molecular results (Smith – Sivasithamparam 2000) showed that the European taxon (*G. adspersum*) is different from *G. australe* (Australia). This explains why *G. adspersum* (Bas.: *Polyporus adspersus*) should be the appropiate name of the European species, which was described from Croatia and the holotype grew on *Carpinus betulus*. This species is presumably identical with *G. linhartii* (Kalchbr.) Z. Igmándy 1968 and *G. europaeum* Steyaert 1961 (Steyaert 1972).

G. adspersum belongs to the '*G. applanatum – australe* complex' (subgen. *Elfvingia*), it has perennial, sessile and non-laccate basidiocarp. It differs from *G. applanatum* by larger spores [(8–)8,5–10(–12) × (5–)5,5–7,5(–8,5) µm], thicker crust [>0,5(–0,75) mm], homogenous reddish brown context, and tube layer without intervening layers (Leonard 1998, Marriott 1998, Ryvarden – Gilbertson 1993). It mainly grows on living broadleaved trees, and in Hungary it is usually found in parks and urban habitats (Igmándy 1991; Papp 2013). In the Mediterranean region of Europe, it was detected from *Pinus pinea* (De Simone and Annesi 2012). In Hungary, *G. adspersum* was also found on the stem of living coniferous trees in a park in Dénesfa (*Abies* sp., IZ2534) and in the Kámoni Arborétum (*Picea abies*, BP80370).

In this study *Ganoderma adspersum* is presented for the first time from *Juglans nigra* and *Ulmus laevis*. Igmándy (1991) also mentioned *G. adspersum* from *Carpinus betulus*, but the specimen is missing from the collection. In total it can be found on 20 different tree genera, but it mainly grows on *Quercus* species in Hungary. Compared to other domestic *Ganoderma* taxa, it is frequently found on non native trees (e.g. *Gleditschia triacanthos*, *Robinia pseudoacacia*, *Morus alba*) *(Table 1)*.

MATERIAL EXAMINED – Bács-Kiskun county: Lakitelek, *Robinia pseudoacacia*, 14.VI.1981., leg.: F. Varga, det.: Z. Igmándy (IZ2701); *Robinia pseudoacacia*, 15.VI.1981 (BP76355); Kelebia, *Robinia pseudoacacia*, VIII.1974 (BP76075); **Baranya county**: Mekényes, VI.1975, *Quercus cerris*, leg.: A. Tóth, det.: Z. Igmándy (BP76063); **Borsod-Abaúj-Zemplén county**: Makkoshotyka, *Quercus petraea*, VII.1980, leg.: B. Kliegl, det.: Z. Igmándy (BP76358); **Budapest**: Csillaghegy, *Acer saccharinum*, 04.IV.2012. leg. et det.: V. Papp (PV608); Pestlőrinc, *Prunus cerasus*, 03.X.1985, leg.: L. Kárpáti, det.: Z. Igmándy (BP90040/IZ3067); **Csongrád county**: Sándorfalva, *Robinia pseudoacacia*, XI.1974, leg.: A. Kmoskó, det.: Z. Igmándy (BP76065); Ásotthalom, *Quercus robur*, 1978, leg.: Polner F.-né, det.: Z. Igmándy (BP76068); **Fejér county**: Alcsutdoboz, *Gleditschia triacanthos*, 22.X.1967, leg.: V. Csapody, det.: Z. Igmándy (BP76353); **Győr-Moson-Sopron county**: Sopron, *Prunus domestica*, XII.1967, leg.: V. Stubnya, det.: Z. Igmándy (IZ1756); Süttör, *Aesculus hippocastanum*, 25.VI.1971, leg.: V. Stubnya, det.: Z. Igmándy (BP76070/IZ1919); Dénesfa, *Abies* sp., III.1980, leg.: J. Kiss, det.: Z. Igmándy (IZ2534); Sopron, Brennberg, *Prunus domestica*, leg.: L. Kárpáti, det.: Z. Igmándy (BP76354/IZ2537); Kapuvár, Iharos-erdő, *Fraxinus* sp., XI.1980, leg.: S. Nagy, det.: Z. Igmándy (BP76360/IZ2638); Sopron, Botanical Garden, *Prunus* sp., 17.II.1981, leg.: M. Kocsó, det.: Z. Igmándy (BP76357/IZ2665); Lövő, *Gleditschia triacanthos*, 26.III.1960, leg. et det.: Z. Igmándy (BP23746/47675); Bősárkány, *Morus* sp., 26.XI.1966, leg.: Z. Igmándy & F. Varga, det.: Z. Igmándy (BP23691); Kapuvár, *Quercus robur*, 04.V.1978, leg.: Z. Igmándy & L. Kárpáti, det.: Z. Igmándy (BP76060); Fertőd, *Tilia* sp., 21.VI.1981, leg. et det.: Z. Igmándy (BP76359); Sopronhorpács, *Tilia* sp., V.1978, leg. P. Ubrankovics, det.: Z. Igmándy (BP76071); *Gymnocladus dioicus*, 04.XI.1979, leg.: L. Kárpáti, det.: Z. Igmándy (BP76354); Mosonmagyaróvár, *Quercus robur*, 1978, leg.: Palrne D.-né, det.: Z. Igmándy (BP76074/ IZ2459); Sopron, *Robinia pseudoacacia*, 23.IV.1978, leg. et det.: Z. Igmándy (BP76061); Nagylózs, *Populus nigra*, 05.IX.1956, leg. et det.: Z. Igmándy (BP23680); **Hajdú-Bihar county**: Debrecen, Haláp, *Gleditschia triacanthos*, IX.1976, leg.: F. Eszes, det.: Z. Igmándy (BP76066/IZ2252); *Robinia pseudoacacia*, IX.1973, leg.: F. Eszes, det.: Z. Igmándy (BP76076); Nagyerdő, *Gleditschia triacanthos*, 07.IV.2012, leg. et det.: V. Papp (PV609); **Heves county**: Gyöngyössolymos, *Quercus* sp., III.1966, leg.: Nagy, det.: Z. Igmándy (BP20334); **Komárom-Esztergom county**: Tata, Öregtó, *Celtis occidentalis*, 12.VIII.1969, leg. et det.: Z. Igmándy (BP55595); Tata, *Salix* sp., 19.VIII.1969, leg.: Z. Igmándy & F. Varga, det.: Z. Igmándy (BP76073); **Pest county**: Horány, *Juglans nigra*, 18.VI.1978, leg.: M. Babos, det.: Z. Igmándy (BP65369); Ócsa, Ócsai-turjános Forest Reserve, *Fraxinus angustifolia* subsp. *danubialis* leg. et det.: V. Papp (PV497); Vácrátót, Vácrátot Botanical Garden,

hardwood, 13.VIII.2013, leg. et det.: V. Papp (PV941); **Somogy county**: Barcs, Középrigóc, *Betula pendula*, 07.VI.1983, leg.: L. Kárpáti, det.: Z. Igmándy (IZ2957); Balatonendréd, *Quercus* sp., 29.VII.1912, leg.: Mágocsy & S. Dietz, det.: G. Moesz, rev.: Z. Igmándy (BP13663); **Szabolcs-Szatmár-Bereg county**: Vámosatya, indet. hardwood, 19.X.2009, leg. et det.: V. Papp (PV968); **Tolna county**: Pörböly, Szomfova, *Populus alba*, 1956.VI.08. leg. et det.: Z. Igmándy (IZ743); Lengyel, *Ulmus laevis*, 28.VIII.2011, leg. et det.: V. Papp (PV460); Hőgyész, *Fraxinus ornus*, 22.X.1964, leg. et det.: Z. Igmándy (BP76049); Szekszárd, 11.X.1927, leg. et det.: L. Hollós, rev.: Z. Igmándy (BP13630); Pörböly, Gemenci Forest, 08.IV.2013, *Quercus robur*, leg. et det.: V. Papp (PV942); **Vas county**: Szombathely, Kámon, *Picea abies*, 04.IX.1982, leg.: B. Kiss & L. Varga, det.: Z. Igmándy (BP80370); Körmend, *Quercus robur*, X.1982, leg.: J. Raszler, det.: Z. Igmándy (BP80358); Sárvár, *Fraxinus* sp., 20.IX.1977, leg. et det.: Z. Igmándy (BP76072); 12.V.1983, leg. et det.: Z. Igmándy (BP80362); Őriszentpéter, Morus sp., 06.IX.1968, leg. et det.: Z. Igmándy (BP76062); Csapod, *Prunus cerasus*, 14.VII.1980, leg.: S. Faragó, det.: Z. Igmándy (BP76069); Sárvár, *Quercus* sp., 29.VII.1967, leg.: Z. Igmándy & F. Varga, det.: Z. Igmándy (BP47331/47664); Tanakajd, *Quercus* sp. X.1968, leg.: E. Barabits, det.: Z. Igmándy (BP47634); Sitke, Bajti, *Quercus robur*, 14.IX.1964, leg.: Z. Igmándy, H. Pagony, F. Varga, det.: Z. Igmándy (BP23645); **Veszprém county**: Pápa, *Platanus* sp., 09.X.1984, leg.: Z. Igmándy & L. Kárpáti, det.: Z. Igmándy (BP90039/IZ3023); Ugod, Bakony Mts., *Morus* sp. XI.1974, leg.: R. Rózsai, det.: Z. Igmándy (BP76064); **Zala county**: Letenye, *Populus nigra*, VII.1971, leg.: M. Szélessy, det.: Z. Igmándy (BP55601/IZ1971); Eszteregnye, *Quercus petraea*, 26.III.1982, leg.: M. Szélessy, det.: Z. Igmándy (BP90041); Kemendollár, hardwood, 13.II.1982, leg.: M. Szélessy, det.: Z. Igmándy (IZ2814); Pölöske, *Quercus* sp., 06.VII.1965, leg. et det.: Z. Igmándy (BP76050); *Fagus sylvatica*, 11.VII.1965, leg. et det.: Z. Igmándy (BP23665).

Ganoderma applanatum (Pers.) Pat., Bulletin de la Société Mycologique de France, 5: 67, 1889
≡ *Boletus applanatus* Pers. 1799
= *Boletus lipsiensis* Batsch 1786 – *Ganoderma lipsiense* (Batsch) G.F. Atk. 1908

Numerous articles were published to clarify the nomenclatural status of *G. applanatum*, (e.g. Redhead et al. 2006, Niemelä – Miettinen 2008, Demoulin 2010). Eventually the Nomenclature Committee for Fungi sanctioned *Boletus applanatus* Pers. 1799 against *B. lipsiensis* Batsch 1786 (Norvell 2010, 2011).

Main morphological characters of *G. applanatum* are the perennial, applanate basidiocarps with thin, non-laccate crust (<5mm), the whitish streaks and patches in the context and the layer of the trama. Characteristically, drawings can be made on its fresh pore surface with a sharp instrument ("artists' fungus"), since the bruised surface turns brown due to an immediate oxidation (Ryvarden – Gilbertson 1993). Another feature is that the tubes are often attacked by the fungivore insect larvae of *Agathomyia wankowiczii*, which causes distinctive galls to form.

G. applanatum is a common and widespread species in Hungary. It mainly grows on logs and stumps as saprophyte and in contrary of *G. adspersum*, often occures in forest habitats (Igmándy 1991). It is a polyphagous species: in Europe, the substrates are mainly deciduous trees, but sometimes it can be found on conifers as well (*Abies*, *Picea*) (e.g. Ryvarden – Gilbertson 1993, Kotlaba 1984). In Hungary, the most common hosts are *Fagus*, *Salix* and *Populus*, but there are details on several other tree species as well (Table 1.). The first data from *Abies alba* and *Fraxinus ornus* are presented here.

MATERIAL EXAMINED – Bács-Kiskun county: Kecskemét, leg. et det.: L. Hollós (BP13655); **Baranya county**: Béda, *Populus* x *euramericana*, 17.VIII.1968, leg. et det.: Z. Igmándy (BP47456); **Borsod-Abaúj-Zemplén county**: Miskolc-Lillafüred, *Acer* sp., 09.V.1957, leg. et det.: Z. Igmándy (BP76142); **Budapest**: Hármashatárhegy, 04.III.1934, *Quercus* sp., leg.: A. Pénzes, det.: Moesz G. (BP13665); **Csongrád county**: Dóc, 13.X.1985, leg.: unknown, det.: M. Babos & I. Krepuska (BP79529); **Fejér county**: Vértes Mts., 14.IV.1938, leg. et det.: G. Bohus (BP13664); Vértes Mts, Csákberény, Juhdöglő-völgy Forest Reserve, *Fagus sylvatica*, 03.VIII.2011, leg. et det.: V. Papp (PV969); **Győr-Moson-Sopron county**: Sopron, *Alnus glutinosa*, 17.III.1950, leg. et det.: Z. Igmándy (BP34476/IZ120); Sopron, *Tilia* sp., 05.V.1952, leg. et det.: Z. Igmándy (IZ183); Sopron, Felső-Tödl, *Tilia* sp., IV.1954, leg.: I. Deák, det.: Z. Igmándy (BP34479); Sopron, Deák-kút, *Abies alba*, 21.III.2012, leg. et det.: I. Szabó & V. Papp (PV604); Sopron, Deák-kút, *Carpinus betulus*, 27.VIII.1957 (IZ870); Sopron, Ferenc-forrás, *Picea abies*, 22.VII.1978, leg. et det.: Z. Igmándy (IZ2385); Sopron, Füzesárok, *Alnus glutinosa*, 01.IX.1968, leg. et det.: Z. Igmándy (BP47633), 16.IX.1973 (BP76137); Csorna, *Alnus glutinosa*, IV.1979, leg.: T. Pillér, det.: Z. Igmándy (BP76135); Dunasziget, *Ulmus* sp., 08.X.1976, leg.: J.

Nyulasi, det.: Z. Igmándy (BP76365); Sopron, *Tilia* sp., 05.VII.1952, leg. et det.: Z. Igmándy (BP20335/34477); **Hajdú-Bihar county**: Debrecen, Nagyerdő, *Quercus* sp., 23.III.1930, leg. et det.: D. Révy (BP95302); Debrecen, *Quercus robur*, X.1978, leg.: L. Földi, det.: Z. Igmándy (BP76144); **Heves county**: Szilvásvárad, Őserdő Forest Reserve, *Fagus sylvatica*, VIII.1954, leg.: J. Győry, det.: Z. Igmándy (BP34480/IZ501); Szilvásvárad, Őserdő Forest Reserve, *Fagus sylvatica*, 29.IV.2011, leg. et det.: V. Papp (PV307); Szilvásvárad, *Fagus sylvatica*, 15.V.1956, leg. et det.: Z. Igmándy (BP76136); Mátraháza, 08.IX.1940, leg. et det.: G. Moesz (BP13654); Bélapátfalva, *Fagus sylvatica*, 25.VII.1956, leg. et det.: Z. Igmándy (BP34474); Nagyvisnyó, *Fagus sylvatica*, 06.VII.1957, leg. et det.: Z. Igmándy (BP34478); **Jász-Nagykun-Szolnok county**: Tiszapüspöki, *Populus* x *euramericana* cv. *serotina*, VIII.1976, leg.: J. Kómár, det.: Z. Igmándy (BP76141); **Komárom-Esztergom county**: Neszmély, *Salix* sp., 13.X.1955, leg.: L. Haracsi, det.: Z. Igmándy (BP23738/34481); **Nógrád county**: Zagyvaróna, Vecseklői-völgy, *Quercus* sp., 24.VIII.1955, leg. et det.: Z. Igmándy (BP23749/34473); Diósjenő, *Fagus sylvatica*, 01.X.1954, leg.: J. Rumszauer,, det.: Z. Igmándy (IZ517); Nagyoroszi, *Alnus glutinosa*, 27.X.1974, leg.: J. Gyürky, det.: Z. Igmándy (BP76138); Magyarnándor, *Quercus* sp., X.1974, leg.: J. Fidlóczky, det.: Z. Igmándy (BP76140); **Pest county**: Pilisszentkereszt, Szurdok, *Fagus sylvatica*, 30.X.2009, leg. et det.: V. Papp (PV20); Pusztavacs, *Populus* sp., VIII.1955, leg.: M. Balázs, det.: Z. Igmándy (IZ717); Szigetmonostor, *Robinia pseudoacacia*, VI.1972, leg.: Padányi & G. Gulyás, det.: Z. Igmándy (IZ2024); Csővár (Cserhát Mts), unknown, 31.VII.1979, leg. et det.: M. Babos, A. Friesz (BP59038); Nagykőrös, *Robinia pseudoacacia*, VII.1976, leg.: L. Nemes, det.: Z. Igmándy (BP76133); Isaszeg, Szentgyörgypuszta, *Populus* sp., 31.X.1966, leg.: M. Babos, E. Véssey, det.: Z. Igmándy (BP76147); Gödöllő, *Salix* sp., VIII.1964, leg.: E. Véssey, det.: Z. Igmándy (BP76143); Pusztavacs, *Populus* sp., VIII.1955, leg.: M. Balázs, det.: Z. Igmándy (BP34475); **Somogy county**: Segesd, *Quercus* sp., XI.1970, leg.: F. Eszes, det.: Z. Igmándy (BP76139); **Szabolcs-Szatmár-Bereg county**: Nyírtelek, *Quercus robur*, 16.IX.1982, leg.: F. Varga, det.: Z. Igmándy (IZ2857); Baktalórántháza, *Prunus avium*, 03.XI.1975, leg. et det.: Z. Igmándy (BP55669); Nyírbéltek, *Betula pendula*, 03.XI.1975, leg. et det.: Z. Igmándy (BP76134); **Tolna county**: Keselyű, Őcsény, *Populus* sp., 14.IV.1960, leg. et det.: Z. Igmándy (BP34321); Szekszárd, Kis-Bükk erdő, unknown, 18.V.1927, leg. et det.: L. Hollós (BP13628); Szekszárd, Sötét-völgy, unknown, 18.VIII.1927, leg. et det.: L. Hollós (BP13613); Fácánkert, *Robinia pseudoacacia*, 11.X.1928, leg. et det.: L. Hollós (BP13631); Hőgyész, *Fraxinus ornus*, 22.X.1964, leg. et det.: Z. Igmándy (BP20409/20443); **Vas county**: Szalafő, *Quercus* sp., 06.IX.1968, leg. et det.: Z. Igmándy (BP47455); Körmend, Tilalmasi-erdő, *Acer pseudoplatanus*, 26.IV.1958, leg.: Z. Igmándy, H. Pagony, det.: Z. Igmándy (BP76146/IZ992); Sárvár, *Quercus robur*, 06.IX.1979, leg.: Z. Igmándy, Gy. Traser, det.: Z. Igmándy (BP76145); Sitke, *Carpinus betulus*, 11.X.1972, leg. et det.: Z. Igmándy (BP76366); Szalafő, *Quercus robur*, 05.VII.1972, leg. et det.: Z. Igmándy (BP75934); **Veszprém county**: Marcaltő, *Salix* sp., XII.1953, leg.: J. Csötönyi, det.: Z. Igmándy (IZ375); **Zala county**: Sormás, *Alnus glutinosa*, VIII.1972, leg.: M. Szélessy, det.: Z. Igmándy (BP55483); Pölöske, *Quercus rubra*, 19.IX.1978, leg.: M. Szélessy, det.: Z. Igmándy (IZ2398); Letenye, *Fagus sylvatica*, V.1984, leg.: J. Csendes, det.: Z. Igmándy (IZ3006); Vétyem, *Fagus sylvatica*, 06.IX.1981, leg. et det.: Z. Igmándy (BP76363).

Ganoderma carnosum Pat., Bulletin de la Société Mycologique de France, 5: 66, 1889
= *Ganoderma atkinsonii* H. Jahn, Kotl. & Pouzar 1980

G. carnosum (syn. *G. atkinsonii*) belongs to the group of annual and stipitate *Ganoderma* species (*G. lucidum* complex). The main morphological characters are the dark and shiny pileus and in general the larger fruitbody (Jahn et al. 1980), as well as the size of the pores – *G. carnosum* (average: 138.46 μm), *G. lucidum* (average: 238.34 μm) – (Cilerdzic et al. 2011). It is difficult to separate the two species (*G. carnosum* and *G. lucidum*) by anatomical characters, but according to Jahn et al. (1980) *G. carnosum* has wider spores [average wide: (7.3)7.4–7.8(8) μm].

It is a south-central European species, and it grows mainly on *Abies alba*, but rarely occures on other coniferous or decideous tree species (Bernicchia 1995, Jahn et al. 1980). In Hungary, the first data of *G. carnosum* was published by Szabó (2012). Up to now, only twolocalities of this species was known from *Taxus baccata* and stump of unknown coniferous tree (cf. *Abies alba*) in Hungary *(Table 1, Figure 1).*

MATERIAL EXAMINED – Csongrád county: Szeged, *Taxus baccata*, III.1984, leg.: Gy. Patkó, det./rev.: I. Szabó & V. Papp (IZ2991); Szeged, Museum garden, *Taxus baccata*, 05.XII.1986, leg. F. Eszes, det. Z. Igmándy (IZ3122); **Győr-Moson-Sopron county**: Sopron, Kecske-patak, cf. *Abies alba*, 14.IX.2008, leg.: B. Dima & L. Albert, det.: B. Dima & V. Papp (PV970).

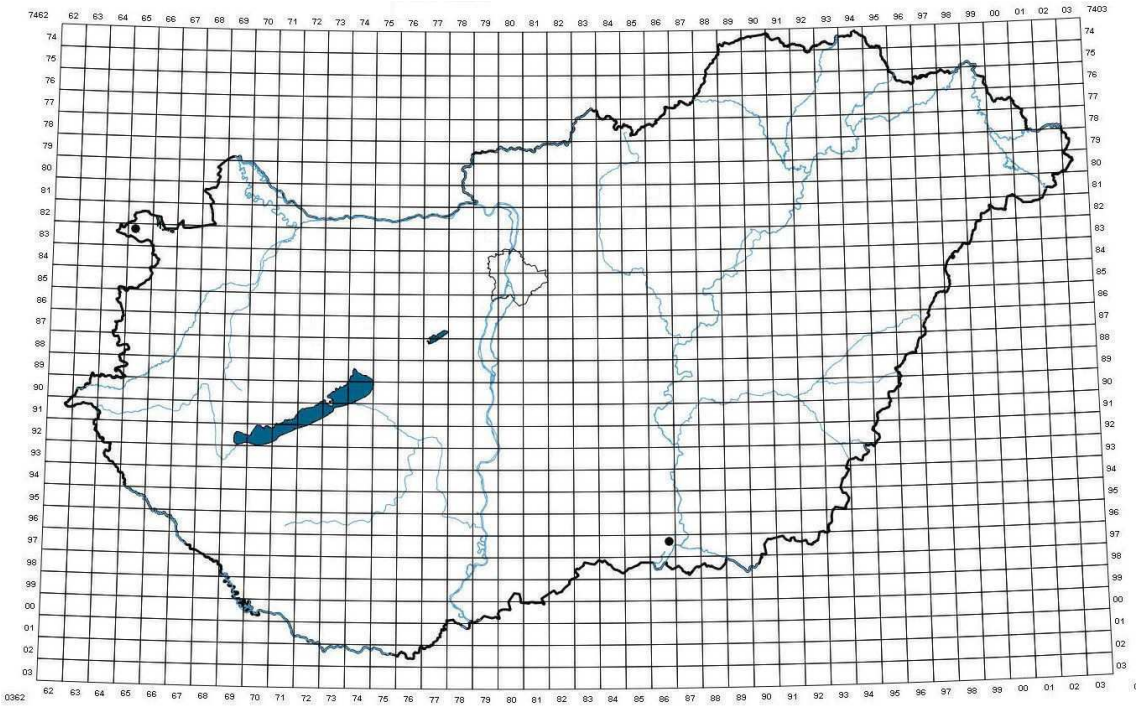

Figure 1. Localities of Ganoderma carnosum in Hungary

Ganoderma cupreolaccatum (Kalchbr.) Z. Igmándy, Acta Phytopathologica Academiae Scientiarum Hungaricae, 3: 234, 1968

≡ *Polyporus cupreolaccatus* Kalchbr. 1885

= *Polyporus laccatus* Kalchbr. 1885

= *Ganoderma pfeifferi* Bres. 1889

G. cupreolaccatum (Bas. *Polyporus cupreolaccatus* Kalchbr. 1885) is presumably identical with *G. pfeifferi* Bres. 1889, which was described from *Abies* (Patouillard 1889), however this taxon is a characteristic species of natural European beech forests (Christensen et al. 2004) and mainly grows on the base of living *Fagus sylvatica* (Ryvarden – Gilbertson 1993). In Europe, it is rarely found on other hardwood species, like *Ulmus laevis, Acer saccharinum* (Szczepkowski – Piętka 2003) or *Aesculus*, *Fraxinus*, *Prunus* and *Quercus* species (Petersen 1987, Ryvarden – Gilbertson (1993).

G. cupreolaccatum (Kalchbr.) Z. Igmándy (syn. *G. pfeifferi* Bres.) has perennial basidiocarp, nevertheless molecular works (e.g. Moncalvo et al. 1995) was shown that it belongs to the annual and laccate '*G. resinaceum*' complex. The old basidiocarps were possibly mistaken for *G. applanatum* (Niemelä – Miettinen 2008). Main characteristics of this species are the laccate pileus, dark brown context and the size of the spores (9–11,5 × 6–9 µm).

In Hungary *G. cupreolaccatum* typically grows on the base of old living *Fagus sylvatica* (e.g. Igmándy 1968, Papp – Siller 2012), that explains why most of the data of this species originate from beech forest reserves. It is also rarely found on other hardwood species – *Acer* (BP20323), *Quercus* (IZ639) – in Hungary. Moesz (1942) reffering to the collection of Schilberszky (Nagytétény, Budapest) published a data of *Ganoderma laccatum* (Kalchbr.) Bourdot & Galzin (synonyms given by the author: *G. pfeifferi* Bres. and *Placodes resinosus* (Schrad.) Quél.), which grew on *Prunus persica*. Since *Prunus* is a particular host for this species, the reconsideration of the data is needed, but the specimen is not found. Igmándy (1970) previously mentioned *Ganoderma cupreolaccatum* only from two localities (Erdősmecske, Pusztavám). Pál-Fám and Lukács (2002) published this species on living *Fagus* in Kőszegi-forrás Forest Reserve (Mecsek Mts). Siller also found it on *Fagus sylvatica*

in Őserdő Forest Reserve (Siller 2004) and in Tátika Forest Reserve (Papp – Siller 2012). Previously the first author reported this species from Dobogókő, Pilisszentlélek (Visegrád Mts) and Juhdöglő-völgy Forest Reserve (Vértes Mts) (Papp – Siller 2012). In this study three new localities are published (Galyatető, Nagykanizsa, Zagyvaróna) *(Table 1, Figure 2)*.

MATERIAL EXAMINED – Baranya county: Erdősmecske, VIII.1965, leg.: Vaday, det.: Z. Igmándy (BP20323); **Fejér county**: Pusztavám, *Acer* sp., 13.X.1955, leg.: L. Haracsi, det.: Z. Igmándy (BP20313); Csákberény, Juhdöglő-völgy Forest Reserve, *Fagus sylvatica*, 15.X.2010, leg. et det.: V. Papp (PV971); *Fagus sylvatica*, 04.III.2011, leg. et det.: V. Papp (PV972); **Heves county**: Mátra Mts, Galyatető, *Fagus sylvatica*, 22.IX.2013, leg. et det.: V. Papp (PV967); **Nógrád county**: Zagyvaróna, Vecseklő-völgy, *Quercus* sp., 24.VII.1955, leg.: Z. Igmándy, det./rev.: V. Papp (IZ639); **Pest county**: Visegrádi Mts, Pilisszentlélek, *Fagus sylvatica*, 27.III.2010, leg. et det.: V. Papp (PV45); Visegrádi Mts, Dobogókő, *Fagus sylvatica*, 24.IV.2011, leg. et det.: V. Papp (PV287); Visegrádi Mts, Dobogókő, *Fagus sylvatica*, 11.VII.2012, leg. et det.: V. Papp (PV643); Börzsöny Mts, Nagy-Hideg-hegy, *Fagus sylvatica*, 12.III.1972, leg.: A. Dobos, det.: Z. Igmándy (BP76034); **Zala county**: Vétyem, *Fagus sylvatica*, 18.VI.1981, leg.: Z. Igmándy & Gy. Traser, det.: Z. Igmándy (BP76364/90042); Vétyem, *Fagus sylvatica*, III.1984, leg.: G. J. Kovácsné, det.: Z. Igmándy (IZ2994); Nagykanizsa, *Fagus sylvatica*, 03.VIII.1982, leg.: M. Szélessy, det.: Z. Igmándy (BP80368/IZ2844).

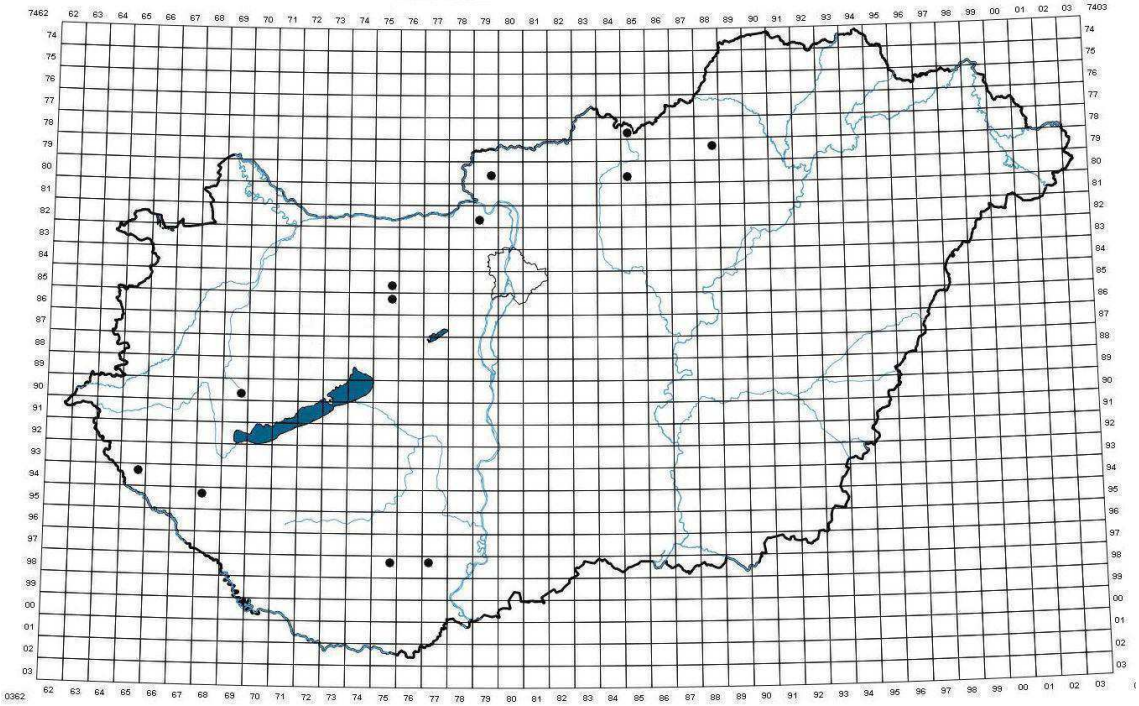

Figure 2. Localities of Ganoderma cupreolaccatum in Hungary

Ganoderma lucidum (Curtis) P. Karst., Revue Mycologique Toulouse, 3 (9): 17, 1881
≡ *Boletus lucidus* Curtis 1781 – *Polyporus lucidus* (Curtis) Fr. 1821
= *Boletus flabelliformis* Leyss. 1761

Ganoderma lucidum is the type species of the genus *Ganoderma* (Karsten 1881), nevertheless taxonomically it is quite problematic (Moncalvo et al. 1995). The morphologically similar species are often identified mistakenly as '*G. lucidum*' all around the world. According to Seo and Kirk (2000) '*G. lucidum*' is the most often incorrectly used name within the genus *Ganoderma* besides *G. applanatum*. For this reason it is difficult to define the real *G. lucidum* s. str. (Park et al. 2012, Szedlay 2002, Wasser 2005). Recent molecular studies showed that certain Chinese taxons, which previously have been identified as *G. lucidum*, are different from the European specimens (*G. lucidum* s. str.) (e.g. Cao et al. 2012, Wang et al. 2009, Wang et al. 2012).

The morphological characters of *G. lucidum* that separates it from other European annual and stipitate *Ganoderma* species (*G. carnosum*, *G. valesiacum*) are the colour of the basidiocarp and context, the size of pores and the host preference (Bernicchia 2005, Ryvarden – Gilbertson 1993). *G. resinaceum* may have short expanding stipe, but it has a robust basidiocarp and usually grows on base of living trees (Igmándy 1991). In the context of this species a wide darker zone can be found, which is absent in *G. lucidum* (Petersen 1987).

The holotype was described from *Corylus avellana* (Moncalvo – Ryvarden 1997), however in Hungary it mainly grows on *Quercus*, *Carpinus* and *Salix* (Igmándy 1991), but it is also known from *Acer* and *Platanus* (Szabó 2012). Igmándy identified it as *G. lucidum* on *Taxus baccata* (Szabó 2012), but following the revision of the speciment, it is prooved to be identical with *G. carnosum*. Previously, *G. lucidum* has not been found in Hungary on *Fagus sylvatica* (PV789) and *Robinia pseudoacacia* (PV461).

MATERIAL EXAMINED – Bács-Kiskun county: Baja, unknown, 18.X.1968, leg.: V. Stubnya, det.: Z. Igmándy (BP76190); Hajós, *Salix* sp., 13.VI.1980, leg.: A. Szalczer, det.: Z. Igmándy (BP76190); **Baranya county**: Marócsa, *Carpinus betulus*, 04.V.1978, leg.: F. Varga, det.: Z. Igmándy (BP76201); **Budapest**: Budai-hegyek, unknown, VI.1957, leg.: I. Szőke, det.: Z. Igmándy (BP76195/IZ881); Vadaskert, *Quercus* sp., 12.X.1934, leg. et det.: A. Pénzes (BP67844), 01.III.1941, leg.: Kőfaragó, V. Gyelnik, det.: G. Bohus (BP28271); Budakeszi, unknown, 29.VIII.1979, leg. et det.: M. Babos (BP65358), 14.III.1982, leg.: O. Dálnoki, det.: G. Bohus (BP78772); Jánoshegy, unknown, 13.VI.1926, leg.: J. Zöldy, det.: J. Tuzson (BP66610), 05.VII.1953, leg. et det.: G. Ubrizsy (BP58939); Hüvösvölgy, *Quercus* sp., 28.VII.1951, leg. et det.: G. Ubrizsy (BP58938); Kamaraerdő, unknown, 30.VI.1985, leg. et det.: M. Rajczy (BP78634); **Fejér county**: Alcsútdoboz, hardwood, 01.V.2013, leg. et det.: V. Papp (PV940); Csákberény, Juhdöglő-völgy Forest Reserve, *Fagus sylvatica*, 10.X.2012, leg. et det.: V. Papp (PV789); **Győr-Moson-Sopron county**: Sopron, unknown, 15.X.1951, leg.: Ö. Apt, det.: Z. Igmándy (IZ55); Sopron, Iker-árok, *Carpinus betulus*, IX.1952, leg.: I. Szodfried, det.: Z. Igmándy (IZ223); Sopron, Fáber-rét, *Carpinus betulus*, 30.VII.1953, leg. et det.: Z. Igmándy (IZ312); Sopron, Váris, *Quercus cerris*, 17.VII.1955, leg. et det.: Z. Igmándy (IZ582); Sopron, Várhely, unknown, 03.VIII.1956, leg.: L. Haracsi, Z. Igmándy, det.: Z. Igmándy (BP76198); Sopron, Vas-hegy, *Carpinus betulus*, IX.1958, leg.: H. Pagony, det.: Z. Igmándy (IZ1103); Sopron, unknown, XII.1965, leg.: Gy. Holdampf, det.: Z. Igmándy (BP76191); Csáfordjánosfa, *Quercus robur*, 27.IX.1981, leg. et det.: Z. Igmándy (BP76368); Sopron, Hotel Lővér, unknown, 21.VII.1985, leg. et det.: B. Lowy (BP78635); **Hajdú-Bihar county**: Debrecen, Nagyerdő, *Quercus* sp., 06.VIII.1957, leg. et det.: Z. Igmándy (BP76200); Debrecen, Haláp, unknown, IX.1973, leg.: F. Eszes, det.: Z. Igmándy (BP76197); **Heves county**: Felsőtárkány, Török-út (Bükk Mts), *Quercus* sp., 01.IX.2005, leg. et det.: T. Sántha (BP99420); Gyöngyösoroszi (Mátra Mts), *Quercus* sp., 16.VIII.2013, leg. et det.: V. Papp (PV939); Síkfőkút, unknown, 12.VI.1974, leg. et det.: M. Babos (BP80465); Kerecsend, unknown, 17.VI.1956, leg.: B. Zólyomi, det.: G. Bohus (BP28274); Síkfőkút, unknown, 27.VIII.1977, leg. et det.: M. Babos (BP80483); **Nógrád county**: Mátraverebély, Szentkút (Mátra Mts), unknown, 10.VIII.1938, leg. et det.: G. Moesz (BP14029); **Pest county**: Nagybörzsöny (Börzsöny Mts), *Quercus* sp., 05.VII.2013, leg.: J. Nagy, det.: V. Papp (PV973); Dobogókő (Visegrád Mts), *Quercus petraea*, 22.IV.2012, leg. et det.: V. Papp (PV615), *Quercus petraea*, 21.VIII.2012, leg. et det.: V. Papp (PV746); Horány, Szigetmonostor, unknown, 11.VII.1982, leg. et det.: M. Babos (BP79139); Vácrátót, Botanical Garden, unknown, 30.XI.1983, leg.: unknown, det.: M. Babos (BP78631); Bag, unknown, 03.X.1955, leg.: B. Zólyomi, det.: G. Bohus (BP28275); Kőhegy (Pilis Mts), unknown, 18.VII.1965, leg.: L. Vajda, det.: M. Babos (BP); Leányfalu, unknown, 09.VII.1979, leg. et det.: M. Babos, G. Bohus, Vidovszky et al. (BP59035); **Somogy county**: Somogyszob, Kaszópuszta, *Acer negundo*, 12.VII.1966, leg. et det.: Z. Igmándy (BP76188); Balatonboglár, *Platanus acerifolia*, 01.VIII.1957, leg. et det.: Z. Igmándy (BP76193); **Tolna county**: Lengyel, Annafürdő, *Robinia pseudoacacia*, 28.VIII.2011, leg. et det.: V. Papp (PV461); Őcsény, Borrévi-erdő, *Salix* sp., 03.IX.1954, leg. et det.: Z. Igmándy (BP34478/IZ461); Pörböly, *Salix alba*, 08.VI.1956, leg. et det.: Z. Igmándy (IZ744); Szekszárd, *Salix* sp., 23.VII.1912, leg. et det.: L. Hollós (BP14023); Szekszárd, Kis-Bükk forest, *Quercus* sp., 23.III.1927, leg. et det.: L. Hollós (BP14025); **Vas county**: Sárvár, hardwood, 06.IX.1979, leg.: Z. Igmándy, Gy. Traser, det.: Z. Igmády (BP76199); Sárvár, *Carpinus betulus*, 20.VIII.1980, leg. et det.: Z. Igmándy (BP76196); Sitke, *Carpinus betulus*, 08.XI.1968, leg. et det.: Z. Igmándy (BP76194); **Zala county**: Sormás, *Quercus* sp., VII.1972, leg.: M. Szélessy, det.: Z. Igmándy (BP76192); Eszteregnye, unknown, VII.1972, leg.: M. Szélessy, det.: Z. Igmándy (BP76369); Pacsa, unknown, 16.VII.1984, leg.: Gy. Bartos, det.: M. Babos (BP78632); Balatongyörök, Gargavölgy, unknown, 15.IX.1927, leg. et det.: G. Moesz (BP14030); **unknown**: S.Kápolna, unknown, VIII.1893, leg. et det.: J. Márton (BP14021); Lepence, unknown, 27.IX.1980, leg. et det.: M. Babos, L. Albert (BP65358); Hortobágy, Ohati-erdő, unknown, 26.VI.1974, leg.: K. Verseghy, S. Orbán, det.: M. Babos (BP51563), 14.XI.1975, leg.: Zs. Komáromi, S. Orbán, det.: M. Babos (BP51550).

Ganoderma resinaceum Boud., Bulletin de la Société Mycologique de France, 5: 72, 1889

G. resinaceum has a robust annual basidiocarp (Igmándy 1991, Mattock 2001, Mohanty et al. 2011), but some authors state that it is perennial (Bernicchia 2005, Ryvarden – Gilbertson 1993). Its microscopic features are very similar to those of *G. lucidum*, but it is different for the lack of the stipe, the size of the pileus and its facultative necrotrophic characters (Igmándy 1991).

In Hungary *G. resinaceum* usually grows at the base of living *Quercus* trees (e.g. Igmándy 1981, Trecker – Szabó 2002), but it occures on other decidous trees (*Platanus acerifolia*, *Pyrus communis*, *Robinia pseudoacacia*, *Salix* spp.) as well (Igmándy 1981, Papp et al. 2012b, Szabó 2012). Previously, it has not been found in Hungary on *Acer saccharinum* (PV480) and *Aesculus hippocastanum* (PV976). Igmándy (1991) mentioned this species from *Mahonia aquifolium* (BP47614/IZ1801), but after examining the speciment, it can be stated that is not identical with *G. resinaceum* and is likely to be different from the accepted European *Ganoderma* species. To determine the speciment, further studies are required.

MATERIAL EXAMINED – Budapest: XI. ker., Lágymányosi str., *Acer saccharinum*, 13.X.2011, leg. et det.: V. Papp (PV480); II.ker., Határ str., *Quercus robur*, 12.VII.2013, leg. : B. Dima, det.: B. Dima & V. Papp (PV974); Wekerle, *Platanus acerifolia*, 19.IX.2012, leg. et det.: V. Papp (PV975); **Győr-Moson-Sopron county**: Sopron, Váris, *Quercus* sp., V.1950, leg. et det.: Z. Igmándy (BP34485/IZ134); Sopron, *Pyrus* sp., XII.1954, leg.: J. Győry, det.: Z. Igmándy (BP34488/IZ527); Sopron, Béka-tó, *Quercus* sp., 23.IX.1956, leg. et det.: Z. Igmándy (BP34482), 07.IX.1969, leg. et det.: Z. Igmándy (BP55488/IZ1840); Sopron, Szárhalmi-erdő, *Quercus petraea*, 24.III.1986, leg.: F. Varga, det.: Z. Igmándy (BP90043/IZ3084); Sopron, Dalos-hegy, *Quercus* sp., 20.X.1963, leg.: A. Szappanos, det.: Z. Igmándy (BP13987); Sopron, Fáber-rét, *Quercus cerris*, 21.IV.1959, leg. et det.: Z. Igmándy (BP34426/47670), 13.XI.1963, leg.: Z. Igmándy, F. Varga, det.: Z. Igmándy (BP47632), 21.IX.1965, leg. et det.: Z. Igmándy (BP47625); Sopron, Deák-tér, *Aesculus hippocastanum*, 09.X.2013, leg.: I. Szabó, det.: I. Szabó & V. Papp (PV976); **Tolna county**: Pörböly, *Robinia pseudoacacia*, 10.VII.1956, leg.: H. Pagony, det.: Z. Igmándy (BP34484/IZ762), Pörböly, Szomfova, *Salix* sp., 08.VI.1956, leg.: H. Pagony, det.: Z. Igmándy (BP34483); Lengyel, Annafürdő, *Quercus cerris*, 08.IX.2013, leg. et det.: V. Papp (PV962); **Vas county**: Őriszentpéter, *Quercus* sp., 15.III.1966, leg.: Z. Igmándy, F. Varga, det.: Z. Igmándy (BP47519); **Veszprém county**: Balatonalmádi, *Salix* sp., 26.VII.2011, leg. et det.: V. Papp (PV555); Szigliget, *Salix alba*, 22.VIII.2013, leg. et det.: V. Papp (PV938); **Zala county**: Keszthely, *Salix alba*, 15.II.1953, leg.: I. Koronky, det.: Z. Igmándy (BP20299/34489/IZ387); Keszthely, *Salix* sp., 25.VII.1967, leg. et det.: Z. Igmándy (BP47335/IZ1717); **unknown**: Bejegyertyános, Rózsáskert, *Quercus robur*, 29.VIII.1956, leg. et det.: Z. Igmándy (BP34486).

4 CONCLUSIONS

Up to now, six species of *Ganoderma* are known in Hungary. *Ganoderma valesiacum* Boud. 1894 is a Central European species occurring predominantly in montane to subalpine regions, in the natural stands of *Larix* (Ryvarden – Gilbertson 1993). In Hungary, the host of this species is not native, only some planted stands are known. Therefore the occurence of *G. valesiacum* in Hungary is not to be excluded, but is unlikely.

In the proposed red list of the Hungarian macrofungi (Rimóczi et al. 1999) only two *Ganoderma* species (*G. adspersum*, *G. resinaceum*) are mentioned, which mostly occure in urban habitats in Hungary (Igmándy 1991, Papp 2013). Due to the data of the specimens it can be stated that these species are not ’vulnerable’ in Hungary. Based on their data *G. carnosum* and *G. cupreolaccatum*, which are clearly rarer, are not included on the list. In Hungary only a few *Abies* stands can be found, which is the main host of *G. carnosum*. Therefore it is probably the rarest species of the genus in Hungary. *Ganoderma cupreolaccatum* has perennial basidiocarp, nevertheless not too much occurrences are known. Due to this reason and its habitat preference *G. cupreolaccatum* has recently been declared protected in Hungary [83/2013. (IX. 25.) VM edict].

Acknowledgements: This work is dedicated to the memory of Prof. Zoltán Igmándy (1925-2000), who was the most prominent Hungarian researcher of poroid wood-inhabiting basidiomycetes. His research activity initiated the modern investigation of polypores in Hungary. We are grateful to Csaba Németh for his help in the preparation of the distribution maps. Bálint Dima is thanked for providing *Ganoderma carnosum* specimens from Sopron.

Table 1. Host preference of the Hungarian Ganoderma species based on the examined fungarium materials

	G. adspersum	***G. applanatum***	***G. cupreolaccatum***	***G. carnosum***	***G. lucidum***	***G. resinaceum***
Abies*	1	1		1		
Acer	1	2	1		1	1
Aesculus*	1					1
Alnus		6				
Betula	1	1				
Carpinus		2			6	
Celtis*	1					
Fagus	1	10	9		1	
Fraxinus	5	1				
Gleditschia*	4					
Gymnocladus*	1					
Juglans	1					
Morus*	3					
Picea	1	1				
Platanus*	1				1	1
Populus	3	6				
Prunus	5	1				
Pyrus						1
Quercus	14	12	1		15	11
Robinia*	6	3			1	1
Salix	1	3			4	5
Taxus				2		
Tilia	2	3				
Ulmus	1	1				
unknown	4	7	1		32	
∑	**58**	**60**	**12**	**3**	**61**	**21**

(*) not native in Hungary. The table shows the numbers of the examined specimens. The shades of the boxes indicate the frequency of *Ganoderma* species on different host genera.

REFERENCES

BERNICCHIA, A. (2005): *Polyporaceae* s.l. Fungi Europaei, 10. Ed. Candusso. Alassio. Italy, 808 pp.

CAO, Y. – WU, S. H. – DAI, Y. C. (2012): Species clarification of the prize medicinal *Ganoderma* mushroom „Lingzhi". Fungal Diversity 56 (1): 49–62.

CAO, Y. – YUAN, H. S. (2013): *Ganoderma mutabile* sp. nov. from southwestern China based on morphological and molecular data. Mycol. Progress 12: 121–126.

CHRISTENSEN, M. – HEILMANN-CLAUSEN, J. – WALLEYN, R. – ADAMČIK, S. (2004). Wood-inhabiting fungi as indicators of nature value in European beech forests. In: Marchetti, M. (ed.), "Monitoring and Indicators of Forest Biodiversity in Europe, from ideas to operationality". Proceedings European Forestry Institute 51: 229–237.

CILERDZIC, J. – VUKOJEVIC, J. – STAJIC, M. – HADZIC, I. (2011): Morpho-physiological Diversity between Lingzhi or Reishi Medicinal Mushroom *Ganoderma lucidium* (W. Curt.:Fr.) P. Karst. and *G. carnosum* Pat. International Journal of Medicinal Mushrooms 13 (5): 465–472.

DEMOULIN, V. (2010): Why conservation of the name *Boletus applanatus* should be rejected. Taxon 59(1): 283–286.

DE SIMONE, D. – ANNESI, T. (2012): Occurrence of *Ganoderma adspersum* on *Pinus pinea*. Phytopathologia Mediterranea 51 (2): 374–382.

FLOOD, J. – BRIDGE, P.D. – HOLDERNESS, M. (2000): Preface. Ganoderma Diseases of Perennial Crops. CABI Publishing, Wallingford, UK.

GOMES-SILVA, A. C. – RYVARDEN L. – GIBERTONI, T. B. (2011): New records of *Ganodermataceae* (Basidiomycota) from Brazil. Nova Hedwigia 92: 83–94.

IGMÁNDY, Z. (1968): Die Porlinge Ungarns und ihre phytopathologische Bedeutung (*Polypori Hungariae*) II. Teil. Acta Phytopathologica Acad. Sci. Hung. 3 (2): 221–239.

IGMÁNDY, Z. (1970): Magyarország taplógombái II. rész. [Polypori Hungariae Teil II.] Mikológiai Közlemények (3): 109–112. (in Hungarian)

IGMÁNDY, Z. (1981): Hazánk csövestaplói (Polyporaceae s.l.) és a fajok növénykórtani jelentősége. [The Polyporaceae s. l. of Hungary and their phytopathological significance.] MTA Dissertation, Budapest. 159 p. (in Hungarian).

IGMÁNDY, Z. (1991): A magyar erdők taplógombái. [The poroid fungi of the Hungarian forests.] Akadémiai Kiadó, Budapest. 113 p. (in Hungarian)

JAHN, H. – KOTLABA, F. – POUZ AR, Z. (1980): *Ganoderma atkinsonii* Jahn, Kotl. & Pouz., spec. nova, a parellel species to *Ganoderma lucidum*. Westfälische Pilzbriefe, 10–11: 97–120.

KARSTEN, P. A. (1881). Enumeratio Boletinearum et Polyporearum Fennicarum, systemate novo dispositarum. Revue Mycologique Toulouse 3: 16–19.

KOTLABA, F. (1984): Common polypores (Polyporales s. l.) collected on uncommon hosts. Czech Mycol. 49 (3–4): 169–188.

KRIEGLSTEINER, G.J. (2000): Die Großpilze Baden-Württembergs. 1. – Ulmer, Stuttgart, 629 pp.

LEONARD, A.C. (1998): Two *Ganoderma* species compared. Mycologist 2: 65–68.

MARRIOTT, J.V.R. (1998): Spore size distribution in *Ganoderma*. Mycologist 3: 131.

MATTOCK, G. (2001): Notes on British *Ganoderma* species – emphasising the annual species and *G. carnosum*. Field Mycol., 2: 60–64.

MOESZ G. (1942): Budapest és környékének gombái. [The fungi of Budapest and surroundings] Királyi Magyar Természettudományi Társulat, Budapest. Botanikai közlemények 39 (6): 281–600. (in Hungarian)

MOHANTY, P.S., HARSH, N.S.K. & PANDEY, A. (2011): First report of *Ganoderma resinaceum* and *G. weberianum* from north India based on ITS sequence analysis and micromorphology. Mycosphere, 4: 469–474.

MONCALVO, J. M. – WANG, H. F. – HSEU, R. S. (1995): Gene phylogeny of the *Ganoderma lucidum* complex based on ribosomal DNA sequences: comparison with traditional taxonomic characters. Mycol. Res. 99: 1489–1499.

MONCALVO, J. M. – RYVARDEN, L. (1997): A nomenclatural study of the *Ganodermataceae* Donk. Syn. Fung. 11. Fungiflora: Oslo, Norway, 114 p.

NIEMELÄ, T. – MIETTINEN, O. (2008): The identity of *Ganoderma applanatum* (Basidiomycota). Taxon 57 (3): 963–966.

NORVELL, L. L. (2010): Report of the Nomenclature Committee for Fungi: 15. Taxon 59 (1): 291–293.
NORVELL, L. L. (2011): Report of the Nomenclature Committee for Fungi: 18. Taxon 60 (4): 1199–1201.
PÁL-FÁM F. – LUKÁCS Z. (2002): A Mecsek hegység nagygombái 2. Mikol. Közl., Clusiana 41 (2–3): 35–44.
PAPP V. – SILLER I. (2012): The Hungarian distribution and taxonomic status of *Ganoderma cupreolaccatum* (syn. *Ganoderma pfeifferi*). Mikol. Közl., Clusiana 51 (1): 77–78.
PAPP V. – GEÖSEL A. – ERŐS-HONTI ZS. (2012*a*): Native *Ganoderma* species from the Carpathian Basin with the perspective of cultivation. Acta Alimentaria, Supplement 41: 160–170.
PAPP V. – RIMÓCZI I. – ERŐS-HONTI ZS. (2012b): Adatok a hazai és európai platánok (*Platanus* spp.) taplóihoz. [Polypore data from the Hungarian and European plane trees (Platanus spp.)] Növényvédelem 48 (9): 405–411.
PAPP V. (2013): The occurence of Hungarian *Ganoderma* species in urban habitat. 2. Transilvanian Horticulture and Landscape Studies Conference. Tirgu-Mures, Marosvásárhely, Romania. p. 26–27.
PARK, Y. J. – KWON, O. C. – SON, E. S. – YOON, D. E. – HAN, W. – NAM, J. Y. – YOO, Y. B. – LEE, C. S. (2012): Genetic diversity analysis of *Ganoderma* species and development of a specific marker for identification of medicinal mushroom *Ganoderma lucidum*. African Journal of Microbiology Research 6 (25): 5417–5425.
PATERSON, R.R.M. (2006): *Ganoderma* – A therapeutic fungal biofactory. Phytochemistry 67: 1985–2001.
PATOUILLARD, N.T. (1889): Le genre *Ganoderma*. Bull. Soc. Mycol. France 5: 64–80.
PETERSEN, J. E. (1987): *Ganoderma* in Northern Europe. The Mycologist 2: 62–67.
REDHEAD, S. A. – GINNS, J. – MONCALVO, J.M. (2006): Proposal to conserve the name *Boletus applanatus* against *B. lipsiensis* (Basidiomycota). Taxon 55 (4): 1029–1030.
RIMÓCZI I. – SILLER I. – VASAS G. – ALBERT L. – VETTER J. – BRATEK Z. (1999): Magyarország nagygombáinak javasolt vörös listája.[The proposed red list of the Hungarian macrofungi] *Mikol. Közl., Clusiana* 38 (1-3): 107–132. (in Hungarian)
ROBERT, V. – STEGEHUIS, G. – STALPERS, J. (2013): The MycoBank engine and related databases. http://www.mycobank.org. (accessed: 15/09/2013)
RYVARDEN, L. (1985): Type studies in the Polyporaceae. 17. Species described by W. A. Murrill. Mycotaxon 23: 169–198.
RYVARDEN, L. (1991): Genera of polypores. Nomenclature and taxonomy. Synopsis fungorum 5. Fungiflora, Oslo, Norway. 363.
RYVARDEN, L. – GILBERTSON, R. L. (1993): European polypores. Vol. 1. (*Abortiporus–Lindtneria*). In: Synopsis Fungorum, 6, Fungiflora A/S, Oslo, 387 pp.
SCHWARZE F.W.M.R. – FERNER, D. (2003): *Ganoderma* on trees – Differentiation of species and studies of invasiveness. Arboricultural Journal 27: 59–77.
SEO, G. S. – KIRK, P. M. (2000): Ganodermataceae: nomenclature and classification. In: Flood, J., Bridge , P.D. & Holderness, M. (Eds): Ganoderma Diseases of Perennial Crops. CABI, Wallingford. pp. 3–22.
SILLER I. (2004): Hazai montán bükkös erdőrezervátumok (Mátra: Kékes Észak, Bükk: Őserdő) nagygombái. [The macrofungi of the Hungarian beech forest reserves (Mátra: North Kékes, Bükk: Virgin forest] PhD értekezés, kézirat. Kertészettudományi (Multidiszciplináris Agrártudományok) Doktori Iskola, Budapest. (in Hungarian)
SMITH, B.J. – SIVASITHAMPARAM, K. (2000): Internal transcribed spacer ribosomal DNA sequence of five species of *Ganoderma* from Australia. Mycol. Res. 104(8): 943–951.
SZABÓ I. (2012): Poroid Fungi of Hungary in the Collection of Zoltán Igmándy. Acta Silv. Lign. Hung. 8: 113–122.
SZCZEPKOWSKI, A. – PIĘTKA, J. (2003): New localities and new host of *Ganoderma pfeifferi* in Poland. Acta Mycologica 38: 59–63.
SZEDLAY GY. (2002): Is the widely used medicinal fungus the *Ganoderma lucidum* (Fr.) Karst. sensu stricto? Acta Microbiol Immunol Hung 49: 235–243.
STEYAERT, R.L. (1961): Genus *Ganoderma* (Polyporaceae) taxa nova. 1. Bull. Jardin Bot. Bruxelles 31: 69–83.

STEYAERT, R. L. (1972): Species of *Ganoderma* and related genera mainly of the Bogor and Leiden herbaria. Persoonia 7 (1): 55–118.

TRECKER K. – SZABÓ I. (2002): Farontó gombák a Ropolyi Erdőrezervátumban. [Wood decaying fungi in the Ropoly Forest Reserve] Mikol. Közl., Clusiana 41 (2-3): 67-94. (in Hungarian)

TRIGOS, Á. – MEDELLÍN, J. S. (2011): Biologically active metabolites of the genus *Ganoderma*: Three decades of myco-chemistry research. Revista Mexicana De Micología 34: 63–83.

WANG, D.-M. – WU, S.-H. – SU, C.-H. – PENG, J.-T. – SHIH, Y.-H. – CHEN, L.-C. (2009): *Ganoderma multipileum*, the correct name for '*G. lucidum*' in tropical Asia. Botanical Studies 50: 451–458.

WANG, X.-C. – XI, R.-J. – LI Y. – WANG, D.-M. – YAO, Y.-J. (2012): The species identity of the widely cultivated *Ganoderma, 'G. lucidum'* (Ling-zhi), in China. Plos One 7 (7): e40857.

WASSER, S.P. (2005): Reishi or Ling Zhi (*Ganoderma lucidum*). in: Coates, P.M., Betz, J.M., Black man, M.R., Cragg , G.M., Levine, M., Moss, J. & White, J.D. (Eds): Encyclopedia of dietary supplements. Marcel Dekker, New York (USA), pp. 3–622.

WELTI, S. – COURTECUISSE, R. (2010): The Ganodermataceae in the French West Indies (Guadeloupe and Martinique). Fungal Diversity 43 (1): 103–126.

DE GRUYTER OPEN DOI: 10.2478/aslh-2013-0007 Acta Silv. Lign. Hung., Vol. 9 (2013) 85–96

Modelling the Potential Distribution of Three Climate Zonal Tree Species for Present and Future Climate in Hungary

Norbert MÓRICZ[a*] – Ervin RASZTOVITS[b] – Borbála GÁLOS[b] – Imre BERKI[b] – Attila EREDICS[b] – Wolfgang LOIBL[a]

[a] Energy Department, Austrian Institute of Technology, Vienna, Austria
[b] Institute of Environmental and Earth Sciences, Faculty of Forestry, University of West Hungary, Sopron, Hungary

Abstract – The potential distribution and composition rate of beech, sessile oak and Turkey oak were investigated for present and future climates (2036–2065 and 2071–2100) in Hungary. Membership functions were defined using the current composition rate (percentage of cover in forest compartments) of the tree species and the long-term climate expressed by the Ellenberg quotient to model the present and future tree species distribution and composition rate. The simulation results using the regional climate model REMO showed significant decline of beech and sessile oak in Hungary during the 21st century. By the middle of the century only about 35% of the present beech and 75% of the sessile oak stands will remain above their current potential distribution limit. By the end of the century beech forests may almost disappear from Hungary and sessile oak will also be found only along the Southwest border and in higher mountain regions. On the contrary the present occurrences of Turkey oak will be almost entirely preserved during the century however its distribution area will shift to the current sessile oak habitats.

potential tree species distribution / composition rate / beech / sessile oak / Turkey oak

Kivonat – Három klímazonális fafaj hazai potenciális elterjedésének modellezése jelenlegi és jövőbeni klímában. A bükk, a kocsánytalan tölgy és a csertölgy potenciális elterjedését és elegyarányát vizsgáltuk Magyarországon a jelenlegi és a jövőben (2036–2065 és 2071–2100) várható klimatikus körülmények között. A vizsgált fafajok jelenlegi elegyarányának (az erdőrészletben elfoglalt terület aránya, %) és a klímának (az Ellenberg index-el kifejezve) az összefüggését használtuk a fafajok elterjedésének modellezéséhez. A REMO regionális klímamodellel történt szimuláció a bükk és a kocsánytalan tölgy elterjedési területének és elegyarányának jelentős csökkenését mutatta a 21. század folyamán. A század közepére a jelenlegi bükk állományok 35%-a, a kocsánytalan tölgy állományok 75%-a maradna a jelenlegi alsó elterjedési határuk felett. A század végére a bükk szinte teljesen eltűnhet Magyarország területéről és a kocsánytalan tölgy is a magasabb hegyvidékekre és a délnyugati határ menti területre húzódhat vissza. Ellenben a csertölgy jelenlegi állományait várhatóan nem érinti számottevően a klímaváltozás, viszont az elterjedési területe a jelenlegi kocsánytalan tölgyes állományok helyét foglalhatja el.

potenciális fafaj elterjedés / elegyarány / bükk / kocsánytalan tölgy / csertölgy

[*] Corresponding author: norbert.moricz@ait.ac.a; Giefinggasse 2, A-1210 VIENNA

1 INTRODUCTION

The present distribution of tree species is influenced by several factors such as historic and current ecological and climatic conditions, natural disturbance regimes and forest management activities. However, climate is generally considered to be one of the most important factor of the potential natural distribution of tree species.

For Central Europe, climate models project about 2–5°C annual mean air temperature rise in the 21st century (IPCC 2007). Climate change is likely to increase the frequency of summer drought in this region (Schär et al. 2004, Bartholy et al. 2007, Beniston et al. 2007, Gálos et al. 2007).

Climate change is considered to unfavourably affect forest ecosystems through the impact on forest growth and regeneration. Numerous studies suggest a decline in forest regeneration (Rennenberg et al. 2004, Penuelas et al. 2007) or extensive forest dieback in mid european latitudes (Berki et al. 2009, Czúcz et al. 2010, Kramer et al. 2010, Lindner et al. 2010) during dryer and warmer climatic conditions as it is already observed in several locations (Allen et al. 2010, Mátyás 2010).

In general the xeric (or rear, trailing) limits of the tree species is difficult to follow due to the more complex ecology and human disturbance. The occurrence of the species is determined here mainly by climatic aridity (Mátyás et al. 2009), contributing to the loss of competitive ability (Loehle 1998, Hogg et al. 2005). However, the change in climatic aridity is more difficult to predict than alone air temperature due to e.g. the high variability of soil water holding capacity. Biotic interactions (e.g. pests and disease), persistence and plasticity of species may also play a major role at xeric range limits (Mátyás et al. 2008, Lakatos and Molnár 2009).

Here we will deal with bioclimatic envelope models (niche models) to examine effects of climate change to a set of the main tree species in Hungary. Niche models rely on statistical correlations between existing species distribution and environmental variables to define a species' tolerance (Pearson & Dawson, 2003). These kind of models are often used to predict the impacts of climate change on species distribution (Rehfeldt et al. 2003, Araujo et al. 2004; Thuiller et al. 2005, Czúcz et al. 2010, Rasztovits et al. 2012). Although the distribution limits are defined through statistical models with considerable uncertainty (Kramer et al. 2010), the predictions of general distribution changes have high ecological and economic significance (Koskela et al. 2007).

Statistical distribution models (SDMs) apply statistical relationship between observed presence/absence or abundance of a given species to a relevant set of limiting environmental factors controlling the distribution of the species (Guisan and Zimmermann 2000).

Numerous studies have focused on particularly important group of major forest tree species, such as beech and oak species predicting potential shifts of forest cover (Rehfeldt et al. 2003, Thuiller et al. 2005, Ohlemüller et al. 2006, Rickebusch et al. 2007, Kramer 2010). But due to the difficulties of modelling at the xeric limits, such distribution studies are scarce (Hogg et al. 2005, Czúcz et al. 2010, Rasztovits et al. 2012).

In this paper we investigate the potential distribution and composition rate of beech (*Fagus sylvatica* L.), sessile oak (*Quercus petrea*) and Turkey oak (*Quercus cerris*) for present (1961–1990) and future climate (2036–2065 and 2071–2100) applying fuzzy membership functions using the relationship between the composition rate of the tree species and long-term climate in Hungary. Although the presence of tree species in Hungary is influenced by human (and will also in the future), the composition rate (%) was used as a kind of probability of occurrence instead of using only the presence/absence information of the species.

All three investigated tree species form extensive forest stands throughout Central Europe and from the forest steppe limit upward, according to their moisture requirement. Turkey oak, sessile oak and beech dominate as climate indicators of the zonal forests.

So far, distribution changes of beech and sessile oak were modeled since they are the most important tree species in forest management in Hungary. Only a few studies are dealing with the distribution change of turkey oak (e.g. Führer et al. 2011). The resistance of turkey oak against droughts may increase the importance of this species in the forest sector considering climate change.

In our study the following research questions are addressed:

1. What is the relation between the tree species composition and climate aridity?
2. How would the current potential distribution and tree species composition change under projected climate conditions?
3. Are the modeled present and future potential distribution of the tree species agree with the results of previous studies?

To answer the research questions (1) we created the Ellenberg climate surfaces for the present (1961–1990) and future (2036–2065 and 2071–2100), (2) coupled the composition information of beech, common oak and turkey oak with EQ to define membership functions, (3) modeled the current and future distribution of the species and (4) compared the present and future distributions with other potential distribution maps.

2 MATERIALS AND METHODS

2.1 Climate data

For modeling the potential vegetation the Ellenberg quotient (*EQ*, Ellenberg 1988) has been used. EQ has been shown as one of the best indicator for tree species distribution (Czúcz et al. 2010, Rasztovits et al. 2012, Stojanovic et al. 2013) defined as the mean temperature of the warmest month (July) divided by the annual precipitation:

$$EQ = 1000 T_{07} P_{ann}^{-1}$$

The precipitation data (approx. 80 stations) was interpolated by Kriging with 50km search radius and 500m resolution. The interpolation was checked with cross-validation namely by leaving out stations with measured data from interpolation and afterwards comparing it to the interpolated value. This has shown that the average deviation was only about 10.2% of the annual precipitation sum.

Air temperature for July (31 stations) was also interpolated using kriging with 500m resolution. The effect of elevation was considered by the SRTM digital elevation model using constant monthly gradients (Peczely 1979).

For the future climate (2036–2065 and 2071–2100) results of the regional climate model simulations by REMO (Jacob et al. 2001, Jacob et al. 2007) were analyzed for the A1B IPCC-SRES emission scenario (*Table 1*).

Table 2. Simulation results of REMO for the future related to the base period 1961–1990 (values are representing country means for Hungary)

Climate variable	1961–1990	2036–2061	2071–2100
July temperature mean	19.6°C	+1.6°C	+3.7°C
Annual precipitation sum	583 mm	+2.59%	–2.2%

For country means, climate change signals for July temperature mean and annual precipitation sum was calculated as the difference of the simulated future and past periods (e.g. 2036–2060 vs. 1961–1990). To avoid the model bias, delta change approach has been applied: the simulated change signals were added to the observed climate in the past. Based on the resulting temperature and precipitation maps**,** EQs have been computed for the future in the same way as for the present climate.

Applying climatic means are not fully appropriate for describing species distribution change driven by climatic change, since the decline of the species is related mostly to prolonged extreme events and subsequent biotic damages (Berki – Rasztovits 2009, Rasztovits et al. 2012). However, lacking reliable projections on extreme events, climatic means were used as surrogates (Mátyás et al. 2008).

2.2 Forest data

As mentioned above the distributions of three tree species were investigated beech, sessile oak and Turkey oak in Hungary for potential distribution modeling. The occurrence and composition data was derived from the Hungarian Forest Inventory database provided by the Central Agricultural Office, gathered in 2012. The database included all the forest compartments containing any of the three tree species. We have used the geometrical centre of the forest compartment polygons as reference point to extract climate parameters from digital climate surfaces.

The Forest Inventory database contained details on site and stand conditions, which allow excluding sites located at microclimatic, edaphic and hydrological extremes, from further analysis. Accordingly, all compartments have been omitted with shallow soil, surplus water effect and steep slopes above 20°.

The composition rate (%) of tree species was defined as the species percentage cover of each forest compartment which reflects the favour of the environmental conditions for the tree species occurrences. The natural equilibrium in the mixture ratio is strongly altered by the forest management even in semi-natural forests but towards the distribution limit of the tree species this selection has no significant effect on the mixture ratio as the ecological conditions overwrite biotic interactions.

2.3 Defining the relation between EQ and the composition rate

We defined the relationship between the EQ and mixture rate to model the current and future potential distribution of the three tree species.

First, the value of the present aridity index (1961–1990) was added to each compartment using zonal statistics. The relations between the composition rates of the species and EQ were then plotted on compartment level. We aggregated the data to equal interval classes of EQ and calculated the average composition rate of each class with the corresponding 95% confidence intervals. Polynomial regressions in the order of four were applied to describe the relationships.

2.4 The fuzzy membership approach

To model the current and future potential distribution of tree species the fuzzy membership has been applied. This approach was selected as it allows to better consider the continuous variation of forest stand composition of tree species due to location characteristics, species competition and forest management.

The approach uses membership functions to classify features of arbitrary range into fuzzy values, between zero and one to indicate the degree of membership. In our case the membership functions were based on the relation between EQ and composition rate of the tree species.

We have used the eCognition software (Definiens 2005). eCognition is usually applied for remote sensing classifications by merging the information of the spectral "bands" of images like orthophotos or satellite images. Here the three tree composition fractions were stored in separate grid layers treated as 3 bands of an image raster. So finally spatial objects of similar tree composition could be delineated through a statistical segmentation process. The extracted objects correspond to certain homogeneity criteria based on a scaling parameter.

The membership functions for the three tree species are evaluated for each object during the classification. The result of the classification is twofold, a fuzzy classification with mixture values of tree species and a discrete classification where each image objects are assigned to of the one tree species with the highest fuzzy share.

3 RESULTS AND DISCUSSIONS

3.1 Relationship of EQ and composition rate

The computed Ellenberg quotient maps show that the aridity will increase in Hungary during the century (*Figure 1*).

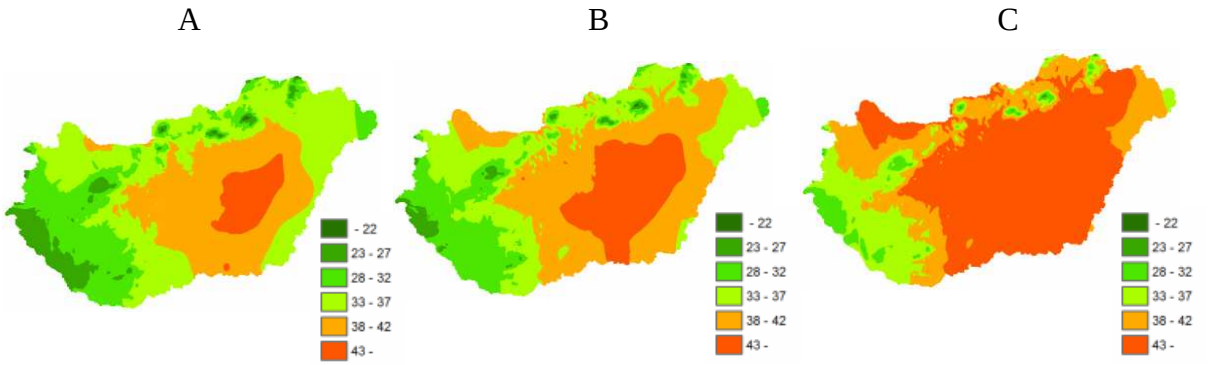

Figure 1. EQ for 1961–1990 (A) for 2036–2065 (B) and for 2071–2100 (C)

For visualization of the dominant spatial occurrences of these species we have used the threshold value of 90% composition rate (*Figure 2*).

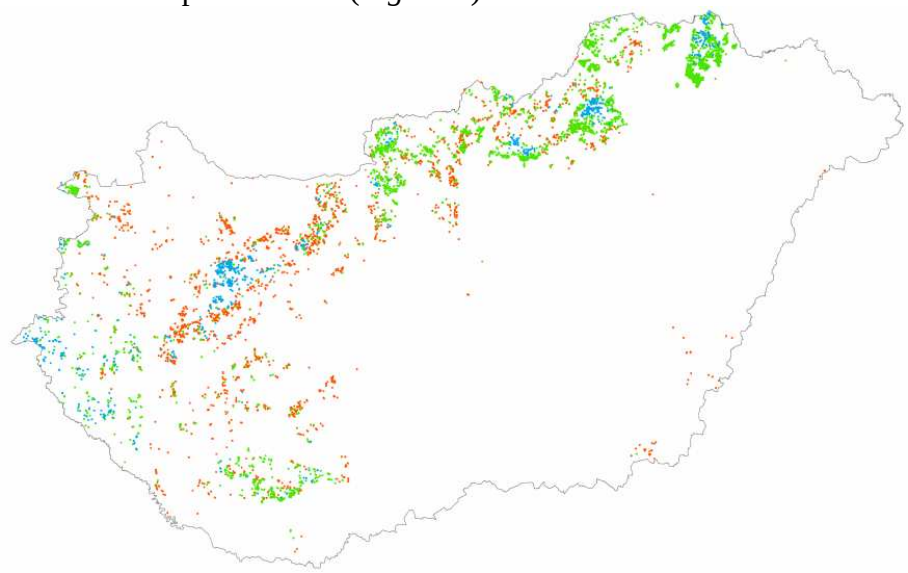

Figure 2. Beech (blue), sessile oak (green) and Turkey oak (red) compartments (with composition rate above 90%) in Hungary

Beech, which is the most climate-dependent among the investigated species, is mainly dominant in the higher mountain areas and in SW-Hungary. The actual distributions of sessile and Turkey oak are disturbed, due to forest management praxis, especially along the xeric limit of the species. Sessile oak is more widespread in the lower parts of the mountains especially in NE-Hungary. Turkey oak occupies the more arid locations along the foothills and lowland regions but it can be also found in more humid conditions as the dominant.

The relationships between EQ and composition rate for each forest compartment have shown no clear correlation in any case of the studied species. Merely, the aggregation of the EQ values to equal classes and the assignment the mean value of the composition rate to the classes have revealed a strong link (*Figure 3*).

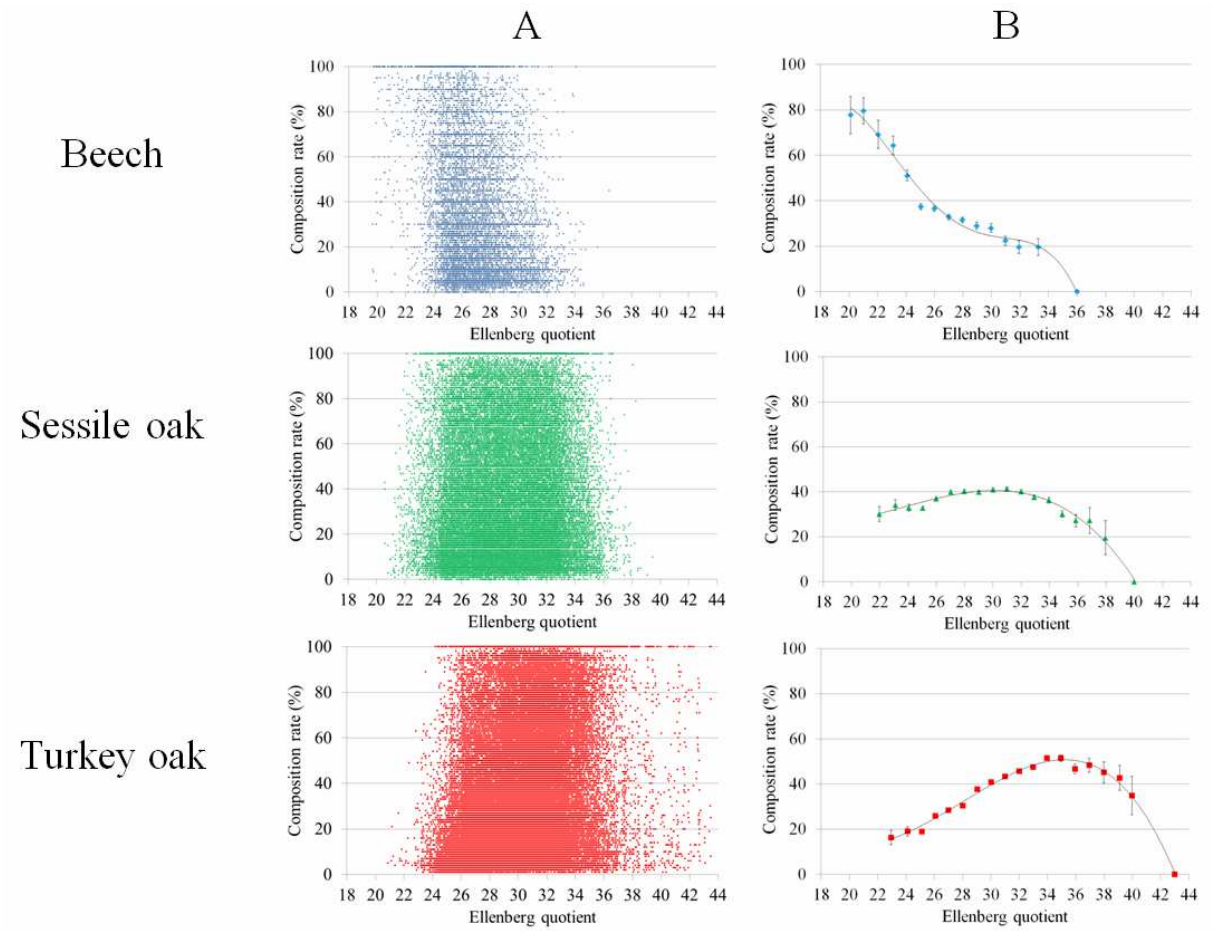

Figure 3. The original (A) and aggregated (B) relationship between the EQ and the composition rate of beech, sessile oak and Turkey oak with corresponding confidence intervals

The membership functions show the degree of suitability of the tree species on a given location using the composition rate as proxy. The lower limit of each tree species was given by the lowest EQ-s of the occurrences. In general the relationships show that the lower limit of each species is approached abruptly, but at different EQ limits. No occurrences of these species were observed above EQ 43. Beech is the dominant tree species at the most humid locations in Hungary, the mixing ratio reaches here up to 80%. The composition rate of sessile oak is surprisingly balanced with around 30–40% in the distribution area, but decreases by approaching its lower limit. The mixing of Turkey oak increases with higher aridity up to 50% until around EQ 35 and then it decreases rapidly as we reach the forest-steppe limit (*Figure 3*).

3.2 Potential distribution of the investigated tree species for recent and future climate

The result of the discrete classification is a map where each tree composition object is assigned to only one tree species. The current potential distribution map is in good agreement with the current distributions of the tree species (*Figure 4*).

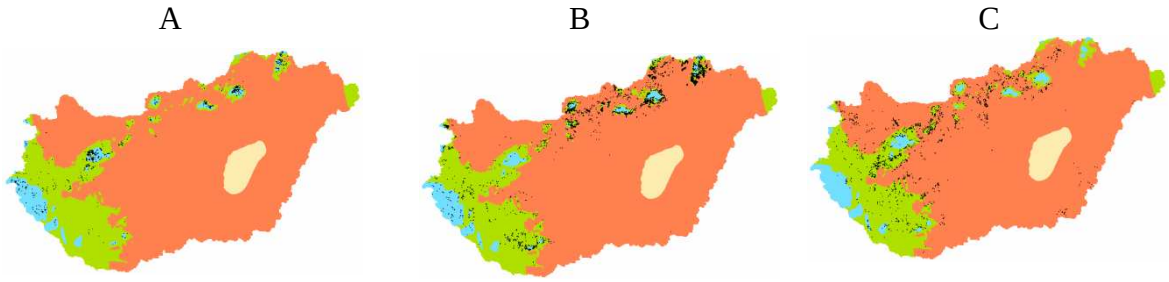

Figure 4. Modeled current tree species distribution maps (A-B-C: beech – blue, sessile oak – green, Turkey oak – red, no forest – white) with the current distribution of beech (A), sessile oak (B) and Turkey oak (C) (with composition rate above 90%)

In case of beech the modeled current tree species distribution pattern covers most of the current pure beech stands. However, some under-prediction can be observed at lower elevations. The lower distribution limit of sessile oak matches well with the forest stands in the Transdanubian region, but there is some substantial difference in the mountains of North-East Hungary. Turkey oak could potentially occupy most of the lowland areas in Hungary except of the most arid places around the center of the Hungarian lowland. Both oak species can be found not only in their dominant area but also in more moist conditions.

The modeled future tree species distribution patterns show large changes due to projected climate change (*Figure 5*).

Figure 5. Modeled future tree species distribution maps for 2036–2065 (A) and 2071–2100 (B), beech – blue, sessile oak – green, Turkey oak – red, no forest – white

The distribution area of beech is expected to decrease substantially till 2050 and will be restricted to the higher mountain areas and along the south-west border. By the end of the century it could disappear totally except of some locations in the highest mountains (e.g in Bükk). Similarly, sessile oak is expected to decline and will be restricted and its occurrence mainly to the south-west of Hungary and in general to higher elevation by 2050 (*Figure 5*). The present occurrences are expected to decrease by about 25%. By the end of the century sessile oak can only be found in higher mountains and probably along the border to Slovenia (*Table 2*).

Table 2. Percentage of occurrences relative to the total occurrences found above the lower limit of potential distribution area presently (1961–1990)

	2036–2061 (%)	2071–2100 (%)
Beech	35.3	1.7
Sessile oak	75.5	13.9
Turkey oak	99.8	96.9

The distribution area of Turkey oak will be about the same by the middle of the century since while it will lose some area in the Hungarian Lowland, it will occupy large tracts of area from sessile oak in the Transdanubian region (*Figure 5*). Finally, by the end of the century the optimum area of this species will also slightly decrease and relocated from the lowland to the hilly and mountainous regions. The area where none of these tree species will find optimal conditions will be significantly greater during the course of the century (*Figure 5*).

The potential composition of the tree species evaluated by the fuzzy membership functions for present and future climates show similar changes (*Figure 6*).

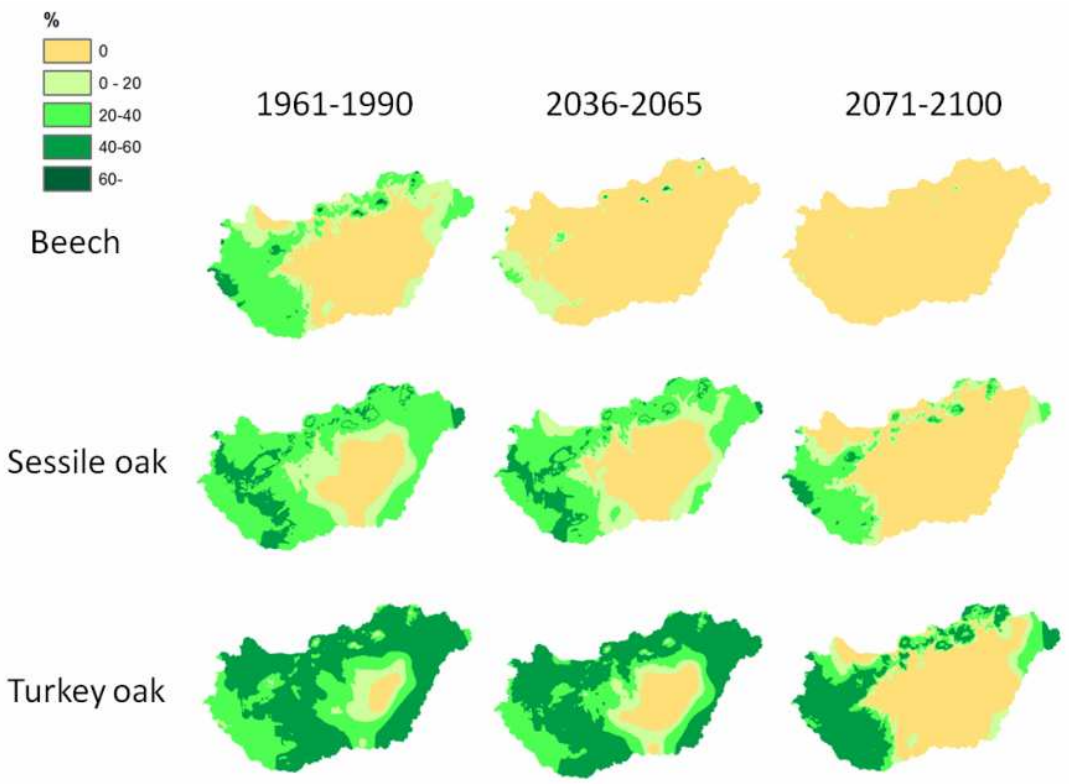

Figure 6. Composition rates of tree species for present (1961–1990) and future climates (2036–2065 and 2071–2100)

Beech is already expected to be a minor tree species for the middle of the century and only some stands may preserve until the end of the century particularly in sites with appropriate microclimatic conditions. The mixture of sessile oak may also decline during the century and the most dominant stands will be concentrated in the mountains (*Figure 6*). The large mixture of Turkey oak in large parts of Hungary will even increase and only by the end of the century it is expected that the mixture may begin to decline especially at lower elevations.

3.3 Comparison with other potential vegetation maps

We have compared our results with similar studies which was not easy due to the wide variety of the applied methods and climate scenarios.

Czúcz et al. (2010) focused on the analysis of climate change impacts at the trailing (xeric) limits of closed forests in Hungary exploring beech and sessile oak forests. Conditional tree regression was applied which have revealed the significance of EQ in distribution modeling. Their results for the HADCM3 A1B scenario showed similar tendencies of decline of the investigated tree species during this century.

The future distribution pattern of the main tree species of the Transdanubian region was modelled by Führer et al. (2011, 2013). For describing the growth of the trees, the forest aridity index was developed, based on phenological patterns of growth. Two future climate scenarios have been applied assuming 1 and 1.7°C increase in summer temperature and decrease of precipitation in summer by 8.2%. The larger temperature change implies that beech may almost entirely disappear from this region. The area of the Turkey oak may remain the same but shifts partly to the area of today's sessile oak. Finally, the area of forest steppe may expand and occupies some of the area from current Turkey oak, similar as projected by our approach.

Rasztovits et al. (2012) has evaluated the habitat suitability of beech forests for three terms in the 21st century in Hungary using different species distribution models. Here a CLM A1B simulation was used. The authors have found that the neural networks (e.g. BP-ANN) and classification tree methods (e.g. CTree) delivered better results than other approaches. BP-ANN predicted a very slight shrinkage of the potential area (8.0%) during 2036–2065. A considerable decrease of the potential area was foreseen only to the end of this century which results that about 45% of the current stands will be out of the potential area. Regionally the most serious decrease was predicted for the sub-Mediterranean region in Southwest Hungary. CTree predicted a more significant shrinkage of beech in all regions of Hungary by losing 67.5% of the area during 2036–2065 and 74.7% during 2071–2100 which was quite in agreement with our results.

3.4 Uncertainties

Our approach is based on the assumption that the potential distribution of beech and common oak are determined by climatic means. The relationship between the potential distribution and the climatic mean may not hold when weather extremes (like droughts) occur with a much higher frequency than nowadays. These act as triggering effect on tree growth decline and pests or diseases that attack populations of weakened vitality and cause mortality (Bréda et al. 2006, McDowell et al. 2007, Lakatos and Molnár 2009). So predictions based on climatic means alone could overestimate the potential distribution of species.

Predictive ecological modelling is usually based on equilibrium between climate and species tolerance. This biotic uncertainty originates from the inadequate understanding of the mainly ecological factors influencing the equilibrium of the species distribution. The genetically set tolerance limits of species are wider than realized ones and this is especially valid for populations near their distribution limits. Climate change may affect also consumes and pathogens that cannot be predicted. The persistence of forest ecosystems is one of the main sources of uncertainty of distribution modelling, which is supported by the wide phenotypic plasticity of trees proven by comparative field tests (Mátyás 2007). The persistence of forests is further reinforced by planned forest management and changing species preferences, which may assist to maintain forests in the future (Mátyás et al. 2009).

Soil conditions (e.g. soil texture, water holding capacity, groundwater depth) were not considered, since fine-scale information for forests compartments was not available, which

could lead to over or underestimation of the potential distribution areas of tree species, compared to the pure climatic based assessment of this study.

A substantial proportion of forest stands are situated on non-zonal sites, which were not accounted by our modelling, but these sites may assist to preserve optimal conditions for the investigated species even if the climate will not be suitable for zonal occurrences.

4 CONCLUSIONS

The composition rate was used for describing the probability of occurrence instead of the presence/absence information of the species. We have defined functions using the recent composition rate and the Ellenberg quotient, both applied to model the present and future tree species distribution and composition rate. We have only considered stands located at zonal positions.

The projections based on the simulation results of the regional climate model REMO have shown a significant decline of beech and sessile oak in Hungary during the century which is in accordance with other study results near the xeric limit of these species. By the middle of the century only about 35% of the present beech and 75% of the sessile oak stands will remain above their current potential distribution limit. By the end of the century beech forest may almost disappear from Hungary and sessile oak will also be found only along the Southwest border and in higher mountain regions. On the contrary the present occurrences of Turkey oak will be almost entirely preserved during the century however its distribution area will be shifted to the Transdanubian region hence occupying large areas of current sessile oak habitat.

This study also underlines the importance of future forest management and conversion strategies from the perspective of the species selection, regeneration and financial issues. The results of the study will be in more detail investigated in an upcoming national project TAMOP dealing with the preparation of a decision support system for forest management in Hungary.

Acknowledgements: The This research was financially supported by the TÁMOP 4.2.2-08/1-2008-0020, the 4.2.2.B-10/1-2010-0018 “Talentum”, the TÁMOP-4.2.2.A-11/1/KONV-2012-0004 and the 4.2.2.A-11/1/KONV-2012-0013 "Agrárklíma" joint EU-national research projects.

REFERENCES

ALLEN, C.D. − MACALADY, A. − CHENCHOUNI, H. − BACHELET, D. − MCDOWELL, N. − VENNETIER, M. − GONZALES, P. − HOGG, T. − RIGLING, A. − BRESHEARS, D.D. − FENSHAM, R. − ZHANG, Z. − KITZBERGER, T. − LIM, J.-H. − CASTRO, J. − ALLARD, G. − RUNNING, S.W. − SEMERCI, A. − COBB, N. (2010): A global overview of drought and heat-induced tree mortality reveals emerging climate change risks for forests. Forest Ecology and Management 259: 660–684.

ARAUJO, M.B. − CABEZA, M. − THUILLER, W. − HANNAH, L. − WILLIAMS, P.H. (2004): Would climate change drive species out of reserves? An assessment of existing reserve-selection methods. Global Change Biology 10: 1618–1626.

BARTHOLY, J. − PONGRÁCZ, R. − GELYBÓ, GY. (2007): Regional climate change expected in Hungary for 2071–2100. Applied Ecology and Environmental Research 5(1): 1–17.

BENISTON, M. – STEPHENSON D.B. − CHRISTENSEN, O.B. − FERRO, C.A.T − FREI, C. − GOYETTE, S. − HALSNAES, K. − HOLT, T. − JYLHÄ, K. − KOFFI, B. − PALUTIKOF, J. − SCHÖLL, R. − SEMMLER, T. – WOTH, K. (2007): Future extreme events in European climate: an exploration of regional climate model projections. Climatic Change 81: 71–95 doi: 10.1007/s10584-006-9226-z.

BERKI, I. – RASZTOVITS, E. – MÓRICZ, N. – MÁTYÁS, CS. (2009): Determination of the drought tolerance limit of beech forests and forecasting their future distribution in Hungary. Cereal Research Communications 37: 613–616.

BRÉDA, N. – HUC, R. – GRANIER, A. – DREYER, E. (2006): Temperate forest trees and stands under severe drought: a review of ecophysiological responses, adaptation processes and long-term consequences. Annals of Forest Science 63: 625–644.

CZÚCZ, B. − GÁLHIDY, L. − MÁTYÁS, CS. (2010): Limiting climating factors and potential future distribution of beech (Fagus sylvatica L.) and sessile oak (Quercus petraea (Mattuscha) Liebl.) forests near their low altitude - xeric limit in Central Europe. Annals of Forest Science 68(1): 99–108.

DEFINIENS (2005): eCognition Professional, Munich.

FÜHRER, E. − HORVÁTH, L. − JAGODICS, A. − MACHON, A. – SZABADOS, I. (2011): Application of a new aridity index in Hungarian forestry practice. Időjárás 115 (3): 205–216.

FÜHRER, E. − JAGODICS, A. – JUHASZ, I. − MAROSI, GY. − HORVÁTH, L. (2011): Ecological and economical impacts of climate change on Hungarian forestry practice. Időjárás 117 (2): 159–174.

GÁLOS B. – LORENZ P.H. – JACOB, D. (2007): Will dry events occur more often in Hungary in the future? Environmental Research Letters 2 034006 (9 pp.)

GUISAN, A. − ZIMMERMANN, N.E. (2000): Predictive habitat distribution models in ecology. Ecological Modeling 135: 147–186.

HOGG, E.H. − BRANDT, J.P. − KOCHTUBAJDA, B. (2005): Factors affecting interannual variation in growth of western Canadian aspen forests during 1951–2000. Canadian Journal of Forest Research 35: 610–622.

IPCC − Summary for Policymakers. – In: Climate Change (2007): The Physical Science Basis. Contribution of Working Group I. [Solomon, S. – Manning, Q.D. – Chen, M. – Marquis, Z. – Averyt, M.K.B.– Miller, H.L. (eds.)]. Cambridge University Press, Cambridge, New York.

JACOB, D. – ANDRAE, U. – ELGERED, G. – FORTELIUS, C. – GRAHAM, L.P. – JACKSON, S.D. – KARSTENS, U. – KOEPKEN, C. – LINDAU, R. – PODZUN, R. – ROCKEL, B. – RUBEL, F. – SASS, H.B. – SMITH, R.N.D. − VAN DEN HURK, B.J.J.M. – YANG, X. (2001): A comprehensive model intercomparison study investigating the water budget during the BALTEX-PIDCAP Period. Meteorology and Atmospheric Physics 77 (1–4): 19–43.

JACOB, D. – BÄRRING, L. – CHRISTENSEN, O.B. – CHRISTENSEN, J.H. − DE CASTRO, M. – DÉQUÉ, M. – GIORGI, F. – HAGEMANN, S. – HIRSCHI, M. – JONES, R. – KJELLSTRÖM, E. – LENDERINK, G. – ROCKEL, B. – SÁNCHEZ, E. – SCHÄR, C. – SENEVIRATNE, S.I. – SOMMOT, S. − VAN ULDEN, A. − VAN DEN HURK, B. (2007): An inter-comparison of regional climate models for Europe: model performance in present-day climate. Climatic Change 81:31–52. doi:10.1007/s10584-006-9213-4.

KOSKELA, J. − BUCK, A. − TEISSIER DU CROS, E. (eds.) (2007): Climate change and forest genetic diversity: Implications for sustainable forest management in Europe. Biodiversity International, Rome, Italy.

KRAMER, K. − DEGEN, B. − BUSCHBOM, J. − HICKLER, T. − THUILLER, W. − SYKES, M. − DE WINTER, W. (2010): Modeling exploration of the future of European beech (Fagus sylvatica L.) under climate change – Range, abundance, genetic diversity and adaptive response. Forest Ecology and Management 259: 2213–2222.

LAKATOS, F. − MOLNÁR, M. (2009): Mass mortality of beech on Southwest Hungary. Acta Silvatica& Lignaria Hungarica 5: 75–82.

LINDNER, M. − MAROSCHEK, M. − NETHERER, S. − KREMER, A. − BARBATI, A. − GARCIA-GONZALO, J. − SEIDL, R. − DELZON, S. − CORONA, P. − KOLSTROM, M. − LEXER, M.J. − MARCHETTI, M. (2010): Climate change impacts adaptive capacity and vulnerability of European forest ecosystems. Forest Ecology Management 259 (4): 698–709.

LOEHLE, CS. (1998): Height growth tradeoffs determine northern and southern range limits for trees. Journal of Biogeography 25: 735–742.

MÁTYÁS, CS. (2007): What do field trials tell about the future use of forest reproductive material? In: Koskela, J, Buck A. and Teissier du Cros, E. (eds.): Climate change and forest genetic diversity: Implications for sustainable forest management in Europe. Biodiversity International, Rome, Italy. pp. 53–69.

MÁTYÁS, CS. − NAGY, L. − UJVÁRI-JÁRMAY, É. (2008): Genetic background of response of trees to aridification at the xeric forest limit and consequences for bioclimatic modeling. In: Strelcova K, Mátyás Cs, Kleidon A (eds.) Bioclimatology and natural hazards. Springer Verlag, Berlin pp. 179–196.

MÁTYÁS, CS. − VENDRAMIN, G.G. − FADY, B. (2009): Forests at the limit: evolutionary-genetic consequences of environmental changes at the receding (xeric) edge of distribution. Annals of Forest Science 66: 800–80.

MÁTYÁS, CS. (2010). Forecasts needed for retreating forests (Opinion). Nature 464: 1271

OHLEMÜLLER, R. − GRITTI, E.S. − SYKES, M.T. − THOMAS, C.D. (2006): Quantifying components of risk for European woody species under climate change. Global Change Biology 12: 1788–1799.

PÉCZELY, GY. (1979): Éghajlattan. Climatology – in Hungarian. Nemzeti Tankönyvkiadó, Budapest.

PEARSON, R. G. – DAWSON, T. P. (2003): Predicting the impacts of climate change on the distribution of species: are bioclimate envelope models useful?. Global Ecology and Biogeography 12 (5): 361–371.

PENUELAS, J. – OGAYA, R. – BOADA, M. – JUMP, A.S. (2007): Migration, invasion and decline: changes in recruitment and forest structure in a warming-linked shift of European beech forest in Catalonia (NE Spain). Ecography 30: 829–837.

RASZTOVITS, E. − MÓRICZ, N. − BERKI, I. − PÖTZELSBERGER E. − MÁTYÁS CS. (2012): Evaluating the performance of stochastic distribution models for European beech at low-elevation xeric limits. Időjárás 116(3): 173–194.

REHFELDT, G.E. − TCHEBAKOVA, N.M. − MILYUTIN, L.I. − PARFENOVA, E.I. − WYKOFF, W.R. − KOUZMINA, N.A. (2003): Assessing population responses to climate in Pinus silvestris and Larix spp. of Eurasia with climate transfer models. Eurasian Journal of Forestry Research 6: 83–98.

RENNENBERG, H. – SEILER, W. – MATYSSEK, R. – GESSLER, A. – KREUZWIESER, J. (2004): Die Buche (Fagus sylvatica L.) – ein Waldbaum ohne Zukunft im südlichen Mitteleuropa? Allgemeine Forst- und Jagdzeitung 175: 210–224.

RICKEBUSCH, S. − GELLRICH, M. − LISCHKE, H. − GUISAN, A. − ZIMMERMANN, N.E. (2007): Combining probabilistic land-use change and tree population dynamics modeling to simulate responses in mountain forests. Ecological Modeling 209: 157–168.

SCHÄR, C. − VIDALE P.L. − LÜTHI, D. − FREI, C. − HÄBERLI, C. − LINIGER, M.A. − APPENZELLER, C. (2004): The role of increasing temperature variability in European summer heatwaves. Nature 427: 332–336 doi: 10.1038/nature02300.

STOJANOVIC, D.B. − KRZIC, A. − MATOVIC, B. − ORLOVIC, S. − DUPUTIE, A. − DJURDJEVIC, V. − GALIC, Z. − STOJNIC, S. (2013): Prediction of the European beech (Fagus sylvatica L.) xeric limit using a regional climate model: An example from southeast Europe. Agricultural and Forest Meteorology 176: 94–103.

THUILLER, W. − LAVOREL, S. − ARAUJO, M.B. − SYKES, M.T. − PRENTICE, I.C. (2005): Climate change threats to plant diversity in Europe. Proceedings of the National Academy of Sciences 102: 8245–8250.

DE GRUYTER OPEN DOI: 10.2478/aslh-2013-0008 Acta Silv. Lign. Hung., Vol. 9 (2013) 97–109

Measuring the Bearing Capacity of Forest Roads with an Improved Benkelman Beam Apparatus

Gergely MARKÓ* – Péter PRIMUSZ – József PÉTERFALVI

Department of Forest Opening Up, Institute of Geomatics and Civil Engineering,
Faculty of Forestry, University of West Hungary, Sopron, Hungary

Abstract – Bearing capacity measurements of roads were traditionally carried out using the Benkelman beam. The Benkelman beam measurements provide the maximum vertical deflection of the pavement under 50 kN of wheel load. Nowadays the bearing capacity of public roads is measured with falling weight deflectometers. Falling weight deflectometer measurements provide the full deflection basin. It is convenient to use these high precision instruments on forest roads, but their application is inefficient and costly. The Department of Forest Opening Up developed a new method to measure the full deflection basin with the Benkelman beam. Besides the instrument improvement the authors developed a new method for the processing of the deflection basin data. Results are presented through the case study of a 2nd class opening up forest road.

Benkelman-beam / forest road / bearing capacity / pavement management system

Kivonat – Erdei utak teherbírásának mérése a Benkelman-gerenda továbbfejlesztett változatával. Az erdészeti szállításban mértékadónak tekinthető tehergépjármű állomány az elmúlt évtizedekben nagy tengelyterhelésű járművekre cserélődött le; ez a folyamat a szállítópályák leromlását felgyorsította. Mindezek miatt az erdőfeltárás témakörében a hangsúly a feltáróhálózatok bővítéséről áthelyeződött a meglévő utak fenntartására és fejlesztésére. Az Erdőfeltárási Tanszéken folyó kutatások – az erdőgazdaságok által megrendelt kutatás-fejlesztési megbízásokkal párhuzamosan – követik ezt a trendet; a cikk az aszfalt kopóréteggel rendelkező pályaszerkezetek teherbírásának roncsolásmentes meghatározása területén elért legújabb eredményeket mutatja be.

Benkelman-gerenda / behajlásmérés/ erdészeti utak teherbírása / útfenntartási rendszer

1 INTRODUCTION

One of the most important, objectively measurable parameters of the road maintenance systems is the bearing capacity of the roads. To define the bearing capacity of the elastic pavements is not an exact task, as we do not have a widely accepted theory to do this. In addition, we can state, that the definition of the bearing capacity of pavements is also difficult. Unlike bearing capacity, stiffness – as the deformation caused by a given weight – can be

* Corresponding author: gergely.marko@gmail.com; H-9400 SOPRON, Bajcsy-Zs. u. 4

defined, and even measured. Instead of defining bearing capacity directly, we usually look for the answers to these questions:

- How long is the remaining lifetime of the pavement?
- Which recovering technology should be used based on the bearing capacity and surface condition of the pavement?
- How thick the stiffening layer covering the pavement should be, to endure the next 10–20 years of traffic?

The study describes development results achieved at the Forest Opening Up Department of the University of West Hungary, through which the deformation of elastic pavements caused by weight can be measured. The advantage of the method is that the whole deflection bowl can be measured applying a low cost equipment.

2 MEASURING THE DEFORMATION OF PAVEMENTS

During the last decades several procedures have been developed to measure the deformations of elastic pavements. Each procedure simulates the relationship between the traffic and the pavement differently. Because of this, the measured results vary slightly. We briefly present the methods that have been used in forestry practice so far. The *Table 1* contains the main features of the measurement tools (Kosztka et al., 2008).

Table 1. Comparison of deflectometers.

Features	Benkelman beam	Lacroix deflectograph	FWD
Tools needed	loaded truck 2 pcs Benkelman beam	measuring vehicle	measuring vehicle
Staff	4 pers.	2 pers.	2 pers.
Stress	static	actually static	dynamic
Simulated speed	0 km/h	3-4 km/h	60-80 km/h
Method of measurement	discrete	permanent	discrete
Frequency of measurement	min. 25 m	4 m	25 m
Daily performance	15 km	20 km	15 km
Measured parameter	central deflection	central deflection	deflection bowl
Data recording	manual	automatic	automatic
Repeatability	satisfactory	average	excellent
Cost of tool	cheap	expensive	expensive

The classic tool to measure deflections is the *Benkelman beam*. During the measurement a rod that stands against the pavement and spins round a horizontal axis is placed between the rear dual tires of a loaded truck at the place of the maximum deflection. The deflection of the pavement can be defined from the displacement measured at the other end of the rod. During the measuring process the truck stands still, so the weight is static (Boromissza 1959).

We can apply the Lacroix Deflectograph to automatically measure the deflections. The principle of this measurement is the same as the principle of the manual method. The difference is in the implementation. Here the deflection meters are fixed to an automatic measuring vehicle, which measures the pavement's deflection every 4 meters while slowly (3–5 km/h) progresses. The deflection measurement technique made by the

Lacroix Deflectograph has not spread in forestry practice because of its circumstantiality and high cost. On the other hand, the former researches at the Forest Opening Up Department showed, that as to the renewal plans of forestry roads, the manual deflection measurement method, which needs simpler tools, leads to the same results (Boromissza 1959, Kosztka et al. 2008).

The public road practice uses the Falling Weight Deflectometer (FWD) to measure the deformations of elastic pavements – that is the deflection bowl – caused by load. The FWD devices, at several points at once, precisely measure the vertical displacement caused by dynamic load with the help of accelerometer sensors placed on the pavement surface. The device measures the temperature of the air and the pavement too. The adaptation studies to establish the application of the dynamic bearing capacity measurement in Hungary began in 1991. According to these, we can state, that the measurement procedure is rapid and objective (Tóth 2007). The measurement technique – according to our experiences of the last years – can be applied successfully in forestry conditions (Kosztka et al. 2008).

3 THE POSSIBILITIES OF DEVELOPING THE MANUAL DEFLECTION MEASUREMENT METHOD

Using the FWD device we can measure the deformations of the pavement surface at several points beside the central deflection, so the shape of the deflection line (deflection bowl) can also be produced. Knowing the shape of the deflection bowl we can estimate parameters that are the input data of pavement design procedures based on mechanical principles. We believe that we should prefer the measurement procedures that make the whole deflection bowl be possible to record. The price and maintenance cost of the Falling Weight Deflectometers are very high, so the bearing capacity measurements on forestry roads can only be carried out by specialist companies that own FWD devices. It seems practical to develop a procedure that enables specialists dealing with forestry roads to independently measure the deflection bowl.

4 THE GEOBEAM AND OTHERS

The Geobeam is an automated Benkelman beam, the development of which began in the 1980's (Tonkin &Taylor). The main purpose of the development was to preserve the simple principle of the manual deflection measurement method while automatically recording the whole deformation line, with little expense increase. During the measurement the sensor of the measuring beam automatically records the vertical displacement while assigns the load position to the measurement. So the deflection bowl can be reconstructed by the appropriate processing software. The position of the load is measured and recorded with the measuring wheel attached to the truck. The resolution of the measuring wheel is 10 mm, which enables very frequent sampling. Unlike the FWD device, the Geobeam records the vertical displacement of a point at different times (Anderson, 2008). The measurement system is shown in *Figure 1.*

The Geobeam provides usable, representative measurement results even in cases when because of the saturated foundation, the FWD tools cannot be reliably applied (consolidation issue) (Anderson, 2008).

Figure 1. The Geobeam measuring equipment (Geotechnics Ltd.)

Naturally, there are several other solutions to improve the manual deflection measurement method beside Geobeam. It is worth mentioning the manual deflectometer applied at the Faculty of Civil Engineering, Bauhaus-Universität in Weimar. This method applies three more sensors beside the central sensor at 25-50-80 cm from the axis of load. The displacements recorded by the sensors are processed and stored automatically by the electronic device fixed onto the measuring beam. This method, just like the FWD tools, records the displacements at different discreet points (4 measured points). With the help of the function fitted to the measured values, different bowl parameters can be computed (Dähnert, 2005). This equipment is shown in *Figure 2.*

Figure 2. Automated Benkelman beam (Dähnert, 2005)

5 THE IMPROVED BENKELMAN BEAM APPARATUS

The procedure developed at the Forest Opening Up Department was the result of the improvement of the manual deflection measure method. The development included planning the measurement process, choosing the necessary accessory equipment, designing and building the central data collecting unit, developing the firmware running on the data collecting hardware and the data collecting and analyzing software running on PC-s.

The development in respect of the equipment basically lies on three pillars:

1. We substituted the traditional Benkelman beams' analogue meters with meters having digital output.
2. During the measurement we record the progress of the truck with an ultrasonic rangefinder.
3. The signal of the digital sensors is recorded then transferred to the netbook that runs the data collector software, using a self-developed central control unit.

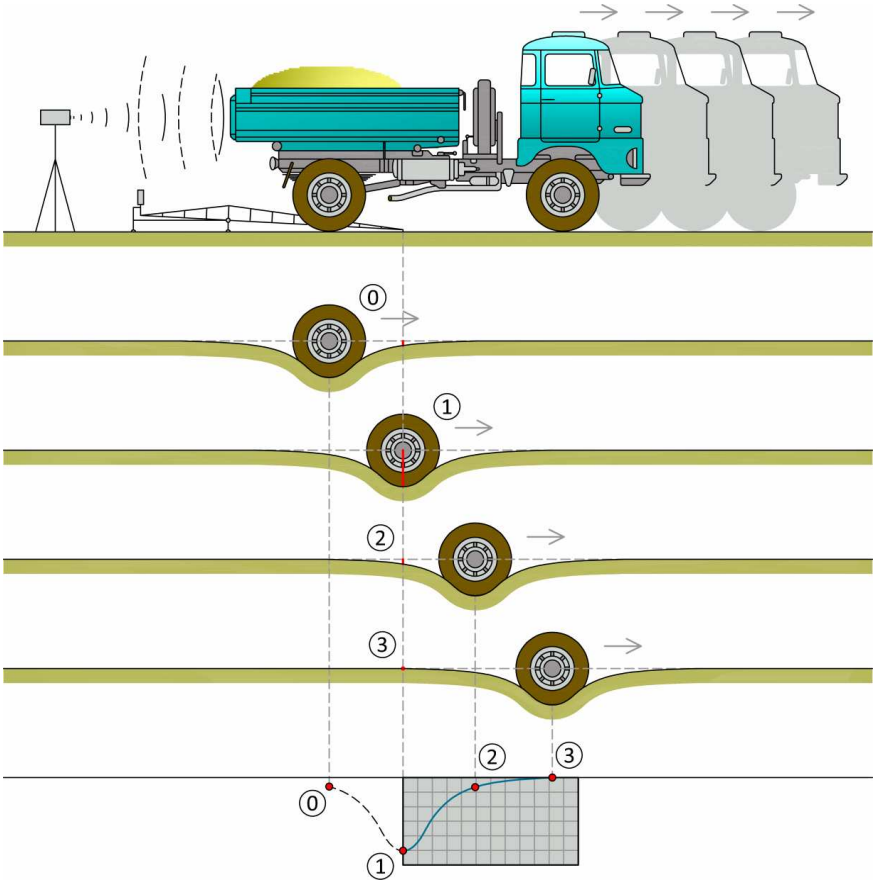

Figure 3. The principle of the improved manual deflection measurement method

The measurement procedure consists of the following steps *(Figure 3)*:

1. Driving a loaded truck with known rear axle load to the segment of the measurement.
2. Placing deflectometers between the dual tires of the rear axle so the measure peak will be in front of the contact line of the wheel.
3. Positioning the digital displacement meters.
4. Positioning the ultrasonic rangefinder placed on a stand.
5. Preparing the data-collector touch-screen netbook to receive the measurement data, checking the data connection with the external hardware.
6. Starting data collection with the data collector software.
7. While the truck slowly drives away, the data collector software records the data of the digital meters and rangefinder sensor.
8. After progressing 5 m ahead, the data collection stops automatically.

The measuring device records the vertical displacement of one point of the pavement by assigning the loading distance to every "reading" of the displacement meters. After properly pre-processing the data flow the shape of the deflection bowl can be drawn.

6 HARDWARE COMPONENTS

We took the following aspects into consideration when we chose the type of digital meter fixed on the Benkelman beam:

- At least 0.01 mm resolution.
- At least 10 Hz measurement frequency.
- At least 25 mm measurement range.
- Open format digital data output.
- Robust design for outdoor measurements.
- The beam is the same diameter (8 mm) as our analogue meters.
- Reasonable price.

After studying the market choice, we chose the type ID-U meter of the Mitutoyo Company. Mitutoyo is one of the leader manufacturers of precision measurement equipment, and the ID-U meter completely meets our requirements listed above. The meter has digital data output, the enclosed data cables have standard connectors by which the equipment can be connected to data collectors manufactured by the company or developed in-house. The DIGIMATIC digital data-exchange format developed by Mitutoyo is well documented and simple. The hardware realization of the communication – logical signal levels, timing, external controllability etc. – enables the sensor to fit in a self-developed microcontroller environment. We record the progress of the truck with a type SRF-08 ultrasonic rangefinder sensor. The main features of the sensor:

- 1 cm resolution.
- 30 cm – 6 m measurement range.
- High sampling frequency (> 20 Hz).
- I_2C standard communication.
- Low price.

The sensor was built in the central data collecting unit's box mentioned later. The central data collecting and control unit is built around a type Microchip 18F2550 microcontroller. The tasks of the instrument group's "brain":

- Connection through a USB HID standard communication protocol, data exchange with the data collecting software running on a PC.
- Synchronized start of the digital displacement meters' and rangefinder sensor's measurements with the frequency of 10 measurements per second.
- Receiving and converting the measurements of the sensors.
- Transferring the results to the data collector software.

The data collector control unit is powered from the PC's USB port. The microcontroller and the components built around it are placed on a self-designed and manufactured printed-circuit. We wrote the program (firmware) run on the microcontroller with the education version of the Microchip MPLAB developer tool, in C language. We placed the control unit in a plastic box, which can be fixed onto a camera stand by a fast connector. The data collecting software is run on a type Vye touch screen netbook. The data collector control unit is shown in *Figure 4*, while the assembled instrument group is shown in *Figure 5*.

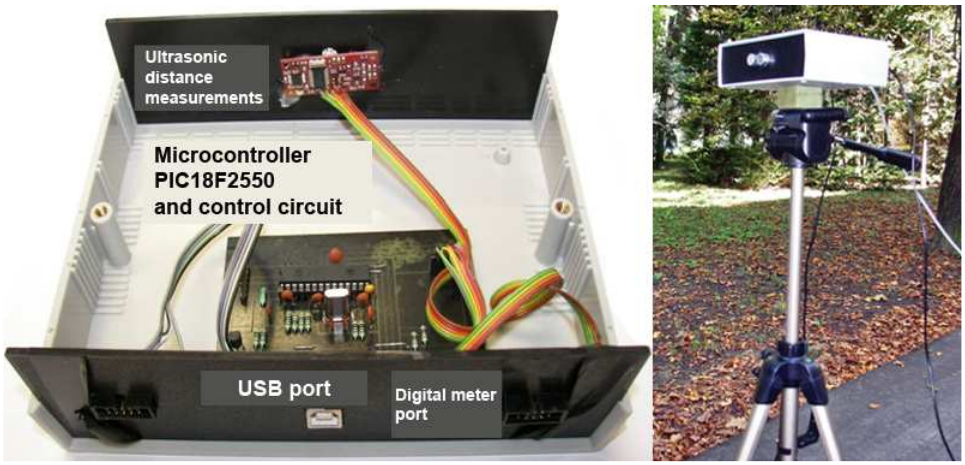

Figure 4. The central data logging unit.

Figure 5. The instrument group in use.

7 SOFTWARE COMPONENTS

During fieldwork the software run on the netbook supports the control, pre-process of the measured data and storage of the measured results. The software written to support the office process of the measurement results provides the following functions:

- Equalization of the measured data series.
- Numerical definition of the function corresponding the mechanical calculi, appropriately describing the shape of the deflection bowl.
- Defining the parameters (length of the deflection bowl, the location of the inflexion point, minimum curve radius, central deformation, shape factor) typical of the shape of the deflection bowl and bearing capacity with the help of the fitted functions.

8 PRE-PROCESS OF THE MEASUREMENT RESULTS

After the general description of the manual deflectometer developed at the Forest Opening Up Department it is practical to review the features of the recorded data series. During the measurement the data collector software records the displacements (*d*) read by the digital meters, records the momentary distance of the wheel load (*x*), and the elapsed time (*t*) from the start of the measurement. The shape of the detected deflection bowl is clearly defined by the function $f : x \rightarrow d$ *(Figure 6).*

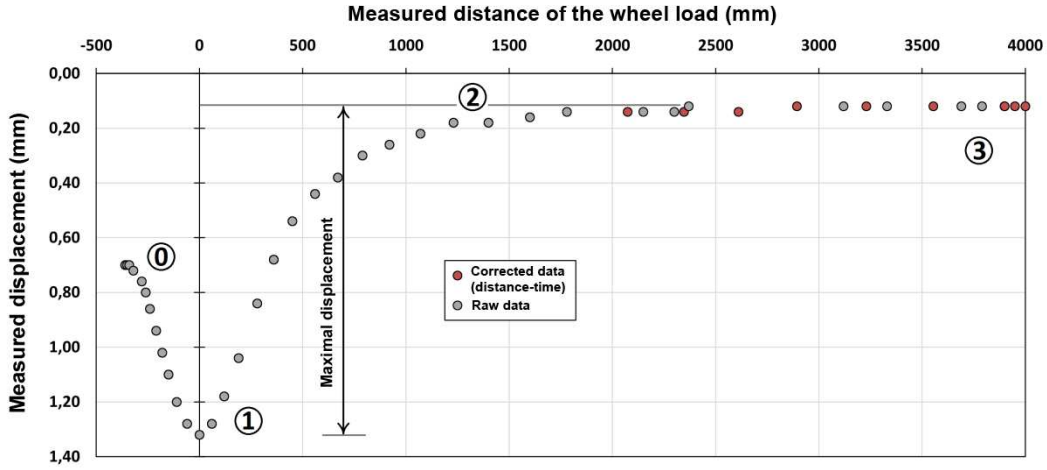

Figure 6. Measured points of the deflection bowl. Red dots represent corrected measurements

On the raw data series it can clearly be seen, that during the measurement the peak of the deflectometer is placed 40-50 cm in front of the wheel contact point. During the first stage of the measurement the pavement structure suffers a gradually increasing shape deformation (0–1) then when it passes the measuring peak, the deformation reaches its maximum (1). As the wheel passes the measuring peak, the pavement structure gradually gains its original shape (2–3). The deformation line can be recorded by the measurement equipment in 5 m length.

As to the raw data, we can also observe, that they more or less vary along a definite trend, so they are charged with noise. Both members of the data pairs (*x*, *d*) describing the deflection bowl are charged with measurement error, the rate of which depends on the features of the sensor that recorded the given parameter. Out of the three recorded parameters the most reliable one is the time (*t*), next is the displacement (*d*), and the last one is the position of the moving wheel load (*x*). We practically start the noise reduction with observing the *x* parameter. The distance-time diagram is the graphic image of the distance covered by the wheel load versus time *(Figure 7)*. We can follow the acceleration of the moving wheel load. The entire load time period is approx. 3 seconds, so the wheel-speed is an average of 5 km/h. This value is similar to the measurement speed of the Lacroix Deflectometers that is why the measurement is not static, but static-like. We can also observe, that the last 5-10 recorded values of the ultrasonic rangefinder (red bordered area) are charged with errors, so they are worth being substituted with a regression function fitted onto the whole measured data-series or with a spline curve. Using this method, we can relatively reliably reduce the number of errors from distance measurement (see the corrected values of *Figure 6*).

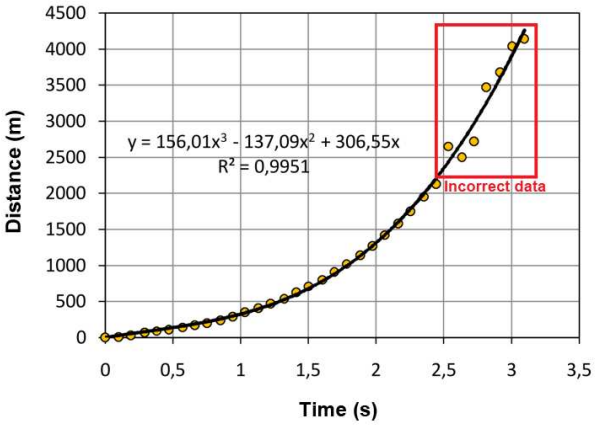

Figure 7. The typical distance-time diagram of the Improved Benkelman Beam Apparatus

In theory, the supporting legs of the manual deflectometer should be far enough from the loaded tires so that they do not participate in the movement of the pavement. Otherwise, the measured values are charged with the so-called foot error (e) *(Figure 8)*. According to the experiences confirmed in Hungary the foot error can be significant as to thin pavements (Kosztka 1978). Because of the outlined problem, the Benkelman-beams with measuring arm of 2:1 have been spread worldwide. In the case of devices like these the distance between the measuring peak (A) and the foot point (B) is twice as long as the distance between the foot point (B) and the meter (C). The extended length is usually enough to place the legs on deformationless area without affecting the controllability of the device (Kosztka 1986). In spite of the developments we have to take foot error into account, as its rate depends on the value of the so-called *co-working length* typical of the pavements (Boromissza 1959). This value may vary within broad limits.

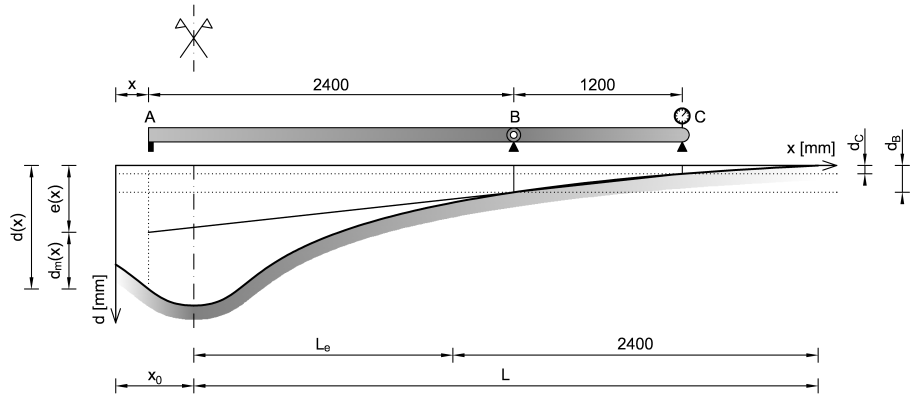

Figure 8. The foot error (e) coming from the support of the measuring arm (B)

The improved manual deflectometer can record the deformation line evolved under load up to 5 meters, so it is possible to estimate the foot error per measured points:

$$c(x) = \left(d_B(x) - d_C(x)\right) \cdot \frac{3600}{1200} + d_C(x) = 3 \cdot d_B(x) - 2 \cdot d_C(x) \qquad (1)$$

where:

e(x) – The value of the foot error evolving from a distance of x from the measuring peak, [mm].
$d_B(x)$ – Displacement measured at the foot point, [mm].
$d_C(x)$ – Displacement measured at the meter, [mm].
3600 – The total length of the deflectometer, [mm].
1200 – Distance between the B and C points of the deflectometer, [mm].

We need to take the foot error into account as to the section of length L_e of the deflection bowl charged with foot error. Taking the foot error into account we can compute the corrected value of the x coordinate point of the deflection line:

$$d(x) = d_m(x) + e(x) \tag{2}$$

where:

- $d(x)$ – The value of the deflection, if the axis of the deflection is placed at a distance of x from the measuring peak, [mm].
- $d_m(x)$ – The measured deflection at a distance of x from the measuring peak, [mm].
- $e(x)$ – The rate of foot error evolving at a distance of x from the measuring peak, [mm].

9 EVALUATING THE MEASUREMENT RESULTS

After the field measurements and pre-processing the data, the first step of the measurement results' evaluation is that we fit a function in numerical way on the measured values, well representing the shape of the bowl:

$$D(x) = \frac{D_0 4r^2}{c \cdot x^2 + 4r^2} = \frac{D_0}{c\left(\frac{x}{d}\right)^2 + 1} \tag{3}$$

where:

- D_0 – The maximum deflection under the loaded disc [mm].
- r – The radius of the loaded disc [mm], $d=2r$.
- c – The shape factor typical of the deflection bowl's shape.
- x – The distance from the centre of the load [mm].

Advantageous feature of the applied function is that it can be continuously differentiated. The first as well as the second derivate can be computed at an optional x place. With the help of the function the complex measurement series (the deflection bowl) can be characterized with two parameters (D_0, c). The detailed description of the suggested function is discussed by Primusz and Tóth (2009).

10 PARAMETERS DESCRIBING THE PAVEMENT'S STIFFNESS

The radius of the circle tangent to the function describing the shape of the deflection bowl at $x = 0$ can be computed in a closed form:

$$R_0 = \frac{2r^2}{c \cdot D_0} \tag{4}$$

where:

- R_0 – Curve radius, [mm].
- D_0 – The maximum deflection measured at the place of load, [mm].
- r – The radius of the ideal, round load surface, [mm].
  We set its value typically to 150 mm.

The minimal curve radius is, beside the central deflection, a value that describes the pavement deformation in a simply interpretable way. We can clearly see, if the pavement is deflected by the repeated loads along a small-radius arc, it will get damaged sooner (fatigue).

Knowing the minimum deflection radius and the thickness of the asphalt layers we can compute the strain of the asphalt layer's bottom line:

$$\varepsilon = \frac{h}{2R} \tag{5}$$

where:

ε – The strain of the asphalt layers' bottom line, [m/m].
h – The thickness of the bonded layers, [m].
R – Curve radius, [m].

We usually use μstrain (μm/m) for strain; to do so, we have to multiply the value received in [m/m] dimension by 10^6. The strain is one of the important parameters of the asphalt pavement layers' lifetime, and it is essential for computing the remaining lifetime of the pavement. The distance of the inflexion point of the function that describes the shape of the deflection bowl measured from the place of load (stiffness radius) is:

$$L = \frac{2 \cdot r}{\sqrt{3 \cdot c}} \tag{6}$$

where:

L – Stiffness radius [mm].
c – The shape factor typical of the deflection bowl's shape.
r – The radius of the ideal, round load surface, [mm].

The latest researches at the Forest Opening Up Department (Primusz–Markó, 2010) showed, that the elastic moduli of the pavement's bonded layers (asphalt) and the non-bonded layers below (base layers + subgrade) can be computed if we know the stiffness radius and the thickness of the pavement layers (asphalt) that have cohesion.

11 APPLICATION OF THE METHOD ON A FOREST ROAD AT HÁRMASTARJÁN

The first application of the improved manual deflectometer in practice was realized on the second-class forestry road of Ravazd Forestry of the Kisalföldi Erdőgazdaság Zrt. in Hármastarján. We executed the deflection measurement in both tracks with sampling at every 50 meters. Both the prototype of the measuring device and the measurement process proved that they are appropriate for usage under normal operating conditions. Studying the time needed for the measurement, we can state, that using this procedure, in one hour, we can measure a 1 km section with 50 m sampling.

After the field measurements we processed the deflection measurements with the software described above. At the measurement points we defined the following parameters:

- Central deflection (D_0, mm).
- The shape factor of the deflection bowl (*c*).
- Minimum curve radius (*R*, m).
- The elastic moduli of the bonded layers (E_k, Mpa).
- The elastic moduli of the non-bonded layers (E_{nk}, Mpa).

The individually defined values by measurement place were displayed on a condition-evaluation longitudinal profile with the "RR" software developed at the Department. Then we defined the borders of the homogeneous sections that we considered conditionally identical. We computed the standard value of the above-mentioned parameters for the homogeneous sections, and then we continued the further analysis using these values. The standard values of the indicator parameters are summarized in *Table 2.*

Table 2. Calculated bearing capacity parameters of the studied pavement

Border segment of the homogeneous sections	Central deflection	Curve radius	Asphalt strain	Moduli	
				Bonded pavement layers	Non-bonded pavement + subgrade
[hm]	D_0 [mm]	R [m]	μ [microstrain]	E_k [Mpa]	E_{nk} [Mpa]
0+00					
	1,25	98	306	3620	84
2+25					
	1,85	61	492	2390	64
11+25					
	1,29	99	303	3660	99
21+75					
	1,26	64	469	1990	94
28+25					
	0,89	107	280	3490	106
31+75					
	1,1	72	417	2560	116
39+00					

12 SUMMARY AND CONCLUSIONS

Researchers of the Institute of Geomatics and Civil Engineering at the University of West Hungary developed a new instrument to measure the full deflection basin with Benkelman beam. A new method for the analysis of the deflection basin is also developed.
Both the prototype of the measuring device and the measurement procedure proved that they are appropriate for usage under normal operating conditions. Studying the time needed for the measurement, we can state, that using this procedure, in one hour, we can measure a 1 km section with 50 m sampling. Measurements were made in both wheel path simultaneously. The next parameters were determined after the field measurements:

- Central vertical deflection.
- Shape coefficient of deflection basin.
- Strain of the bottom of the asphalt layer.
- Minimal radius of curvature.
- Young-modulus of the asphalt layer.
- Young-modulus of the granular subgrade.

New results are presented via the case study of a 2nd class opening up forest road.

Acknowledgements: The development research was supported by the R & D contract of 2010 berween NymE-ERFARET Nonprofit Ltd. and the Kisalföld Erdőgazdaság Co. Special thanks to László Balázs technician, Balázs Kisfaludi and Balázs Biczó PhD students for their assistance in field measurements.

REFERENCES

ANDERSON, S. (2008): Pavement Deflection Measurements Using the Geobeam. Mechanistic Design and Evaluation of Pavements, 2008 Workshop, link: http://www.pavementanalysis.com

BOROMISZA T. (1959): Útburkolatok behajlása. [Deflection of pavements.] Mélyépítéstudományi Szemle, 1959/12. p.: 564–571. (in Hungarian).

DÄHNERT, M. (2005): Messwert gestützte Ermittlung der Tragfähigkeit von bestehenden Strassen, Diplomarbeit, Bauhaus-Universität Weimar, Fakultät Bauingenieurwesen, Professur Verkehrsbau.

KOSZTKA M. (1978): Erdei utak pályaszerkezetének teherbírása. [Bearing capacity of forest road pavements.] Manusscript. Erdészeti és Faipari Tudományos ülés, Budapest, 1978. (in Hungarian).

KOSZTKA M. (1986): Erdészeti utak fenntartási rendszere. [Maintenance system of forest road networks.] CSc thesis. Sopron, 1986. (in Hungarian).

KOSZTKA M. – MARKÓ G. – PÉTERFALVI J. – PRIMUSZ P. – TÓTH CS. (2008): Erdészeti utak teherbírásának mérése. [Measuring bearing capacity on forest roads.] MTA Agrárműszaki Bizottság, XXXII. Kutatási és Fejlesztési Tanácskozás, 2008. január 22., Gödöllő, 2008. 32/3: 75–79. (in Hungarian).

TÓTH CS. (2007): A teherbíróképesség meghatározásának ellentmondásai és lehetőségei. [Inconsistencies and prospects in the determination of road bearing capacity.] Közúti és Mélyépítési Szemle, 8 (57): 13–20. (in Hungarian).

PÉTERFALVI J. – MARKÓ G. – PRIMUSZ P. (2010): Az erdészeti utak teherbírásmérési módszerének továbbfejlesztése a KAEG Zrt. Hármastarjáni erdészeti útjának példáján. [Improved methodology for measuring bearing capacity of forest roads on KAEG Ltd. example.] NymE-ERFARET Kutatási Jelentés, Erdőmérnöki Kar, Geomatikai, Erdőfeltárási és Vízgazdálkodási Intézet, Sopron, 2010. (in Hungarian).

PRIMUSZ P. – TÓTH CS. (2009): A behajlási teknő geometriája. [Geomerty of the deflection bowl.] Közlekedésépítési szemle, 12 (59): 18–24 (in Hungarian).

PRIMUSZ P. – MARKÓ G. (2010): Kétrétegű pályaszerkezetmodellek paramétereinek meghatározása FWD mérések alapján. [Parameter calculation of twolayered pavement models based on falling weight deflectometer measurements.] Közlekedésépítési szemle, 7 (60): 8–13. (in Hungarian).

DE GRUYTER OPEN DOI: 10.2478/aslh-2013-0009 Acta Silv. Lign. Hung., Vol. 9 (2013) 111–117

The Thermal Insulation Capacity of Tree Bark

Zoltán PÁSZTORY* – Ildikó RONYECZ

University of West Hungary, Hungary

Abstract – Nowadays increasing emphasis is placed on improving the quality of different insulation materials, and on developing such from materials of natural origin. The present research focuses on the thermal insulation capacity of the chipped bark of different broadleaved and coniferous wood species. We examined the bark of five tree species: black locust, a poplar clone, larch, spruce, and Scotch pine and compared their insulation characteristics to the traditionally used insulation materials. Results indicate that the thermal insulation capacity of chipped tree bark is comparable to that of generally used insulation materials, such as glass wool. Moisture content influences the thermal insulation capacity of chipped bark of the five examined species. Since energy requirement of producing chipped tree bark is very low, and it contributes also to storing carbon, therefore its CO_2 balance is more advantageous compared to that of traditional fibrous or foamy insulation materials.

tree bark / insulation capacity / moisture content / CO_2 footprint

Kivonat – A fakéreg hőszigetelési tulajdonságai Manapság egyre nagyobb hangsúlyt fektetnek a különböző szigetelőanyagok javítására. A tanulmány bemutatja a különböző lombos- és tűlevelű fafajok kérgének hőszigetelő képességét. Öt fafajt vizsgáltunk meg: az akácot, a Pannonia nyár klónt, az erdeifenyőt, a vörösfenyőt és a lucfenyőt. A tanulmány mind a kezdő nedvességtartalmú, mind a 12%-os nedvességtartalomra szárított kérgeket vizsgálja. A kutatás megmutatta, hogy a fakéreg hasonló hőszigetelési tulajdonságokkal rendelkezik, mint más, általánosan használt szigetelő anyagok. A fakéreg feldolgozása alacsony energiafelhasználással jár és CO_2 mérlege is lényegesen jobb, mint a hagyományos szigetelő anyagok.

fakéreg / hőszigetelő képesség / nedvességtartalom / CO_2 lábnyom

1 INTRODUCTION

Hungary produces about 500 thousand cubic meters per year of bark from forest harvests, spread evenly across the areas of primary wood processing. The proportion of bark of the harvested tree can be as much as 10–20%, depending on the species and diameter of the tree (Sopp – Kolozs 2000). The bark of processed wood is mostly used for generation of energy (Ragland et al. 1991), for mulching (Colorado Master Gardeners Program 2009), and for extracting of chemical compounds (Hoong et al. 2011), among other uses (Harkin – Rowe 1971, Pedieu et al. 2009). Since the bark does not possess a mechanical stability similar to wood, its use for insulation is mainly possible in the form of chips or particles. Skogsberg and

* corresponding author: pasztory@fmk.nyme.hu; H-9400 SOPRON, Bajcsy Zs. u. 4.

Lundberg (2005) have shown that processed bark – applying proper treatment and technology – can be used as loose-fill insulation material.

The insulation capacity of tree bark plays an important role in case of forest fire also. The thick and well insulating bark protects the cambium layer of the tree and thus mitigates the damaging effects of fire (Bauer et al. 2010, Wang – Wangen 2011). Dimitri (1968) investigated the thermal conductivity of beech wood bark and found that the most significant and major factor is its moisture content. The effect of moisture content on thermal conductivity is well investigated as far as wood is concerned but much less for bark.

The CO_2 balance projected on the specific insulation effect is presumably better when using bark, compared to the use of other insulation materials (Buchanan – Levine 1999, Börjesson – Gustavson 2000, Gustavsson – Sathre 2006). Bark used for insulation purposes has obviously a higher economic value than lower value functions such as burning or as mulching. The bark insulation can be recycled at the end of its service life for energy or other purposes without polluting the environment. During its life as an insulation material, the carbon accumulated in the bark does not burden the atmosphere and helps reducing the emission of CO_2 which is an important greenhouse gas.

Finally, the bark contains protective materials (such as tannin, suberin) in higher amounts than wood, and thus the bark has natural protective elements against decay. Thus, bark used as insulation material will need less chemical protection compared to other materials used for insulation, contributing to possible lower costs.

We investigated the bark of five tree species (black locust, a poplar clone 'Pannonia', larch, spruce, and Scotch pine) that are common across most of Europe. We aimed to investigate, determine and compare the specific thermal insulation capacity of the bark of these species, and to compare these capacities with other customary insulation materials. Developing new and more specific knowledge in this area will further expand the possibilities of using natural and recyclable resources as alternatives for thermal insulation. This also means potentially greater energy savings and reduction of the CO_2 footprint, through storing carbon and avoiding the release of CO_2 from burning. Possible use of bark for thermal insulation means new alternatives to other customarily used insulation materials that need more energy resources to produce and that also release CO_2 in the production process.

2 MATERIALS AND METHODS

The chosen broadleaved timber species are black locust (*Robinia pseudoacacia*) and the poplar clone 'Pannonia' (*Populus euramericana cv. Pannonia*). Both species have especially big bark-to-wood proportion of about 12–20 % based on the diameter of the trunk; however, their bark contains a lot of additional incrustation substances, and therefore are not suitable for mulching. Nevertheless, the high content of incrustation substances provides an advantage with respect to resistance to decay and therefore increases the durability.

The three coniferous species chosen are larch (*Larix decidua*), spruce (*Picea abies*), and Scotch pine (*Pinus silvestris*). Scotch pine and spruce have scaly outer bark which peels off in thin lamellas.

During timber processing, the bark that is removed usually comes off in different broken particles and has considerable moisture content. For comparability purposes, the bark samples from the five chosen species were chipped with the same chipping technology and device. Hence, the resulting particle size of the bark is almost the same for all five species, with little differences as summarized in *Table 1*. *Figure 1* shows the material prepared for testing.

Figure 1. Chipped bark of black locust is placed in the measurement box for testing.

Table 1. Particle size of chipped bark samples

Dimension	particle size (mm)
Thickness	1 – 26
Width	5 – 27
Length	10 – 48 (100)

The pine bark broke into flat, disc-like pieces because the bark layers are stronger compared to the other species. However, the bark of broadleaved species is structurally different, with ca. 100 mm long inner bark fibers appearing in black locust and poplar bark chips due to the higher proportion of inner bark in the material compared to the conifers. The inner bark content is different in amount and structure among wood species, with the difference being more pronounced between broadleaved and conifer species. There are differences in bark density also among species (MacFarlane – Luo 2009, Gryc et al. 2010).

According to Freire et al. (2002) and So et al. (2006), there are more significant differences between the outer bark and the inner bark in terms of structure and chemical components. The inner bark fibers play a cross-linking role in the chip; they also form further air layers between the bark elements reducing the connecting surfaces of bark pieces. Similar to the fibrous insulation materials, such as rock and glass wool, the wood bark fibers have air layers or space between them, so that they can improve the air-filling ratio of the system.

Another basic difference in the bark chips is density. The inner bark body of conifers has sieve cells whereas broadleaved trees have sieve tubes which develop from the fusion of more cells, so the bark of the latter has a more porous structure and consequently lower density. With respect to the firmness of the inner bark structure, Scotch pine has stalk fibers only while spruce and larch have sclereids, but the two broadleaved species examined have both sclereids and stalk fibers (Molnár 2004).

The heat flow through bark samples of the five tree species was measured. To help ensure that the heat fluxes in the test samples are parallel to each other and perpendicular to the surface, the width of the measuring surface should be greater compared to the thickness of the test sample. Moreover, the lateral heat fluxes were reduced by lateral insulation of the samples.

The bark measurement box had the dimensions 500 mm × 500 mm × 50 mm, with measurements on the middle 120 mm x 120 mm cross section as the transmitting area. No bonding materials were used, the chips were loosely scattered in the measuring box (*Figure 1)*. Density was not measured because the aim was to fill up the measurement box at 50 mm height similarly for all species. The coefficient of thermal conductivity λ was determined in steady state heat flow condition. The heat flow (or heat flux) Q in watts is given by the equation

$$Q = \frac{\lambda * A * \Delta T}{d}$$

where *d* is the thickness (50 mm) of the sample and *ΔT* is the temperature difference between warm and cold sides in Kelvin. Thus, the units of λ are *W/mK* which are obtained from the equation above when the heat flow values are measured. Steady state conditions were obtained by measuring heat flow to the cooler side every minute, defining "steady state" as the state when successive measurements per minute gave the same results to three decimals for a period of 30 minutes. The steady state thermal condition measurement was repeated 100 times. The λ values were determined as the average value of 100 data points.

Using the *z*-test, the thermal conductivity data were examined to determine if the sample size was representative of the whole population.

3 RESULTS AND DISCUSSIONS

Wet bark has a higher coefficient of thermal conductivity than bark with 12% moisture content, as shown in Table 2. The results also indicate that the thermal insulation qualities of the chipped bark of the five chosen species are comparable at 12% moisture content, with values ranging between 0.0613 *W/mK* and 0.0765 *W/mK*. In contrast, the initial moisture content of the bark samples varies significantly across the five species, with poplar having a higher value compared to the other four species. The lowest value (black locust) is almost three times that of poplar. *Figure 2* clearly shows the influence of moisture content on thermal conductivity across the five species.

Chipped wood and the air trapped within the bark pieces created a composite system. The heat is transmitted partly through the trapped air flow and through the linked thermal bridge system created by the contacting chip elements. The more the air flow and the size of contact surfaces decline, the more efficient the evolved thermal resistance is.

Static air of 0.025 *W/mK* value improves the thermal conductivity of the composite system. The basic thermal conductivity of broken bark also influences the thermal insulation capacity of the system. The thermal insulation values of chipped wood bark were comparable to the generally used insulation materials. The thermal insulation capacity of rock and glass wool is between 0.035–0.05 *W/mK*; for polystyrene this value is between 0.033–0.045 *W/mK* depending on density.

The flat disc-like shape of the bark of the spruce results in high contact surfaces and less blocked air ratio. In contrast, black locust has high inner bark content, and this causes more inner bark fibers to lower the contact surfaces of the bark elements and increase the proportion of blocked air. Results indicate that the thermal conductivity at 12% moisture content of chipped wood barks of broadleaved species are lower compared to the values for

the coniferous species. Therefore the high inner bark content of the broadleaved wood species tends to positively affect the insulation capacity of the system.

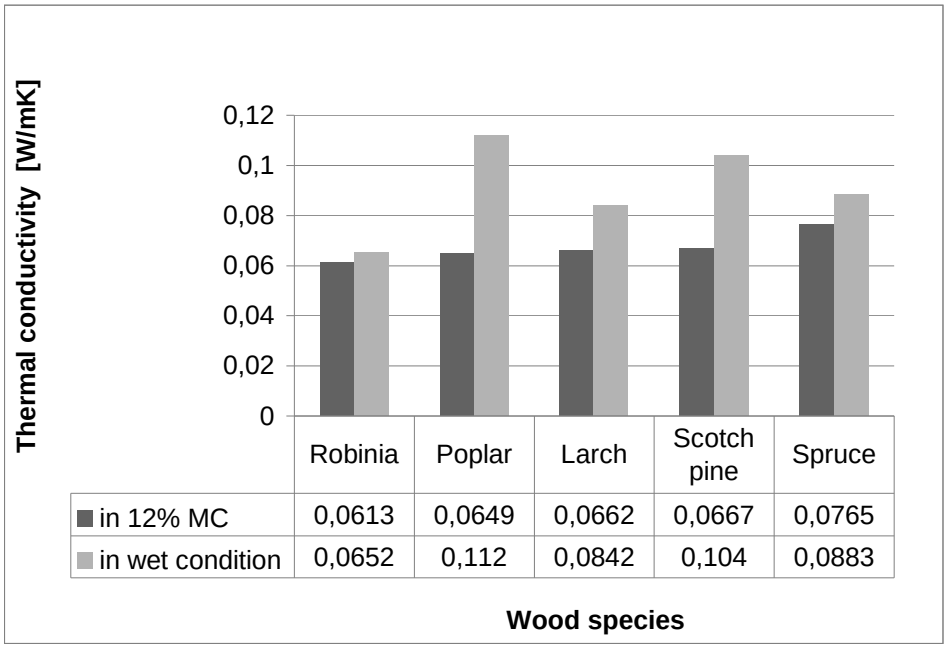

Figure 2. Thermal conductivity of different chipped wood barks in different moisture content

The results clearly support the effect of moisture content on the thermal insulation capacity of chipped bark (*Table 2.*). The high specific heat and good thermal conductivity of water influenced the thermal conductivity values unfavorably. Water fills cell lumen and provides better heat transfer in cell walls; on the other hand, the water vapor is able to transfer high amount of heat because of its high specific and latent heat. The heat difference can result also in vapor flow and, consequently, the heat transfer is increased by the specific heat amount of transferred vapor.

Table 2. Relationship between moisture content and thermal conductivity

Wood species	Heat conductivity at 12% MC	Heat conductivity under wet condition		MC difference	Difference of heat conductivity [1]	Change of heat conductivity in percentage relation in 1% of MC change [2]
	(W/mK)	(W/mK)	MC (%)	(%)	(%)	((W/mK)/MC%)
Robinia	0.0613	0.0652	14.3	2.3	6.36	2.77
Poplar	0.0649	0.1120	40.2	28.2	72.57	2.57
Larch	0.0662	0.0842	24.2	12.2	27.19	2.23
Scots p	0.0667	0.1040	35.9	23.9	55.92	2.34
Spruce	0.0765	0.0883	22.8	10.8	15.42	1.43

[1] Difference of heat conductivity = (Heat conductivity under wet condition – Heat conductivity at 12%MC) / Heat conductivity at 12%MC *100%

[2] Change of heat conductivity in percentage relation in 1% of MC change = Difference of heat conductivity / MC difference

The coefficient of thermal conductivity measured at 12% moisture content indicates little difference between species except for spruce shows in the Table 2. Black locust had the highest value at 0.0613 *W/mK*, followed by poplar at 0.0649 *W/mK*, with only 5.5% difference between these two species. The larch has 7.4%, and Scotch pine has 8.1% higher coefficient of thermal conductivity than that of the black locust. The second column of *Table 2* shows that spruce has 19.8% higher thermal conductivity than black locust. The high thermal conductivity value of the chipped spruce bark seems to be influenced by the particle structure form. Note that the data in column 2 consider one degree Kelvin difference only, but at higher temperatures the value has to be multiplied by the temperature; thus, a smaller difference can mean a much higher thermal flux for higher temperatures.

The effect of moisture is shown the last column of Table 2. In the case of black locust, the 2.3% moisture content difference makes a 6.36% difference in the coefficient of thermal conductivity, which translates to a 2.77% change of heat conductivity per moisture percentage. For poplar, the 28.20% moisture content difference resulted in 72.57% change of heat conductivity which shows 2.57 change of coefficient of thermal conductivity for each moisture content percentage. The data for the larch and Scots pine also show similar values.

The value of spruce (last column last row in Table 2) is lower than for other wood species. The explanation is the disc-like shape of spruce bark and in its higher heat conductivity values under 12% moisture content conditions.

4 CONCLUSIONS

The results of the study have several significant implications:

- Compared to the coniferous species, the barks of the broadleaved species have lower thermal conductivity, possibly due to their high inner bark content, that positively affect their insulation quality. This suggests that bark of broadleaved species may be better thermal insulators than those of conifers.
- Thermal conductivity is better the lower the air flow and the smaller the contact surfaces of the bark. The longer fibers from the inner bark of broadleaved species affects their thermal conductivity positively compared to the conifer species.
- Our study also shows that the thermal insulation capacity of bark is comparable to generally used insulation materials such as glass wool and rock wool.
- The water content strongly influences the heat conductivity of wood bark chips. 1% change in MC influences the thermal conductivity 2.23% to 2.77% for all species except spruce. Of the five species examined, spruce has also the lowest value indicating it is not the best candidate for thermal insulation purposes.

The project results suggest that the use of wood bark for thermal insulation material has a significant potential. The use of bark for insulation needs further exploration of the connection between moisture content and thermal conductivity. Modification/preservation methods may lead to a product that will have a very good eco-balance. Further research is needed to etablish optimal size and form of chip elements in detail and to compare and determine optimal insulation capacity for bark from other species.

Acknowledgements: This study was supported by the Environment conscious, energy efficient buildings TAMOP-4.2.2.A–11/1/KONV-2012-0068 project sponsored by the EU/European Social Foundation. We express our cordial thanks to Lita C. Rule and Kristóf Mohácsi for their useful suggestions on the manuscript.

REFERENCES

BAUER, G. – SPECK, T. – BLÖMER, J. – BERTLING, J. – SPECK, O. (2010): Insulation capability of the bark of trees with different fire adaptation. J Mater Sci 45:5950–5959

BÖRJESSON, P. – GUSTAVSSON, L. (2000): Greenhouse gas balances in building construction: wood versus concrete from life-cycle and forest land-use perspectives. Energy Policy 28 575–588

BUCHANAN, A. H. – LEVINE, A.B. (1999): Wood-based building materials and atmospheric carbon emissions. Environ. Sci. Policy 2, 427–437.

COLORADO MASTER GARDENERS PROGRAM (2009): Mulching with Wood/Bark Chips. Grass Clippings, and Rock, Colorado State University Extension

DIMITRI, L. (1968): Untersuchungen über den Einfluß des Wassergehaltes, der Rindendicke und der Darrdichte auf die Wärmeleitung der Buchenrinde. Holz als Roh und Werkstoff 26(3):95–100

FREIRE, C.S.R. – SILVESTRE, A.J.D. – PASCOAL, N.C. – CAVALEIRO, J.A.S. (2002): Lipophilic extractives of the inner and outer barks of Eucalyptus globulus. Holzforschung 56(4):372–379

GRYC, V. – VAVRČÍK, H. – ŠLEZINGEROVÁ, J. – KOŇAS, P. (2010): Basic density of spruce wood, wood with bark, and bark of branches in locations in the Czech Republic. TRACE – Tree Rings in Archaeology, Climatology and Ecology, Vol. 8: Proceedings of the DENDROSYMPOSIUM 2009, April 16th – 19th 2009, Otočec, Slovenia. GFZ Potsdam, Scientific Technical Report STR 10/05, Potsdam : 151 – 156.

GUSTAVSSON, L. – SATHRE, R. (2006): Variability in energy and carbon dioxide balances of wood and concrete building materials. Building and Environment 41 940–951

HARKIN, J.M. – ROWE, J.W. (1971): Bark and its possible uses. Research note FPL, 091 56 p

HOONG, Y.B. – PARIDAH, M.T. – LOH, Y.F. – JALALUDDIN, H. – CHUAH, L.A. (2011): A new source of natural adhesive: Acacia mangium bark extracts co-polymerized with phenol-formaldehyde(PF) for bonding Mempisang (Annonaceae spp.) veneers. International Journal of Adhesion & Adhesives 31 (2011) 164–167

MACFARLANE, D.W. – LUO, A. (2009): Quantifying tree and forest bark structure with a bark-fissure index. Can. J. For. Res. 39: 1859–1870

MOLNÁR, S. (2004): Faanyagismeret [*Wood Science*]. Szaktudás Kiadó, Budapest (in Hungarian)

PEDIEU, R. – RIEDL, B. – PICHETTE, A. (2009): Properties of mixed particle boards based on white birch (Betula papyrifera) inner bark particles and reinforced with wood fibres. Eur. J. Wood Prod. 67: 95–101

RAGLAND, K.W. – AERTS, D.J. – BAKER, A.J. (1991): Properties of Wood for Combustion Analysis. Bioresource Technology 37: 161–168

SKOGSBERG, K. – LUNDBERG, A. (2005): Wood chips as thermal insulation of snow, Cold Regions Science and Technology 43: 207– 218

SO, C.L. – EBERHARDT, T.L. (2006): Rapid analysis of inner and outer bark composition of Southern Yellow Pine bark from industrial sources. Holz als Roh- und Werkstoff 64: 463–467

SOPP, L. – KOLOZS, L. (2000): Fatömeg-számítási táblázatok [Wood volume tables]. Állami Erdészeti Szolgálat, Budapest pp 24–27 (in Hungarian)

WANG, G.G. – WANGEN, S.R. (2011): Does frequent burning affect longleaf pine (*Pinus palustris*) bark thickness? Can. J. For. Res. 41: 1562–1565

DE GRUYTER OPEN DOI: 10.2478/aslh-2013-0010 Acta Silv. Lign. Hung., Vol. 9 (2013) 119–133

Aerial Image Classification for the Mapping of Riparian Vegetation Habitats

Szilvia KOLLÁR[a,c*] − Zoltán VEKERDY[b,c,d] – Béla MÁRKUS[c]

[a] Department of RIM, Faculty of Spatial Planning, Technical University of Dortmund, Germany
[b] Department of Water Resources, ITC Faculty of the University of Twente, Enschede, the Netherlands
[c] Department of Geoinformation Science, Faculty of Geoinformatics, University of West Hungary, Székesfehérvár, Hungary
[d]Department of Water and Waste Management, Szent István University, Gödöllő, Hungary

Abstract – In the current study, aerial image analysis has been applied to map vegetation communities in a riparian wetland ecosystem, Szigetköz (Hungary). Remote sensing offers an objective and time-effective method for the detection of detailed vegetation habitats with the use of high resolution aerial photos combined with ancillary botanical and silvicultural data. Three images of the same test site, acquired in three different years have been analysed by sample-based semi-automated image classification technique. Due to the heterogeneous nature of the target vegetation classes, besides using spectral features (e.g. vegetation indices) textural descriptors were also involved in the classification procedure. The most appropriate parameters have been chosen using a statistical feature selection method based on the Jeffries-Matusita distance. The accuracy assessment proved for each scene that the combined use of spectral and textural features gave the best classification results in comparison to the exclusive use of spectral or textural measures. The here-applied feature set can be applied for the analysis of similar riparian sites.

remote sensing / high resolution imagery / riparian wetland / texture analysis

Kivonat – Légifelvételek osztályozása vizes élőhelyek térképezése céljából. A tanulmány célja légi-felvételek elemzésére szolgáló módszer kidolgozása vizes élőhelyek vegetációtérképezéséhez, melyet a szigetközi folyómenti mintaterületen vizsgáltunk. A hagyományos terepi felméréssel szemben a távérzékelés lehetővé teszi vizes élőhelyek megközelítően objektív és gyors térképezését nagy felbontású légifelvételek és kiegészítő botanikai és erdészeti adatok felhasználásával. A mintavételen alapuló fél-automatikus képosztályozás eredményesnek bizonyult a kiválasztott három képre alkalmazva (adott tesztterület három időpontra). A vegetációs célosztályok heterogén természetéből adódik, hogy a spektrális jellemzők (vegetációs index) vizsgálata mellett texturális jellemzők bevonására is szükség van az osztályozási algoritmusok kialakításához. A legjelentősebb paramétereket a Jeffries-Matusita statisztikai kiválasztó módszer segítségével határoztuk meg. Megbízhatósági elemzés alapján a spektrális és texturális jellemzők együttes alkalmazása adta a legjobb osztályozási eredményeket a kizárólag spektrális vagy texturális paraméterek felhasználásával szemben. Hasonló ártéri területek növényzeti térképezéséhez a kiválasztott jellemzők alapértelmezett alkalmazása javasolt.

távérzékelés / nagy felbontású felvétel / folyómenti vizes élőhely / texturális elemzés

* Corresponding author: szilvia.kollar@tu-dortmund.de; August-Schmidt-Str. 10, DE-44221, DORTMUND

1 INTRODUCTION

Rapid and extensive change of ecosystems in the last 50 years induced a significant decrease in the variety of life forms (Millennium Ecosystem Assessment 2005). Since by the end of 2010 it became clear that the loss of biodiversity could not be stopped, a new strategy (EU 2020 biodiversity strategy) has been developed, linked to the European Habitats Directive and the Birds Directive (Lang et al. 2013). Besides this policy framework, appropriate technology is needed for observation, where satellite Earth Observation (EO) emerged as a powerful monitoring device. Beyond satellite imagery, the use of archive aerial photography is essential, for the historical characterization of variability within ecosystems and hereby for the development of strategies related to the management of ecological integrity (Landres et al. 1999). The analysis of high resolution images with additional in-situ measurements can compete with traditional field surveying of complex vegetation communities considering cost- and time-effectiveness. The visually-based, solely manual interpretation of imagery is inefficient due to its high subjectivity, as well as due to the rapid development of digital image analysis techniques and automated information extraction methods which result in feasible investigation of larger areas with high spatial resolution. Nevertheless, the image classification techniques of high resolution images for vegetation habitats are not straightforward. Due to the heterogeneous nature of these communities at high geometric resolution, traditional pixel-based digital image classifiers do not give satisfactory results (Levick – Rogers 2008, Kamagata et al. 2008, Addink et al. 2007, Johansen et al. 2010). Therefore, the application of object-based algorithms, after appropriate segmentation approaches, emerged (Blaschke et al. 2011). In addition to that, numerous studies have postulated that a supplementary approach is needed to spectral classification regarding vegetated areas and forest structures from high resolution images (Lévesque – King 2003, Zhang 2001), since target features cannot be differentiated on the sole basis of spectral reflectance. The characterization of image texture became the backbone of various remote sensing related applications, e.g. the analysis of landscape heterogeneity, biophysical parameters, forest structural characteristics, prediction of species distribution and biodiversity patterns (Morgan et al. 2010). Many texture features can be added to a certain study, however, since classification cost increases with the number of features, it is reasonable to reduce this number and utilize only the necessary features for performing a classification (Richards − Jia 2006). In other words, finding the best suited characteristics is a prerequisite for an efficient classification approach, therefore, statistical feature separability methods have been applied aiming at emerging those parameters which have high significance and could be best used in the differentiation of diverse vegetation habitats (Bindel et al. 2011, Mahmoud et al. 2011).

The present study aims at finding an appropriate semi-automated classification method with the use of texture characteristics in order to map predefined vegetation habitats based on high resolution aerial imagery. The analysis is based on a test site in a riparian wetland ecosystem (Szigetköz, Hungary) applied to three different years. Image classifications are carried out independently, however, their comparable use by transferring the descriptive measures from the recent image into another is investigated as well.

2 STUDY SITE

Wetlands in general are among the world's most productive ecosystems and reached a critical vulnerable state recently, wherefore their conservation and sustainable development strategy has been formulated in the Ramsar Convention on Wetlands (1971).

The Szigetköz Danubian floodplain together with the Slovakian Csallóköz is the most extensive riparian wetland in the Upper-Danube region, displaying a high species diversity of

flora and fauna (Illés − Szabados 2008). The region is part of the Fertő-Hanság National Park (FHNP) with 37 500 ha area, of which 9157 ha became landscape protected in 1987 and nowadays it is included in the list of NATURA 2000 SPA (special protected area) and IBA (important bird areas) (Szabó 2005).

Due to the diversion of the Danube into a side channel in 1992, related to the construction of the Gabčikovo Hydroelectric Power Plant, severe changes occurred in the discharge pattern of the old riverbed of the Danube, with a decrease of the average discharge approximately to 20% (Ijjas et al. 2010). It has been reported in the same study of Ijjas et al. (2010) that the unique diverse pattern of habitat types have been significantly affected by the changed flow and sediment regime, and an alteration has been detected from aquatic or aquatic-related species to more terrestrial ones. Medium resolution Landsat satellite image analysis showed negative changes of the normalized vegetation indices in short-term (1992–1993) (Smith et al. 2000), caused by dropping groundwater levels, as were documented and modelled in the region (Vekerdy – Meijerink 1998). Similarly to that, changes were detected in the wetness values based on the Tasseled Cap transformation of Landsat, however, from 1997 a continuous regeneration is experienced, except for older willow species (Kristóf 2005).

Blaschke et al. (2011) listed numerous vegetation studies, where advanced remote sensing techniques have been applied to the analysis of high resolution imagery (≤10 m/pixel) in the recent years, though, in the test site of the present research, vegetation habitat classifications have been mainly based on traditional field survey. Available archive aerial imagery has been often used as unprocessed background information for visualization purposes as a basic layer for vector data representation (Takács − Molnár 2009). While land use/land cover classification of such images has been mainly based on visual image interpretation (Licskó 2002), in the field of forestry Illés − Somogyi (2005) have given an example for the application of a supervised digital image processing algorithm for the detection of different species and their state of health, but they did not reach satisfactory results.

In our research, for detailed vegetation analysis an approximately 2.5 km^2 area has been chosen as a test site, near to the village Dunaremete *(Figure 1)*.

3 DATA

Archive aerial photo series with high spatial resolution (≤ 5 m/pixel) are available at more Hungarian institutions about the chosen test site. For our experiment we used the ones summarized in *Table 1*.

As a pre-processing phase, imagery from 2008 and 2005 has been resampled to the coarser geometric resolution of the image 1999 (1.25 m/pixel) in order to support comparable image analysis techniques for all dates, since textural parameters depend on the spatial resolution of the imagery.

Any kinds of vegetation-related studies need the support of in-situ measurements as reference data. Therefore, botanical maps have been gathered, where the field survey was based on the framework of the National Biodiversity Monitoring System (Takács − Molnár 2009) focusing on the mapping of Á-NÉR types (Á-NÉR = the Hungarian abbreviation of General National Habitat Classifying System) (*Figure 1, Table 2*). Besides the botanical view of habitat complexes, it was also essential to involve silvicultural databases (*Figure 1, Table 2*), in order to aid the selection of target vegetation classes. Personal field inspection of a part of the test site has been carried out in November, 2010. Nevertheless, it has to be mentioned, that the ancillary data have been acquired in different time from the image dataset, and this brings some additional uncertainties into the image interpretation procedure.

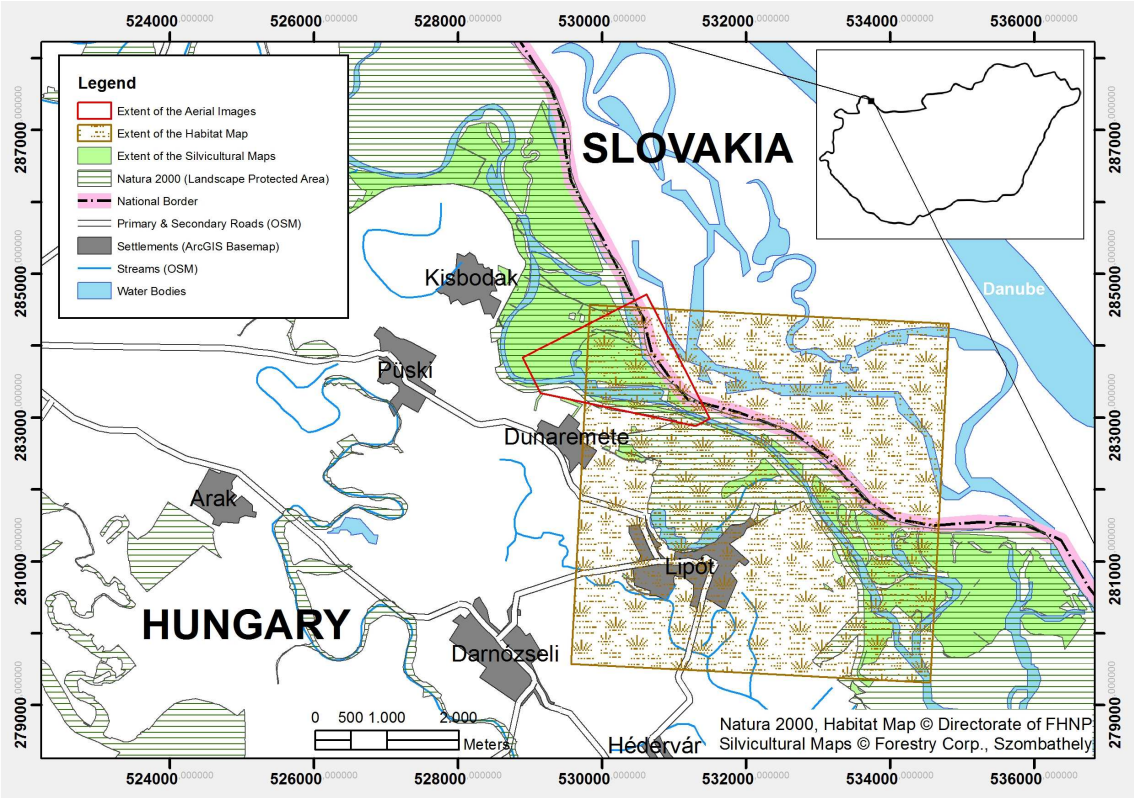

Figure 1. Test site in the Szigetköz Danubian floodplain

Table 1. Aerial imagery

Imagery	Orthophoto 2008	Orthophoto 2005	Orthophoto 1999
Source	Institute of Geodesy, Cartography and Remote Sensing (FÖMI), Budapest		University of West Hungary, Phare CBC Project, EUROSENSE*
Scale	1 : 74 000**	1 : 30 000	1 : 30 000
Original Ground Spatial Resolution	0.5 m/pixel	0.5 m/pixel	1.25 m/pixel
Spectral Resolution	NIR, G, B	RGB	NIR, R, G
Camera Type	UltraCamX	RC 20	Wild RC 20
Applied Film Type	Digital, Color IR	Color	Color IR
Acquisition time	06.08.2008	29.07.2005	03.08.1999
Solar azimuth angle	125.6°	209.4°	111.6°

* CBC: Cross-Border-Cooperation; EUROSENSE: http://www.eurosense.com
** However, because of the digital camera, the given scale cannot be directly compared to the others.

Table 2. Ancillary data

Ancillary data	Habitat map	Silvicultural map
Thematic information	Á-NÉR habitat type	First type of forest stand
Scale	1 : 12 500	1 : 10 000
Acquisition year	2000, 2004	2003
Acquisition time period	July-October	Spring-sommer-autumn
Source	Directorate of FHNP	Forestry Directorate, Szombathely

4 METHODS

4.1 Object-based image analysis

Object-based image analysis (OBIA) technique, contrary to pixel based approaches, offers an efficient solution for high spatial resolution mapping with a potential extension for larger areas in a relatively rapid manner, due to the integration of spatial complexity. OBIA consists of (1) image segmentation: clustering of pixels into homogeneous objects, (2) classification: labeling of objects and (3) modeling based on the characteristics of objects (Johansen et al. 2010b). As the first step, the segmentation approach is mainly based on the concept from Tobler (1970), also known as the first law of geography, saying that "everything is related to everything else, but near things are more related than distant things".

According to that, images of each year have been firstly analysed concentrating on the separation of`the spectrally differentiable 'Water bodies', like the first part of a hierarchical classification. In that case, after quadtree and multi-resolution segmentation approaches, the classification was based on vegetation indices (*Table 3*) and brightness values (average of the three original bands). In addition, manual corrections were needed, especially concerning the image from 2005.

Table 3. Vegetation indices applied to images with different spectral resolutions

Orthophoto	2008	2005	1999
Spectral bands	NIR, G, B	R, G, B	NIR, R, G
Vegetation Index	modified NDVI: (NIR-B)/(NIR+B)	(G-R)/(G+R) (Gitelson et al. 2002)	NDVI: (NIR-R)/(NIR+R)

4.2 Target vegetation classes

Further classes are related to vegetation habitats, where the selection of target classes was based on a synoptic view of the aerial photos (2008, 2005, 1999) and additional information, concentrating on the most occurring and characteristic vegetation patterns which can be "easily" identified by human eye in the visual image interpretation process. Reed (R), Hybrid Poplar (HP), Domestic Poplar (DP), Willow (W) and Willow & Poplar (WP) classes (*Figure 2*) have been defined as target classes for the image classification for each year, except for class Domestic Poplar (in the Hungarian designation "hazai nyáras") which was only present in 2008. It has not been intended to identify each of the occurring classes in the test site, but those ones which cover an area with a significant size.

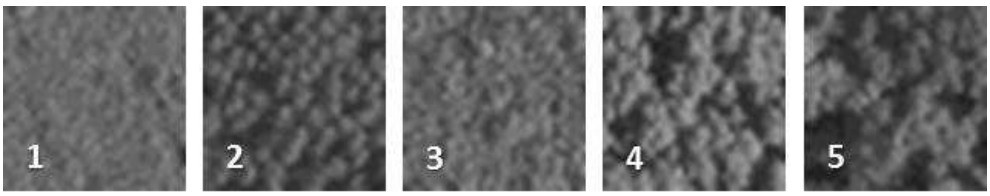

*Figure 2. Target vegetation classes represented by 40 m * 40 m square samples (2008, PC1, GSR: 1.25 m/pixel)*
1: Reed, 2: Hybrid Poplar, 3: Domestic Poplar, 4: Willow, 5: Willow & Poplar

4.3 Analysis of textures

In case of very high resolution (VHR) imagery the spectral characteristics (radiometric values in various bands) of a single pixel cannot describe forest stands or even an individual tree, therefore, information is needed on the local neighborhood of each pixel, either by the generalization for the stand (substand) or by the analysis of the texture of larger spatial units, like square-shaped windows/polygons. Local textures can be described by spatial statistical measures, grouped into three types, (1) first-order statistics, e. g. standard deviation, (2) second-order statistics based on co-occurrences and (3) semi-variances or autocorrelations within a pixel neighborhood (Tuominen − Pekkarinen 2005).

4.3.1 The grey-level co-occurrence matrix

Grey-level co-occurrence matrices (GLCM) belong to second-order statistics and have been successfully applied in numerous studies for land-cover/vegetation analysis of remotely sensed imagery (Berberoglu et al. 2007; Hájek 2008), showing significant improvements in the classification accuracies (Franklin et al. 2000; Carleer − Wolff 2006). Taking a grey-scale image with a given brightness value range (in our case $L = 256$ *due to the* 8 bit data), the GLCM is an $L \times L$ matrix, where the value for each cell is defined by the number of occurrences of a given grey-level-combination of 2 pixels (a pixel pair, with a defined h distance and θ direction which are given for a concrete matrix) divided by the total possible number of grey level pairs (Richards − Jia 2006). Depending on the various h and θ chosen, there are different GLCMs. Haralick et al. (1973) defined 14 various metrics derived from each matrix to use as texture measures.

In summary, variables which have to be defined for GLCM calculations are (1) moving window (object) size; (2) direction of the offset (mentioned as θ before); (3) distance of the offset (h); (4) image channel used; (5) specific metrics as defined by Haralick et al. (1973). Regarding the direction of the offset, the all directional feature is often applied, meaning the average of all the directions (0°, 45°, 90°, 135°), especially when the observed classes are not directionally biased (Laliberte − Rango 2009). The distance of pixels is normally set to 1, i.e. for the comparison of direct neighbours (Trimble 2013). We applied GLCM on the first principal component (PC1) calculated from the three bands of each aerial photo to best represent the texture of the photo (coefficients for PC1 *regarding 2008*: 0.659, 0.485, 0.575; *regarding 2005*: 0.579, 0.590, 0.563; *regarding 1999*: 0.685, 0.488, 0.541).

Similar to the case described above regarding the image analysis of VHR imagery, by the application of object-based image analysis technique the core of the analysis procedure is not any more the pixel itself, but "an extended neighborhood", the image segments or objects, which are typically the sets of spectrally similar pixels coming from a multi-resolution segmentation approach (Benz et al. 2004). However, due to the fact that target vegetation communities are spectrally heterogeneous, another type of segmentation ("chessboard") is privileged in our investigations, where the image scene is divided into unique-sized objects (squares) with a predefined size. This means actually that the minimum mapping unit of the classification has changed from 1.25 m/pixel to 20 m/pixel, but with additional information on the texture.

4.3.2 The semi-variogram

Moving window sizes or in our example, the square image object sizes are critical for any texture analyses. The internal spatial variability of the target class(es) will determine the ground resolution element (here the grid size), before unnecessary intra-parcel variability would be detected (Curran 1988). In this regard, semi-variogram analysis has been applied in numerous studies to choose the most appropriate window size for GLCM computation (Carr −

Miranda 1998; Treitz − Howarth 2000; Tsai − Chou 2006; Szantoi et al. 2013). The variogram (or semi-variogram) is frequently used as a measure of spatial continuity, as well as a multiscale directional measure of surface roughness (Trevisani et al. 2009). The mathematical structure model of the empirical semi-variogram is defined as (Curran 1988):

$$\gamma(h) = \frac{1}{2m} \sum_{i=1}^{m} [z(x_i) - z(x_{i+h})]^2 \quad (1)$$

where x is a geographic point, $z(x)$ is its attribute value (in our case, the radiometric value, DN) and m is the number of point pairs separated by vector h. For the graphs of the semi-variograms $\gamma(h)$ is visualized for increasing h**.** The larger $\gamma(h)$ is, the less similar are the pixels divided by a given h vector (often named as *lag*). Range is one of the most important characteristics of the semi-variogram, which is a point on the h axis where $\gamma(h)$ reaches its maximum, or rather for sample data where $\gamma(h)$ reaches approximately 95% of the sill - which is the maximum level of $\gamma(h)$ (Curran 1988).

In the current research, since target classes are vegetation habitats with repetitive patterns, their semi-variograms are rather periodical, but anisotropic. The visualization of the semi-variogram graphs help to identify approximately one period as the appropriate size for further texture investigations. Semi-variograms for 4 window sizes (*10 ×10, 20 ×20, 30 ×30, 40 ×40 m*) have been compared for the image 2008 calculated on the PC1, choosing certain samples from the predefined target vegetation classes (*Figure 2*). Corresponding to the solar azimuth angle of the image acquisition of 2008, directional variograms have been computed along the direction of the supposed minimum continuity (126°) in order to describe variability and as well along the direction of maximum continuity (perpendicular to 126°, thus 36°). These analyses (*Figure 3*) proved that the use of around *20 m ×20 m* (16 ×16 pixels for the 1.25 m/pixel GSR) square-objects is reasonable as basis for the texture analysis.

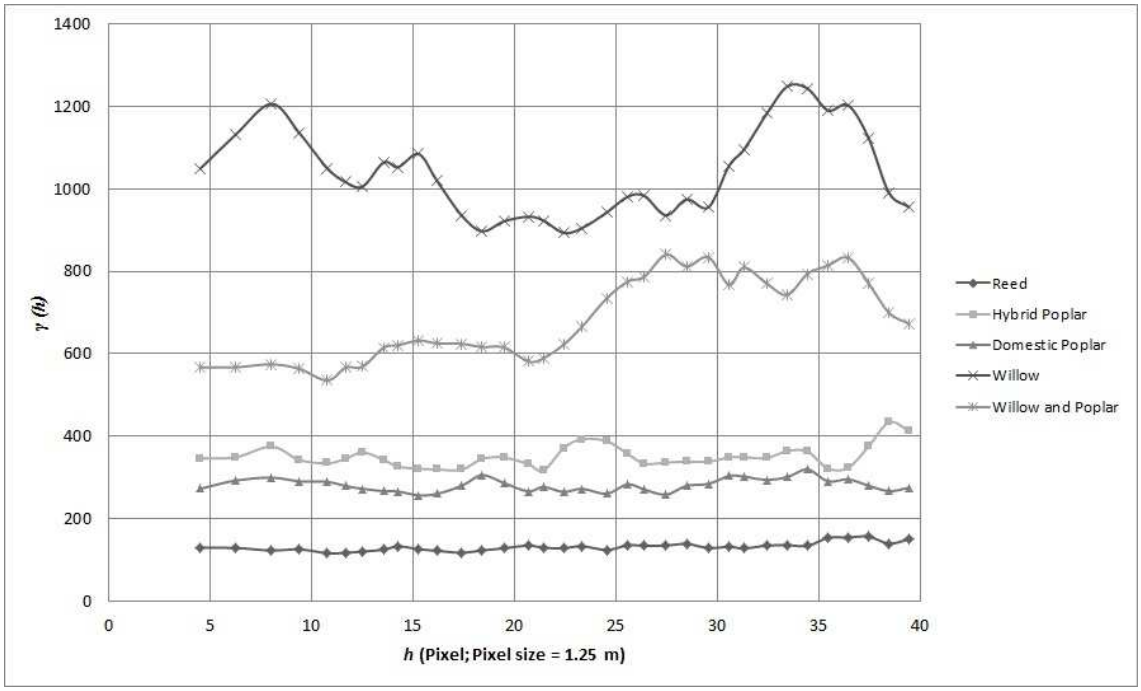

Figure 3. Directional semi-variograms (regarding the solar azimuth angle: 126° of the image acquisition 2008) for different vegetation classes

This was supported by the findings of Tuominen − Pekkarinen (2005) who applied 20 m × 20 m square-shaped windows, stating that this size would lead to near-optimal results regarding forest stand inventories based on the analysis of aerial photography.

4.4 Statistical feature selection method

In a recent study (Kollár et al. 2013) related to the present research project GLCM entropy (ENT), correlation (CORR) and standard deviation (STDEV) have been chosen from the texture measures based on literature references (Hall-Beyer 2007) and empirical observations by the comparison of feature value ranges of certain class-pairs. There, besides the all-directional type, directional textures have been analyzed as well, applied to those angles which were the nearest to the solar azimuth angle of each image acquisition (*Table 1*). For 2008 the use of the all-directional, for 2005 and 1999 the directional textures in the combined feature set (together with vegetation index) provided the best classification accuracies (Kollár et al. 2013).

The current attempt aimed at a statistically based feature selection method for the analysis and the choice of the most appropriate textural features from a larger number of measures, which have been analysed as well in the study of Laliberte − Rango (2009) complemented with two other measures. The issue of feature selection has been a general problem in image analysis methods, more specifically in pattern recognition related applications in order to minimize the classification error (Peng 2005, Pereira et al. 2007, Laliberte et al. 2012, Silva et al. 2012). Besides aiming at higher classification accuracies, the application of feature selection methods has been related to the reduction of redundant information in order to speed up the classification approach by an optimal decrease in the evaluated features (Mahmoud et al. 2011, Bindel et al. 2011). Determination of the mathematical separability of classes has been a common procedure, where feature reduction is performed by checking how separable various spectral classes remain when reduced sets of features are applied (Richards − Jia 2006). From the group of probabilistic measures the Bhattacharyya distance (*B*) is one of the most popular measures (Mahmoud et al. 2011):

$$B = \frac{1}{8}(m_1 - m_2)^2 \times \frac{2}{{\delta_1}^2 + {\delta_2}^2} + \frac{1}{2}\ln\left[\frac{{\delta_1}^2 + {\delta_2}^2}{2\delta_1\delta_2}\right] \quad (2)$$

which has been stated as a convenient equation for normal distributions, but not rejecting the complete group of non-Gaussian cases and also discussed for a family of gamma distributions (Fukunaga 1990). However, the infinite nature of B concerning a range of a half-closed interval [0, ∞) makes its interpretation difficult. Therefore, a similar measure, but with a finite dynamic range has been introduced, called Jeffries-Matusita distance *(JM)* (Richards − Jia 2006).

$$JM = 2(1 - e^{(-B)}) \quad (3)$$

Silva et al. (2012) have summarized that generally JM values above 1.8 are the indicators for a good separability, the distance value below 1.8 would mean the possibility of confusion in the classification process between classes.

In our study 8–8 GLCM features (all-directional and directional) and 4–4 GLDV (gray level difference vector) statistics have been analyzed for the best separability measures, where GLDV is a sum of the diagonals of the GLCM and a measure of the absolute differences of neighbors (Laliberte − Rango 2009). Target classes have had a minimum of 20 grid samples for each year. The basis for the texture calculations was the first principal component layer. As mentioned before, GLCM can be directional (related to the solar azimuth angle of each

image) and non-directional (the average of the directional features) and here both have been applied. For *d* (distance), 1 has been chosen as default, calculated in the object-based image analysis software eCognition Developer 8.9. Besides textures, vegetation indices (*Table 3*) and two other spectral descriptors (average of PC1 and average of the Green band) have been added as well to the separability analysis.

JM measures for image 2008 are shown in detail in *Table 4* for the selected textures (each one of them is all directional, *Table 5*) next to one spectral characteristic. Although, the separability value for GLCM Mean was only bigger than 1.8 for 2 class pairs, one of them (HP-SP) represents a unique case since those classes have not been separable by any other texture features. Besides this consideration, we can also take into account, that there might be class pairs which are not clearly separable and the step concerning the selection of target classes should be revised. *Table 4* indicates an example where the class pairs SP-WP and W-WP are not separable without confusion (white fields, where *JM* is under 1.8). From the investigations regarding 2005, 1999 pairs of HP-WP and W-WP have been inseparable.

Table 4. JM measures for vegetation class pairs, concerning the selected textural and spectral features

	HP-SP	HP-W	HP-WP	HP-R	SP-W	SP-WP	SP-R	W-WP	W-R	WP-R	Number of pairs where JM ≥ 1.8
GLCM STDEV	0.0	1.9	1.6	1.8	2.0	1.7	1.8	0.5	2.0	2.0	6
GLDV ENT	0.7	1.6	0.4	0.9	1.9	0.5	1.8	1.4	2.0	1.8	4
GLCM CONT	0.5	1.6	0.4	1.0	1.8	0.7	1.9	1.3	1.9	1.8	4
GLCM MEAN	1.9	1.4	0.4	2.0	0.4	1.0	1.0	0.4	1.1	1.4	2
mNDVI	1.9	2.0	1.9	2.0	1.1	0.6	1.9	0.2	1.0	1.3	5

Table 5. GLCM measures chosen after separability analysis

Texture Measure	Formula
GLCM Contrast (CONT)	$\sum_{i,j=0}^{N-1} P_{i,j}(i-j)^2$
GLCM Mean (MEAN)	$\frac{\sum_{i,j=0}^{N-1} P_{i,j}}{N^2}$
GLCM Standard Deviation (STDEV)	$\sum_{i,j=0}^{N-1} P_{i,j}(i, j-\mu_{i,j})$
GLDV Entropy (ENT)	$\sum_{k=0}^{M-1} V_k(-\ln Vk)$

P_{ij} is the normalized gray-level value in the cell i,j of the matrix, N is the number of rows or columns, $\mu_{i,j}$ are the mean of row i and column j, V_k is the normalized gray-level difference vector, and $k = |i-j|$.

4.5 Semi-automated classification algorithm

The complete image analysis with texture calculations was performed using the object-based image analysis software eCognition Developer 8.9. The applied supervised classification algorithm is based on a membership value based fuzzy class evaluation, where the membership values concerning one specific feature from the selected feature set are computed from the training grid cells. The fuzzy nature of the algorithm means that there are three potential classes in the evaluation for a certain object (here: grid cell), with the label of the best class, calculated from the membership value based class descriptions for the selected feature set (Trimble 2013). Semi-automated refers to the general nature of classification approaches as part of the digital image analysis techniques where pixels or grid cells are classified in an almost automatic manner. Although the part of training sample selection is still subjective, chosen by the analyst, the labeling of objects later on is based on the derived characteristics and chosen algorithms.

In traditional supervised classifications, firstly training samples are chosen from a concrete image where, based on their characteristics (usually the statistical descriptions), the whole image can be classified into the groups of predefined classes. In case of aerial image time series regarding a certain test site and short time period, the following question arises: whether it is possible to classify different-year images based on the training samples from a given year. In the current study, training samples have been collected from the 2008 image and the derived class descriptions have been tested for the 1999 image, which has a different spectral, but due to the earlier resampling (regarding the 2008 image) the same geometric resolution.

5 RESULTS AND DISCUSSION

Due to the fact that the acquisition times of botanical and forest inventories did not overlap with the aerial images, reference data cannot be directly taken. Thus, just like for the training stage of the classification, samples for accuracy assessment were taken from the target classes at locations different from the training areas. *Table 6* summarizes the overall accuracies and Kappa coefficient measures for the 9 classifications, regarding the 3 different feature sets applied to each year.

Table 6. Accuracy assessment of the fuzzy classification results concerning different feature sets

	Year 2008 (CIR)		Year 2005 (RGB)		Year 1999 (CIR)	
Features applied	Overall acc.	Kappa	Overall acc.	Kappa	Overall acc.	Kappa
Mean of PC1, VI	0.78	0.72	0.50	0.35	0.60	0.47
4 textures only	0.91	0.89	0.88	0.84	0.82	0.76
4 textures, VI	0.96	0.94	0.90	0.87	0.84	0.79

Accuracy measures have shown that the use of texture parameters leads to significant improvements in comparison to solely spectral bands based classifications, however, best classification results were reached with the application of a combined set of spectral (vegetation index) and textural descriptors.

The following three maps in *Figure 4* present the best classification results for the test site (2008, 2005, 1999).

Classification results for the different images (2008, 2005, 1999) come from independent image analyses based on sample selection in each year. Nevertheless, after visual interpretation target vegetation classes regarding species composition remained nearly the

same between 1999 and 2008 for the most of the site, that's why it was reasonable to analyse the classification algorithm based on the same class descriptions for the former year 1999.

The identification of water bodies in image 1999 worked well with the application of the "transferred" algorithm applied originally to image 2008 (a combination of the use of vegetation index and brightness). Contrary to that the predefined vegetation classes could not be detected in the 1999 image. Because of temporal differences "stable" vegetation classes are changing (growth) as well and any change in the texture patterns is critical for the given (transferred) membership functions in the classification algorithm. In addition, the here-applied classification scheme does not cover the complete test site (unclassified area covers more than 30% in case of image 2008 and more than 20% for images 2005, 1999) which leads to difficulties regarding class transferability for different years and sites, that's why the reconsideration of target classes is vital. However, an extension of the classification scheme without primary ground reference information (field survey concerning the last image, 2008) isn't straightforward either. Complementary classes could partly come from habitat maps (in the concrete example, Dunaremete, 2004: vegetation on edges and dams, other hardwood, arable land), from silvicultural inventory (domestic poplar-acacia) and from visual interpretation (bare soil mixed with grass, road, young stand, shadow). The application of the same supervised classification method described before, however, with additional samples, resulted in 87% overall accuracy and showed a significant decrease in the unclassified area. It has to be emphasized that although we have been concentrated on a classification scheme mainly based on species composition, one of the additional classes: domestic poplar-acacia has been classified into the same group as a certain hybrid poplar stand with the same age (referring to the silvicultural information), which leads to the consideration of forest stand classification based on age structure.

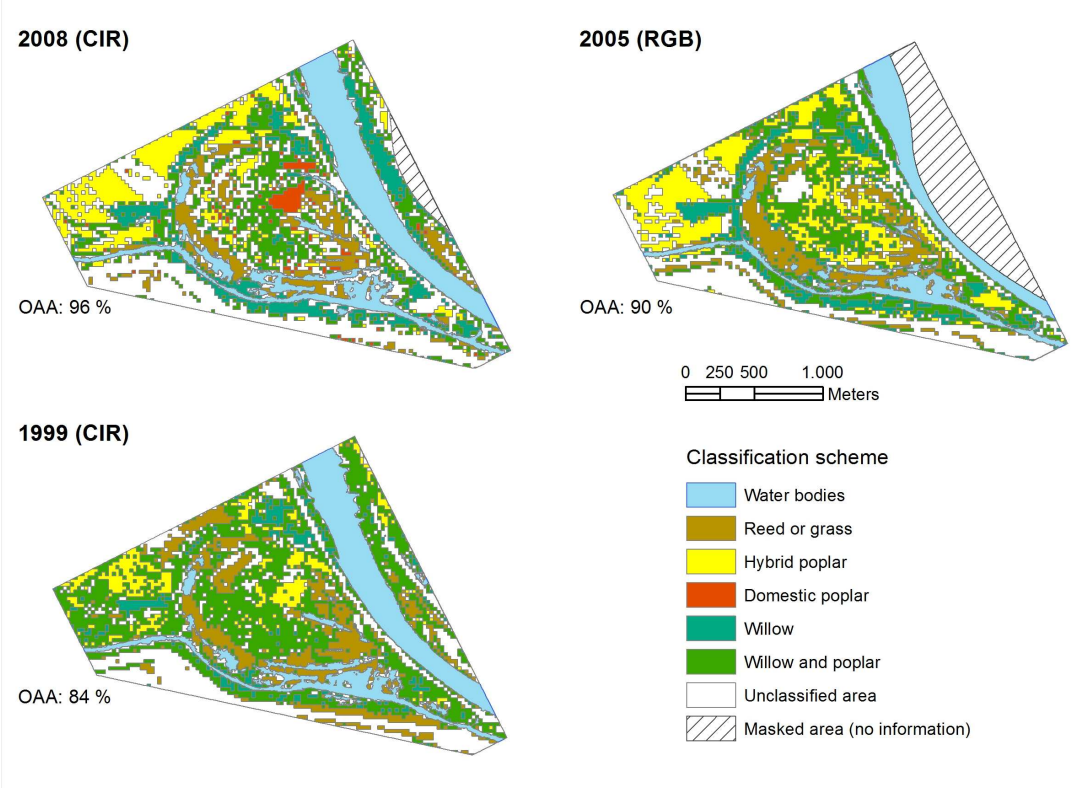

Figure 4. Classification results based on the fuzzy (membership value based) classification, for three different years (2008, 2005, 1999) with the use of the combined (textural and spectral) feature set

Beyond these aspects, the lack of reliable ancillary information for the former years makes it difficult to conduct a detailed analysis with appropriate accuracy. Monitoring approaches often apply post-classification change detection, which is an essential tool for the evaluation of quantitative and qualitative changes in the observed (vegetation) classes. Nevertheless, this type of analysis requires high classification accuracies for each analysed year. We have seen that overall classification accuracy decreases significantly from 2008 to 1999, however, for each scene it was higher than 80%. Considering the accuracy calculation procedure it is vital, that in the earlier-mentioned measures (*Table 6*) misclassification of the background (expected as unclassified area) has not been involved. Experimental accuracy calculations complemented with background reference samples, only applied to the 2008 image, have resulted in 9% decline (from 96% to 87%) regarding the overall accuracy and 0.10 decrease (from 0.94 to 0.84) concerning the Kappa index. These values emphasize the significance of more detailed accuracy assessment and the further improvement of classification results, before the application of reasonable change detection methods.

6 CONCLUSIONS AND FUTURE WORK

Generally speaking, aerial imagery based semi-automatic image analysis aids vegetation monitoring approaches, helps to understand the ecological structures (vegetation patches) in a faster manner and has the potential to analyse processes (temporal changes) and hereby, supports the work of botanical and silvicultural surveyors with habitat maps.

Based on the findings of the current study, the combined set of spectral (vegetation index) and textural (derived from GLCM/GLDV) features is suggested to be analysed and further involved in image classification algorithms for the mapping of riparian vegetation habitats. Based on the accuracy assessment the combination of spectral and textural features provided the best classification results in comparison to the sole use of spectral or textural descriptors. During the analysis of textural and spectral descriptors (features) the utilization of a statistical feature selection method (e.g. Jeffries-Matusita measure) has been proved to be essential in order to find the best fitting descriptors and to make reliable estimates of class signatures, especially in those cases where the selection of training pixels/objects is restricted due to the small size of the test site (Richards − Jia 2006). Regarding the remark (made in the previous section) concerning the similarities between different vegetation habitats (hybrid poplar and domestic poplar-acacia), it should be further investigated based on other test sites whether the age structure of forest stands significantly influences the vegetation habitat classification mainly based on species composition and if texture based image analysis could help to investigate forest stand ages.

Uncertainty originates from various sources in ecosystem mapping, already in the training phase of the supervised classification, e.g. definition of classes, subjectivity of the field surveying based reference data and the mixed pixel (in our case: mixed object) problem (Rocchini et al. 2013). In case of differing acquisition times in image and reference data, a significant difficulty is often present, since the identification of a certain land cover type cannot be precise. Accuracy assessment can only take into account those objects for proof where the identification of a given class is reliable.

The current study proved that the direct transfer of texture measures derived from one image transferred to a former one, and thereby the detection of the same or similar vegetation habitats in the former year cannot be worked out based on an incomplete classification scheme and the applied membership function based classification algorithm. For this reason and for the improvement of recent results, a complete cover of vegetation classes and the use of advanced classification algorithms have to be analysed in the further research.

Acknowledgements: We wish to extend our thanks to the University of West Hungary, Faculty of Forestry for the provided PhD grant (2008–2011), to the Trimble Geospatial Munich for providing the eCognition Developer software; to the Fertő-Hanság National Park (Sarród) and to the Forest Inspectorate in Szombathely for giving us access to the botanical and silvicultural data, and to István Hahn (ELTE, Budapest) for his guidance during the field investigations and for his support regarding the botanical aspects of the study.

REFERENCES

ADDINK, E. A. − JONG, S. M. de − PEBESMA, E. J. (2007): The Importance of Scale in Object-based Mapping of Vegetation Parameters with Hyperspectral Imagery. Photogrammetric Engineering & Remote Sensing 73 (8), 905–912.

BENZ, U. C. − HOFMANN, P. − WILLHAUCK, G. − LINGENFELDER, I. − HEYNEN, M. (2004): Multi-resolution, object-oriented fuzzy analysis of remote sensing data for GIS-ready information. ISPRS Journal of Photogrammetry and Remote Sensing 58 (3–4), 239–258.

BERBEROGLU, S. − CURRAN, P. − LLOYD, C. − ATKINSON, P. (2007): Texture classification of Mediterranean land cover. International Journal of Applied Earth Observation and Geoinformation 9 (3), 322–334.

BINDEL, M. − HESE, S. − BERGER, C. − SCHMULLIUS, C. (2011): Feature selection from high resolution remote sensing data for biotope mapping. In: C. Heipke, K. Jacobsen, F. Rottensteiner, S. Müller, U. Sörgel (Eds.): High-Resolution Earth Imaging for Geospatial Information. Hannover, June 14–17. ISPRS. XXXVIII-4/W19 (ISPRS Archives).

BLASCHKE, T. − JOHANSEN, K. − TIEDE, D. (2011): Object-Based Image Analysis for Vegetation Mapping and Monitoring. In: Q. Weng (Ed.): Advances in Environmental Remote Sensing: Sensors, Algorithms and Applications. United States: CRC Press Taylor & Francis Group, 241–271.

CARLEER, A. P. − WOLFF, E. (2006): Urban land cover multi-level region-based classification of VHR data by selecting relevant features. Int. J. of Remote Sensing 27 (6), 1035–1051.

CARR, J. R. − MIRANDA, F. P. de (1998): The semivariogram in comparison to the co-occurrence matrix for classification of image texture. Geoscience and Remote Sensing, IEEE Transactions on 36 (6), 1945–1952.

CURRAN, P. J. (1988): The semivariogram in remote sensing: An introduction. Remote Sensing of Environment 24 (3), 493–507.

FRANKLIN, S. E. − HALL, R. J. − MOSKAL, L. M. − MAUDIE, A. J. − LAVIGNE, M. B. (2000): Incorporating texture into classification of forest species composition from airborne multispectral images. International Journal of Remote Sensing 21 (1), 61–79.

FUKUNAGA, K. (1990): Introduction to Statistical Pattern Recognition. Second Edition. San Francisco San Diego: Morgan Kaufmann Academic Press.

GITELSON, A. A. – KAUFMAN, Y.J. – STARK, R. – RUNDQUIST, D. (2002): Novel algorithms for remote estimation of vegetation fraction. Remote Sensing of Environment 80, 76–87.

HÁJEK, F. (2008): Process-based approach to automated classification of forest structures using medium format digital aerial photos and ancillary GIS information. Eur J Forest Res 127 (2), 115–124.

HALL-BEYER, M. (2007): The GLCM Tutorial Home Page. Available online at http://fp.ucalgary.ca/mhallbey/tutorial.htm, updated on 21/02/2007, checked on 6/12/2012.

HARALICK, R. M. − SHANMUGAM, K. − DINSTEIN, I. (1973): Textural Features for Image Classification. Man and Cybernetics Systems 3 (6), 610–621.

IJJAS, I. − KERN, K. − KOVÁCS, GY. (Eds.) (2010): Feasibility Study. The Rehabilitation of the Szigetköz Reach of the Danube. Budapest.

ILLÉS, G. − SOMOGYI, Z. (2005): A szigetközi ártéri erdők egészségi állapotának ortofotókon alapuló elemzése és értékelése. [Health condition of the forests of Szigetköz based on orthophotos.] Tájökológiai Lapok 3 (2), 335–360. (in Hungarian)

ILLÉS, G. − SZABADOS, I. (2008): 20 éves az erdészeti monitoring a Szigetközben. [20 years of monitoring in Szigetköz.] Erdészeti Kutatások 2007–2008 92, 95–120. (in Hungarian)

JOHANSEN, K. − ARROYO, L. A. − PHINN, S. − WITTE, C. (2010a): Comparison of Geo-Object Based and Pixel-Based Change Detection of Riparian Environments using High Spatial Resolution Multi-Spectral Imagery. Photogrammetric Engineering & Remote Sensing 76 (2), 123–136.

JOHANSEN, K. − BARTOLO, R. − PHINN, S. (2010b): SPECIAL FEATURE – Geographic Object-Based Image Analysis. Journal of Spatial Science 55 (1), 3–7.

KAMAGATA, N. − HARA, K. − MORI, M. − AKAMATSU, Y. − LI, Y. − HOSHINO, Y. (2008): Object-based classification of IKONOS data for vegetation mapping in Central Japan. In: T. Blaschke, S. Lang, G. J. Hay (Eds.): Object-Based Image Analysis - Spatial Concepts for Knowledge-Driven Remote Sensing Applications. Berlin Heidelberg: Springer-Verlag, 459–475.

KOLLÁR, Sz. − VEKERDY, Z. − MÁRKUS, B. (2013): Geostatistical Characterization of Wetland Habitats. In: M. Neményi, L. Varga, F. Facskó, I. Lőrincz (Eds.): Science for Sustainability. International Scientific Conference for PhD Students. Győr, Hungary, March 19–20. Sopron: University of West Hungary Press, 106–111.

KRISTÓF, D. (2005): Távérzékelési módszerek a környezetgazdálkodásban. [Remote sensing methods in environmental management.] PhD thesis, University of Szent István, Gödöllő (in Hungarian)

LALIBERTE, A. − BROWNING, D. − RANGO, A. (2012): A comparison of three feature selection methods for object-based classification of sub-decimeter resolution UltraCam-L imagery. International Journal of Applied Earth Observation and Geoinformation 15, 70–78.

LALIBERTE, A. − RANGO, A. (2009): Texture and Scale in Object-Based Analysis of Subdecimeter Resolution Unmanned Aerial Vehicle (UAV) Imagery. IEEE Trans. Geosci. Remote Sensing 47 (3), 761–770.

LANDRES, P. B. − MORGAN, P. − SWANSON, F. J. (1999): Overview of the use of natural variability concepts in managing ecological systems. Ecological Applications 9 (4), 1179–1188.

LANG, S. − CORBANE, C. − PERNKOPF, L. (2013): Earth Observation for Habitat and Biodiversity Monitoring. T. Jekel, A. Car, J. Strobl, G. Griesebner (Eds.): GI_Forum 2013. Creating the GISociety. GI Forum. Salzburg. Berlin/Offenbach: Herbert Wichmann Verlag, 478–486.

LÉVESQUE, J. − KING, D. J. (2003): Spatial analysis of radiometric fractions from high-resolution multispectral imagery for modelling individual tree crown and forest canopy structure and health. Remote Sensing of Environment 84 (4), 589–602.

LEVICK, S. R. − ROGERS, K. H. (2008): Structural biodiversity monitoring in savanna ecosystems: Integrating LiDAR and high resolution imagery through object-based image analysis. In: T. Blaschke, S. Lang, G. J. Hay (Eds.): Object-Based Image Analysis - Spatial Concepts for Knowledge-Driven Remote Sensing Applications. Berlin Heidelberg: Springer-Verlag, 477–491.

LICSKÓ, B. (2002): A Szigetköz digitális felszínborítás térképeinek elkészítése légi felvételek kiértékelésével. [Digital mapping of Szigetköz by evaluating aerial photos.] Térinformatika (3), 13–15. (in Hungarian)

MAHMOUD, A. − ELBIALY, S. − PRADHAN, B. − BUCHROITHNER, M. (2011): Field-based landcover classification using TerraSAR-X texture analysis. Advances in Space Research 48 (5), 799–805.

MILLENNIUM ECOSYSTEM ASSESSMENT (Ed.) (2005): Ecosystems and Human Well-being: Synthesis. Washington, DC., Island Press

MORGAN, J. L. − GERGEL, S. E. − COOPS, N. C. (2010): Aerial Photography: A Rapidly Evolving Tool for Ecological Management. BioScience 60 (1), 47–59.

PENG, H. (2005): Feature Selection Based on Mutual Information: Criteria of Max-Dependency, Max-Relevance, and Min-Redundancy. IEEE Transactions on Pattern Analysis and Machine Intelligence 27 (8), 1226–1238.

PEREIRA, R. R. − AZEVEDO MARQUES, P. M. − HONDA, M. O. − KINOSHITA, S. K. − ENGELMANN, R. − MURAMATSU, C. − DOI, K. (2007): Usefulness of Texture Analysis for Computerized Classification of Breast Lesions on Mammograms. J Digit Imaging 20 (3), 248–255.

RICHARDS, J. A. − JIA, X. (Eds.) (2006): Remote Sensing Digital Image Analysis. An Introduction. 4th Edition. Heidelberg: Springer-Verlag

ROCCHINI, D. − FOODY, G. M. − NAGENDRA, H. − RICOTTA, C. − ANAND, M. − HE, K. S. et al. (2013): Uncertainty in ecosystem mapping by remote sensing. Computers & Geosciences 50, 128–135.

SILVA, C. − MARCAL, A. − PEREIRA, M. − MENDONÇA, T. (2012): Separability analysis of color classes on dermoscopic images. In: A. Campilho, M. Kamel (Eds.): ICIAR 2012. Part II. LNCS 7325. Berlin; Heidelberg: Springer-Verlag, 268–277.

SMITH, S. − BÜTTNER, G. − SZILAGYI, F. − HORVATH, L. − AUFMUTH, J. (2000): Environmental impacts of river diversion: Gabcikovo Barrage System. Journal of Water Resources Planning and Management 126 (3), 138–145.

SZABÓ, M. (2005): Vizes élőhelyek tájökológiai jellemvonásai a Szigetköz példáján. [Landscape ecological features of wetlands exemplified by the Szigetköz region] PhD thesis ELTE, Budapest, (in Hungarian)

SZANTOI, Z. − ESCOBEDO, F. − ABD-ELRAHMAN, A. − SMITH, S. − PEARLSTINE, L. (2013): Analyzing fine-scale wetland composition using high resolution imagery and texture features. International Journal of Applied Earth Observation and Geoinformation 23 (0), 204–212.

TAKÁCS, G. − MOLNÁR, ZS (Eds.) (2009): National Biodiversity Monitoring System XI. Habitat mapping. 2nd modified edition. Vácrátót; Budapest: Hungarian Academy of Sciences, Insitute of Ecology and Botany; Ministry of Environment and Water

TOBLER, W. (1970): A computer movie simulating urban growth in the Detroit region. Economic Geography 46 (2), 234–240

TREITZ, P. − HOWARTH, P. (2000): High Spatial Resolution Remote Sensing Data for Forest Ecosystem Classification: An Examination of Spatial Scale. Remote Sensing of Environment 72 (3), 268–289.

TREVISANI, S. − CAVALLI, M. − MARCHI, L. (2009): Variogram maps from LiDAR data as fingerprints of surface morphology on scree slopes. Nat.Hazards Earth Syst.Sci. (9), 129–133.

TRIMBLE (Ed.) (2013): eCognition Developer. Reference Book, Trimble Germany GmbH.

TSAI, F. − CHOU, M.-J. (2006): Texture augmented analysis of high resolution satellite imagery in detecting invasive plant species. Journal of the Chinese Institute of Engineers 29 (4), 581–592.

TUOMINEN, S. − PEKKARINEN, A. (2005): Performance of different spectral and textural aerial photograph features in multi-source forest inventory. Remote Sensing of Environment 94 (2), 256–268.

VEKERDY, Z. − MEIJERINK, A. M. J. (1998): Statistical and analytical study of the propagation of flood-induced groundwater rise in an alluvial aquifer. Journal of Hydrology (205), 112–125.

ZHANG, Y. (2001): Texture-Integrated Classification of Urban Treed Areas in High-Resolution Color-Infrared Imagery. Photogrammetric Engineering & Remote Sensing 67 (12), 1359–1365.

DE GRUYTER OPEN DOI: 10.2478/aslh-2013-0011 Acta Silv. Lign. Hung., Vol. 9 (2013) 135–146

Mapping Forest Regeneration from Terrestrial Laser Scans

Gábor BROLLY* – Géza KIRÁLY – Kornél CZIMBER

Department of Forest Opening Up, Institute of Geomatics and Civil Engineering,
Faculty of Forestry, University of West Hungary, Sopron, Hungary

Abstract – Location, spread, abundance and density of forest regeneration are key factors in understanding forest dynamics as well as in operational management of uneven-aged stands. Simulation of forest growth, silviculture and planning of skid road networks require accurate and objective methods for locating forest regeneration. Terrestrial laser scanning has high potential for tree mapping, however, the development of automatic processing methods has been focused on mature trees so far. This study introduces an automatic procedure to locate individual trees with 3–6 meter height from terrestrial laser scanner data. The method has been validated on three sample quadrates representing different stand structures and it succeeded in detecting 79–90% of trees extracted manually from the point cloud. Out of the investigated stand features, stem density had the strongest impact on the performance, while branching intensity slightly affected the detection rate. The results highlight that terrestrial laser scanning has the ability for the quantitative evaluation of regeneration, providing a prospective tool for surveying forests of contiguous cover.

LIDAR / TLS / forestry / tree detection / regeneration / voxel

Kivonat – Erdei újulat térképezése földi lézeres letapogatás adataiból. Az erdei újulati foltok helye, kiterjedése, borítottsága és törzsszáma kulcsfontosságú tényezők az erdődinamikai folyamatok feltárásában és a többkorú faállományok kezelésében. A fatermési modellek előállítása, az üzemi gyakorlatban végzett erdőművelés valamint erdőfeltárás pontos és objektív módszereket kíván az újulat helyének meghatározására. A földi lézeres letapogatás kiválóan alkalmas törzstérképek előállítására, ám az adatok feldolgozásához szükséges eljárásokat eddig csak szálerdőkre fejlesztettek ki. A tanulmány olyan automatikus eljárást mutat be, ami 3–6 méter magasságú faegyedek lézeres letapogatás adataiból történő azonosítását teszi lehetővé. Három, különböző jellegű újulati foltban létesített mintaterületen a ponthalmaz vizuális interpretációjával azonosított törzsek 79–90%-át sikerült automatikus úton felismerni. Az eljárás teljesítményét a vizsgált állományjellemzők közül elsősorban a törzsszám befolyásolta, míg az ágak mennyiségének hatása elenyésző. Az elért eredmények rámutatnak, hogy a földi lézeres letapogatás alkalmas az újulat mennyiségének felmérésére, így a folyamatos borítású erdők leírásának ígéretes eszköze lehet.

LIDAR / földi lézerszkennelés / erdészet / újulat / faegyed kimutatása / voxel

* Gábor Brolly: gbrolly@emk.nyme.hu; H-9400 SOPRON, Bajcsy-Zs. u. 4.

1 INTRODUCTION

The expansion of nature-based silviculture in Europe has been generating variability in age and complexity in structure of forest stands. In forests of contiguous cover, the development of the regeneration strongly depends on the adjacent mature trees through the allocation of light and nutrients. Operational planning, treatment and administrative control of uneven-aged stands require detailed geospatial information on trees with heterogeneous size. For instance, the location of both mature trees and regeneration patches must be taken into consideration at marking trees for cutting or at decision support in forest opening up e.g. planning the fine network of transportation paths.

Moreover, a geospatial database including mature trees and regeneration has apparent value as input for scientific purposes to understand forest growth or to simulate the effects of regeneration cuttings. To locate trees of heterogeneous size, a sensor is needed with (1) effective range to record objects at a distance of at least 30 meter and (2) capacity of identifying fine structures such as juvenile tree stems.

Terrestrial laser scanning (TLS) is an active remote sensing technology holding great promise for supporting forestry applications. TLS data capture results in 3D point cloud of object surfaces that can be processed by visual interpretation (Hopkinson et al. 2004, Watt – Donoghue 2005) or automatic procedures (Aschoff – Spiecker 2004, Bienert et al. 2007). The output involves the map of individual stem locations and the related tree metrics; typically diameter at breast height (DBH) and tree height. The location and estimation accuracies of the derived tree models are in accordance with the requirements of operational forestry, which has been confirmed in studies of various geographic regions over the temperate zone (e.g. Király – Brolly 2007). It is not surprising that most of the investigations concluded that TLS has high potential in supporting ground-based forest inventories (Thies – Spiecker 2004, Pueschel et al. 2013). Moreover, TLS-derived tree attributes can be combined with airborne laser scans to extend the parameter retrieval into larger area (Lindberg et al. 2012).

Algorithms on tree detection and DBH estimation imply that stems can be approximated by a cylinder in a given height interval, therefore their horizontal cross-section has circular shape (Simonse et al. 2003). Usefulness of this assumption on stem geometry has been verified in two and three-dimensional stem mapping approaches (Brolly – Király 2009a). In comparison to mature trees, juvenile ones intercept fewer point measurements at a constant distance from the scanner because they cover smaller area. In addition, point measurements are frequently scattered on the rough surface of stems. Since the amount of stem surface points is low and their pattern introduces high degree of irregularity, the existing tree mapping methods have difficulties in detecting juvenile trees. However, the high sampling density of TLS allows for the automatic detection of thin linear features such as twigs suggesting the possibility to detect juvenile trees from the point cloud. For instance, Bucksch and Fleck (2011) scanned trees from four directions at a distance of about four meters with angular step width of 0.036 degrees. The automatic extraction of branch structure resulted correlation of up to 0.99 in comparison to manually measured branch diameters.

The amount and spatial distribution of light transmitted through the upper canopy specify the density, composition and growth of the regeneration, therefore crown models are essential for the investigation of the eco-physiological process of trees and the simulation of gap dynamics. In addition to tree positions, 3D structural models including stem and crown can be derived from the point cloud. Crown models account for the originating and end point of the branches as well as their length, diameter and orientation. Branches have been modelled as a set of cylinders in telescopic arrangement whose parameters were specified by minimizing the squared distance of the surface and the corresponding point measurements (Pfeifer et al. 2004). Gorte and Pfeifer (2004) proposed a directed graph structure to reveal branch hierarchy

by storing the preceding and succeeding shoots in each node. Bucksch and Fleck (2011) demonstrated the capacity of high-density TLS data to reconstruct the fine structure of tree crowns including twigs with diameter of 1–2 cm. Danson et al. (2007) developed a procedure for the assessment of directional canopy gap fraction, which showed good agreement with the estimates derived from hemispherical photos. Henning and Radtke (2006) estimated Plant Area Index (PAI) by converting the TLS point cloud in a 3D grid structure and assessing the presence of vegetable matter upon the number of pulses passing through each cell and the number of intercepted pulses. Coté et al. (2009) created architectural model of trees from TLS data to provide basis for the computation of reflectance properties of the canopy in a radiation transfer analysis.

Although TLS has been used extensively to investigate the upper canopy, there has been little effort to take advantage of this technique in studying the structure of understory. Characteristics of the stand structure at the age of 'saplings' (achieving 3–6 meter height) are similarly important from ecologic respect as trees tend to vary in height, form and quality at this age thus the competition is especially strong. Mapping and structural reconstruction of juvenile trees based on in-situ TLS data has been still challenging, as present tree detection methods are not suitable for the recognition of small vegetation components in the understory.

This study is focusing on the development of automatic detection of trees with height of 3–6 m from the point cloud to extend the use of TLS over stands of contiguous forest cover and in this way, widen its field of potential applications in forestry. The method presented in this paper has been introduced in a PhD thesis (Brolly 2013).

2 MATERIAL AND METHOD

Juvenile tree mapping has to meet some specific requirements. First, 3D approaches are preferred because the horizontal slices of the point cloud provide few stem surface points for reliable detection. In regrowth patches, considerable amount of data is returned from irrelevant entities, such as branches and foliage surrounding the stems, which must be eliminated by filtering. Filtering of irrelevant data can be regarded as a classification according to 'stem' or 'other vegetation components'. Natural forest regeneration is characterized by high density and heavy branching resulting in data gaps in stem point measurements or even occlusion of trees especially farther from the scanner. Stem detection algorithm must overcome data discontinuity by the aggregation of the corresponding tree fragments.

Considering these expectations, the developed procedure is composed of two modules, i.e. filtering and objects detection addressing the following issues:

1. Conversion of the point cloud into regular 3D data structure
2. Filtering of irrelevant data, including side branches and leaves
3. Reconstruction of stems by the aggregation of stem fragments.

2.1 Sample site

The algorithm was validated on a terrestrial laser scanner point cloud captured in the region of Pilisszentkereszt (N47.722, E18.860), Hungary, in the altitude of 430–500 meters. The multi-layered stand is composed of 55% beech (*Fagus sylvatica*), 23% sessile oak (*Quercus petraea*) and 12% hornbeam (*Carpinus betulus*) over 10.5 ha area. The mean age of trees associated with the dominant and subdominant canopy layers was 100 and 50 years respectively at the data acquisition. The site has been subject to long-term regeneration managed by the Pilisi Parkerdő Zrt according to the Pro Silva directives since 1999, which resulted in 2–10 meter high natural regeneration patches.

Three quadrates of 5 × 5 meters labelled with ‘P1’, ‘P2’ and ‘P3’ were delineated within three distinct regeneration patches. All the sample quadrates are located in a slope of 10° with South-West aspect and characterized by different stem density and branching frequency. Both factors are expected to have influence on tree detection because stem density is related to the degree of occlusion while branches generate irrelevant point measurements being potential error sources.

Stem positions were identified by visual interpretation of the point cloud and they were used as reference trees for the assessment of the automatic stem detection. Stem positions were located at 1.30 meter height above ground level following the manual filtering of stem point measurements. Only the trees with height exceeding two meters were involved in the reference data set. Branching frequency was assessed subjectively for each quadrate during the interpretation. Sample quadrate P1 is considered as the simplest case as stem counts (n_1 = 41 trees) and branching frequency are relatively low here. The quadrate P2 is characterized by the highest stem density (n_2 = 212). Trees (n_3 = 58) within quadrate P3 have wider crown relative to the trees within the two other quadrates. The shrub-layer is of 0.5 meter height with low abundance; therefore, it has little influence on the stem detection.

2.2 Data acquisition

The whole study site was scanned in leaf-less state of the stand by combining the data captured from 38 scanning positions using Riegl LMS-Z 420i instrument on April 2009. The range finding unit of the instrument utilizes near infrared laser with beam divergence of 0.25 mrad (Riegl, 2010). The scanning was conducted at tilted axis of +50° and –30° applying angular stepwidth of 0.07° for horizontal and vertical direction. The point cloud was recorded and georeferenced by the piLine Ltd. The mean 3D error of the georeferencing was 0.05 meter. The digital terrain model (DTM) of the study site as well as the map of mature trees (DBH>10 cm) were created in the course of previous studies (Brolly – Király 2009b). The location of the three sample quadrates and the arrangement of scanning positions are depicted in *Figure 1*.

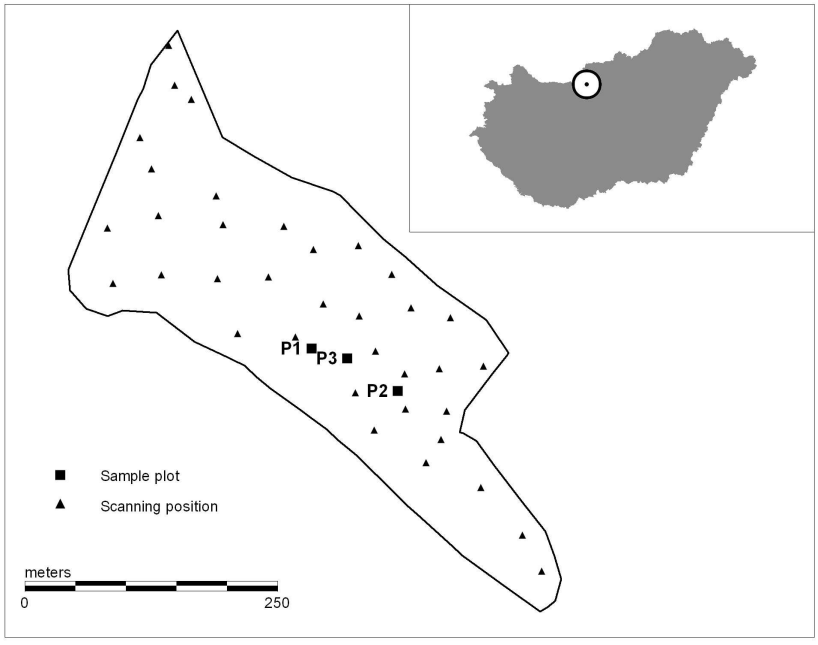

Figure 1. Sample quadrates and scanning positions on the study site

2.3 Data structure

Tree models created in this study are composed of connected cubic elements of equal size also referred to as volumetric elements or briefly *voxels* (Kaufman et al. 1993). The associated voxel space is a kind of grid data structure that can be considered as the extension of raster data structure into the 3D domain. Owing to the regular construction, neighbourhood relations are relatively simple to characterize; a single voxel can share six faces, twelve sides and eight vertices with maximum 26 connected neighbours. Voxel data structure can be used effectively in object detection by adapting the tools of digital image processing so it has appeared optimal for the extraction of juvenile trees.

The georeferenced point cloud was converted into a binary voxel space. Voxels containing at least one point measurements were set to 'filled'. The vertical extent of the voxel space was limited to the elevation between 0.5 and 3.5 meters above the DTM as this interval is dominated by stem surface points.

The grid resolution was specified by visual evaluation of voxel space subsets with different voxel size. Voxel size of 5 cm deemed adequate for all the sample quadrates considering point spacing within the quadrates and the size of trees to be detected.

Adjacent filled voxels constitute connected regions. The smallest region consists of a single voxel, i.e. each voxel belongs to exactly one connected region. Connected regions can be delineated using region growing algorithms, e.g. the Connected Component Labelling (Jain et al. 1995). Connected voxel regions can be translated to *voxel objects* by creating a spatial database that allows identification and access of the unique regions. Voxel objects can be characterized by attributes concerning their geometry and neighbourhood relations. Juvenile trees are usually represented by multiple voxel objects due to the obscuring effects of neighbouring stems and the resulting data gaps. In order to assess the stem number and locate individual tree positions, the corresponding voxel objects must be aggregated. The set of coherent voxel objects can be regarded as one *disconnected voxel object*, representing a complete tree model composed of isolated tree fragments.

2.4 Filtering

Juvenile tree stems can be visually perceived as linear patterns surrounded by irregularly distributed data with altering density originating from branches and dry leaves. In juvenile age, stems and crowns are not separated into distinct vertical zones because the natural pruning has just begun. The crown and lateral branches of juvenile trees generate considerable amount of laser returns. These data are irrelevant for tree mapping; furthermore, they induce false detections. To reduce irrelevant data, a local filtering was developed.

The structuring element used in the filtering defines a 3D region of space around its central voxel. The filtering value is defined as the counts of filled voxels within the defined region. The shape of the structuring element must ensure high filtering values for vertically elongated features. To design appropriate structural element, the following guidelines should be taken into account: (1) The filtering is anisotropic in vertical direction hence the structuring element must be elongated along its vertical axis. (2) The filtering has no preference in horizontal direction so the structuring element is radially symmetric. (3) The filtering must be tolerant of vertical direction because of leaning stems thus the size of the structuring element widens out around the central voxel. These considerations lead to the structure illustrated in *Figure 2*.

The filtering value is computed for each filled voxel. Voxels with filtering value below a predefined threshold are assumed to be vegetation components apart from stems so they can be removed from the data set. The parameters of the filtering applied in this study were the following: radius = 5, height = 11, threshold of filtering value $\geq$ 5. (Dimensions refer to spacing between voxel midpoints.)

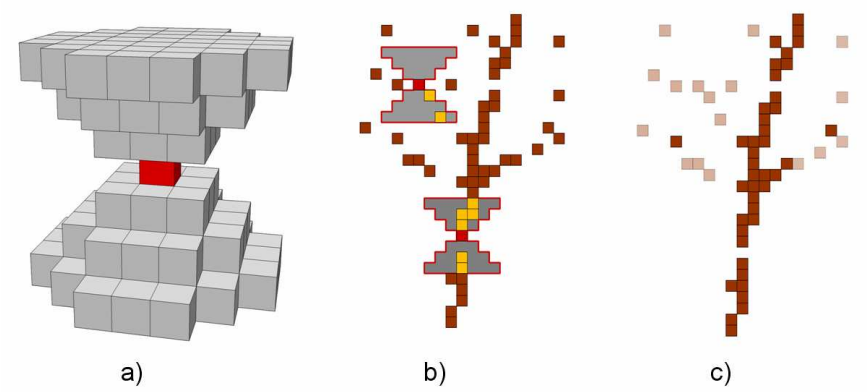

Figure 2. Filtering of irrelevant data. a) Structuring element with radius of three voxels and height of six voxels, (b-c) the concept of the operation

2.5 Reconstruction of stems from fragments

Adjacent voxels in any of the 26 directions are organized into objects by Connected Component Labelling algorithm. Stems are usually composed of multiple objects due to data discontinuity resulting from the obscuring effects of neighbouring trees. Voxel objects representing stem fragments are the basic elements of the subsequent reconstruction procedure. It is practical to generalize the objects to one-voxel-thin *vertical axis* representing the horizontal dimension and orientation of the fragments. *Vertical axis* of a contiguous object is defined as the set of connected voxels with solely upper or lower adjacency (lateral adjacency is forbidden). In this way, the voxel count of a vertical axis is the same as the vertical extent of the object. However, since diagonal adjacency is also allowed, its shape is not necessarily vertical. Vertical axes are extracted by finding the shortest path between the lowest and the highest voxel of the objects. To do so, objects are represented as graphs where the vertices correspond to voxel positions and the edges denote adjacency relations. The shortest path within the resulting graph is obtained by using Dijkstra's algorithm (Cormen et al. 1990). Objects in which no path without lateral adjacency between the highest and lowest voxel exists, are considered atypical for representing young trees. In this case, the region remains in the voxel space but it is excluded from the subsequent processing so it cannot be used in stem reconstruction.

Voxel objects (i.e. vertical axes) represent fragments of either stems or branches; however, they cannot be distinguished based on their shape properties. In the next step, objects that belong to each other are aggregated into disconnected voxel objects representing complete trees. High number of combinations among the objects is possible, so a rule set is needed which favours to the aggregation of stem fragments and skip the branches. Three assumptions have been formulated concerning the shape of stems. (1) Stems are vertically extensive features. (2) The shape of stems is approximately straight. (3) Overlying fragments are vertically close to each other; data gaps separating them are short.

Considering these theories, three variables have been introduced to reveal the spatial relationship of any two fragments within the voxel space. Knowing the coordinates of the voxels constituting the vertical axes, the Euclidian distance between the end voxels as well as the path length between them is computed as input. The three variables stand for the extent (E), shape (S) and gap distance (G) of the resulting disconnected vertical axis. Detailed derivation of the formulae can be found in Brolly (2013). Each of the variables is normalized into the interval of [0, 1] with the theoretically maximum return value of the corresponding function. The degree of conformity of the disconnected vertical axis to the hypothetical stem shape is quantified using the aggregation factor A, which is yielded as the product of the three variables:

$$A = E \cdot S \cdot G$$

Computation of *A* can be extended over the aggregation of disconnected vertical axes so a stem can consist of any number of fragments.

The algorithm initiates by the computation of *A* for any possible object pairs. The aggregation takes place in the order of descending value of *A*, so the assignment resulting in highest degree of conformity to the assumed stem shape is realized first (*Figure 3*). Following each aggregation, the values of *A* with respect to its neighbouring objects are recomputed. As vertical axes contain only vertical or diagonal adjacency, the size of any object (regardless its continuity) is limited to the vertical extent of the voxel space. The aggregation routine is being iterated until the threshold of 0.01 on the aggregation value of potential object pairs is exceeded. This threshold prevents the aggregation of distant fragments that probably belong to different trees. The majority of the resulting disconnected objects represent stem fragments although some of them constitute branches or meaningless groups of voxels arranged accidentally in linear pattern. Tree stems are assumed to be the largest vertical features within regrowth patches, so voxel counts of disconnected objects can be used to distinguish stems from other vegetation fragments. The optimal threshold of 20 voxels was specified by visual evaluation of the classification in the three sample quadrates. Lower thresholds resulted in misclassified branches, while higher ones lead to omission of stems.

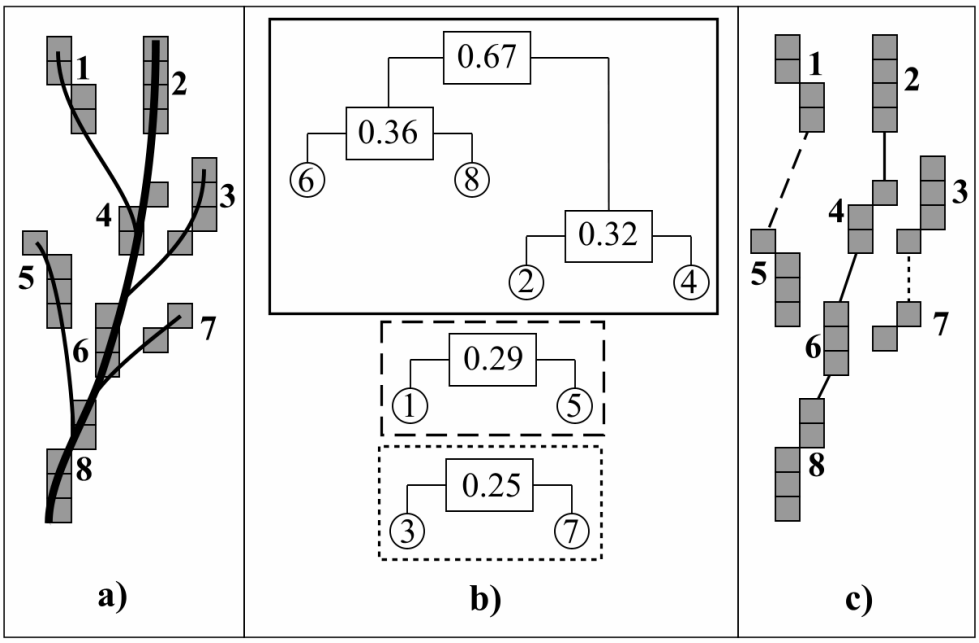

Figure 3. Aggregation of tree fragments. a) Components represented as voxel objects labelled by 1–8, b) Assignment according to the maximum of aggregation factor, c) Resulting disconnected objects composed of fragments (1, 5); (2, 4, 6, 8) and (3, 7)

3 RESULTS AND DISCUSSION

3.1 Filtering

Filtering is considered efficient if surface points of irrelevant vegetation are reduced but stem point measurements are preserved. The proportion of eliminated points indicates filtering intensity, while the retained stem surface points denote filtering reliability. Filtering is a pre-processing step of tree mapping, so its actual value emerges indirectly in the results of stem detection.

The performance of anisotropic filtering in sample quadrates P1, P2 and P3 is given in *Table 1*. The majority of the total voxels has been eliminated from quadrates P1 and P3. The relative low filtering intensity in quadrate P2 is explained with high stem density resulting in elevated number of stem voxels. Although at P3, where the stem density is 34% higher relative to that of P1, the filtering intensity is only slightly different. Higher voxel counts per individuals in P3 indicate larger crown size and / or higher degree of branching frequency, which has been only partially removed by the filtering.

The proposed anisotropic filtering is adequate to remove irrelevant data arranged in random pattern *(Figure 4)* preserving stems even if their main orientation is inclined. According to this tolerance in orientation, acute-angled branches cannot be removed by this filtering method.

Table 1. The effect of the filtering on data amount within the sample quadrates

Quadrate	Tree counts	Voxel counts		Voxel counts / tree	
		Original	Removed [%]	Original	Preserved
P1	41	11806	58.0	228	121
P2	212	38371	36.8	181	114
P3	58	22020	58.8	380	156

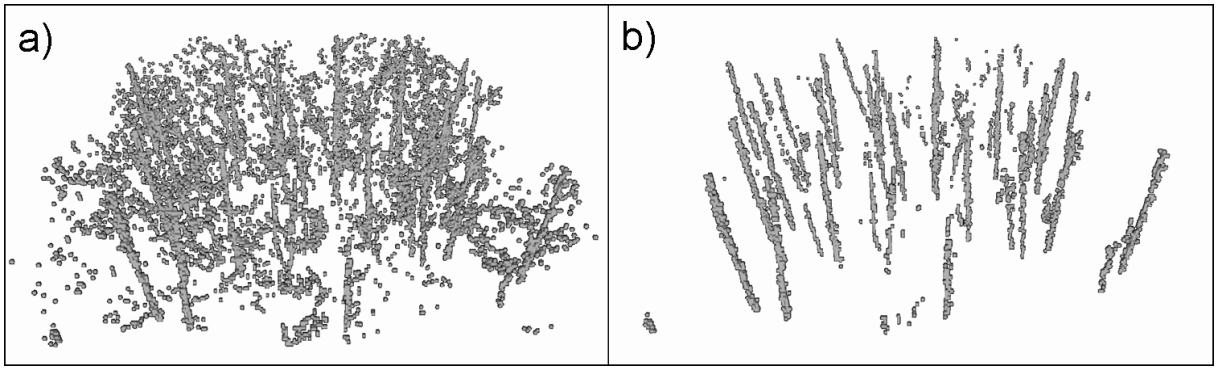

Figure 4. a) Perspective view of the voxel space generated from the total measurement data of sample quadrate P1. b) The result of filtering

3.2 Tree mapping

The tree detection algorithm provides tree positions in a given reference height and the vertical axis of stems. Knowing tree positions, the boundary of regrowth patches can be delineated and stem density within the patches can be estimated directly.

The validation of extracted tree positions for the sample quadrates are given in *Table 2*. Correct detections refer to extracted stem positions with matching reference trees within a positional tolerance of 10 cm. The matching must be unambiguous, i.e. exactly one reference tree can be assigned to a given model position and vice versa. Omissions are undetected trees, while misclassifications are false detections. Omission rate is normalized by the total number of reference trees, thus it complements detection rate to 100%. Misclassification rate is proportional to the number of correct detections.

The highest detection rate was achieved in quadrate P1, where both stem density and branching frequency are moderate. The highest omission rate as well as the highest misclassification rate was found in quadrate P2 where the stem density is the highest. Stem density appears to have the main impact on the overall performance of stem detection.

Although stem density in P2 is over three times greater than in the other two quadrates, the corresponding reduction in detection rate is relative low. Due to the high branching frequency in P3, the filtering was less effective so the remaining tree fragments show high diversity in shape. Detection rate of 87.9% only slightly underperforms that of achieved in quadrate P1 (90.2%), implying that branching frequency has minor relevance on stem detection. This can be traced back to the generalization of voxel regions to vertical axes, as the latter represent the branch-free subset of stem fragments. Generalization of objects to their vertical axis can be regarded as a kind of filtering as well that highlights the main direction of the objects and eliminates the remaining parts irrespective of the degree of structural complexity.

Table 2. Results of the automatic tree detection

Sample quadrate	P1	P2	P3
Reference trees	41	212	58
Correct [%]	90.2	79.3	87.9
Omission [%]	9.8	20.7	12.1
Misclassification [%]	9.8	25.7	10.5

3.3 Modelling

The reconstructed stems are illustrated in *Figure 5.* The individuals are represented in the voxel space by their generalized vertical axes. Due to data discontinuity, the vertical axes are composed fragments resulting in disconnected models. This concept enables to reconstruct standing juvenile trees including the slightly inclined ones.

Tree models at the three sample quadrates differ in structural properties, which are attributed to the distinct stand characteristics *(Table 3).* Although tree density is considerably different in sample quadrates P1 and P2, the fragmentation degree (i.e. the number of objects having been connected for each detected stem) is almost the same. Undetected stems in P2 are assumed to be fragmented more so that the resulting aggregated objects are too small and they cannot be classified as stems.

Detection rate shows close agreement with mean voxel counts composing the vertical axes. There is no difference in height among the tree models because the vertical extent of the voxel spaces is limited to the stem region, which is equal for the three sample areas. So the reason for the variation in voxel counts of vertical axes is not the diversity in height but the ratio in size of fragments and data gaps. High stem density in P2 is assumed to result smaller fragments separated by larger data gaps. Vertical axes composed of fewer voxels explains the higher omission rate.

One could expect that the heavy branching in P3 generate higher degree of occlusion consequently higher degree of fragmentation. As the mean object counts is the lowest in this quadrate, it seems the leaf-less lateral branches are too thin to cause data discontinuity at the applied voxel resolution thus branching had small impact on stem detection.

Table 3. Fragmentation degree of tree models

Sample quadrate	P1	P2	P3
Mean object counts / tree	3.8	3.8	2.9
Maximum object counts / tree	9	9	8
Mean voxel counts (vertical axis) / tree	45.4	38.8	47.7

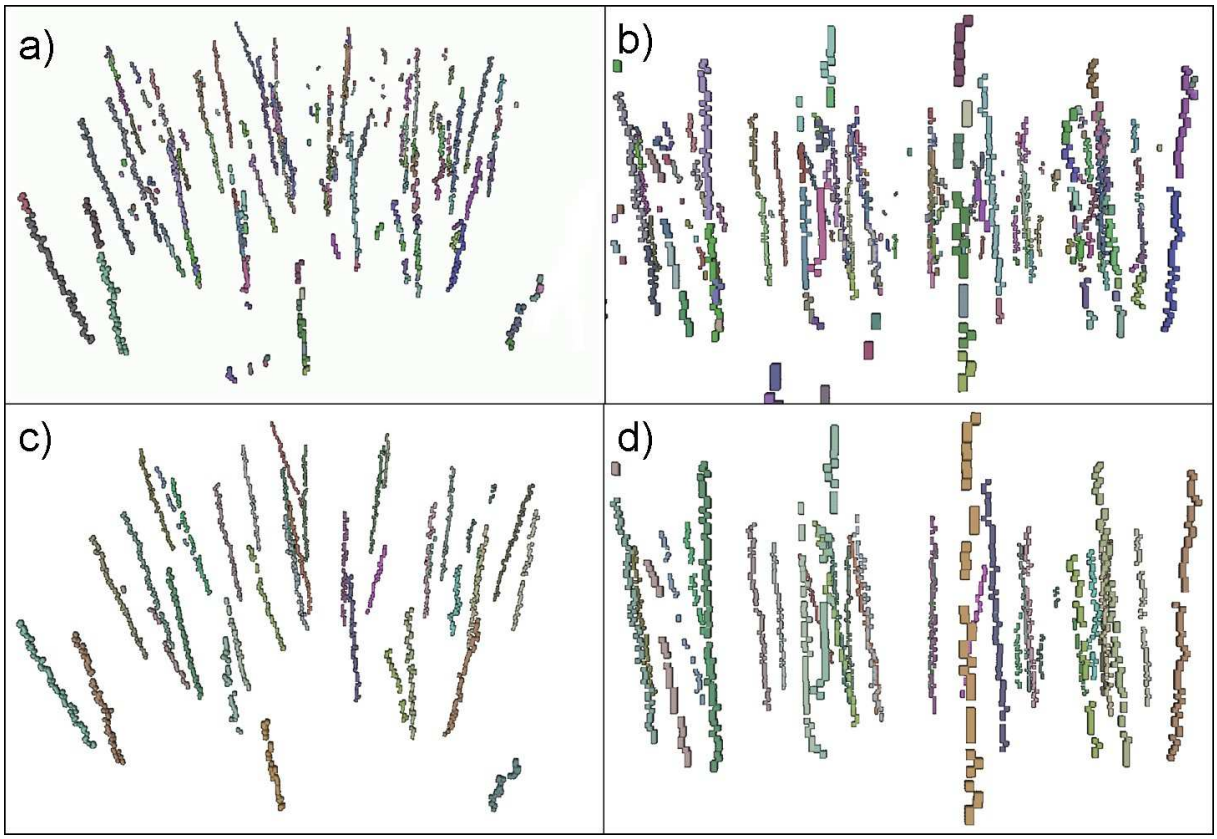

Figure 5. Reconstruction of juvenile tree stems. Fragments are distinct objects without thematic coherence indicated by different colours. a) Perspective view of the fragments over the sample quadrate P1, b) front view of a magnified subset. Following the aggregation, the corresponding fragments constitute stem models represented by identical colours. c) Perspective view of the disconnected stem models in sample quadrate P1, d) front view of a magnified subset

The overall performance of tree mapping and modelling depends on the method used for the calculation of shape properties and on the rule of object aggregation. The advantage of the presented stem detecting algorithm is that only two parameters (threshold on the aggregation factor and threshold on the voxel counts) are needed to control the aggregation of stem fragments and to classify disconnected voxel objects. It is assumed that the optimal value of these two parameters can be found iteratively by refinement either of the parameters and checking the result. A prospective way for developing the aggregation rule has been suggested where each object is represented by a cylinder along its axis and the pair-wise overlaps between the cylinders are checked. It is assumed that the using of overlapping cylinders would especially be powerful if they were representing the variation in diameter, as two stem fragments are more likely to be coherent if their diameter is similar. Since the algorithm does not take diameter in account at present stage, this is a potential way of development. However, measuring diameters of juvenile trees requires voxel size of approximately one centimetre, which is five-times smaller than what was used in this study.

4 CONCLUSION

The proposed algorithm allows for mapping of juvenile trees in regeneration patches with comparable detection rate achieved by recent automatic methods applied at mapping of mature trees. This highlights the potential of high-resolution TLS data to characterise understory vegetation.

To detect juvenile trees with fine structure, three-dimensional data structure is suggested. In contrast, there is a wide range of methods for mapping mature trees by various, computationally less demanding two-dimensional approaches. Detection of juvenile stems requires considerably high data density. Spacing of laser point measurements successively decreases afar from the scanner, putting limitation to the effective detection range surrounding a single scanning position. For operational mapping of uneven aged stands by TLS, a multi-level approach seems to be practical, where mature trees are extracted by using two-dimensional methods followed by the detection of juvenile trees within regeneration patches. Regeneration patches could be delineated using interpretation of the density map of the TLS point cloud within the height interval of 1–4 meters above the DTM. Limitation in mapping range from a single scanning has economic issue at practical surveying of large areas through the increased number of station set-ups; therefore, the proposed method is advisable rather for plot-based sampling of regeneration. Despite the effective filtering of point measurements being relevant for tree mapping purpose, the extraction of seedlings smaller than a few meters is still challenging because of their similarity in structure to shrubs and herbal vegetation. The proposed algorithm was designed to detect and reconstruct broadleaved stems in leaf-less state. Leaf-less state is highly recommended for scanning regeneration to minimize obscuring effects from leaves, however, it hinder the classification of tree species even using full-waveform information. As the geometric properties of conifers considerably different, the mapping of conifer regeneration needs further investigations.

Acknowledgement: The data acquisition was financed by the Pilisi Parkerdő Co., which is highly appreciated. The authors thank the anonymous reviewers whose valuable comments and recommendations helped to improve the quality of this manuscript.

REFERENCES

ASCHOFF, T. – SPIECKER, H. (2004): Algorithms for the automatic detection of trees in laser scanner data. In: Proceedings of the ISPRS working group VIII/2, "Laser-Scanners for forest and Landscape assessment". Freiburg, Germany. 3-6 October 2004. 71-75.

BIENERT, A. – SCHELLER, S. – KEANE, E. – MOHAN, F. – NUGENT, C. (2007): Tree detection and diameter estimations by analysis of forest terrestrial laserscanner point clouds. International Archives of Photogrammetry, Remote Sensing and Spatial Information Sciences 36 (3/W52), 50–55.

BROLLY, G. – KIRÁLY, G. (2009a): Algorithms for stem mapping by means of Terrestrial Laser Scanning. Acta Silvatica et Lignaria Hungarica 5: 119–130.

BROLLY, G. – KIRÁLY, G. (2009b): Lézeres letapogatás feldolgozása erdei környezetben. [Processing laser scans over forested environment.] In: Lakatos, F. – Kui, B. (eds.): Nyugat-magyarországi Egyetem, Erdőmérnöki Kar: Kari Tudományos Konferencia Kiadvány. Sopron. 12 October 2009. 29–34. (in Hungarian)

BROLLY, G. (2013): Locating and parameter retrieval of individual trees from terrestrial laser scanner data. Ph.D. dissertation, University of West Hungary, Sopron, Hungary, 104 p. Online: http://ilex.efe.hu/PhD/emk/brollygabor/disszertacio.pdf

BUCKSCH, A. – FLECK, S. (2011): Automated detection of branch dimensions in woody skeletons of fruit tree canopies. Photogrammetric Engineering and Remote Sensing 77 (3): 229–240.

CORMEN, T. H. – LEISERSON, C.F. – RIVEST, R.L. (1990): Algoritmusok. [Algorithms] Műszaki Könyvkiadó, Budapest. 884 p. (in Hungarian)

COTE, J.F. – WIDLOWSKI, J.L. – FOURNIER, R.A. – VERSTRAETE, M.M. (2009): The structural and radiative consistency of three-dimensional tree reconstructions from terrestrial lidar. Remote Sensing of Environment 113: 1067–1081.

DANSON, F.M. – HETHERINGTON, D. – MORSDORF, F. – KOETZ, B. – ALLGÖWER, B. (2007): Forest Canopy Gap Fraction From Terrestrial Laser Scanning. IEEE Geoscience and remote sensing letters 4 (1): 157–161.

GORTE, B. – PFEIFER, N. (2004): Structuring laser-scanned trees using 3d mathematical morphology. ISPRS- International Archives of Photogrammetry, Remote Sensing and Spatial Information Sciences 35 (Part B): 39–45.

HENNING, J.G. – RADTKE, P.J. (2006): Ground-based laser imaging for assessing three-dimensional forest canopy structure. Photogrammetric Engineering and Remote Sensing 72 (12): 1349–1358.

HOPKINSON, C. – CHASMER, L. – YOUNG-POW, C. – TREITZ, P. (2004): Assessing forest metrics with a ground-based scanning LIDAR. Canadian Journal of Forest Research. 34: 573–583.

JAIN, R. – KASTURI, R. – SCHUNCK, B.G. (1995): Machine Vision. McGraw-Hill, Inc., ISBN 0-07-032018-7; 549 p.

KAUFMAN, A. – COHEN, D. – YAGEL, R. (1993): Volume graphics. IEEE Computer 26 (7): 51–64.

KIRÁLY, G. – BROLLY, G. (2007): Tree height estimation methods for terrestrial laser scanning in a forest reserve. International Archives of Photogrammetry, Remote Sensing and Spatial Information Sciences. 36 (3/W52): 211–215.

LINDBERG, E. – HOLMGREN, J. – OLOFSSON, K. – OLSSON, H. (2012): Estimation of stem attributes using a combination of terrestrial and airborne laser scanning. European Journal of Forest Research 131 (6): 1917–1931.

PFEIFER, N. – GORTE, B. – WINTERHALDER, D. (2004): Automatic reconstruction of single trees from terrestrial laser scanner data. ISPRS- International Archives of Photogrammetry, Remote Sensing and Spatial Information Sciences 35 (Part B): 114–119.

PRO SILVA (2012): Pro Silva Principles. Pro Silva Europe. 69 p. Online: www.prosilvaeurope.org

PUESCHEL, P. – NEWNHAM, G. – ROCK, G. – UDELHOVEN, T. – WERNER W. – HILL, J. (2013): The influence of scan mode and circle fitting on tree stem detection, stem diameter and volume extraction from terrestrial laser scans. ISPRS Journal of Photogrammetry and Remote Sensing 77 (1): 44–56.

RIEGL (2010): Data sheet LMS-Z420i, 03/05/2010. Riegl Laser Measurement System GmbH, Horn, Austria. Online: www.riegl.com

SIMONSE, M. – ASCHOFF, T. – SPIECKER, H. – THIES, M. (2003): Automatic determination of forest inventory parameters using terrestrial laser scanning. In: Proceedings of the ScandLaser Scientific Workshop on Airborne Laser Scanning of Forests. Umea, Sweden. 2–4 September, 2003. 271–257.

THIES, M. – SPIECKER, H. (2004): Evaluation and future prospects of terrestrial laser scanning for standardized forest inventories. In: Proceedings of the ISPRS working group VIII/2, "Laser-Scanners for forest and Landscape assessment". Freiburg, Germany. 3–6 October 2004. 192–198.

WATT, P.J. – DONOGHUE, D.N.M. (2005): Measuring forest structure with terrestrial laser scanning. International Journal of Remote Sensing 26 (7): 1437–1446.

DE GRUYTER OPEN DOI: 10.2478/aslh-2013-0012 Acta Silv. Lign. Hung., Vol. 9 (2013) 147–159

Depth and Areal Distribution of Cs-137 in the Soil of a Small Water Catchment in the Sopron Mountains

Ervin KISS* – Péter VOLFORD

OSJER Laboratory, Institute of Wood and Paper Technology, University of West Hungary, Sopron, Hungary

Abstract – The study presents the depth and areal distribution of Cs-137 activity concentration in the forest soils of Farkas Trench, a small water catchment in the Sopron Mountains, in 2001 and 2010, moreover the possible reason of the alteration in activity concentration. The Cs-137 activity values were measured in 30 plots in 2001, and in 5 in 2010. In 2001, the depth distribution of Cs-137 activity concentration in the measurement plots was shaped in accordance with a decreasing exponential function. It appeared in the 2010 data that the highest Cs-137 activity concentration had shifted lower from the top layers, and the depth distribution changed along an increasing or a stagnating function until a depth of 4 to 6 cm (in function of slope inclination), then along a decreasing function. In 2001, activity concentration in the surface soil layers (0 – 2 cm) altered between 15 and 609 Bq/kg, whereas in 2010 between 26 and 72 Bq/kg. A correlation was found between activity concentration in the surface soil layer and slope inclination. It was concluded that one of the main reasons for differences in distribution of Cs-137 activity concentration was the differing extent of soil movement.

Cs-137 distribution / Cs-137 activity concentration / forest soil

Kivonat – Cs-137 mélységi és területi eloszlása a Soproni hegyvidék egy kis vízgyűjtőjének talajában. A tanulmány bemutatja a Farkas-árok, a Soproni-hegység egy kis vízgyűjtője, erdei talajában a Cs-137 aktivitáskoncentráció mélységi és területi eloszlását 2001 és 2010-ben, valamint az aktivitáskoncentráció változás lehetséges okát. A Cs-137 aktivitás értékek 2001-ben 30, 2010-ben 5 helyen lettek mérve. 2001-ben a mérési helyek Cs-137 aktivitáskoncentrációjának mélységi eloszlása a talajban csökkenő exponenciális függvény szerint alakult. A 2010-es mérések adataiban látható volt, hogy a legmagasabb Cs-137 aktivitáskoncentráció a felső rétegekből lejjebb tolódott, és a mélységi eloszlás 4–6 cm mélységig egy növekvő, vagy stagnáló függvény (lejtőszög függvényében), majd egy csökkenő függvény szerint változott. 2001-ben a felszíni talajrétegek (0–2 cm) aktivitáskoncentrációja a mintavételi pontokban 15 és 609 Bq/kg között, míg 2010-ben 26 és 72 Bq/kg között változott. A felszíni talajréteg aktivitáskoncentrációja és a lejtőszög között összefüggést lehetett kimutatni. A területi eloszlás lejtőszög függéséből azt a következtetést vontuk le, hogy a Cs-137 aktivitáskoncentráció területi eltérésének egyik fő oka az eltérő mértékű talajvándorlás volt.

Cs-137 eloszlás / Cs-137 aktivitáskoncentráció / erdei talaj

* Corresponding author: ervink@freemail.hu; H-9400 SOPRON, Bajcsy-Zsilinszky u. 4.

1 INTRODUCTION

Fallout of caesium-137 (Cs-137) is associated worldwide with the nuclear weapon tests performed in the 1950s and 1960s (Du et al. 1998). In addition, the 1986 Chernobyl reactor accident has also made its effect felt in our home country, as a result of which the Cs-137 activity concentration which had originated from earlier atmospheric nuclear weapon tests increased in the soil. Cs-137 arrived at the surface by dry and wet deposition, then, due to natural processes in the environment, a significant portion of it migrated into the soil. Its depth and areal distribution was set by how it was bound in the soil. Since Cs-137 is strongly bound to clay minerals and to the organic matter in the soil, this radioisotope can even be used to follow soil movement (Du et al. 1998).

In general, the depth distribution of Cs-137 in undisturbed soils shows an exponential decrement in function of soil depth. Even though the Cs-137 concentrations of undisturbed sites show great spatial variation, still the depth distribution will chiefly depend on soil type and on soil structure, on the differing distribution of clay minerals and of organic matter (Du et al. 1998). Walling and Quine (1992) surveyed the depth distribution of Cs-137 in several soil species in the United Kingdom. They concluded that activity concentration strongly decreases by depth, more than 75 per cent of the total activity is to be found in the uppermost 15 cm layer, and the total Cs-137 accumulation of the soil strictly correlates with the total fallout amount. Berg and Shuman (1995) carried out studies in coniferous forests, and the results of their 3D model created on the basis of measurements showed that in any equilibrium state, up to 85 per cent of the active radiocaesium is found in the soil. Furthermore, Cs-137 migration, according to the predictions, is rather slow, its most essential part taking place within the uppermost 10 cm of the soil profile.

The objective set in this study was to study the depth and areal distribution of Cs-137 activity concentrations in undisturbed forest soils in a small water catchment in the Sopron Mountains, and to serve with data about Cs-137 accumulation to serve as a basis for surveys to come, for estimating soil movement.

2 MATERIAL AND METHODS

2.1 Study area

The examination was carried out in one of the small water catchments of the Sopron Mountain Range, in the Farkas Trench *(Figure 1)*.

The Farkas Trench (0.63 sq. km) is a southwest-northeast oriented trench along a branch of Rák Brook. The altitude of the outlet is 401 m above the sea level and the highest point of the catchment reaches 545 m. Terrestrial clastic rocks deposited at different siltation conditions (conglomerate, gravel, sand, silt) on crystalline shale bedrock. Average slope of Farkas Creek exceeds 21%, valley-bottom has 7.7% inclination (Csáfordi et al. 2010 p. 4). On the basis of fluvial sediment, podzolic brown forest soils, highly acidic non-podzolic brown forest soils and lessivated brown forest soils have evolved (Gribovszki et al. 2006 p. 85). At the lowermost third of the trench, even landslides can be traced. Mediterranean, continental and also oceanic effects can be sensed in the local climate. Long-time average precipitation of the area is 917 mm, but as an example, in the 2001 examination year there was only 607 mm (Gribovszki et al. 2006). Farkas Trench is mostly covered by forests, with deciduous and coniferous vegetation present alike (Csáfordi 2010). The main conifer species is Norway spruce (*Picea abies*), the main deciduous beech (*Fagus sylvatica*). From 2001 on there have been clear cuttings performed at several sites along the trench, which have probably affected precipitation intake and runoff (Gribovszki et al. 2006).

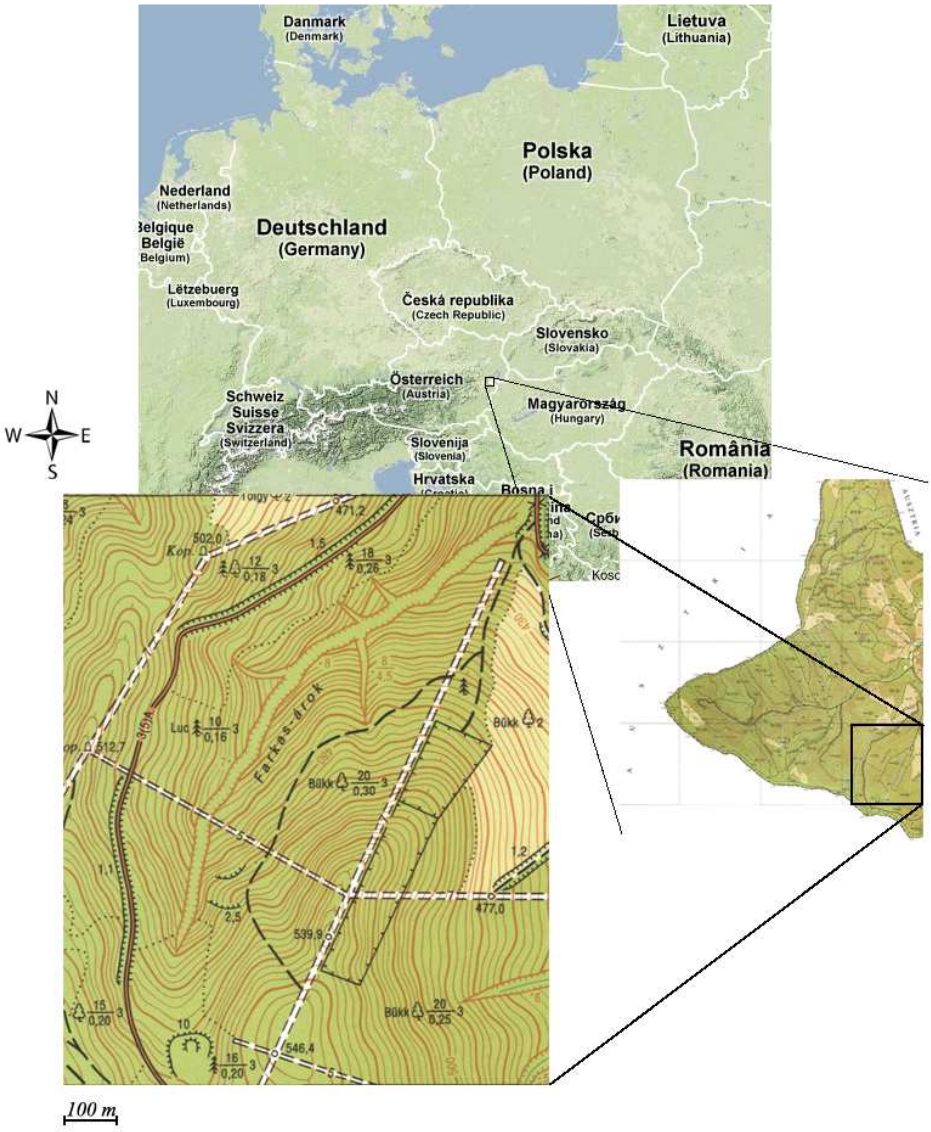

Figure 1. Location of the studied water catchment

2.2 Cs-137 deposition values

Cs-137 accumulated in the examined area originates from two sources. One of them is the fallout originating from nuclear weapon tests, the other one being the Cs-137 amount deposited during the 1986 Chernobyl reactor accident. According to the data in the literature (Pellet 2006), in the examined area the extent of deposition originating from Chernobyl *(Figure 2)* was nearly one magnitude level higher than the activity concentration of nuclear weapon test origin *(Figure 3)* present in the soil at the time of the accident. Thus, the activity values determined during the examination give information primarily about the period which has passed since 1986.

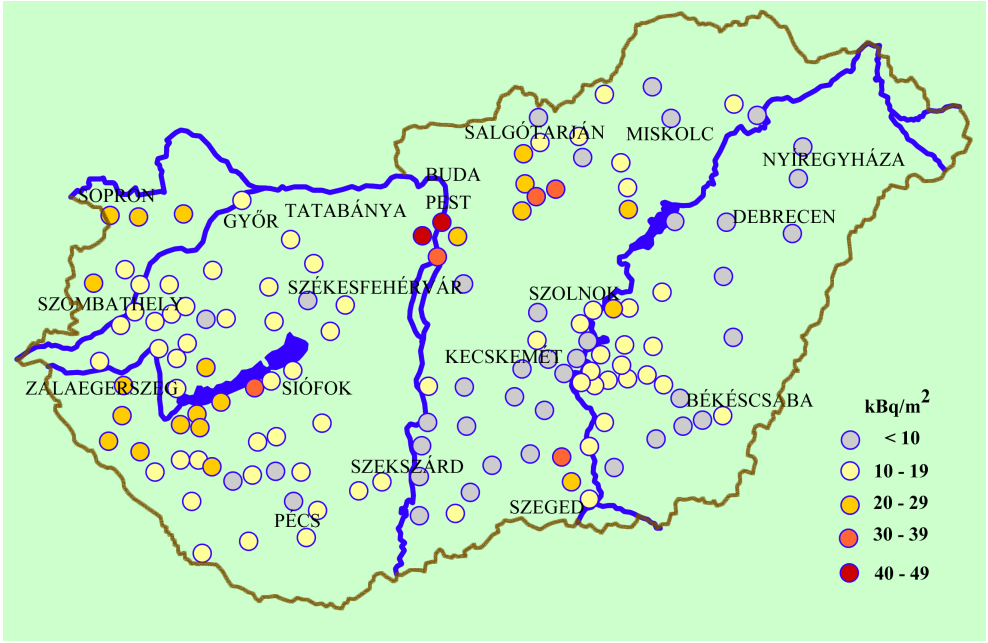

Figure 2. Soil surface Cs-137 pollution in Hungary in 1986, after the Chernobyl accident (Pellet 2006)

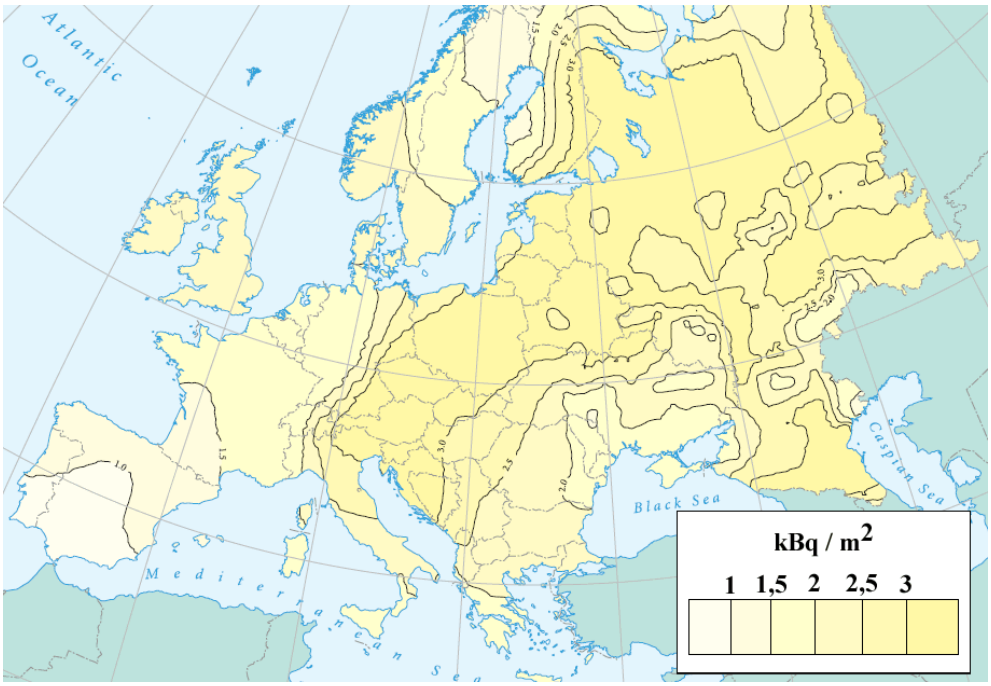

Figure 3. Europe's Cs background pollution before the Chernobyl accident (Pellet 2006)

2.3 Measurement method

When sampling an undisturbed area, acquiring the soil samples without significantly disturbing the area is an important consideration. Sampling device and method have to be such that they either do not disturb or mix up the different layers of the soil, or only to a minimal extent.

Sampling took place within the examined area at 30 plots (numbered points from 1 to 3, and L1/1 to L9/3) in 2001, then at 5 plots (numbered points from L1-2010/0 to L1-2010/4) in 2010 *(Table 1) (Figure 4)*.

Table 1. EOV coordinates of the sampling plots, and their measured slope inclination

Site	EOV(Y) (m)	EOV(X) (m)	Slope (deg.)	Site	EOV(Y) (m)	EOV(X) (m)	Slope (deg.)
1	455493	260122	<4	L5/1	455470	260536	38,8
2	455657	260371	<4	L5/2	455534	260495	17,7
3	455951	260909	<4	L6/1	455428	260415	18,8
L1/1	455899	260926	4,6	L6/2	455472	260398	16,1
L1/2	455905	260910	9,3	L7/1	455371	260333	25,1
L1/3	455911	260899	8,4	L7/2	455312	260336	26,3
L2/1	455891	260950	29,3	L8/1	455392	260329	22,7
L2/2	455890	260977	9,4	L8/2	455429	260318	16,7
L3/1	455874	260903	8,1	L8/3	455469	260311	15,6
L3/2	455880	260888	6,3	L8/4	455521	260295	19,1
L3/3	455886	260862	11,9	L9/1	455375	260267	32,8
L4/1	455727	260796	28,2	L9/2	455417	260230	17,3
L4/2	455736	260791	16,5	L9/3	455435	260207	26,2
L4/3	455745	260743	11,8	L1-2010/1	455932	260943	21,6
L4/4	455762	260720	16,9	L1-2010/2	455939	260948	7,8
L4/5	455765	260680	13	L1-2010/3	455932	260940	13,3
L4/6	455778	260643	15,3	L1-2010/4	455923	260922	9,1
				L1-2010/0	455919	260911	< 4

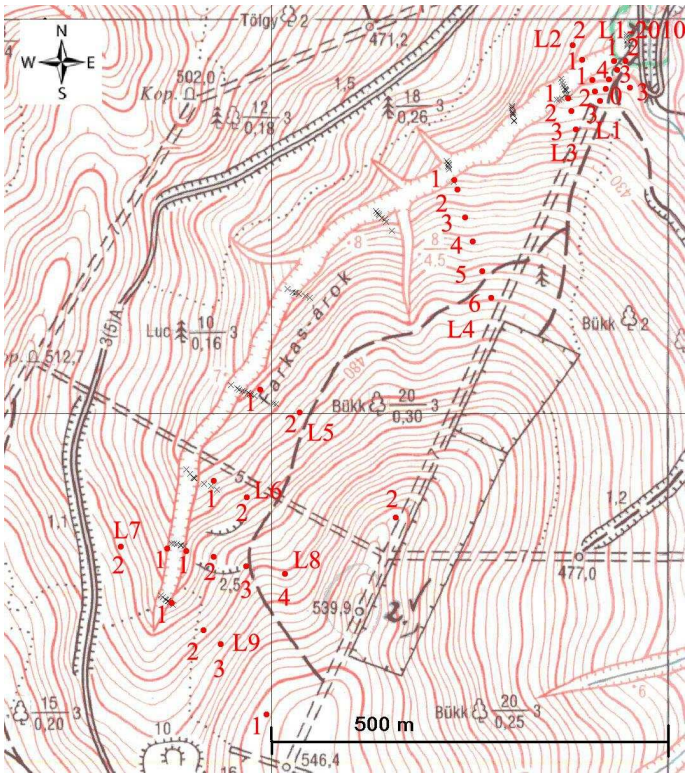

Figure 4. Location of the sampling plots

Sampling was performed using a sampler made of steel plates, down to a depth of 10 to 12 cm, by 2-cm depth intervals. The sampler consisted of a one lateral side opened metal frame (size: 20*25 cm, high: 20 cm) and a horizontal metal plate (frame fitting). In some plots trowel was used to the layers separation instead of the metal plate (due to the roots). Preliminary sampling demonstrated that a significant portion of the Cs-137 amount is found in the uppermost 10-cm layer, hence the sampling depths were adjusted accordingly. In 2001,

at the plots with minor (< 4 degrees) slope inclination at a depth of 10 cm, measured Cs-137 activity concentrations were at least one magnitude level lower than in the surface layer. Samples collected in the area were measured after drying, pulverizing, sieving (< 2 mm). By measuring, 0.5 or 1-liter Marinelli sample dishes were used, the weight of the samples was determined on a certified Precisa 3100D scale. Cs-137 activity of the samples was determined by gamma spectrometry in the OSJER (Hungarian Radiation-Monitoring Detection and Verification System) laboratory at the University of West Hungary. Cs-137 activity was measured using a high-resolution ORTEC HPGe detector (Gem-10185), moreover by a PC-attached multi-channel (8K) ORTEC analyser card. For evaluating the measurements, the ORTEC Maestro software which belongs to the card was used. Measurement duration was 1800 or 3600 s. Channel-energy calibration of the software programme was completed by using Co-60, Cs-137 and Am-241 certified standard sources of known activity.

Activity referring to a given isotope of the sample can be calculated from the area under the net gamma peak (661.62 keV in case of Cs-137) determined using the Maestro programme using the following formula *(Eq. 1)* (Bódizs 1997):

$$A = \frac{N}{\eta_{Ei} \cdot K\gamma_{Ei} \cdot t_m} \tag{1}$$

Where:

A – is activity referring to a given isotope of the sample (Bq).

N – net area of the gamma peak generated by that given isotope (impulse).

$K\gamma_{Ei}$ – the Ei-energy gamma radiation yield by that given isotope, expressing the number of gamma quanta at a certain energy referring to 100 radioactive decaying atomic nuclei.

η_{Ei} – the efficiency value read from the energy-efficiency curve referring to a given geometry of Ei-energy radiation. It expresses how many of all the gamma photons emitted by the radiating source at a certain energy are registered in the full energy peak.

t_m – measurement duration (live time) (s).

Knowing the activity values thus derived one can calculate the activity concentration, A_K, (Bq/kg), of the sample referring to one mass unit (*Eq. 2*), (A – being the activity referring to a certain isotope in the sample (Bq), m – the mass of the sample (kg)):

$$A_K = A / m \tag{2}$$

The activity concentrations can be converted to the inventory (Bq/m^2) according to the following *Eq. (3)* (FANG et al. 2006):

$$CPI = \sum_{i=1}^{n} C_i \times B_i \times D_i \times 10^3 \tag{3}$$

where:

CPI – is Cs-137 point inventory (Bq/m^2),

i – is the No. of soil horizon,

Ci – is Cs-137 activity concentration of the *i*th soil horizon (Bq/kg),

Bi – is bulk density of the *i*th soil horizon (g/cm^3), and

Di – is thickness of the *i*th soil horizon (m).

Even with properly set measurement devices, random statistical errors may occur. *Equation 4*, which describes the time-dependence of radioactive decay, only gives a probability.

$$N_t = N_{t0}e^{-\lambda t} \tag{4}$$

(λ = decay constant, t = time, N_{t0} = number of initial radioactive nuclei)

The simple unweighted average of measured impulse number (N_i) and the empirical standard deviations (s) of measurement points calculated from an average are described by the following formulas (Pátzay 2008):

$$\bar{N} = \frac{\sum_{i=1}^{n} N_i}{n} \tag{5}$$

$$s = \pm\sqrt{\bar{N}} \approx \sqrt{N_i} \tag{6}$$

$$s = \pm\sqrt{\frac{\sum_{i=1}^{n}\left(N_i - \bar{N}\right)^2}{n-1}} \tag{7}$$

With the first standard deviation formula (*Eq. 6*) only the errors arising from the decay, while with the second formula (*Eq. 7*) the errors arising from the decay as well as those arising from measurement device fluctuation, can be estimated. If the standard deviations calculated in these two ways nearly match (difference < 10 %), then the measurement device error is negligible compared to the error arising from decay fluctuation.

3 RESULTS

Vertical distribution of Cs-137 in undisturbed soil (Blagoeva – Zikovsky 1995, Perrin et al. 2006, Porto et al. 2001, Zhiyanski et al. 2008) has been examined in several studies. For this purpose, evenly decreasing two-parameter functions were fitted to the measured values of the profile, by computer (Blagoeva – Zikovsky 1995):

$$C\,(X) = A \times X^{-B} \tag{8}$$

$$C\,(X) = A \times exp(-B \times X) \tag{9}$$

$$C\,(X) = A / (1 + B \times X) \tag{10}$$

where the x is the depth in cm and C the activity concentration in Bq/kg. The best fitting was displayed by the second function (*Eq. 9*).

Based on worldwide published data, Cs-137 concentration distribution by depth in undisturbed soil profiles was classified into three groups (Du et al. 1998). The three types of regression functions are the following:

$Cs = a \times e^{-bz}$ $\quad (a>0, b>0)$

$Cs = a \times (1-(k-z/H)^b) \times (k-z/H)^{b-1}$ $\quad (a>0, b>1 \text{ and } 0<k<=1)$

$Cs = a*(1-z/H)^b$ $\quad (a>0, b>=0)$

where Cs is the concentration of Cs-137 at a given depth (Bq/kg), z represents the given depth in the soil profile (m), a, b and k are coefficients of the used function and H is the thickness in which Cs-137 can be detected.

3.1 Depth distribution of Cs-137 at the sampling plots in 2001

The Cs-137 activity concentration and inventory values of the soil samples acquired at the sampling plots as determined by measurement appear in the following table *(Table 2)*.

Table 2. Cs-137 activity concentration by each soil layer at the sampling plots and Cs-137 inventories of the 1-3 sampling plots

Site	Cs-137 concentration (Bq/kg)					
	Soil depth					
	0 – 2 cm	2 – 4 cm	4 – 6 cm	6 – 8 cm	8 – 10 cm	10 – 12 cm
1	608.8	360.5	150.4	46.8	36.2	
2	449.0	344.6	108.0	27.0	7.1	
3	489.5	250.2	88.8	25.2	15.5	
L1/1	572.1	326.6	199.8	169.2	88.3	
L1/2	438.1	165.8	58.9	34.3	25.1	
L1/3	493.0	208.8	106.8	36.2	19.6	
L2/1	112.4	91.4	39.6	13.7	12.0	
L2/2	255.7	157.2	98.2	43.5	17.5	
L3/1	233.2	248.3	121.1	53.5	23.7	
L3/2	408.9	229.0	103.0	48.5	26.2	
L3/3	368.4	146.5	60.7	11.2	7.0	
L4/1	70.2	62.2	27.9	15.5	10.4	
L4/2	169.2	117.4	38.2	12.5	9.7	
L4/3	156.9	129.4	100.8	42.5	19.4	
L4/4	310.7	135.9	35.4	18.1	10.4	
L4/5	331.0	141.2	27.0	20.2	11.9	
L4/6	310.2	125.8	48.3	20.7	12.4	
L5/1	104.0	107.1	67.5	38.4	18.1	
L5/2	390.6	242.4	161.2	36.4	21.5	
L6/1	155.1	93.6	43.3	26.9	14.2	
L6/2	235.1	253.1	125.1	51.4	16.4	
L7/1	15.5	8.4	3.3	3.6	2.6	
L7/2	158.2	130.6	83.6	38.5	20.1	
L8/1	165.0	131.2	92.2	41.2	21.7	
L8/2	328.9	120.4	48.7	32.0	14.5	
L8/3	397.4	227.4	53.6	19.7	10.1	
L8/4	255.5	160.2	46.4	32.6	13.6	7.5
L9/1	38.8	68.4	35.2	12.4	8.2	
L9/2	221.7	73.2	29.6	7.5	6.0	
L9/3	202.1	103.6	7.9	0.9	2.0	

Site	Cs-137 inventory (Bq/m^2)
1	10569.9
2	9137.0
3	8909.8

The values for some soil profiles from among the values derived are shown in function of soil depth in the following figures as examples. First, 3 sample plots with lesser slope steepness *(Figure 5)*, then, a slope-directed sampling series *(Figure 6)*. On fitting regression functions onto the sampled values it was realised that by the plots with lesser steepness (< 4 degrees) exponential functions provide the best match. As the slope grade grows, this Cs-137 profile alters, too. At the plots which have greater slope inclination, a decrease in Cs-137 activity concentration of the top layers appeared. With the consideration that Cs-137 is strongly bound to soil, this decrease in soil Cs-137 activity suggests soil movement.

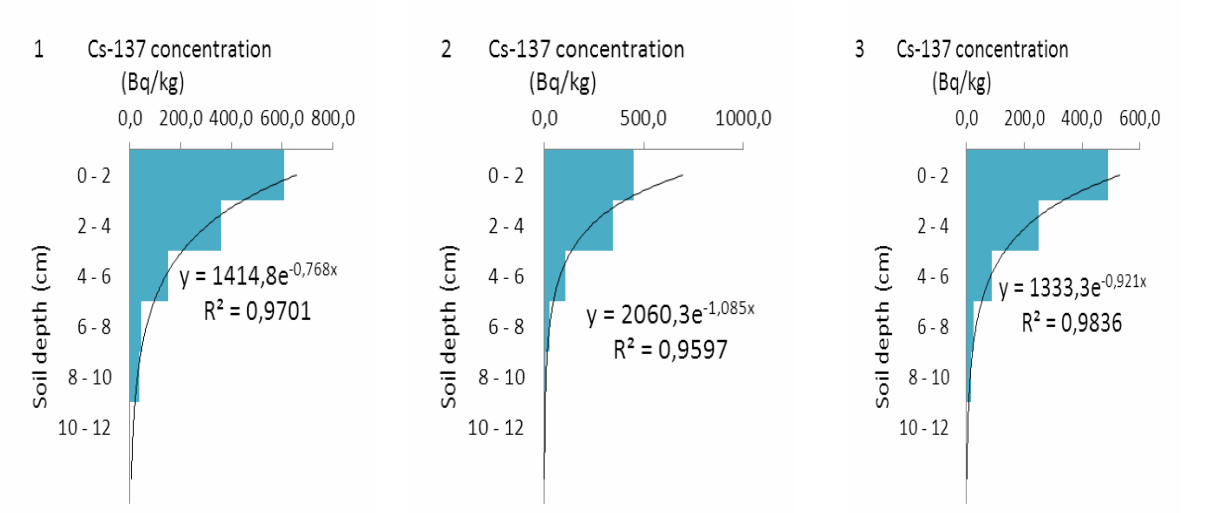

Figure 5. Cs-137 activity concentration distribution by depth in the soil of sampling plots 1 to 3 (slope < 4 degrees)

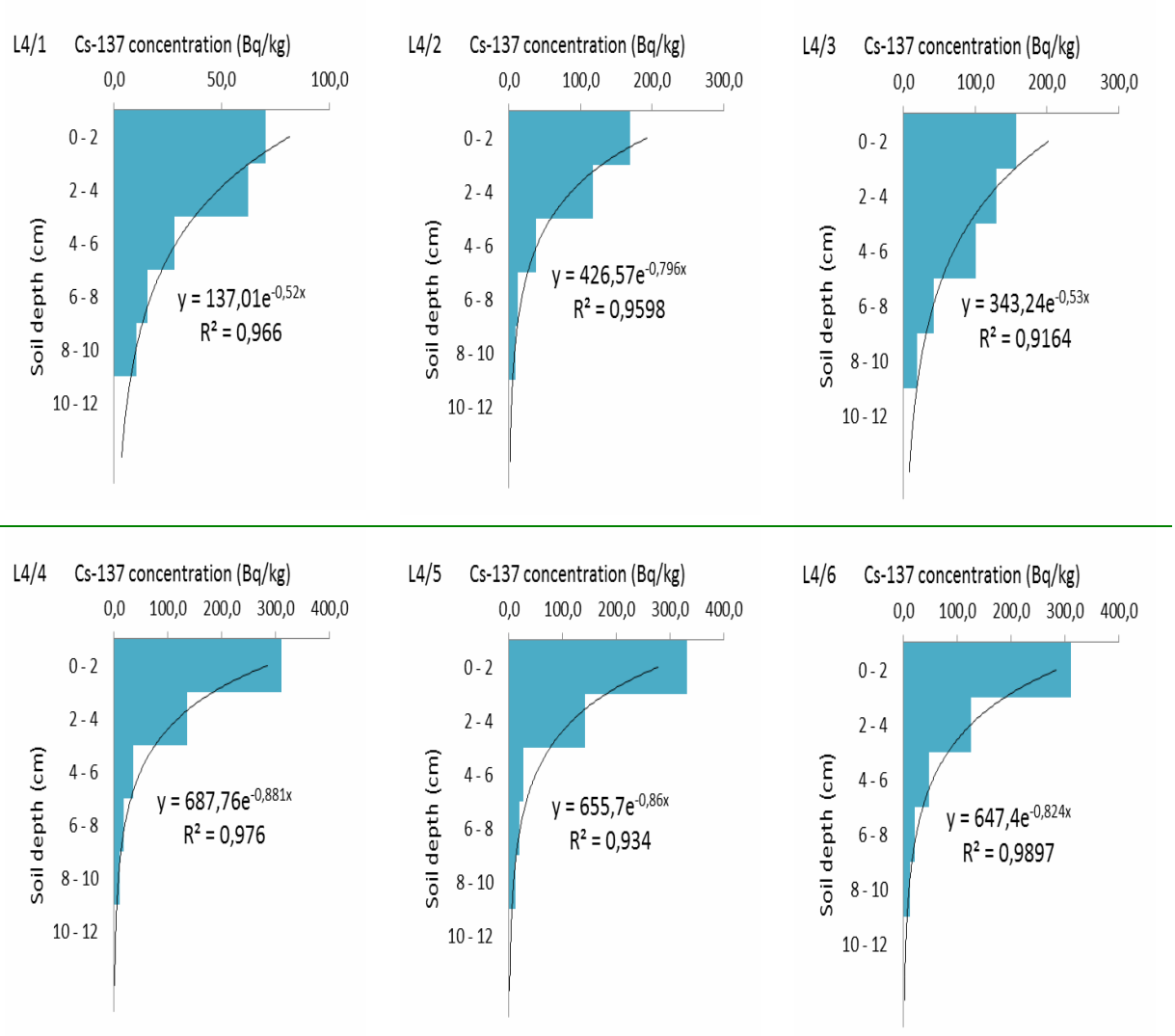

Figure 6. Along a slope (at the L4/1 – L4/6 measurement points) the Cs-137 activity concentration distribution by depth in the soil (slope > 4 degrees)

3.2 Depth distribution of Cs-137 at the sampling plots in 2010

The 2010 repetition of sampling was performed by a smaller number of samples in the lower part of the area. The Cs-137 activity concentration and inventory values determined by measurements of the soil samples taken at the sampling plots appear in *Table 3*.

Table 3. The Cs-137 activity concentrations of the sampling plots in each soil layer and Cs-137 inventory of the L1-2010/0 sampling plot

Site	Cs-137 concentrations (Bq/kg)					
	Soil depth					
	0 – 2 cm	2 – 4 cm	4 – 6 cm	6 – 8 cm	8 – 10 cm	10 – 12 cm
L1-2010/1	26.0	42.0	41.3	29.4	19.8	
L1-2010/2	45.6	69.4	76.0	58.0	29.8	
L1-2010/3	32.6	42.9	59.4	52.8	23.7	
L1-2010/4	29.8	58.9	80.4	47.2	38.2	11.1
L1-2010/0	72.1	62.7	79.4	47.5	33.4	8.9

Site	Cs-137 inventory (Bq/m^2)
L1-2010/0	3887.6

The Cs-137 profile of the slightly sloped sampling plot (< 4 degrees) altered showing stagnating values to a depth of 4 to 6 cm, then exponentially decreasing ones *(Figure 7)*.

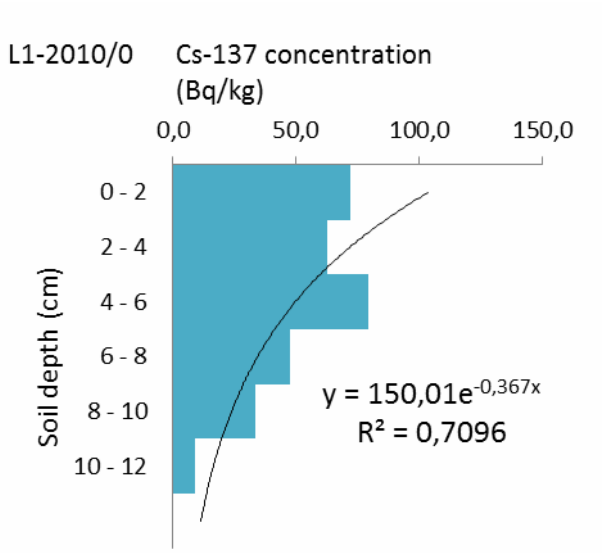

Figure 7. Depth distribution of Cs-137 in the soil at the L1-2010/0 measurement point (slope < 4 degrees)

During the recent period since 2001, at the sampling plot with small slope grade (< 4 degrees) one of the factors shaping the profile besides a slight extent of soil displacement and the natural radioactive decay must have been the vertical migration of Cs-137, as a consequence of which the highest Cs-137 activity concentration shifted to the 4 to 6 cm deep zone. A similar phenomenon was experienced at the sampling plots with greater slope grades, but there, in addition to the aforementioned, also soil movement did shape the surface-close Cs-137 distribution *(Figure 8)* to a great extent.

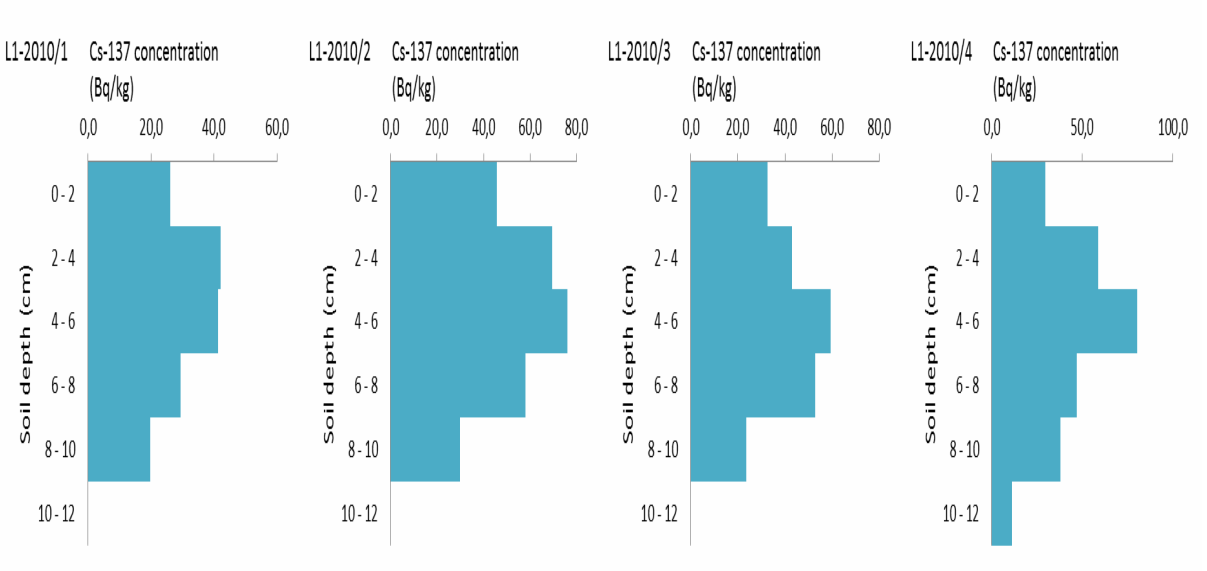

Figure 8. Cs-137 activity concentration depth distribution in the soil at the L1-2010/1 - L1-2010/4 measurement points (slope > 4 degrees)

From this soil profile alteration, one can deduce the vertical speed of movement, which can be estimated based on the samples to be 4 to 6 cm in 9 years (0.44 to 0.66 cm/yr) in the soil of the area. Arapis et al. (1997) estimate this value to be between 0.4 and 1.2 cm/yr. In order to gain better understanding of the presumed phenomenon, further samplings will be needed in the future, through which the presumed Cs-137 relocation can be traced.

3.3 The dependence of Cs-137 activity concentration on slope inclination

On creating a graphic representation of the Cs-137 activity concentration of the surface-close (0 to 2 cm) layer of sampling plots in function of slope inclination it became apparent that there is a connection between Cs-137 activity concentration at the surface and slope inclination. The regression line fitting to the values derived is shown in *Figure 9.* Based on the connection between the data it was concluded that one of the main reasons of differing surface activity values was soil movement (considering that Cs-137 is tightly bound to the organic matter and the clay minerals of soils).

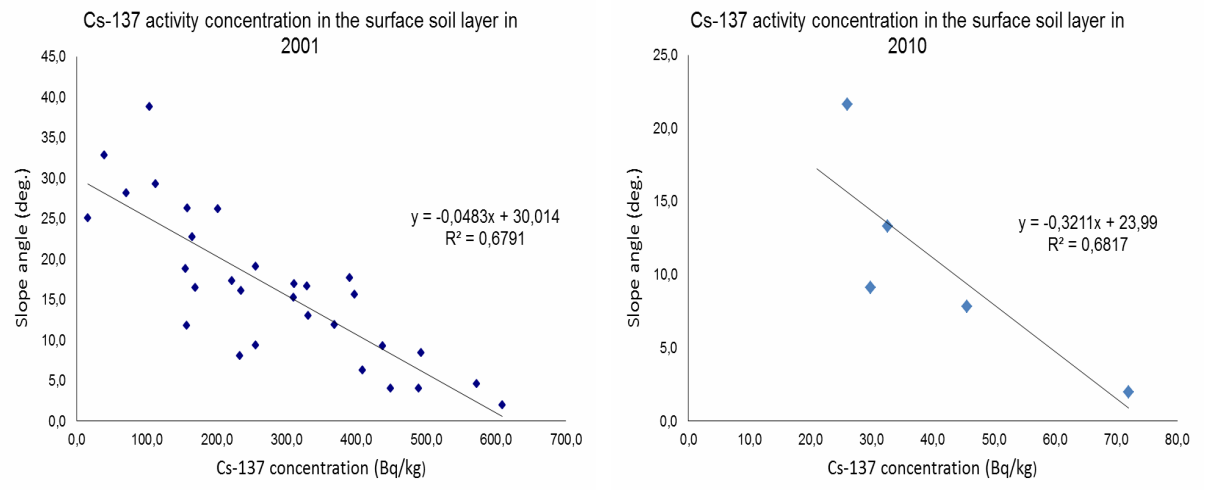

Figure 9. Slope inclination dependence of surface-close (0 to 2 cm) Cs-137 activity concentration of the measurement points in 2001 and 2010

4 SUMMARY AND CONCLUSIONS

Measurements on soil samples of a small water catchment (Farkas Trench) of the Sopron Mountains showed that there is Cs-137 isotope present in the area in well measurable quantities. In 2001, the depth distribution of Cs-137 activity concentration in the soil of the tested area took the shape of an exponential function. When fitting regression functions to the sampled values it was found that at the plots with lesser slope steepness (< 4 degrees) exponential functions provided the best match. As slope inclination increased, so did this Cs-137 profile. At sampling plots owning greater inclination a decrease in Cs-137 activity concentration of the top layers appeared. In 2001, at the sampling points, the activity concentration of the surface layers (0 to 2 cm) of the soil varied between 15 and 609 Bq/kg, whereas in 2010 between 26 and 72 Bq/kg. An interconnection between activity concentration in the surface soil layer and slope inclination could be indicated. From the slope inclination dependence of areal distribution it was concluded that one of the main reasons of areal alteration of Cs-137 activity concentration was differing extent of soil movement.

It appeared in the 2010 measurement data that the highest Cs-137 activity concentration had shifted lower from the top layers, and the depth distribution was altering along an increasing or a stagnating function to a depth of 4 to 6 cm (in function of slope inclination), then along a decreasing function. From this soil profile alteration the vertical migration speed could be deduced, which can be estimated to be 0.44 to 0.66 cm/year in the soil in the area.

Acknowledgements: We would like to thank Dr. Ferenc Divós, Manager of the OSJER Laboratory, for facilitating this research, moreover all the colleagues at the Institute of Geomatics and Civil Engineering of the University of West Hungary for assisting in the field work.

REFERENCES

ARAPIS, G. – PETRAYEV, E. – SHAGALOVA, E. – ZHUKOVA, O. – SOKOLIK, G. – IVANOVA, T. (1997): Effective migration velocity of 137Cs and 90Sr as a function of the type of soils in Belarus. Journal of Environmental Radioactivity 34 (2), 171–185.

BERG, M.T. – SHUMAN L.J. (1995): A three-dimensional stochastic model of the behavior of radionuclides in forests II. Cs-137 behavior in forest soils. Ecological Modelling 83: 373–386.

BLAGOEVA, R. – ZIKOVSKY, L. (1995): Geographic and Vertical Distribution of Cs-137 in Soils in Canada. J. Environ. Radioactivity, Vol. 21 No. 3: 269 – 274.

BÓDIZS, D. (1997): Félvezető-detektoros gamma-spektroszkópia, laboratóriumi gyakorlat, [Gamma Spectroscopy with Semi-Conductor Detector, laboratory training notes] BME Nukleáris Technikai Intézet, Budapest: 11. (in Hungarian)

CSÁFORDI, P. (2010): Erózióveszélyeztetettség vizsgálata a Soproni-hegység erdősült kisvízgyűjtőjén az USLE és az EROSION-3D modellekkel. [Soil erosion risk assessment with the models USLE and EROSION-3D in the small forested catchment of Sopron Hills.] In: Proceedings of the "Environmental management conference for the liveable countryside". Siófok, Hungary. September 2010. 189–198. (in Hungarian)

CSÁFORDI, P. – GRIBOVSZKI, Z. – KALICZ, P. (2010): Contribution of surface erosion to sediment transport in a small forested headwater catchment in the Sopron Hills. Journal of Landscape Management 1 (2): 3–11.

DU, M. – YANG, H. – CHANG, Q. – MINAMI, K. – HATTA, T. (1998): Caesium-137 fallout depth distribution in different soil profiles and significance for estimating soil erosion rate. Sciences of Soils Vol. 3: 23–33.

FANG H. J., YANG X. M., ZHANG X. P. AND LIANG A. Z. (2006): Using 137Cs Tracer Technique to Evaluate Erosion and Deposition of Black Soil in Northeast China. Pedosphere 16 (2): 201–209.

GRIBOVSZKI, Z. – KALICZ, P. – KUCSARA M. (2006): Streamflow Characteristics of Two Forested Catchments in the Sopron Hills. Acta Silvatica Lignaria Hungarica vol.2: 81–92.

PÁTZAY, GY. (2008): Mérési módszerek. In: Somlai, J.: Sugárvédelem. [Measurement methods. In: Somlai, J.: Radiation protection] HEFOP 3.3.1-P.-2004-0900152/1.0). 70-73 (in Hungarian)

PELLET, S. (2006): Magyarországi hatások (Csernobil – 20 év után), OAH konferencia, [Hungary effects (Chernobyl – after 20 years), in Hungarian Atomic Energy Authority Conference] Budapest, Hungary. (in Hungarian) Online: http://www.haea.gov.hu/web/v2/portal.nsf/att_files/eloadasok/$File/csereaps.ppt?OpenElement

PERRIN, J. – CARRIER, F. – GUILLOT, L. (2006): Determination of the vertical distribution of radioelements (K, U, Th, Cs) in soils from portable HP-Ge spectrometer measurements: A tool for soil erosion studies. Applied Radiation and Isotopes 64: 830–843.

PORTO, P. – WALLING, D.E. – FERRO, V. (2001): Validating the use of caesium-137 measurements to estimate soil erosion rates in a small drainage basin in Calabria, Southern Italy. Journal of Hydrology 248: 93–108.

WALLING, D.E. – QUINE, T.A. (1992) The use of caesium-137 measurements in soil erosion surveys. In: Erosion and Sediment Transport Monitoring Programmes in River Basins. IAHS Publication, no. 210: 143–152.

ZHIYANSKI, M. – BECH, J. – SOKOLOVSKA, M. – LUCOT, E. – BECH, J. – BADOT, P.M. (2008): Cs-137 distribution in forest floor and surface soil layers from two mountainous regions in Bulgaria. Journal of Geochemical Exploration 96: 256–266.

DE GRUYTER OPEN DOI: 10.2478/aslh-2013-0013 Acta Silv. Lign. Hung., Vol. 9 (2013) 161–169

Assessment of Quality-related Risks by the Use of Complex Networks

Tamás CSISZÉR*

Cziráki József Doctoral School of Wood Science and Technology, University of West Hungary, Sopron, Hungary

Abstract – This study introduces the NTS network as a new way of analysing, verifying and improving quality-related risk assessment. NTS is based on a network science approach that models complex systems by graphs. By using *N, T* and *S-Graphs* as the elements of NTS, risk events that play special role in the risk management system can be identified. Based on their characteristics, the strength of their potential causal connections can be recalculated, providing more precise predictions of the occurrence frequencies of events.

network science / risk assessment / optimization / FMEA / NTS graphs

Kivonat – Minőségi kockázatok elemzése komplex hálózatok segítségével. A tanulmány bemutatja a minőségügyi kockázatok közötti kapcsolatok elemzésére használható NTS hálózatot, amelynek segítségével - a kockázati események valós előfordulása alapján - értékelhetők és javíthatók a minőségi kockázatok elemzésének eredményei. Az NTS alkalmazása a hálózattudomány újszerű megközelítésén alapul, amely gráfok segítségével modellezi a komplex rendszereket. Az NTS elemeinek, az ún. N-, T- és S-gráfoknak a használatával azonosíthatók azok a kockázati események, amelyek speciális szerepet játszanak a kockázatmenedzsment rendszerben. Ismerve a jellegzetességeiket, az események közötti potenciális okozati kapcsolatok újraértékelhetők, amelynek eredményeképpen megbízhatóbb előrejelzés adható az egyes események előfordulási gyakoriságára.

hálózattudomány / kockázatelemzés / optimalizálás / FMEA / NTS gráfok

1 INTRODUCTION

Quality-related risk assessment aims to identify, analyze and prioritize events that may cause quality problems of products and processes. Experts try to evaluate the probability and effect of risks prior to the implementation of a new process and to the manufacturing of a new product. There might be cause-effect connections among 'risk events'. Therefore, to ensure the proper performance of risk assessment, we must handle them as elements of a complex system, and take their connections into consideration as well.

There are many ways of modelling and analyzing complex systems. One of the emerging toolsets is coming from the field of network science. It structures systems in graphs, emphasizing the connectivity that forms the network and influences its characteristics. By

* Corresponding author: csisztam@gmail.com; H-2120 DUNAKESZI, Kazinczy u. 6a

representing risk events with vertices and their causal connections with edges, we construct a risk-network, with which a deeper insight into the structure of potential problems can be obtained, and more analyses can be conducted in order to validate and improve the output of the risk assessment.

Since there may be many difficulties with the raw material and manufacturing conditions in industrial technology, a new approach of risk assessment can be relevant and useful for researchers and engineers as well.

In the followings we briefly introduce network science basics related to the topic of this article, define and describe the NTS network as a new tool in risk assessment, and finally demonstrate how this method can be utilized and what kind of conclusions can be drawn based upon it.

2 BRIEFLY ABOUT NETWORK SCIENCE

Network science deals with complex systems. It models and analyzes these systems by graphs. The main purposes are to identify and define network models that are independent from the entities of the system, describe the characteristics of the networks, and give predictions to the reaction of the system to different influences, like modifying the number of vertices or the weights of the edges.

Networks can be featured by certain attributes. The degree of a node and the degree distribution of a network show how many edges are linked to the vertices and whether there are some nodes that are significantly ‘richer’ or more important than others (Newman 2003). By creating a graph, we can see whether it is a connected network or there are separated nodes or groups of nodes within the graph. This can be useful when we want to find the shortest or fastest path between two different parts of the system.

Vertices can have different roles according to their position. Some of them function as bridges, connecting two parts of the graph. Others are hubs with high degrees and centrality, and, as such, have huge effect on processes running in the network. There can be isolated nodes as well, with no links to others (Csermely 2005).

Networks are not static; many changes can be detected during their lifetime. A network starts when two or more entities create one or more connection among themselves. When a new node is introduced to the network, it gets connected to one or more original ones according to a network specific rule. One of the widely accepted theories defines this rule as the ‘power law’, where the probability of forming a connection is proportional to the degree of the original node. This has been modified by some other works implementing different variables. (Dorogovtsev 2000). The general principle is that the probability of connecting is proportional to the importance and some ‘individual characteristics’ of vertices.

Networks can be fragmented as well. When one or more links are eliminated due to some events, nodes or sub-graphs get separated from the network. This process can make the whole network unable to operate, i.e. to ensure the flow of information, material or other exchangeable among vertices.

Knowing the structure, the attributes and the operation rules of the network, we can deeply understand the given complex system. Thus we can establish a robust system that would be more protected from intentional or accidental problems.

3 QUALITY-RELATED RISK ASSESSMENT

3.1 Traditional approaches

Several methods exist that provide tools for quality-related risk assessment. One of the most widely spread ones is the Failure Modes and Effects Analysis (FMEA). This mainly qualitative method can be used to analyse the probability and the effect of potential failures associated with a process or a product.

The purpose of FMEA is to mitigate the risk by reducing either the severity, or the probability of an incident. First of all, potential failures need to be listed. For each one, three factors should be calculated: 1) probability, i.e. the likelihood of occurrence; 2) severity, i.e. the worst case scenario of negative effect; 3) detection, i.e. how easy it is to detect the problem during operation. The combination of factors is the risk level. Based on this level, preventive, detective and corrective actions can be defined (Stamatis 2003).

Another method called Fault Tree Analysis (FTA) builds a hierarchical structure of undesired events and their potential causes. It defines logical connections among causes by Boolean operators and calculates the probability of an event from the probabilities of causes (Andrews 2012).

Both FMEA and FTA are aimed at identifying and analysing potential problems and trying to reduce their negative effects. While FMEA is a deductive, top-down methodology, focusing on the effects of an initial event, FTA is an inductive, bottom-up method, considering the potential causes of a failure as an undesired effect. FMEA builds a cause-effect tree from the root; FTA builds the same tree from the crown. If we apply FMEA and FTA together, the result will be a complex system with negative events and the causal connections among them. This system could be modelled by a network that can handle the data of probabilities and logical relationships. In order to keep the risk assessment results updated during the operation, information of real occurrences needs to be handled too. By analysing this network regularly, the theoretical structure of potential failures and the performance of risk management can be improved.

3.2 Definition of the NTS network

NTS consists of failures or, in a broader sense, risk events as vertices and common occurrences or presumed causal connections among them as directed edges. Edges can be weighted according to the strength of connection between cause and effect. In the analysis phase, the weight of an edge is

$$S_{Ae,Ac} = P(A_c)P(A_e) \quad (1)$$

where $S_{Ae,Ac}$ the weight or strength of an edge between A_c as the cause, and A_e as the effect, whilst P is the probability of the occurrence of an event. If there are several causes, the value of $P(A_c)$ is the combination of the probabilities of these causes $(A_{c1}, A_{c2}\ldots A_{cn})$. There are two different cases:

1) events that can cause the effect only when they occur together;
   A_{c1} AND A_{c2} => $P(A_c) = P(A_{c1})P(A_{c2})$;

2) events that can cause the effect separately;
   A_{c3} OR A_{c4} => $P(A_c) = P(A_{c3}) + P(A_{c4})$.

Figure 1 shows the graph representation of a simple system. A_{c1} and A_{c2} are represented together by one vertex in graph; A_{c3}, A_{c4} and A_e are separate vertices.

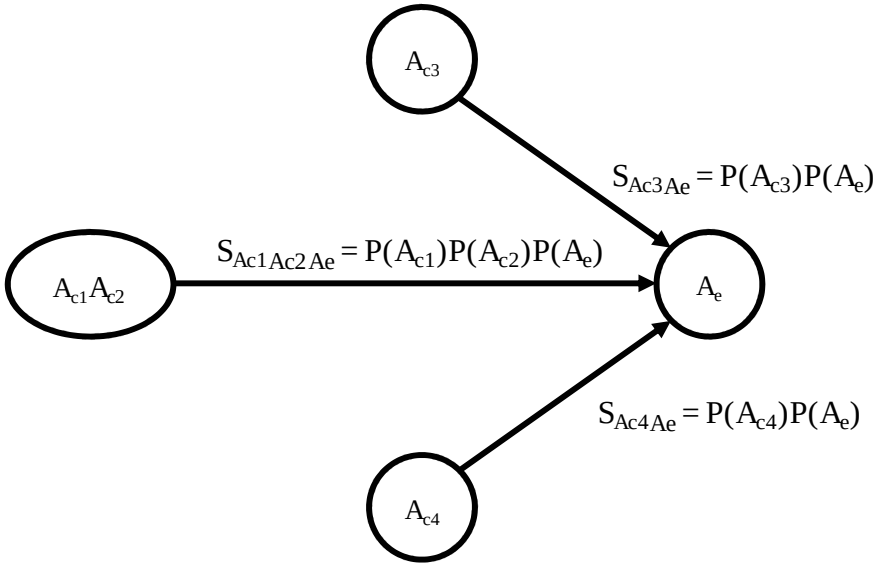

Figure 1: Graph representation of cause-effect connections of events

Since vertices $A_{c1}A_{c2}$, A_{c3} and A_{c4} are independent from each other,

$$P(A_e) = P(A_{c1}A_{c2}) + P(A_{c3}) + P(A_{c4}) \quad (2)$$

The weights of links can be calculated, as follows:

$$S_{Ac3Ae} = P(A_{c3})(P(A_{c1}A_{c2}) + P(A_{c3}) + P(A_{c4})) \quad (3)$$

$$S_{Ac1Ac2Ae} = P(A_{c1})P(A_{c2})((P(A_{c1}A_{c2}) + P(A_{c3}) + P(A_{c4})) \quad (4)$$

$$S_{Ac4Ae} = P(A_{c4})((P(A_{c1}A_{c2}) + P(A_{c3}) + P(A_{c4})) \quad (5)$$

This means that without knowing the probability of the occurrence of the final effect, we can calculate the weights of the links among a risk event and its potential causes.

3.3 The use of NTS

These weights are theoretical, since their calculation is based on prediction. If we want to validate these values, we have to calculate them based on data coming from the running process. There are two indicators that can be used to estimate the strength of connection (*S*) in the operational phase. The first one is the number of simultaneous occurrences (*N*), the other one is the time difference between the occurrences of cause and effect (*T*). The higher the *N* and the lower the *T*, the higher will be *S*. Consequently higher *N/T* ratios result in higher *S* values. *T* can be calculated as the average number of occurrences of common detections.

3.3.1 N-Graph

Let's assume that, from the analysis phase, we have a list of risk events related to the quality of a manufacturing process. When an event (*A1*) is detected, it has to be noted as a potential root cause. If, within a certain time period after *A1*, another event is detected, we record the time that passed between detections. Let this period be 4 seconds. The strength of the link between *A1* and *A2* is

$$S_{A1A2} = N/T = 1/4 = 0.25 \quad (6)$$

When a third event is detected e.g. 5 seconds after *A2*, the same calculation can be done. So, the strength of the link between *A2* and *A3* is

$$S_{A2A3} = N/T = 1/5 = 0.2 \quad (7)$$

Now we have a small connected group with three vertices and two edges. *Figure 2* shows the graph that represents this triplet.

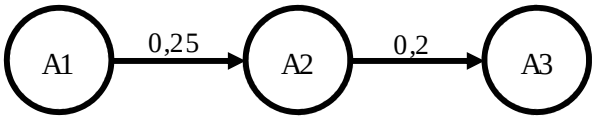

Figure 2: Graph representation of event connections with the weights of connections indicated above the edges

We do not know yet whether *A1* or *A2* or both together caused *A3*, we just know that there is a chance that the common occurrence may reflect a causal connection.

Let us assume that, two minutes later, *A2* is detected again. Two conclusions are possible: 1) *A3* caused *A2*, or 2) this is an independent occurrence. Based on the elapsed time and on professional experience, we can make a decision concerning the existence of a causal connection. If we think that there is no causal connection, or there can be, but the time is much longer than the time has passed between the former detections, we can take *A2* as a first event of a new cause-effect chain. Obviously, if there is no significant lag between them, and a causal connection is possible, *A3* may cause *A2*, so the link between them is bi-directional. Since 2 min is much longer than the previously detected durations, now *A2* starts a new graph. Obviously, this does not mean that *A3* could not have caused *A2*, since we have no evidence that *A2* is certainly the reason of *A3*. Continuing this event monitoring and detection process, we can get short event-chains consisting of connected groups of vertices (*Figure 3*).

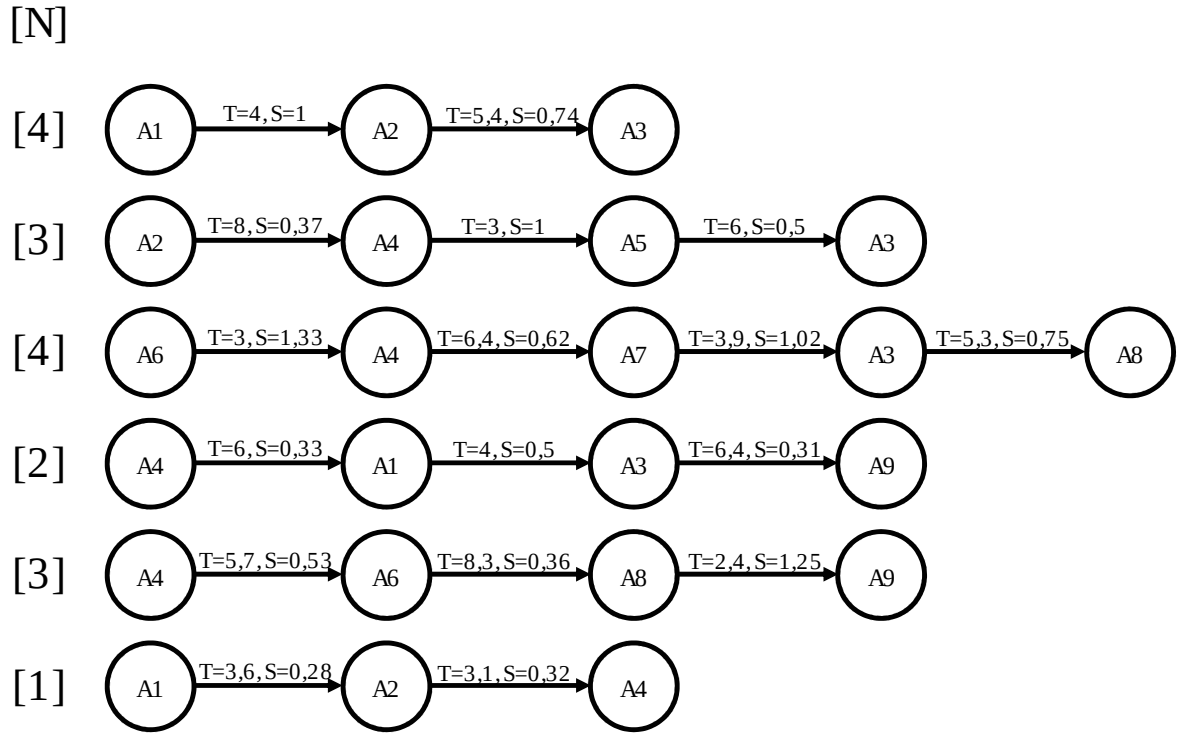

Figure 3: Event-chains with the attributes of links as follows: N (Nr. of common occurrences), T (average time between the occurrences of events), S (weight of edge).

In order to get a connected network from event-chains, we should merge them by using only one vertex for the same event. Since all of the attributes of the links (*N, T, S*) can reflect the strength of a causal connection, they can be used to create separate networks with *N, T* and *S* as the weights of edges.

The *N-Graph* (*Figure 4*) shows how frequently the events occurred together. The weight of the edge is reflected by the thickness of the arrow, the number on the arrow and the two-dimensional distance between the linked vertices.

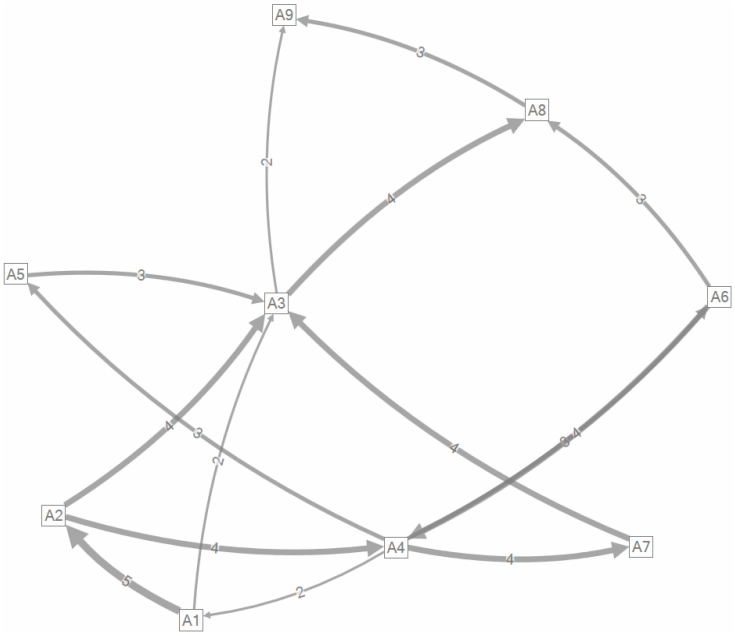

Figure 4: N-Graph

The degree parameters of vertices are listed in *Table 1*. The weights and the in- and out-connection ratios of edges are presented in *Table 2*.

Table 1. Degree parameters of vertices of the N-Graph

Vertex	Weighted in-degree	Weighted out-degree	Weighted degree
A1	2	7	9
A2	5	8	13
A3	13	6	19
A4	8	12	20
A5	3	3	6
A6	3	7	10
A7	4	4	8
A8	7	3	10
A9	5	0	5

Table 2. The weights and the out- and in-connection ratios of edges of the N-Graph

Vertex 1	Vertex 2	Weight	Out-connection frequency ratio[1] (%)	In-connection frequency ratio[2] (%)
A1	A2	5	71.4	100.0
A2	A3	4	50.0	30.8
A2	A4	4	50.0	50.0
A4	A5	3	25.0	100.0
A5	A3	3	100.0	23.1
A6	A4	4	57.1	50.0
A4	A7	4	33.3	100.0
A7	A3	4	100.0	30.8
A3	A8	4	66.7	57.1
A4	A1	2	16.7	100.0
A1	A3	2	28.6	15.4
A3	A9	2	33.3	40.0
A4	A6	3	25.0	100.0
A6	A8	3	42.9	42.9
A8	A9	3	100.0	60.0

1 – Weight of the current edge / weighted out-degree of Vertex 1 as the start node
2 – Weight of the current edge / weighted in-degree of Vertex 2 as the end node

The following main conclusions can be drawn from *N-Graph* and the associated tables:

1) Every event follows at least one other event (in-degree is never zero);
2) *A9* is not followed by any other event (its out-degree is zero);
3) *A3* and *A4* play central roles, since their weighted degrees are the highest;
4) The weighted in-degree of *A3* (13) is approx. twice as big as its out-degree, so *A3* tends to occur as a successor, rather than a predecessor;
5) Contrary to *A3*, for instance, *A4* tends to occur as a predecessor rather than a successor, since its out-degree is 12 and its in-degree is 8;
6) According to the out-degree frequency ratio of the *A5-A3* connection, when *A5* occurs (three-times), it always causes *A3*. In contrast, according to the out-degree frequency ratio of the *A5-A3* connection, *A3* is caused by *A5* in 3 cases, which is only 23,1% of all occurrences of *A3* (13).

Applying the *N-Graph*, we can come to the following general conclusions:

1) The higher the out- or in-degree frequency ratio of a connection, the higher the probability of their common occurrence;
2) If the in-degree of a vertex is higher than its out-degree, the event tends to be a successor of other events;
3) If the out-degree of a vertex is higher than its in-degree, the event tends to be a predecessor of other events;
4) If the in-degree of a vertex is zero, it starts an event-chain or its predecessors are unknown;
5) If the out-degree of a vertex is zero, it ends an event-chain or their successors are unknown;
6) Isolated vertices (both their in- and out-degrees are zero) have no connections with other events in the N-Graph.

3.3.2 T-Graph

The *T-Graph (Figure 5)* is created based on the time that passes between the occurrences of vertices. The shorter the time, the stronger the connection and the larger the weight of edge.

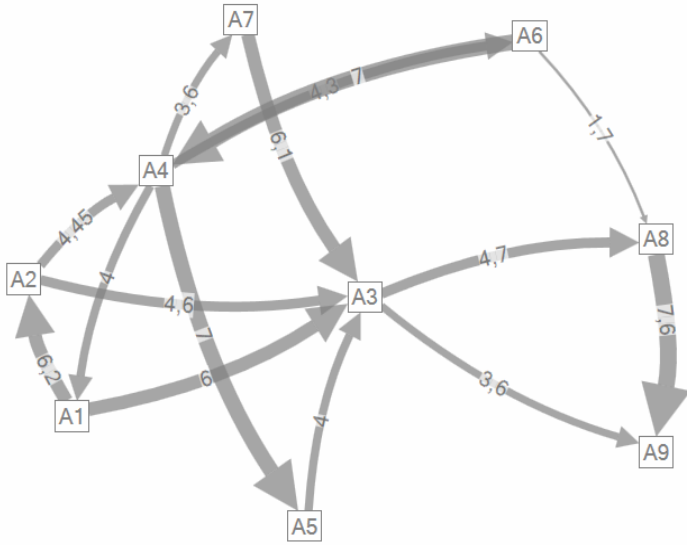

Figure 5: T-Graph

In the T-Graph we can identify the possible sequences of events. For example, if *A1* occurs, *A2* and/or *A3* are also likely to occur, approx. 6 seconds later. When *A3* occurs, we have to take appropriate measures in order to prevent the occurrence of *A8* and *A9*. From the *T-Graph*, we do not know what the probability of a successor's occurrence is.

3.3.3 S-Graph

The *S-Graph (Figure 6)* shows the relative probability of an event's occurrence after the occurrence of its predecessor has been detected. The relative probability is the weight of the edge between the predecessor and the successor, divided by the sum of the weights of the out-edges of the predecessor. For example, if we detect the occurrence of *A1*, the relative probability of the occurrence of *A2* is 4.8/(3. + 4.8) = 0.558. The relative probability of the occurrence of *A3* is 3.8/(3.8 + 4.8) = 0.442. This means that the occurrence of A2 is more probable. Since A2 can cause A3 too, the relative probability of the occurrence after the detections of A1 and A2 is (3.8/(3.8 + 4.8)) + ((4.8/(3.8 + 4.8))(5.6/(5.6 + 2.6)))=0.442 + 0.558 × 0.683 = 0.82.

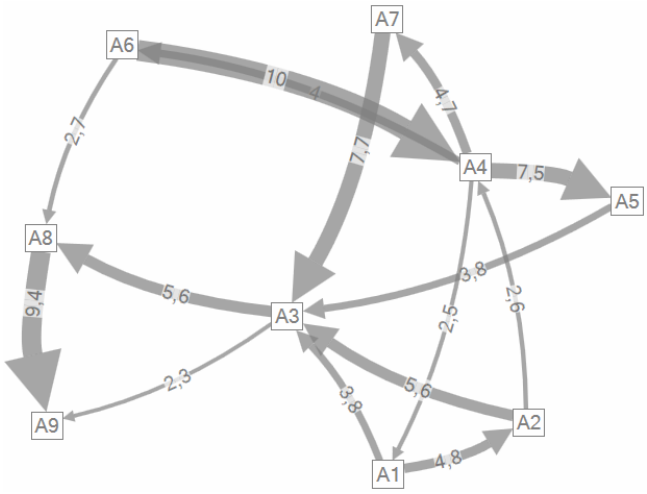

Figure 6: S-Graph

By calculating the relative probability of every possible event-chain, we can quantify the strength of connections and the chance that a failure occurs.

3.4 Conclusions

The *N*, *T* and *S-Graphs*, collectively named NTS, show the events that play specific roles in risk assessment. Based on the analysis of connectivity, we can verify and modify the results of risk assessment and we can create new risk management strategies and actions. Some of the general conclusions based on the NTS analysis are as follows:

1) The higher the *S* and the relative probability, the larger the probability of the existence of causal connection between vertices. This means that if this connection has not been identified formerly, preventive actions need to be defined and applied.
2) The larger the out-degree of a vertex in the *N-Graph*, the more important role the associated event plays as a possible cause of problem. This means that the risk management activities have to be focused on the prevention and detection of this event.
3) The bigger the in-degree of a vertex in the *N-Graph*, the more likely its occurrence is. This means that we have to count on its frequent occurrence, so the introduction of risk mitigation measures is strongly advised.
4) The lower the average time between the occurrences of two connected events in the *T-Graph*, the faster we have to react to prevent the occurrence of its successor. This means that we have to define actions that can be conducted in a very short time.

Finally, it is important to emphasise that NTS is only an approximation of the existence of a causal connection. In order to prove the causality, NTS and other professional investigation tools need to be applied on the long run.

REFERENCES

ANDREWS, J. (2012): Introduction to Fault Tree Analysis. In: 2012 Annual Reliability and Maintainability Symposium. USA. January 2012. 1–3

CSERMELY, P. (2005): A rejtett hálózatok ereje. [The power of hidden networks] Vince Kiadó, Budapest. (in Hungarian)

DOROGOVTSEV, S.N. (2000): Structure of growing networks with preferential thinking, Phys. Rev. Lett. 85, 4633.

NEWMAN, M.E.J. (2003): Random graphs as models of networks. In: Bornholdt, S. (ed.): Handbook of Graphs and Networks, Wiley-VCH Gmbh & Co. KGaA, Weinheim. 35–68

STAMATIS, D.H. (2003): Failure Mode and Effect Analysis, ASQ Quality Press, Milwaukee

Guide for Authors

Acta Silvatica et Lignaria Hungarica publishes original reports and reviews in the field of forest, wood and environmental sciences. ASLH is published in serial volumes. It is online accessible under: http://aslh.nyme.hu

Submission of an article implies that the work has not been published previously (except in the form of an abstract or as part of a published lecture or academic thesis), that it is not under consideration for publication elsewhere. Articles should be written in English. All papers will be reviewed by two independent experts.

Authors of papers accepted for publication should sign the Publishing Agreement that can be downloaded from the homepage (http://aslh.nyme.hu).

All instructions for preparation of manuscripts can be downloaded from the homepage.

Contents and Abstracts of the Bulletin of Forest Science

Bulletin of Forest Science (Erdészettudományi Közlemények) is a new journal supported by the Hungarian Forest Research Institute and by the Faculty of Forestry of the University of West Hungary. The papers are in Hungarian, with English summaries. The recent issue (Vol. 3, Nr. 1, 2013) contains the following papers (with page numbers in brackets), the full papers can be found and downloaded in pdf format from the journal's webpage (www.erdtudkoz.hu).

Abstract – The Síkfőkút Project site was established in 1972 by Pál Jakucs as part of the Man and the Biosphere (MAB) program for long term ecological research in a typical Hungarian climazonal sessile oak - turkey oak forest. For the 40 year jubilee, this paper gives a summary and overview about its establishment, goals, facilities, results, international connections, and silvicultural importance.

Abstract – The Food and Agriculture Organization of the United Nations (FAO) Commission on Genetic Resources for Food and Agriculture published their first reports on the state of plant and animal genetic resources in 1996 and 2007, respectively. The third such report, The State of World's Forest Genetic Resources, is scheduled for publication in 2013. Although Hungary takes part in monitoring of conservation activities on forest genetic resources at international context, the country report for the above mentioned initiative was the first comprehensive assessment of management and conservation issues in the last decades. This paper gives a short summary of the country report, concentrating primarily on the domestic forest gene conservation strategy, measures and activities, its legislation, financial background and international aspects. Additionally, overview on the present state of genetic investigations, breeding and forest reproductive material production, marketing and deployment, based on data from 2010-11, is also included.

Abstract – In order to project the effects of expected climatic changes, distribution of European beech (*Fagus sylvatica*) and sessile oak (*Quercus petraea*) were analysed at the xeric limits in Hungary. A fine-scale analysis was combined with sophisticated screening for

climate-dependent (zonal) occurrences. For both species, temperature and precipitation conditions in late spring and summer appear as principal variables determining the probability of presence. For beech, the importance of Ellenberg's climate quotient supports its sensitivity to summer drought. The calculated range shifts are drastic, similar to other results of statistic models. The applied approach allows a finer distinction of climatic threats on local scale and draws the attention to the urgency of preparative measures and application of proper silvicultural technologies.

Abstract – A transition system to continuous cover forestry has been introduced at large scale (over 5,000 hectares) by Királyrét Directorate of the Ipoly Erdő Ltd. Due to the short time period since the start of the transition in 2007, the processes including natural regeneration are not well known. Of the 6,000 gaps created, we included 124 using stratified sampling by stand age, dominant tree species and time since gap opening. Position and size of the gaps as well as cutting damage were noted. Sapling cover and browsing damage were estimated for each tree species in three size categories.

Two thirds of the gaps exceeded the diameter of stand height and more than half of them have an oblong shape. Forestry operations caused stem damage in 51% of the gaps and saplings were harmed in 21 cases. During the sampling 23 tree species were registered 30% of which did not occur in the adjacent stand. Sapling cover was highest in the 20-150 cm size category reaching 3% for the dominant and 9% for the admixing tree species. Game pressure was high and affected especially saplings between 20-150 cm, sprouts and admixing tree species.

Abstract – One of the greatest challenge of the continuous cover forest management is to choose a suitable gap size in a given forest stand that will help the regeneration of economically significant woody species, but possibly control the competitors of the cutting site and undesired woody species, hereby reduce the necessity of nursing. The hemispherical photos (or fish-eye photos) taken of the gaps in the survey are about to reveal, that how little information is obtained from a simply measured gap size when determining the light conditions of a gap. From the findings, it can be suggested to forest researchers who are working with the transformation system that they take simple fish-eye photos alongside the estimation of ground level gap size, from which accurate canopy closure and real light conditions can be evaluated.

Abstract – One station of the forest water cycle is the forest litter, which can retain more water from the precipitation than its own dry weight. This study examined the litter water storage depending on the dry weight for three species (spruce, beech, sessile oak). The results obtained with the method of collecting litter showed that the leaves can be uptaken by the maximum amount of water depends on especially the dry weight of the litter. According to our measurement the maximum water content of the litter per kilogram dry weight is 2.1-2.2 litres.

Abstract – In Hungary the black locust (*Robinia pseudoacacia*) is one of the most important exotic stand-forming tree species. Its importance is increasing in many other countries, too. As a result of a partly new selection programme eight black locust clones have been improved for setting up clone trials and seed orchards. In the paper the juvenile growth and the stem quality of micropropagated black locust clones were evaluated under sandy soil conditions. At age of 10 the clones 'MB17D3/4', 'MB17D3/10' as well as 'PV 201E2/4' appeared to be the most promising ones for quality wood production. Tissue culture method can be considered as a suitable tool for clonal propagating superior individuals and offering new prospects for rapid mass cloning of selected genotypes.

Abstract – As a result of new developments in technology, harvesters may no longer be confined to conifer forests only. Several studies carried out in black locust, Turkey oak and beech stands have justified the use of these machines in hardwood stands. Evaluating the results of the cost and time analyses we concluded that harvesters are more efficient in several cases compared to traditional wood cutting with chainsaws.

Abstract – This paper discusses the analysis of the complex economic models between selection system based on "Dauerwald" principles (continuous cover forestry) in the early transformation period and in the traditional rotation system in beech stands. The analysis is carried out both subcompartment level and forest blocks (management) level and compares the performances. From the results obtained it can be found, that in beech stands in the selection system is able to reach at least the same economic efficiency in both levels such as in the traditional rotation system.

Abstract – The most important requirement for forestry units managing state owned forests is to carry out sustainable forest management. Among the many criteria of sustainable forest management the maintenance of a stable financial background is essential. Providing the financial background is almost solely based upon the incomes generated from marketable forest based products and services, of which timber is predominant. Studying the potential incomes from timer is therefore of high importance for both the representative of the state as the owner and the forest management units. This income can be considered as the basis of calculating the trusteeship fee. This paper presents an applicable method to calculate long term profitability of forest management.

Abstract – In this paper, we suggest a model of fitting a new type of saturation curve, namely a sinus curve, which can extend the application of saturation curves and life curves for forest yield database. The greatest advantage of the model is its flexibility can be realized in fitting either with or without inflection point. The initial values can easily be given for the regression procedure implemented in computer. The output of the programme consists of five parameters. Beside the usual graphical illustration the algorithm makes possible to show the differences between, for instance, black locust-tree production sites by exact calculation.

Abstract – The genus *Rubus* L. with over 700 European species belongs to the taxonomically most complicated groups of vascular plants. The representatives of the genus form a complex of few sexual diploid species and a plenty of polyploid apomicts. New morphotypes originated as result of occasional hybridization and segregation can be stabilized by renewed apomixis. Batological research was suffered from methodological and taxonomical inaccuracies for a long time, with the description of innumerable individual morphotypes, which were mainly resolved by the new, modern species concept developed in the last 40 years ("Weberian reform"). A scale of distribution extents was established and widely accepted for taxonomic classification, and only uniform morphotypes with sufficiently large distribution areas have been classified as species. The authors give an overview on development of taxonomical concepts and special methods of modern *Rubus* research beside a short summary of former and recent batological activity in Hungary.

Abstract – Coverage, richness and composition of bryophytes were compared between spruce and beech forest stands in the Sopron mountains. The highest coverage of bryophytes species in beech forests had *Hypnum cupressiforme*, which was followed by terricollous species like *Atrichum undulatum* and *Dicranella heteromalla*. The most dominant species in the spruce stands was *Brachythecium velutinum*; *Brachythecium rutabulum* and *Fissidens taxifolius* had slightly lower cover. The cover of bryophytes in beech stands was twice as high as in spruce stands. The total bryophyte coverage was very small in both forest types. The proportion of stands without bryophytes was the same in beech and spruce forest stands. Greater richness of bryophyte was found in beech stands than in spruce stands. The most frequent species were *Hypnum cupressiforme* and *Brachythecium velutinum* in both forest stands. The bryophyte flora was richer in native beech forests, than in spruce stands, which were planted on natural beech forests sites. However, the bryophyte composition of beech and spruce stands show considerable similarity. Generally, the older spruce plantations had unfavorable effect on the bryophyte diversity.

Abstract – Our research focused on the distribution of European mistletoe (*Viscum album*) in five Central European countries (Hungary, Slovakia, Czech Republic, Poland and Romania). Regarding to the distribution of mistletoe in the different countries no accurate assessment have been made yet, therefore our review was based on the assessment of available literature records. The host plants of mistletoe are very different in the analyzed countries. It's notable, that many species from the broadleaf trees, such as *Acer pseudoplatanus*, *Robinia pseudoacacia*, *Populus* × *euramericana*, *Sorbus aucuparia*, or from conifers the silver fir (*Abies alba)* are the most common hosts almost all countries.

Abstract – Mycology is a rapidly developing discipline, which has strong connections to the forestry management. To discover these relationships, mycological investigation was carried out in the Sopron Mts (Western Hungary). The monitoring was started in 2010, and it has not been ended so far. Different sampling methods were applied (e.g. random field work, small and large sampling plots) in the past three fruiting periods of macrofungi to understand their applicability. Altogether 364 taxa were documented. Based on our preliminary results, the Sopron Mts is a species rich, diverse area from mycological point of view. Ecologically as well as economically, macrofungi play important role in the life of the forests and forestry managements (e.g. indicator function, nature conservation, health condition, decay of litter and dead wood, secondary source of income, etc.), and their knowledge has several future possibilities in practical use.

Abstract – In two consecutive years (2011 and 2012), the bird communities of two pine plantations, two pedunculate oak and one gray poplar stands were studied in the Tanulmányi Forest of Ásotthalom. For the survey the quadrate method was used. Altogether 735 individuals of 34 bird species were detected. The surveyed biocoenoses were compared with various ecological parameters (diversity, the level of consistency, similarity measures and hierarchical cluster analysis based on Jaccard). In the two study years, species richness, density and diversity were the highest in the oak stands. The highest similarity was between the two oak sites while it was the lowest between the pine and the oak sites. In the dendrogram of the hierarchical cluster analysis the deciduous and the coniferous quadrates are well separated. At each level the breeding bird occurrence was constant for the terricol and the fruticicol species. The ratio of the dendricol and the arborical species was higher in the oak sites.

Abstract – The Collembola fauna was studied in the region of Ähtäri (Western Finland) in five different habitats (coniferous, deciduous and mixed forests). During the survey a total of 2007 specimens belonging to 32 species were collected. The most abundant species was *Folsomia fimetarioides* occurring in high numbers in all sampled habitats. Species richness and diversity were the highest in the pine forest, while total abundance peaked in the soil samples of the birch forest. Despite of the different plant composition of the sampled forests, community similarity (Bray-Curtis) was relatively high (41%<).

Abstract – Two species of the family Melolonthidae have particular importance in forest management in Hungary; the maybeetle (*Melolontha melolontha*) and the forest cockchafer (*Melolontha hippocastani*). Present knowledge about the two species are presented in details in this article. Earlier experiences with decreasing their damage as well as newer technological experiments are evaluated on the basis of Hungarian literature.

Abstract – Macrolepidoptera communities and their diversity was compared in three different forest stands (sessile oak, beech and mixed sessile oak forests) in the Sopron Mountains. The monitoring was carried out from May to November 2008, using portable light traps and we identified a total of 349 species and 8,046 individuals in 12 families. The results suggest that the mixed forest stand has higher diversity of macrolepidoptera species. The diversity was determined using Shannon and Simpson diversity models. To compare diversity values, Hutcheson's t-test was used. Furthermore, the diversity values were ranked by Rényi's diversity ordering. The results show higher diversity in the mixed oak forest stand, while the beech forest stand had lower diversity of macromoth communities. Ranking of the unmixed oak forest stand was not possible.

Abstract – The light-trap method is based on the insects's behaviour to fly to artificial light, therefore it can also be used to examine light pollution. Light pollution can lead to change in insect behaviour and reproduction. The aim of this study was to examine the effect of light pollution on insect behaviour using three different type of light sources. The investigation was done with Jermy-type light traps from June to August, and the tests were done according to the moon phases. The trap captures varied strongly. Flies (*Diptera*), cicadas *(Hemiptera*) and moths (*Lepidoptera*) were eudominant and dominant in the traps. There is a regionally varied, significant relation between the light sources and trapped insect orders.

Abstract – Leaf miners are good models to study multitrophic interactions, including the regulating potential of their parasitoids. Only a few studies have been published concerning the parasitoids of the Central European and Hungarian leaf miners. In 2011 and 2012 we studied the parasitoid complexes of 9 leaf mining species developing on 4 different species of oaks. The samples were kept in individual rearings. In the two years we collected 1,936 samples. From these rearings 28 different parasitoid species have emerged. After comparing our rearing results with those in the scientific literature, we have concluded that our results include novel and unpublished host-parasitoid associations.

Abstract – We have estimated birth rate in wild boar *Sus scrofa* by counting embryos in the uterus of females killed in the course of individual or drive hunts. Counting corpora lutea in the ovaries gave information, on embryo/corpus luteum rate, which can be useful for estimating birth rate in early stages of pregnancy. In the latter cases we multiplied the number of corpus luteum by the embryo/corpus luteum rate to estimate the birth rate. Birth rate was estimated in different age groups, separately. Age was estimated by means of teeth wear. Survival was estimated by direct observations counting the piglet/female ratio in matrilineal groups. The method is suitable for assessing summer survival only, as 8-9 month after birth matrilineal groups begin to disintegrate. Average estimated birth rate was 6.7 (N=51). We found positive linear relationship between conception rate and age of female, conception rate and body mass, respectively. In late stages of pregnancy, embryo/corpus luteum rate proved to be 0.83±0.15. Recruitment of piglets to the female population was low: more than half of them perished by the end of September. The highest mortality rate occurred in the first weeks of the piglets' lives.